Developmental Regulation of Prion Expression in Cattle and Mouse Embryonic Stem Cells

Oscar Alejandro Peralta Troncoso

Dissertation submitted to the faculty of the Virginia Polytechnic Institute and State University in partial fulfillment of the requirements for the degree of

Doctor of Philosophy

in

Biomedical and Veterinary Sciences

Willard H. Eyestone, Chairman

William R. Huckle

Ludeman A. Eng

Xiang-Jin Meng

Jill C. Sible

Mary Lynn Johnson

July 25th, 2008

Blacksburg, Virginia

Keywords: Cellular prion protein (PrP^C), Embryogenesis, Gene expression, Embryonic stem cells, Neural differentiation, Prion gene (Prnp), Reproductive tract, Somatic tissues

Developmental Regulation of Prion Expression in Cattle and Mouse Embryonic Stem Cells

Oscar A. Peralta Troncoso

ABSTRACT

The host encoded cellular prion protein (PrP^C) is an N-linked glycoprotein tethered to the cell membrane by a glycophosphatidylinositol (GPI) anchor. Under certain conditions, PrP^C can undergo conversion into a conformationally-altered isoform (PrP^{Sc}) widely believed to be the pathogenic agent of transmissible spongiform encephalopathies (TSEs). Thus, tissues expressing PrP^C are potential sites for conversion of PrP^{Sc} during TSE pathogenesis. Although much is known about the role of PrP^{Sc} in prion diseases, the normal function of PrP^C is poorly understood. Lines of mice and cattle in which PrP^C has been ablated by gene knockout show no major phenotypical alterations other than resistance to TSE infection. However, recent reports using Prnp-null mouse models have suggested the participation of PrP^C in neural stem/progenitor cell proliferation and differentiation. The first objective in our study was to map the expression of PrP^C in twenty six somatic and reproductive tissues in ruminants. Our second objective was to characterize the ontogeny of PrP^C expression during bovine embryonic and early fetal development. Finally, we used a mouse embryonic stem cell (mESC) model to study the potential role of PrP^C during neurogenesis. In adult tissues, intense expression of PrP^C was detected in the central nervous system (CNS), thymus and testes, whereas the liver, striated muscle and female reproductive tissues showed the lowest expression. We observed that PrP^C was associated with tissues undergoing cellular differentiation including spermatogenesis, lymphocyte activation and hair follicle regeneration. Analyses in bovine embryos and fetuses indicated peaks in expression of PrP^C at days 4 and 18 post-fertilization, stages associated with the maternal-zygote transition and the maternal recognition of pregnancy and initiation of placental attachment, respectively. Later in development, PrP^C was expressed in the CNS where it was localized in mature neurons of the neuroepithelium and emerging neural trunks. Based on these observations, we hypothesized that PrP^C was involved in neurogenesis. We tested this hypothesis in a murine embryonic stem cell model (mESC). mESC were induced to form embryoid bodies (EBs) by placing them in suspension culture under differentiating conditions and allowed to differentiate *in vitro* for 20 days. We detected increasing levels of PrP^C starting on day 12 (8.21- fold higher vs. day 0; $P < 0.05$) and continuing until day 20 (20.77-fold higher vs. day 0; $P < 0.05$). PrP^C expression was negatively correlated with pluripotency marker Oct-4 ($r = -0.85$) confirming that mESC had indeed differentiated. To

provide a more robust system for assessing the role of PrP^C in neural differentiation, mESC were cultured with or without retinoic acid (RA) to encourage differentiation into neural lineages. Induction of EBs with retinoic acid (RA) resulted in an earlier up-regulation of PrP^C and nestin (day 12 vs. day 16; $P < 0.05$). In addition, immunofluorescence studies indicated co-expression of PrP^C and nestin in the same cells. The results of these experiments suggested a temporal link between PrP^C expression and expression of nestin, a marker of neural progenitor cells. We next tested whether PrP^C was involved in RA-enhanced neural differentiation from mESC using a PrP^C knockdown model. Plasmid vectors designed to express either a PrP-targeted shRNA or scrambled, control shRNA were transfected into mESC. Stable transfectants were selected under G418 and cloned. PrP-targeted and control shRNA clones, as well as wild-type mESC, were differentiated in presence of RA and sampled as above. PrP^C expression was knocked down in PrP-targeted shRNA cultures between days 12 and 20 (62.2 % average reduction vs. scrambled shRNA controls). Nestin expression was reduced at days 16 and 20 in PrP^C knockdown cells (61.3% and 70.7%, respectively vs. scrambled shRNA controls). These results provide evidence that PrP^C plays a role in the neural differentiation at a point up-stream from the stages at which nestin is expressed. In conclusion, the widely distributed expression of PrP^C in ruminant tissues suggests an important biological role for this protein. In the present work we have provided evidence for the participation of PrP^C in the differentiation of mESC along the neurogenic pathway.

ACKNOWLEDGMENTS

First, I would like to express my gratitude to my advisor Dr. Will Eyestone for his patience, encouragement and support in the completion of my doctorate degree. It was a great experience to work with Dr. Eyestone, he is a very enthusiastic and knowledgeable person, and an excellent scientist. I would also like to thanks my committee members Dr. William Huckle, Dr. Ludeman Eng, Dr. Xiang-Jin Meng, Dr. Jill Sible and the external examiner Dr. Mary Lynn Johnson for their guidance throughout this project. My gratitude to Kathy Lowe for her permanent and friendly support. I also would like to thanks the staff of the CREATE Lab for their assistance in my work.

This dissertation is dedicated to my wife Cecilia Zuleta, my parents Maria and Oscar, and my brothers Nicolas and Rodrigo. Their continue support and love made possible for me to achieve this degree. Thanks.

TABLE OF CONTENTS

Page number

LIST OF FIGURES

Page number

CHAPTER IV

CHAPTER V

INTRODUCTION

The complex nature of prions has intrigued the scientific community during the last 70 years. Since the first indication of scrapie infectivity in 1937 and the experimental transmission of the scrapie agent in sheep the same year, prions and their associated diseases, have been under constant investigation. Furthermore, the formulation of the prion hypothesis in 1966 and the discoveries by Prusiner in 1982, opened a completely new perspective in the understanding of these infectious proteins. One of the most interesting aspects of the prion hypothesis is the presence of a host-encoded isoform (PrP^{C}) with the autocatalytic or induced capacity to change its secondary configuration into a pathogenic isoform (PrP^{Sc}). Despite intense research undergoing during the last 20 years to probe this hypothesis, the most compelling evidence is yet to be reported. Another enigmatic aspect of the prion biology is the potential physiological function of PrP^{C}, a protein that is widely distributed in mammalian tissues and intensely expressed in the nervous system. PrP^{C} has been associated to several biological roles including cellular adhesion, signaling and protection. Recently, one study reported a positive association between PrP^{C} and differentiation of neural cells. These researchers argued that PrP^{C} was associated in a dose-dependent manner with differentiation of multipotent precursors into mature neurons *in vitro*. Moreover, analyses in mouse brain showed the PrP^{C} played a role in the proliferation of neural precursor cells.

In the present work, we described our efforts to better understand the potential function of PrP^{C}. In chapters two and three we mapped the expression of PrP^{C} in 30 different tissues of the bovine. These analyses characterized PrP^{C} as widely distributed protein expressed in organs with different physiological functions. This wide distribution and intense expression in neurons and lymphoreticular cells suggest that PrP^{C} may have an important physiological function. Chapter four focused on the developmental characterization of PrP^{C} during bovine embryogenesis. The stage-specific expression of PrP^{C} during pre-implantation stage suggests the participation of this protein in the early embryonic development. Thereafter analyses in fetuses showed an intense expression of PrP^{C} during the early development of the nervous system. This data led us to hypothesize a potential contribution of PrP^{C} in neurogenesis. This hypothesis was tested in the last chapter of this work. Analysis of PrP^{C} expression in mouse embryonic stem cell (mESC) showed a positive association between PrP^{C} expression and the marker for neural stem/progenitor cells, nestin. The final experiment demonstrated that the knockdown of PrP^{C} expression results in the significant reduction of nestin levels indicating a direct or indirect association between these proteins. This data represents evidence for the contribution of PrP^{C} in neurogenesis and support the reports of others indicating the participation of PrP^{C} as a neural differentiation factor.

CHAPTER I

PRION BIOLOGY AND BOVINE SPONGIFORM ENCEPHALOPATHY

INTRODUCTION

Transmissible spongiform encephalopathies (TSEs) are neurodegenerative, fatal diseases with no early diagnosis, treatment or cure (Collinge, 2001). Several species are affected by TSEs including human (Creutzfeldt-Jakob disease, Gerstmann-Straussler-Scheinker, Kuru, Fatal familial insomnia), bovine (spongiform encephalopathy), ovine (scrapie), deer (chronic wasting disease) and mink (transmissible encephalopathy). TSEs display a wide spectrum of clinical signs, neuropathology and epidemiology that result in difficult diagnosis and control. Despite their diverse presentations, all TSEs stem from the infectious, spontaneous or hereditary conversion of PrP^{C} into the pathogenic isoform PrP^{Sc} (Soto, 2006). The unpredictable properties of PrP^{Sc} and the potential zoonotic transmission of the bovine spongiform encephalopathy (BSE) have generated intense concern in the international community over animal product biosecurity. One of the most critical aspects of the TSE-infectious agent is the capacity to cross the species barrier from cattle to human through the consumption of beef products. Worldwide, 172 people have fallen victim to the variant CJD (vCJD) during 2008, and epidemiologists predict the presentation of more cases in the coming years due to existing pre-clinical or subclinical infection (Collee et al., 2006; NCJDSU, 2008). The first case of BSE was detected in USA in 2003, resulting in the ban of meat importation from USA to 53 countries with a drastic drop in 83% of the imports. Translated into economic terms, BSE produced a loss of 5 billion dollars which corresponded to 4% of the gross domestic agriculture product (Coffey et al., 2005).

The scientific community has been intrigued with the complex nature of prions for over 70 years. The first indication of prion infectivity was reported in 1937 in Scotland after immunization of sheep against louping ill. The vaccines used were accidentally elaborated from brain extracts obtained from animals infected with scrapie (Gordon, 1946). The fact that eight percent of the immunized animals developed scrapie, with the experimental transmission of the agent performed the same year, the infectious capacity of scrapie among sheep and goats was demonstrated (Cullie and Chele, 1939). In 1959, Hadlow suggested that Kuru, a neurodegenerative disease that affected New Guinea tribes might be similar to scrapie due to similarities in epidemiology, clinical signs and pathological findings. This hypothesis was later confirmed in 1965 by the successful transmission of Kuru to chimpanzees after incubation of 18 to 21 months (Gajdusek et al., 1965). One year later, Alper and colleagues reported that the molecular weight of the scrapie agent was significantly lower compared to a conventional virus (Alper et al., 1966). Moreover, Apler showed that the scrapie agent was able to resist doses of ultraviolet radiation (UV) sufficient to

inactivate nucleic acids. These experiments led to the formulation of the protein-only hypothesis, which described the scrapie agent as a particle conformed by a proteinaceous structure devoid of nucleic acids with the unique capacity to autoreplicate (Griffith, 1967). In the 1980s, Prusiner reported abundant experimental data in support of this hypothesis and proposed for the first time the term "prion" to describe the scrapie agent. Prion was defined as small proteinaceous infectious particle which was resistant to inactivation by most procedures that modify nucleic acids (Prusiner, 1982). This controversial suggestion supported the idea of a scrapie agent consisting only of an infectious protein and discredited the model that included a small nucleic acid in the core of the protein. Furthermore, one of the most intriguing aspects of the prion biology was the discovery of a host-encoded cellular prion protein or PrP^{C} (Oesch et al., 1985). This discovery guided to the formulation of the prion hypothesis that postulates that the agent responsible for prion propagation is originated by autocatalytic conversion of PrP^{C} into the pathogenic isoform. Physical contact between both isoforms induces instability of the PrP^{C} mainly α-helicoidal structure and results in its conversion into a predominantly β-sheet configuration characteristic of PrP^{Sc}.

Although the involvement of PrP^{C} in the infection of TSEs has been well documented, the function of PrP^{C} remains inconclusive. During the last decades, there have been several reports describing roles for PrP^{C} as an antioxidant, cytoprotective, cell adhesion and mitogenic agent (Manson et al., 1992; Martins et al., 2001; Zanata et al., 2002; Chiarini et al., 2002). However, recent studies have demonstrated the capacity of PrP^{C} to bind molecules involved in signal transduction such as the neural cell adhesion molecule (N-CAM) and laminin. Binding of PrP^{C} to these molecules results in neurite outgrowth and neuronal proliferation and migration (Santuccione et al., 2005; Graner et al., 2000). A recent report indicated that PrP^{C}-null mice exhibited an impaired capacity of self-renewal of hematopoietic stem cell populations after serial transplantation in the bone marrow (Zhang et al., 2005). Furthermore, PrP^{C} was positively associated with proliferation of neural cells *in vivo* and differentiation of multipotent neural precursors *in vitro* (Steele et al., 2005). Since PrP^{C} is highly expressed in the nervous tissue, PrP^{C} mediation or activation of cell signaling involved in proliferation or differentiation suggests a role for PrP^{C} in the development of the nervous system; however, further evidence is required to elucidate this hypothesis.

The complex presentation of TSEs and the novel properties of the PrP^{Sc} have opened many questions yet to be answered. During the last years, research in prion biology has mainly focused on determination of the pathogenesis of TSEs and the development of diagnostic and therapeutic methods. However, further research in prion biology will continue to be the foundation for understanding the complex nature of TSEs and how these diseases can be controlled.

PRION BIOLOGY

PrP^{C} structure. The structure of PrP^{C} is highly conserved among species and throughout evolution, suggesting an important biological role (Riek et al., 1996; Gossert et al, 2005). Before post-translational modification, PrP^{C} is composed of a sequence of 253 amino acids with a slight variation between species depending on the number of octapeptide repeats (Prusiner and Scott, 1997). The octapeptide repeat region is an eight-amino acid repetitive motif composed of residues P(H/Q)GGG(-/G)WGQ and located in the N-terminal region of the protein (Moore et al., 2006). During protein maturation, PrP^{C} is exposed to several modifications in the rough endoplasmic reticulum (ER) including replacement of the peptide signal located between amino acids 232-253 with a glycophosphatidylinositol (GPI) anchor. Additionally, two asparagines at amino acids 181-197 are glycosylated and one disulfide bridge is added between two cysteine residues 179-214 (Prusiner, 1998; Harris, 2003). The mature protein is divided in two distinct regions: a flexible and essentially unstructured N-terminal region between amino acids 23-125 and a C-terminal region containing three alpha-helicoidal structures and a short beta-sheet motif between amino acids 126-231 (Abid and Soto, 2006). Asparagine glycosylation will determine variations in the biochemistry of the mature protein resulting in mono-, di- or un-glycosylated forms with molecular weights of ~28, 34 and 25 Kb, respectively (Russelakis-Carneiro et al., 2002; Priola and Vorberg, 2006). PrP^{C} is found as a mixture of these forms with variable proportions depending on the tissue and animal species (Russelakis-Carneiro et al., 2002).

The usual cellular location of PrP^{C} is attached by the GPI anchor to membrane domains rich in cholesterol and sphingolipids known as lipid raft (Martins et al., 2002, DeMarco et al., 2005). However, part of the pool of PrP^{C} can be internalized via clathrin-mediated endocytosis and accumulate inside the Golgi

apparatus. Furthermore, some of the internalized protein is recycled to the cytoplasmatic membrane by kinesin anterograde transport (Harris et al, 1996; Sunyach et al., 2003; Hachiya et al., 2004). It is uncommon for membrane-anchored proteins to be internalized by clathrin-mediated endocytosis since they are devoid of a cytoplasmic domain that usually recruits clathrin-coated pits. However, this process may be facilitated by unknown proteins that interact with PrP^{C}, enabling endocytosis of the molecule (Harris et al., 1996). Although the specific location for PrP^{C} conversion has not yet been determined, it is believed that formation of PrP^{Sc} occurs inside the cell and not in the extracellular suspension. PrP^{C} has been detected inside endosomes and lysosomes which potentially participate as conversion sites (Martins et al., 2002). The low pH maintained inside these organelles may facilitate PrP^{C} conversion as demonstrated by experiments in which acid pH favored aggregation of recombinant PrP^{C} into PrP^{Sc}-like structures (Bocharova et al., 2005). Alternatively, the pool of PrP^{C} that remains attached to the plasma membrane may find a favorable environment for conversion in lipid rafts that promote protein interaction and recruit accessory molecules (Hooper and Taylor, 2006).

Prnp gene structure. The prion gene (Prnp) has homologues in all vertebrates with conserved regions between mammals and birds (Premzl and Gamulin 2007). Prnp is located in chromosome 2 in mouse, 13 in bovine and 20 in human (Sparkes et al, 1986; Ryan and Womack, 1993). The 5' flanking region of bovine Prnp shows an 89% homology with the sheep and only 46-62% homology with the mouse, rat, hamster and human sequences (Inoue et al., 1997). Bovine, sheep, mouse and rat Prnp possess three exons with the protein coding sequence located entirely within the third exon (Fig. 1; Chesebro et al., 1985; Oesch et al., 1985; Inoue et al., 1996). Using chloramphenicol acetyltransferase (CAT) plasmids, the promoter region of the bovine gene was detected in the region between -88 and -30 relative to the transcription start site, similar to the rat promoter region (Inoue et al., 1997). Several regulatory regions including the promoter has been identified in the bovine Prnp with the major region of transcriptional control located upstream of the initiation site. The promoter sequence is rich in G+C features, lacks a TATA box and contains potential binding sites for Sp-1 transcriptional factors (Inoue et al., 1997). Several variables have been reported to influence Prnp expression under *in vitro* conditions including nerve growth factor (NGF), rate of prion infection and epigenetic changes (Graner et al., 2000; Bueler et al., 1993; Martins et al., 2002). However, *in vivo* factors such as the physiological status of the host may influence Prnp expression as well. A recent study reported that Prnp gene expression may be affected by heat shock proteins under stress conditions (Haigh et al., 2007).

Polymorphic variations in the coding sequence of the ovine Prnp gene have been reported to control the susceptibility to scrapie. The major mutations associated with susceptibility or resistance are located at codons 136 (A or V), 154 (R or H) and 171 (R, Q or H) (Clouscard et al., 1995; Hunter et al., 1996). Animals with PrP genotypes V136 R154Q171/VRQ, ARQ/VRQ and ARQ/ARQ are the most susceptible to scrapie, whereas homozygous or heterozygous AHQ and heterozygous ARR animals show only marginal susceptibility. ARR/ARR sheep are considered to be fully resistant (Hunter et al., 1996).

Prion Hypothesis. The prion hypothesis or protein-only hypothesis postulates that the agent responsible for prion propagation is originated by autocatalytic conversion of PrP^{C} into the pathogenic isoform (Griffith, 1967). Conversion into PrP^{Sc} involves a drastic alteration in the protein configuration as well as in the biochemical properties. Crystallography studies indicate that in normal state 47% of the PrP^{C} structure is composed of α-helix and only 3% β-sheet secondary configuration. In the conversion process, the β-sheet configuration is increased to 43-45 % and the α-helix structure is reduced to 17-30% (Pan et al., 1993; DeMarco et al., 2005, Fig.2). Therefore, the newly formed PrP^{Sc} structure is highly planar and stable showing strong resistance to temperature, pH, disinfectants and enzymatic degradation (Taylor, 2000).

Additional supporting evidence of the prion hypothesis has been originated from studies that reported resistance to prion infection in mice lacking the Prnp gene (Bueler et al., 1993). These knockout models not only evidenced the requirement of a host-encoded PrP^{C} protein for the infection process but also allowed a better understanding of the pathogenesis of TSEs. However, the most compelling evidence to probe this theory is yet to be reported. Some researchers claimed that a confirmatory experiment will consist in the *in vitro* conversion of PrP^{C} molecules into a pathogenic isoform with the capacity to induce TSE infection (Chesebro, 1998). Mutations induced to recombinant PrP^{C} have resulted in destabilization of the protein configuration and formation of a PrP^{Sc}-like molecule; however, this mutated agent was unable to induce prion disease (Chiesa et al, 1998; Bocharova et al., 2005). It is possible that additional factors including a transitional form of PrP and host-derived proteins or non-protein compounds (chaperones, glycosaminoglycans or short nucleic acids) are required to sustain *in vitro* generation of PrP^{Sc} (Castilla et al., 2005; Aguzzi et al., 2007). Hamster PrP^{C} was only converted to PrP^{Sc} when cell lysate was added to the reaction (Deleault et al., 2005). Moreover, mice co-expressing both human and mice PrP were resistant to prion replication as consequence of the interaction of mice PrP^{C} with an additional factor (termed protein X) that inhibited human PrP^{C} conversion (Telling et al., 1995). Recent

studies reported the *in vitro* generation of PrP^{Sc} molecules using a protein misfolding cyclic amplification technique (PMCA) that allows the repetitive amplification of the misfolding event (Castilla et al., 2005). Although, the newly formed PrP^{Sc} generated by this technique was able to infect wild-type Syrian hamsters, the use of crude brain homogenates to amplificate these molecules may have also resulted in the addition of different components responsible for the infection.

Two distinct models have been proposed to explain the autocatalytic conversion of PrP^{C}, a process not mediated by nucleic acids that challenge the central dogma of molecular biology. The template-assisted model postulates a thermodynamically stable conversion between both PrP isoforms (Fig. 3). PrP^{C} conversion is induced by PrP^{Sc} and is mediated by an intermediate and heterodimeric unit before the formation of a homodimeric PrP^{Sc}. The process is catalyzed by a yet unidentified protein X that has chaperone-like properties and facilitates aggregation of both isoforms (Cohen and Prusiner, 1998). Protein X promotes PrP^{C} conversion by binding a discontinuous epitope in the globular C terminal region of the protein (Kaneko et al., 1997). Newly formed PrP^{Sc} can eventually agglutinate and precipitate, forming amyloid precursors detected in some TSEs (Prusiner, 1990; Cohen et al., 1999). A second model termed nucleation-polymerization, proposes a similar thermodynamic equilibrium between both isoforms (Fig. 3). However, after PrP^{C} conversion, the model describes a highly unstable and transient PrP^{Sc} molecule that would be stabilized only by forming ordered aggregates. The stabilized oligomers act as nuclei to recruit monomeric PrP^{Sc} in a process that displaces the thermodynamic equilibrium and accelerates PrP^{Sc} formation (Caughey, 2001; Caughey and Lansburry, 2003).

Despite a bulk of evidence in support of the prion hypothesis, alternative models suggesting the participation of viral particles, virinos and small RNAs have also been proposed. Co-sedimentation of retroviral RNA with PrP^{Sc}, and purification of short RNA fragments from infectious fractions suggest the participation of nucleic acids as part of the infectious particle (Akowitz et al., 1990, 1994). The virino model describes the TSE agent as a proteinaceous structure containing nucleic acids with a virus-like conformation (Chesebro, 1998). The finding that prions have a variety of strains that correlates with a species-specific symptomology and histopathology in TSEs has also been used as evidence to support the virino model (Chesebro, 1998). However, the strain phenomenon can be explained by the variation in PrP^{Sc} protein secondary structure and not necessarily by the existence of viral strains containing nucleic acids (Prusiner, 1998). Furthermore, several biochemical properties displayed by scrapie agents indicate the absence of nucleic acids. The molecular weight (< 50 kDa), diameter (4 to 6 nm) and width (1 nm) of

the scrapie agent predicted a reduced core volume (14.1 m3) with insufficient capacity to store enough nucleic acids to encode a viral protein (Prusiner, 1982). Additionally, the prion agent has shown high resistance to UV radiation (42,000 J/m2) and nuclease digestion.

PrP^C Function. Despite intense investigation during recent years, the function of PrP^C remains enigmatic. Some studies have suggested a cellular protective role of PrP^C against oxidative stress. Experiments have showed that neurons obtained from Prnp knockout mice and cultured *in vitro* display higher susceptibility to oxidative agents such as hydrogen peroxide, xanthine oxidase and copper ions compared to wild-type neurons (Brown et al., 2002). Moreover, brain tissue collected from Prnp knockout mice exhibited biochemical changes including increased levels of protein carbonyls and lipid peroxidation products, which are indicative of oxidative stress (Wong et al., 2001). An extensive body of evidence has accumulated suggesting the binding of Cu+2 ions to the PrP^C octapeptide repeat region. Copper (Cu+2) is an essential element that participates as an enzymatic cofactor in the biochemical pathways of all aerobic organisms. However, Cu +2 can also catalyze the formation of reactive oxygen species such as the hydroxyl radical (Martins et al., 2001). The binding of Cu +2 to PrP^C may limit the capacity to catalyze the formation of such toxic oxidative radicals (Martin et al., 2001; Vassallo and Herms, 2003). Some researchers have questioned this antioxidant property due to the super-physiological concentrations of Cu +2 required to activate this process (Westergard et al., 2007). Alternatively, PrP^C may modulate the activity of the Cu/Zn superoxide dismutase (Cu/Zn SOD) enzyme that showed cellular protective function against oxidative stress (Wechslberger et al., 2002; Brown et al., 2001). Analyses in brain tissue obtained from Prnp knockout mice have shown only 10-50% of the normal Cu +2 loading capacity and Cu/Zn SOD enzymatic activity. In contrast, the enzymatic activity and copper loading of Cu/Zn SOD was increased in mice over-expressing PrP^C (Brown et al., 1997).

Several lines of evidence have proposed a cytoprotective role of PrP^C against internal or environmental stresses that initiate apoptosis. This anti-apoptotic potential is primarily based on the capacity of PrP^C to inhibit the action of the apoptotic protein Bax (Bounhar et al., 2001). PrP^C-induced blocking of Bax may be direct, for example by inhibiting its mitochondrial translocation, conformational change, or oligomerization. Alternatively, PrP^C may act upstream of Bax, affecting the activity of BH3, Bcl-2 or Bcl-X_L, or downstream, suppressing the effects of Bax in the release of cytochrome c or activation of Apaf-1 and caspases (Roucou et al., 2005; Westergard et al, 2007). PrP^C could also affect the calcium Bax-mediated secretory pathway in the ER. Other studies have reported a close similarity between the

homologous domain of the anti-apoptotic protein Bcl-2 and the PrP^C octapeptide region. This analogy in the protein structure may allow PrP^C to mimic Bcl-2 function and induce cell survival (Roucou et al., 2005; Westergard et al., 2007).

In addition to the cytoprotective role, PrP^C has been also implicated as a cell proliferation and differentiation factor. Recently it was reported that PrP^C-null mice exhibited an impaired capacity of self-renewal of hematopoietic stem cell populations after serial transplantation in the bone marrow (Zhang et al., 2005). The potential mitogenic capacity has also been supported by studies showing a decrease in T lymphocyte proliferation in mice devoid of PrP^C (Bainbridge et al., 2005). The role of PrP^C in differentiation was suggested by high levels of expression in cells that ceased proliferation and became differentiated into neurons during early stages of mice embryogenesis (Tremblay et al., 2007). In a recent report, PrP^C displayed a positive effect in the proliferation of neural precursor cells and showed a positive correlation with neuronal differentiation (Steele et al., 2006). In this study, mice over-expressing PrP^C exhibited an increased multipotent neural precursor proliferation in neurogenic regions of the brain. In contrast, ablation of PrP^C resulted in lower neural precursor differentiation compared to wild-type controls.

The capacity of PrP^C to bind to several different molecules has opened the idea that this protein may exert its function in association with a ligand. The location of PrP^C in the extracytoplasmic face of the lipid bilayer restricts the interaction to transmembrane and secreted proteins. Transmembrane variants of PrP^C could potentially interact with cytoplasmic partners; however, these forms are normally present in low amounts in the absence of predisposing mutations in the PrP^C molecule (Stewart et al., 2001). The membrane association and the interaction with ligands suggest the hypothesis that PrP^C may activate transmembrane signaling processes associated to neuronal survival, neurite outgrowth, and neurotoxicity. The stress inducible protein STI-1 has been implicated as a co-chaperone molecule that form part of the heat shock protein (HSP) macromolecular complexes Hsp70 and Hsp 90 (Zanata et al., 2002). The interaction between PrP^C and STI-1 showed high affinity and specificity resulting in neuroprotective functions through the mediators of the cAMP dependent protein kinase (AMPc/PKA) pathway (Zanata et al., 2002; Chiarini et al., 2002). Additionally, interaction with STI-1 induced neuritogenesis through the MAPK pathway as a parallel effect to neuroprotection (Lopes et al., 2005). Neuronal growth has also been observed during PrP^C interaction with the neuron cell adhesion protein N-CAM after its recruitment from lipid rafts and the activation of Fyn kinase (Santuccione et al., 2005). Treatment of cultured neurons

with recombinant PrP^C enhances neurite outgrowth and neuronal survival, concomitant with activation of several kinases, including fyn, PKC, PKA, PI-3 kinase/Akt and ERK (Kanaani et al, 2005; Santuccione et al., 2005).

Laminin is an important glycoprotein of the basal membrane and plays an important role in neuronal proliferation, growth and migration (Westergard et al., 2007). Studies have showed that PrP^C binding to the receptor of laminin is specific and saturable and results in dendritic extension, neuronal migration, axonomic regeneration and suppression of cell death induced by kainic acid injection (Graner et al., 2000, Martin et al., 2001). PrP^C can also interact with the cytoplasmic protein laminin receptor precursor (LRP), which may serve as an endocytic receptor for cellular uptake of both PrP^C and PrP^{Sc} (Gauczynski et al., 2006).

Although, PrP^C has been reported as a cellular anti-apoptotic factor, some experiments have suggested its involvement as neurotoxin effects. Synthetic peptide PrP 106-126 has been used to mimic the effect of PrP^{Sc} on cultured cells (Selvaggini et al., 1993). Incubation with this peptide showed toxic effects on cultured neurons and neuronal cell lines, but only in those that express PrP^C (Forloni et al., 1993; Brown et al., 1994a). These studies suggest that PrP^C may mediate PrP^{Sc} pathogenic action through a signaling pathway.

PrP^C role in TSE pathogenesis. The pathogenesis of TSEs including the mechanism of neuronal degeneration has not been completely elucidated. It is now becoming clear, however, that PrP^{Sc} kills neurons by virtue of its ability to perturb the normal and physiological activities of PrP^C (Westergard et al., 2007). The presence of PrP^{Sc} alone in neuronal cells may result in toxic effects by several mechanisms including blocking axonal transport, interfering with synaptic function, or triggering apoptotic pathways (Westergard et al., 2007). Alternatively, the potential association between PrP^{Sc} and PrP^C during the pathogenic process may result in the loss of PrP^C anti-apoptotic activity, resulting in neuronal death. Evidence that argues against this theory is based on the small phenotypic effect and lack of any features of TSEs observed after ablation of PrP^C either prenatally or postnatally (Bueler et al., 1992; Mallucci et al., 2002). However, it is possible that neurodegeneration may be consequence of both loss and gain in function, by loss of the cytoprotective activity of PrP^C that may become essential in the disease state due to cellular or organism stress.

Another hypothesis for the TSE-pathogenic effect postulates the alteration or subversion of the normal PrP^{C} neuroprotective function. PrP^{C} may act as a membrane-anchored signal transduction that transmits the PrP^{Sc} toxic effect (Chesebro et al., 2005). Neurons obtained from PrP^{C} knockout mice and cultured in vitro were resistant to apoptosis induced by exposure to the synthetic peptide PrP 106-126 (Brown et al., 1994a). This phenomenon may be the consequence of a PrP^{Sc}-induced aggregation of cell surface PrP^{C} that generate a neurotoxic rather than a neuroprotective signal. Cross-linking of PrP^{C} using anti-PrP antibodies resulted in apoptosis of neurons in vivo (Solforosi et al., 2004). Alternatively, amino acid sequences (PrPΔ 105-125) in the PrP^{C} structure have been reported to have receptor activity with cytoprotective functions. These receptor sequences may be blocked by PrP^{Sc} resulting in the delivery of a neurotoxic signal (Li et al., 2007).

BOVINE SPONGIFORM ENCEPHALOPATHY

Epidemiology. Bovine spongiform encephalopathy (BSE) was reported for the first time in the UK in 1986 (Wells et al., 1987). The disease achieved epidemic proportions during the 1990s with more than 182,000 cases worldwide recorded between November of that year and July of 2008. BSE has been detected in 24 countries worldwide showing a decreasing trend in the number of cases since 2003 (2167), 2004 (879), 2005 (561), 2006 (201), 2007 (169) (OIE, 2008).

The origin of BSE has not been clarified but several theories have been formulated. One of these theories postulates the inter-species transmission from scrapie-infected sheep to cattle. Cows became infected after consumption of protein concentrate made from carcasses of sheep contaminated with scrapie. Scrapie has affected sheep for 200 years, is endemic in the UK and is present in a number of countries worldwide (Schwartz, 2003). Although contamination of feed with infected ovine carcasses is possible; experimental transmission of scrapie agent to the bovine has proved difficult, making this hypothesis improbable (Cutlip et al., 1994). A second theory involves the spontaneous destabilization and conversion of PrP^{C} into PrP^{Sc}. Spontaneous or atypical BSE cases have been reported recently, and animals affected by this disease may have served as a source of protein supplements for cattle feed thus spreading the disease in

this manner (Capiobianco et al., 2007). However, one of the most controversial theories to explain the contamination of animal concentrate is the human origin of BSE. Funeral rituals in areas of India involve the cremation of cadavers and the disposal of human remains to rivers. Some of these remains may have been collected by "bonepickers" and used to elaborate bone meal that eventually might have been contaminated with human TSE. By this process, contaminated bone and meat meal exported from the India to Europe and used for animal consumption may have served as a source of BSE transmission (Colchester and Colchester, 2005).

Causal agent. Detection of PrP^{Sc} is highly correlated with the pathology and diagnosis of BSE. However, the sole presence of PrP^{Sc} as the pathogenic agent of TSEs has been debated. Mice infected with scrapie agent developed lesions in areas of the brain that showed low levels of PrP^{Sc} (Parchi and Gambetti, 1995). Moreover, no brain damage was reported in transgenic mice over-expressing PrP^{Sc} (Chiesa and Harris, 2001). These reports suggest that cellular damage is a consequence not exclusively of PrP^{Sc} but also require the participation of additional cofactors including a transitional form of PrP and host-derived proteins or non-protein compounds (glycosaminoglycans or short nucleic acids; Aguzzi et al., 2007). In this scenario, PrP^{C} may play an important role as a mediator in PrP^{Sc} pathogenesis. Mice infected with PrP^{Sc} in which Prnp gene was knocked out from the beginning or during the infectious process showed that PrP^{C} expression is required for cellular damage (Brandner et al., 1996; Mallucci et al., 2003).

Pathogenesis. There are several origins of prion disease pathogenesis that remain to be understood. It is believed that the TSE agent is passed under natural conditions from one animal to the other through oral ingestion. Indeed, the transmission of the PrP^{Sc} agent by the oral pathway has great relevance in some TSEs (e.g. variant Creutzfeldt-Jakob disease, Kuru and BSE). This is not the case in spontaneous forms of this disease in which genetic predisposition seems to be the causative factor (e.g. spontaneous Creutzfeldt-Jakob). Although oral ingestion of the agent is the most commonly known form of contamination, other ways of infection cannot be overlooked, such as injection of contaminated products, skin injuries or iatrogenic ways (Mabbot and MacPherson, 2006). The transport of PrP^{Sc} through the intestinal mucosa is mediated by microfold cells (M cells) located within the epithelium villus and follicle-associated epithelium (FAE) of the Peyer's patches, through the process of transcytosis (Heppner et al., 2001). Under physiological conditions, M cells sample contents of the intestinal lumen and present these antigens to the host immune system for immunomodelation. Some pathogenic microorganisms and potentially PrP^{Sc} can exploit M cells transcytosis to gain entry into mucosal tissues (Neutra et al., 1996).

The transport of TSE agents across the intestinal epithelium; however, might not be entirely mediated by M-cell-transcytosis. PrP^{Sc}-proteon complexes originated from CJD brain homogenate can be endocytosed by intestinal epithelial cells (Caco-2 cells) and transcytosed in vesicular structures by a ferritin-dependent mechanism (Mishra et al., 2004).

After transport through the intestinal mucosa, PrP^{Sc} particles are captured by several types of cells including macrophages, lymphocytes and dendritic cells (DCs) and presented to follicular dendritic cells (FDCs) in the lamina propia. The precise involvement of macrophages in TSE pathogenesis is uncertain but these cells may mediate the transport and also the impairment of PrP^{Sc} accumulation. A recent *in vitro* study showed that macrophage depletion resulted in an earlier increase in PrP^{Sc} accumulation in the lymphoid tissue (Maignien et al, 2005). Lymphocytes are also situated intraepithelial, but are unlikely to be involved in transporting PrP^{Sc} as they do not acquire measurable levels of this agent following intra-intestinal exposure (Huang et al., 2002). DCs are a distinct lineage from stromal derived FDCs that sample antigens in the periphery and deliver them to lymphoid tissues to initiate an immune response (Shortman and Liu, 2002). The location of DCs beneath intraepithelial M cells and their capacity to acquire intestinal antigens by inserting their dendrites between tight junctions (independently from M cells) make these cells good candidates to transport PrP^{Sc} to lymphoid tissues (Beekes and McBride, 2000).

Analysis of the distribution of the PrP^{Sc} within the nervous system of orally inoculated rodents indicates that the agent subsequently spreads from the gut-associated lymphoid tissue (GALT) to the CNS through the enteric nervous system in a process known as neuroinvasion (Beekes and McBride, 2000). The enteric nervous system is an important component of the autonomic nervous system and regulates intestinal motility and secretions through stimuli from sympathetic and parasympathetic nerves. PrP^{Sc} reaches the CNS by spreading in a retrograde direction along efferent fibers of both sympathetic and parasympathetic nerves until they contact the spinal cord. It is not understood how PrP^{Sc} initially spread from the FDCs to the peripheral nervous system. This process may be mediated by mobile intermediate cells or exosomes derived from FDCs, DCs or macrophages that transport PrP^{Sc} particles from FDCs to the peripheral nervous system (Mabbot and MacPherson, 2006). Potential neuroinvasion through the blood-brain barrier has also been suggested; however, the localization of PrP^{Sc} deposits and blood vessels in brains of patients with vCJD does not reflect a haematogenous pattern (Armstrong et al., 2003; Mabbot y MacPherson 2006).

Histopathological changes. In general, histopathological changes observed in TSEs are associated with spongiform degeneration, vacuolization, astrogliosis and PrP^{Sc} deposition (Budka, 1995, MacDonald et al., 1996). However, astrogliosis and neuronal loss are not evident in BSE compared to other TSEs. The presence of amyloid plaques are rare in classic BSE and are mostly found in the thalamus. In contrast, atypical BSE or Bovine Amyloidotic Spongiform Encephalopathy (BASE) has been characterized by the presence of large plaques mainly in the white matter. The molecular signature of BASE also differs from BSE and resembles CJD (Casalone et al., 2004). Several theories have been proposed to explain BASE presentation including spontaneous occurrence of TSE in animals as in sporadic CJD. Classic BSE is also characterized by spongiosis and vacuolization of the neuropil and neuronal bodies through simple or multiple vacuoles in the neuronal perikarya (Wells et al., 1989). Neural tissues most consistently and severely affected are the solitary tract nucleus, the spinal tract nucleus of the trigeminal nerve, and the central gray matter of the midbrain (Wells et al., 1989). Neuropil vacuolization of the target nuclei is considered to be pathognomic in BSE. Intraneuronal vacuolation is also observed in BSE, but this feature alone in the absence of neuropil vacuolation is not confirmatory. Vacuolated neurons particularly in certain locations such as the red nucleus may be an incidental finding in cattle (Gavier-Widen et al., 2001). Immunohistochemical analysis consistently reveals PrP^{Sc} accumulation in the brain, with distribution similar to but often more widespread than neuropil vacuolation. Patterns of PrP^{Sc} deposition in the brain include intraneuronal, perineuronal, linear, fine punctuate and coarse particulate (Wells and Wilesmith, 1995). PrP^{Sc} cannot readily be detected in tissues outside bovine CNS; however, limited involvement of the Peyer's patches has been documented in experimentally induced and naturally acquired cases of BSE (Terry et al., 2003).

Diagnosis. All diagnostic methods currently available require post-mortem confirmation. Despite characteristic clinical signs, diagnosis of BSE cannot rely solely on the clinical course and requires histopathological analysis. Initial histopathological diagnosis is based on vacuolar changes in the brain, observation of florid plaques, astrogliosis and neuronal loss. However, presentation of cases with no evident or ambiguous histopathological changes requires confirmation through more specific and sensitive methods such as immunohistochemistry, western blot and/or ELISA (Gavier-Widen et al., 2005, OIE, 2004). Given the pivotal role played by PrP^{Sc} in TSE pathogenesis, diagnostic methods rely on PrP^{Sc} detection by specific antibodies and partial proteinase K digestion that allows differentiation between both PrP isoforms. In recent years, some antibodies have claimed to differentiate between PrP^{C} and PrP^{Sc};

however, none of these molecules have proved suitable for direct identification of PrP^{Sc} (Korth et al., 1997; Curin et al., 2004; Zou et al., 2004).

Consistent early accumulation of PrP^{Sc} and vacuolar lesions in the medulla oblongata at the level of the obex (brainstem) make this area of the brain an optimal site for the post-mortem diagnosis of BSE. An appropriate sample for BSE diagnosis should include the solitary and trigeminal tract nuclei (Jeffrey and Gonzales, 2004). Brainstem sample may be conveniently obtained by introducing a commercially available, long, spoon-shaped metal or disposable instrument with cutting edges through the foramen magnum to facilitate sampling of the brainstem. Alternatively, the sample could be obtained by dismantling the calvarium (e.g. when retrieving the whole brain for rabies diagnosis). The brainstem sample should be promptly refrigerated (at 4°C not frozen) or fixed in 10% formaldehyde until shipment to the diagnostic laboratory to avoid post-mortem decomposition (Gavier-Widen 2005, USDA, 2006).

Several diagnostic methods based on immunological techniques have been validated and officially accepted for BSE. Currently, the BioRad diagnostic immunoassay is used as a rapid test for BSE detection. Advantages of this method include easy manipulation, fast results (24 h), high sensitivity, and detection of PrPSc infection during preclinical stages (Soto, 2006). This immunoassay is based on the capture of PrP^{Sc} present in the sample by antibodies attached to a microtitulation plate. Incubation of captured PrP^{Sc} by anti-PrP antibodies allows secondary antibody detection and visualization with a colorimetric reaction. However, high presentation of false positive results by this method recommends the use of confirmatory techniques (USDA, 2005). High specificity, visualization of the spongiform lesions and PrP^{Sc}-specific immunostaining make the immunohistochemistry a primary choice for confirmatory diagnosis of BSE. This method requires formalin-fixation and paraffin-embedding of the samples. Tissue is sectioned and mounted in glass slides. Mounted tissue sections are exposed to proteinase K digestion and epitope unmasking through immersion in citric buffer. PrPSc is detected by incubation with anti-PrP antibodies followed by secondary antibodies associated to horseperoxidase staining or fluorescence dyes (OIE, 2004). Samples with moderate levels of decomposition may not be suitable for the immunohistochemistry method but may be used for western blot analysis. This method has similar specificity compared to immunohistochemistry but does not allow histological analysis. Currently, this technique can be performed in a short period of time with high sensitivity. Tissue sample lysates are treated with proteinase K for PrP^{C} digestion. Total protein contained in samples are separated by electrophoresis in 12% SDS polyacrylamide gels and blotted into nitrocellulose or polyvinylidene

fluoride (PVDF) membranes. PrP^{Sc} is specifically detected by incubation with anti-PrP antibodies followed by secondary antibodies.

The requirement of a pre-mortem diagnostic method is desirable considering the inability to apply conventional methods for nucleic acids or antiserum detection such as PCR or ELISA. During the last years, substantial efforts have been applied in the development of PrP^{Sc}-specific antibodies for the potential diagnostic of infectivity in fluids and tissues. Despite the significant differences in secondary structure between both PrP isoforms, the development of such antibodies is still incomplete (Demart et al., 1999, Groschup et al., 1997, Kascsak et al., 1997, Curin et al., 2004). PrP^{Sc} has been detected in the blood of infected animals, which represents a potential strategy for early diagnosis of TSEs (Castilla et al., 2005). However, levels of PrP^{Sc} in blood are very low making even highly sensitive techniques such as immunocapillary electrophoresis unable to detect the agent (Schmerr and Jenny., 1998). One important step in the development of such a diagnostic tool was the recently reported development of a protein misfolding cyclic amplification technique (PMCA). This method was able to simulate PrP^{Sc} replication in a test tube and increase the detection threshold of this protein by 10 million times (Castilla et al., 2005). This new technology enables an efficient, specific and rapid detection of prions offering great promise for developing a noninvasive early diagnosis of TSEs.

Conclusions. The complex nature of the prion biology has intrigued the scientific community for more than 70 years and yet there are many questions to be answered. The establishment of the controversial prion hypothesis opened a new perspective in protein biology that involved the participation of these molecules in diseases as pathogenic and infectious agents. Not only TSEs, but other neurodegenerative diseases such as Alzheimer's have showed to be the consequence of the misfolding and deposition of host-encoded proteins with severe neuropathology. Currently, there are no ways to cure, treat or immunize against these diseases, and the consequences for public health and economic costs have proven to be tremendous. However, important advances during the last years in the evaluation of prion biology have allowed a better understanding of the pathogenesis of this disease and have opened new opportunities for treatment.

One of the most intriguing aspects in prion biology is the still enigmatic physiological function of the PrP^{C}. This mysterious protein has been implicated in several biological processes including cellular

protection against oxidative stress and apoptosis, cell-to-cell adhesion, cellular proliferation and differentiation. Recently, important evidence has been reported supporting the idea that PrP^C is involved in signaling pathways associated with cellular proliferation and differentiation. In the present work, we first describe the analyses performed to characterize the expression of PrP^C in several somatic and reproductive tissues. These analyses suggest the participation of PrP^C in various physiological processes involving cellular differentiation and tissue development. Therefore, in the final two chapters we describe the efforts to elucidate the potential participation of PrP^C in cellular differentiation by the utilization of developmental models including embryos and embryonic stem cells.

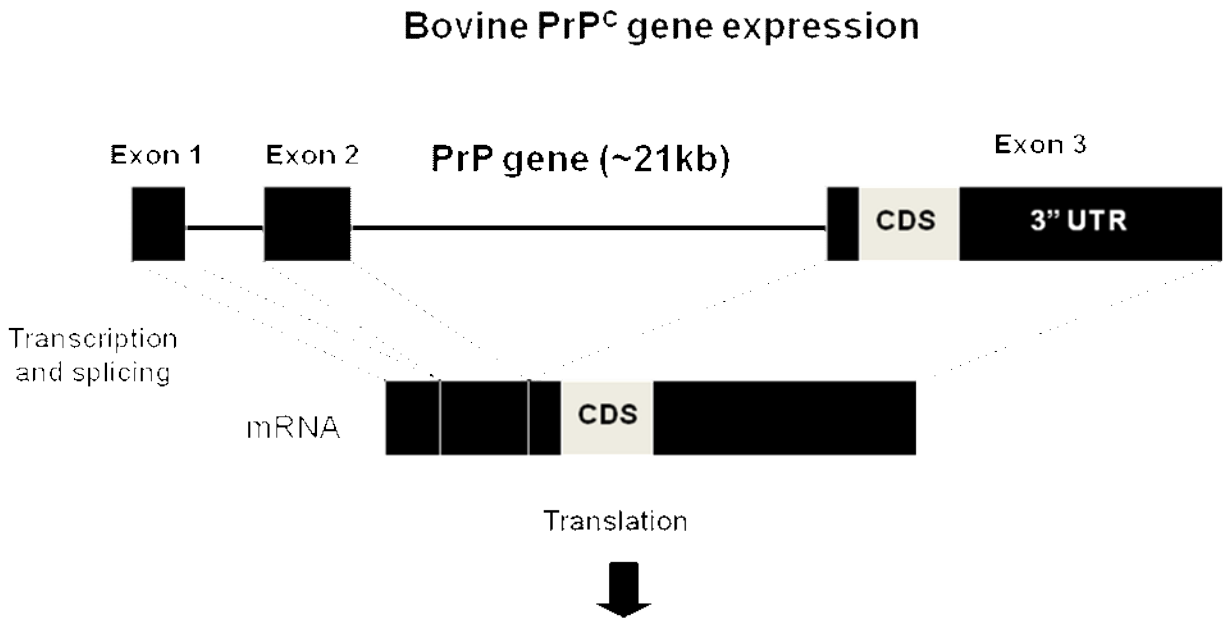

Figure 1. Structure of the Prnp gene and mRNA. The Prnp gene size is aproximate 21 kb. After transcription and splicing, the mRNA molecule is formed by the exons 1, 2 and 3. Exon 3 carries the coding sequence that encodes the PrP^C protein after translation.

PrP isoforms structure

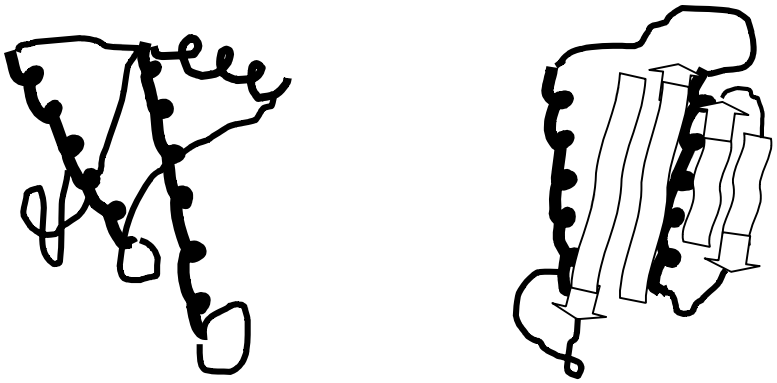

Figure 2. Structure of PrP^{C} and PrP^{Sc} isoforms. PrP^{C} and PrP^{Sc} have important differences in secondary protein configuration. Structure of PrP^{C} is conformed by a high α-helicoidal (47%) and low β-sheet configuration (3%). In contrast, PrP^{Sc} is characterized by high β-sheet (43-45%) and low α-helicoidal (17-30%) proportion.

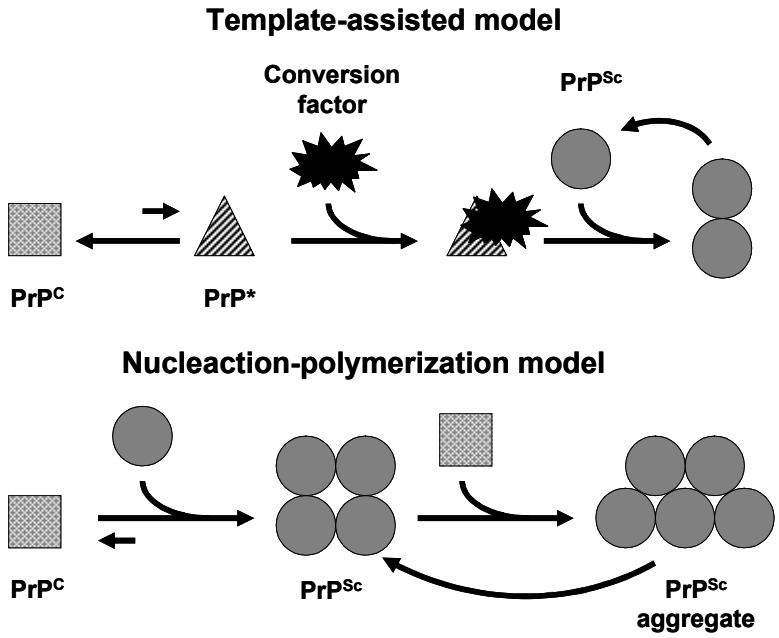

Figure 3. Models for conversion between PrP^{C} and PrP^{Sc}. The template assisted model includes the participation of a conversion factor that mediates PrP conversion. The nucleation-polymerization model describes a PrP^{Sc} heterodimer intermediate complex that induces aggregation and conversion. Both models propose a thermodynamic equilibrium for PrP^{C}-PrP^{Sc} conversion (Soto, 2006).

LITERATURE CITED

Abid K, Soto C. 2006. The intriguing prion disorders. Cell Mol Life Sci 63, 2342-2351.

Aguzzi A, Heikenwalder M, Polymenidou M. 2007. Insights into prion strains and neurotoxicity. Nat Rev Mol Cell Biol 8, 552-561.

Akowitz A, Sklaviadis T, Manuelidis EE, Manuelidis L. 1990. Nuclease-resistant polyadenylated RNAs of significant size are detected by PCR in highly purified Creutzfeldt-Jakob disease preparations. Microb Pathog 9, 33-45.

Akowitz A, Sklaviadis T, Manuelidis L. 1994. Endogenous viral complexes with long RNA cosediment with the agent of Creutzfeldt-Jakob disease. Nucleic Acids Res. 22, 1101-1107.

Alper T, Haig DA, Clarke MC. 1966. The exceptionally small size of the scrapie agent. Biochem Res Commun 22, 278-284.

Armstrong RA, Cairns NJ, Ironside JW, Lantos PL. 2003. Does the neuropathology of human patients with variant Creutzfeldt-Jakob disease reflect haematogenous spread of the disease? Neurosci Lett 348, 37-40.

Bainbridge J, Walker KB. 2005 The normal cellular form of prion protein modulates T cell responses. Immunol Lett 15, 147-150.

Beekes M, McBride PA. 2000. Early accumulation of pathological PrP in the enteric nervous system and gut-associated lymphoid tissue of hamsters orally infected with scrapie. Neurosci Lett 278, 181-184.

Berg LJ. 1994. Insights into the role of the immune system in prion diseases. Proc Natl Acad Sci USA 18, 91, 429-432.

Bocharova OV, Breyedo L, Parfenov AS, Salnikov VV and Baskakov IV. 2005. In vitro conversion of full-length mammalian prion protein produces amyloid form with physical properties of PrP (Sc). J Mol Biol 346, 645-659.

Bounhar Y, Zhang Y, Goodyer CG, LeBlanc A. 2001. Prion protein protects human neurons against Bax-mediated apoptosis. J Biol Chem 19, 39145-39149.

Brandner S, Isenmann S, Raeber A, Fischer M, Sailer A, Kobayashi Y, Marino S, Weissmann C, Aguzzi A. 1996. Normal host prion protein necessary for scrapie-induced neurotoxicity. Nature 379, 339-343.

Brown DR, Herms J, Kretzschmar HA. 1994. Mouse cortical cells lacking cellular PrP survive in culture with a neurotoxic PrP fragment. NeuroReport 5, 2057-2060.

Brown DR, Schulzschaeffer WJ, Schmidt B, Kretzschmar HA. 1997. Prion protein-deficient cells show altered response to oxidative stress due to decreased SOD-1 activity. Exp Neurol 146, 104-112.

Brown DR. 2001. Prion and prejudice: normal protein and the synapse. Trends Neurosci 24, 85-90.

Brown DR, Nicholas RS, Canevari L. 2002. Lack of prion protein expression results in a neuronal phenotype sensitive to stress. J Neurosci Res 67, 211-224.

Budka H, Aguzzi A, Brown P, Brucher JM, Bugiani O, Gullotta F, Haltia M, Hauw JJ, Ironside JW, Jellinger K. 1995. Neuropathological diagnostic criteria for Creutzfeldt-Jakob disease (CJD) and other human spongiform encephalopathies (prion diseases). Brain Pathol 5, 459-466.

Bueler H, Fischer M, Lang Y, Fluethmann H, Lipp H-P, DeArmond SJ, Prusiner SB, Aguet M, Wissmann C. 1992. Normal development and behavior of mice lacking the neuronal cell-surface PrP protein. Nature 356, 577-582.

Bueler H, Aguzzi A, Sailer A, Greiner RA, Autenried P, Aguet M and Weissman C. 1993. Mice devoid of PrP are resistant to scrapie. Cell 73, 1339-1347.

Casalone C, Zanusso G, Acutis P, Ferrari S, Capucci L, Tagliavini F, Monaco S, Caramelli M. 2004. Identification of a second bovine amyloidotic spongiform encephalopathy: molecular similarities with sporadic Creutzfeldt-Jakob disease. Proc Natl Acad Sci USA 101, 3065-3070.

Capobianco R, Casalone C, Suardi S, Mangieri M, Miccolo C, Limido L, Catania M, Rossi G, Di Fede G, Giaccone G, Bruzzone MG, Minati L, Corona C, Acutis P, Gelmetti D, Lombardi G, Groschup MH, Buschmann A, Zanusso G, Monaco S, Caramelli M, Tagliavini F. 2007. Conversion of the BASE prion strain into the BSE strain: the origin of BSE? PloS Pathog 3, e31.

Castilla J, Saa P, Hetz C, Soto C. 2005. In vitro generation of infectious scrapie prions. Cell 121, 195-206.

Caughey B. 2001. Interactions between prion protein isoforms: the kiss of death? Trends Biochem Sci 26, 235-242.

Caughey B, Lansbury PT. 2003. Protofibrils, pores, fibrils, and neurodegeneration: separating the responsible protein aggregates from the innocent bystanders. Annu Rev Neurosci 26, 267-298.

Chesebro B, Race R, Wehrly K, Nishio J, Bloom M, Lechner D, Bergstrom S, Robbins K, Mayer L, Keith JM, Garon C, Haase A. 1985. Identification of scrapie prion protein-specific mRNA in scrapie-infected and uninfected brain. 315, 331-333

Chesebro B. 1998. BSE and prions: uncertainties about the agent. Science 279, 42-43.

Chesebro B, Trifilo M, Race R, Meade-White K, Teng C, LaCasse R, Raymond L, Favara C, Baron G, Priola S, Caughey B, Masliah M, Oldstone. 2005. Anchorless prion protein results in infectious amyloid disease without clinical scrapie. Science 308, 1435-1439.

Chiesa R, Harris DA. 2001. Prion diseases: what is the neurotoxic molecule? Neurobiol Dis 8, 743-763.

Chiarini L, Freitas A, Zanata S, Brentani R, Martins V, Linden R. 2002. Cellular prion protein transduces neuroprotective signals. EMBO J 21, 3317-3326.

Chiesa R, Piccardo P, Ghetti B and Harris DA. 1998. Neurological illness in transgenic mice expressing a prion protein with an insertional mutation. Neuron 21, 1339-1351.

Clouscard C, Beaudry P, Elsen JM, Milan D, Dussaucy M, Bounneau C, Schelcher F, Chatelain J, Launay JM, Laplanche JL. 1995. Different allelic effects of the codons 136 and 171 of the protein gene in sheep with natural scrapie. Journal of General Virology, 76, 2097-2101.

Coffey B, Mintert J, Fox S, Schroeder T, Valentin L. 2005. The economic impact of BSE on the US beef industry: product value losses, regulatory costs, and consumer reactions. In: Kansas State University.

Cohen FE, Prusiner SB. 1998. Pathologic conformations of prion proteins. Annu Rev Biochem 67, 793-819.

Cohen FE. 1999. Protein misfolding and prion diseases. J Mol Biol 293, 313-320.

Colchester AC, Colchester NT. 2005. The origin of bovine spongiform encephalopathy: the human prion disease hypothesis. Lancet 366, 856-861.

Collee JG, Bradley R, Liberski PP. 2006. Variant CJD (vCJD) and bovine spongiform encephalopathy (BSE): 10 and 20 years on: part 2. Folia Neuropathol 44, 102-110.

Collinge J. 2001. Prion diseases of humans and animals: their causes and molecular basis. Annu Rev Neurosci 24, 519-550.

Cullie J, Chele PL. 1938. La tremblante du mouton est bien inoculable C. R. Acad Sci (Paris) 206, 78-79.

Curin Serbec V, Bresjanac M, Popovic M, Pretnar Hartman K, Galvani V, Rupreht R, Cernilec M, Vranac T, Hafner I, Jerala R. 2004. Monoclonal antibody against a peptide of human prion protein discriminates between Creutzfeldt-Jacob's disease-affected and normal brain tissue. J Biol Chem 279, 3694-3698.

Cutlip RC, Miller JM, Race RE, Jenny AL, Katz JB, Lehmkuhl HD, DeBey HM, Robinson MM. 1994. Intracerebral transmission of scrapie to cattle. J Infect Dis 169, 814-820

Deleault NR, Geoghegan JC, Nishina K, Kascsak R, Williamson RA, Supattapone S. 2005. Protease-resistant prion protein amplification reconstituted with partially purified substrates and synthetic polyanions. J Biol Chem 280, 26873-26879.

DeMarco ML, Daggett V. 2005. Local environmental effects on the structure of the prion protein. C R Biol 328, 847-862.

Demart S, Fournier JG, Creminon C, Frobert Y, Lamoury F, Marce D, Lasmezas C, Dormont D, Grassi J, Deslys JP. 1999. New insights into abnormal prion protein using monoclonal antibodies. Biochem Biophys Res Commun 265, 652-657.

Forloni G, Angeretti N, Chiesa R, Monzani E, Salmona M, Bugiani O, Tagliavini F. 1993. Neurotoxicity of a prion protein fragment. Nature 362, 543-546.

Gajdusek DC, Gibbs CJ Jr, Alpers M. 1966. Experimental transmission of a kuru-like syndrome to chimpanzees. Nature 209, 794-96.

Gauczynski S, Nikles D, El-Gogo S, Papy-Garcia D, Rey C, Alban S, Barritault D, Lasmezas CI, Weiss S. 2006. The 37-kDa/67-kDa laminin receptor acts as a receptor for infectious prions and is inhibited by polysulfated glycanes. J Infect Dis 194, 702-709.

Gavier-Widen D, Wells GA, Simmons MM, Wilesmith JW, Ryan J. 2001. Histological observations on the brains of symptomless 7-year-old cattle. J Comp Pathol 124, 52-59

Gordon WS. 1946. Advances in Veterinary Research. Vet Rec 58, 516.

Gossert AD, Bonjour S, Lysek DA, Fiorito F, Wuthrich K. 2005. Prion protein NMR structures of elk and of mouse/elk hybrids. Proc Natl Acad Sci USA 102, 646-650.

Graner E, Mercandante AF, Zanata SM, Orestes VF, Cabral ALB, Veiga SS, Juliano MA, Roesler R, Walz R, Minetti A, Izquierdo I, Martins VR, Bretani RR. (2000) Cellular prion protein binds laminin and mediates neuritogenesis. Mol Brain Res 76, 85-92.

Griffith JS. 1967. Self-replication and scrapie. Nature, 215, 1043-1044.

Groschup MH, Harmeyer S, Pfaff E. 1997. Antigenic features of prion proteins of sheep and other mammalian species. J Immunol Methods 207, 89-101.

Hachiya NS, Watanabe K, Yamada M, Sakasegawa Y, Kaneko K. 2004. Anterograde and retrograde intracellular trafficking of fluorescent cellular prion protein. Biochem Biophys Res Comm 315, 802-807.

Hadlow WJ. 1959. Scrapie and kuru. Lancet 2, 289-290.

Haigh CL, Wright JA, Brown DR. 2007. Regulation of prion protein expression by noncoding regions of the Prnp gene. J Mol Biol 368, 915-927.

Harris DA, Gorodinsky A, Lehmann S, Moulder K, Shyng SL. 1996. Cell biology of the prion protein. Curr Top Microbiol Immunol 207, 77-93.

Harris, DA. 2003. Trafficking, turnover and membrane topology of PrP. Br Med Bull. 66, 71-85.

Heppner FL, Christ AD, Klein MA, Prinz M, Fried M, Kraehenbuhl JP, Aguzzi A. 2001. Transepithelial prion transport by M cells. Nature Med 7, 976-977.

Hooper NM, Taylor DR. 2006. The prion protein and lipid rafts (Review). Mol Mem Biol 23, 1, 89-99.

Huang F-P, Farquhar CF, Mabbot NA, Bruce ME, MacPherson GG. 2002. Migrating intestinal dendritic cells transport PrPSc from the gut. J Gen Virol 83, 267-271.

Hunter N, Foster JD, Goldmann W, Stear MJ, Hope J, Bostock C. 1996. Natural scrapie in a closed flock of Cheviot sheep occurs only in specific PrP genotypes. Archives of Virology 141, 809-824.

Inoue S, Tanaka M, Horiuchi M, Ishiguro N, Shinagawa M. 1997. Characterization of the bovine protein gene: The expression requires interaction between the promoter and intron. J Vet Med Sci 59, 175-183.

Jeffrey M, Gonzales L. 2004. Pathology and pathogenesis of bovine spongiform encephalopathy and scrapie. Curr Topics Microbiol Immunol 284, 65-97.

Kanaani J, Prusiner SB, Diacovo J, Baekkeskov S, Legname G. 2005. Recombinant prion protein induces rapid polarization and development of synapses in embryonic rat hippocampal neurons in vitro. J Neurochem 95, 1373-1386.

Kaneko K, Zulianello L, Scott M, Cooper CM, Wallace AC, James TL, Cohen FE, Prusiner SB. 1997. Evidence for protein X binding to a discontinuous epitope on the cellular prion protein during scrapie prion propagation. Proc Natl Acad Sci USA. 94, 10069-10074.

Kascsak RJ, Fersko R, Pulgiano D, Rubenstein R, Carp RI. 1997. Immunodiagnosis of prion disease. Immunol Invest 26, 259-268.

Korth C, Stierli B, Streit P, Moser M, Schaller O, Fischer R, Schulz-Schaeffer W, Kretzchmar H, Raeber A, Braun U, Ehrensperger F, Hornemann S, Glockshuber R, Riek R, Billeter M, Wuthrich K, Oesch B. 1997. Prion (Prpsc)-specific epitope defined by a monoclonal-antibody. Nature 390, 74-77.

Li A, Christensen HM, Stewart LR, Roth KA, Chiesa R, Harris DA. 2007. Neonatal lethality in transgenic mice expressing prion protein with a deletion of residues 105-125, EMBO J 26, 548-558.

Lopes MH, Hajj GN, Muras AG, Mancini GL, Castro RM, Ribeiro KC, Brentain RR, Linden R, Martins VR. 2005. Interaction of cellular prion and stress-inducible protein 1 promotes neuritogenesis and neuroprotection by distinct signaling pathways. J Neurosci 25, 11330-11339.

Mabbott NA, MacPherson GG. 2006. Prions and their lethal journey to the brain. Nat Rev Microbiol 4, 201-211.

Maignien T, Shackweh M, Calvo P, Marce D, Sales N, Fattal E, Deslys JP, Couvreur P, Lasmezas CI. 2005. Role of gut macrophages in mice orally contaminated with scrapie or BSE. Int J Pharm 298, 293-304.

Mallucci GR, Ratte S, Asante EA, Linehan J, Gowland I, Jefferys JG, Collinge J. 2002. Post-natal knockout of prion protein alters hippocampal CA1 properties, but does not result in neurodegeneration. EMBO J 21, 202-210

Mallucci GR, Dickinson A, Linehan J, Klohn PC, Brandner S, Collinge J. 2003. Depleting neuronal PrP in prion infection prevent disease and reverses spongiosis. Science 302, 871-874.

Manson J, West JD, Thomson V, McBride P, Kaufman MH, Hope J. 1992. The prion protein gene: a role in mouse embryogenesis? Development 115, 117-122.

Martins V, Mercadante A, Cabral A, Freitas A, Castro R. 2001. Insights into the physiological function of cellular prion protein. Braz J Med Biol Res 34, 585-595.

Martins VR, Linden R, Prado M, Walz R, Sakamoto AC, Izquierdo I, Brentani RR. 2002. Cellular prion protein: on the road for functions. FEBS Letters 512, 25-28.

McDonald ST, Sutherland K, Ironside JW. 1996. Prion protein genotype and pathological phenotype studies in sporadic Creutzfeldt-Jakob disease. Neuropathol Appl Neurobiol 22, 285-292.

Mishra RS, Basu S, Gu Y, Luo X, Zou WQ, Mishra R, Li R, Chen SG, Gambetti P, Fujioka H, Singh N. 2004. Protease-resistant human prion protein and ferritin are cotransported across Caco-2 epithelial cells: Implications for species barrier in prion uptake from the intestine. J Neurosci 24, 11280-11290.

Moore RA, Herzog C, Errett J, Kocisko DA, Arnold KM, Hayes SF, Priola SA. 2006. Octapeptide repeat insertions increase the rate of protease-resistant prion protein formation. Protein Science 15, 609-619.

Neutra MR, Frey A, Kraehenbuhl JP. 1996. Epithelial M cells: gateways for mucosal infection and immunization. Cell 86, 345-348.

Oesch B, Westaway D, Walchili M, Mckinley MP, Kent SB, Aebersol R, Barry RA, Tempst P, Teplow DB, Hood LE, Prusiner SS and Weissman C. 1985. A cellular gene encodes scrapie PrP 27-30 protein. Cell 40, 735-746.

Office International des Epizooties (OIE). 2004. Bovine spongiform encephalopathy. In: Manual of diagnostic tests and vaccines for terrestrial animals (mammals, birds and bees), 5th ed. Vol I, Paris.

Office International des Epizooties (OIE). 2008. Number of reported cases of bovine spongiform encephalopathy (BSE) in farmed cattle worldwide. http://www.oie.int/eng/info/en_esbmonde.htm

Palmer MS, Dryden AJ, Hughes JT, Collinge J. 1991. Homozygous prion protein genotype predisposes to sporadic Creutzfeldt-Jakob disease. Nature 352, 340-342.

Pan KM, Baldwin M, Nguyen J, Gasset M, Serban A, Groth D, Mehlhorn I, Huang Z, Fletterick RJ, Cohen FE and Prusiner. 1993 Conversion of alpha-helices into β-sheets features in the formation of scrapie prion proteins. Proc Natl Acad Sci USA 90, 10962-10966.

Parchi P, Gambetti P. 1995. Human prion disease. Curr Opin Neurol 8, 286-293.

Premzl M, Gamulin V. 2007. Comparative analysis of prion genes. BMC Genomics 8, 1.

Priola S, Vorberg I. 2006. Molecular aspects of disease pathogenesis in the transmissible spongiform encephalopathies. Mol Biotech, 33, 71-88.

Prusiner SB. 1982. Novel proteinaceous infectious particles cause scrapie. Science 216, 136-144.

Prusiner SB. 1990. Novel structure and genetics of prions causing neurodegeneration in humans and animals. Biologicals 18, 247-262.

Prussiner SB and Scott MR. 1997. Genetics of prions Annu Rev Genet 31, 139-175.

Prusiner SB. 1998 Prions. Proc Natl Acad Sci USA 95, 13363-13383.

Riek R, Hornemann S, Wider G, Billeter M, Glockshuber R, Wuthrich K. 1996. NMR structure of the mouse prion protein domain PrP (121-321). Nature 11, 180-182.

Roucou X, Giannopoulos PN, Zhang Y, Jodoin J, Goodyer CG, LeBlanc A. 2005. Cellular prion protein inhibits proapoptotic Bax conformational change in human neurons and in breast carcinoma MCF-7 cells. Cell Death Differ 12, 783-795.

Russelakis-Carneiro M, Saborio GP, Anderes L, Soto C. 2002. Changes in the glycosylation pattern of prion protein in murine scrapie. Implications for the mechanism of neurodegeneration in prion diseases. J Biol Chem 277, 36872-36877.

Ryan AM, Womack JE. 1993. Somatic cell mapping of the bovine prion protein gene and restriction fragment length polymorphism studies in cattle and sheep. Anim Genet 24, 23-26.

Santuccione A, Sytnyk V, Leshchyns'ka I, Schachner M. 2005. Prion protein recruits its neuronal receptor NCAM to lipid rafts to activate p59fyn and to enhance neurite outgrowth. J Cell Biol 169, 341-354.

Schmerr MJ, Jenny A. 1998. A diagnostic test for scrapie-infected sheep using a capillary electrophoresis immunoassay with fluorescent-labeled peptides. Electrophoresis 19, 409-414.

Schwartz M. 2003. How the cows turned mad. Berkeley: University of California Press.

Selvaggini C, De Gioia L, Cantu L, Ghibaudi E, Diomede L, Passerini F, Forloni G, Bugiani O, Taglivini F, Salmona M. 1993. Molecular characteristics of a protease-resistant, amyloidogenic and neurotoxic peptide homologous to residues 106-126 of the prion protein. Biochem Biophys Res Commun. 194, 1380-1386.

Shortman K, Liu Y-J. 2002. Mouse and human dendritic cell subtypes. Nature Rev Immunol 2, 151-161.

Solforosi L, Criado JR, McGavern DB, Wirz S, Sanchez-Alavez M, Sugama S, DeGiorgio LA, Volpe BT, Wiseman E, Abalos G, Masliah E, Gilden D, Oldstone MB, Conti B, Williamson RA. 2004. Cross-linking cellular prion protein triggers neuronal apoptosis *in vivo*. Science 303, 1514-1516.

Soto C. 2006. Prions. The new biology of proteins. CRC Press. Boca Raton, FL, USA

Sparkes RS, Simon M, Cohn VH, Fournier RE, Lem J, Klisak I, Heinzmann C, Blatt C, Lucero M, Mohandas T, DeArmond SJ, Westaway D, Prusiner SB, Weiner LP. 1986. Assignment of the human and mouse prion protein genes to homologous chromosomes. Proc Natl Acad Sci USA 83, 7358-7362.

Steele AD, Emsley JG, Ozdinler PH, Lindquist S, and Macklis J. 2006. Prion protein (PrPC) positively regulates neural precursor proliferation during developmental and adult mammalian neurogenesis. PNAS, 103, 3416-3421.

Stewart RS, Harris DA. 2001. Most pathogenic mutations do not alter the membrane topology of the prion protein. J Biol Chem 276, 2212-2220.

Sunyach C, Jen A, Deng J, Fitzgerald KT, Frobert Y, Grassi J, McCaffrey MW and Morris R. 2003. The mechanism of internalization of glycosylphosphatidylinositol-anchored prion protein. EMBO J. 22, 3591-3601.

Taylor DM. 2000. Inactivation of transmissible degenerative encephalopathy agents: a review Vet J 159, 10-17.

Telling GC, Scott M, Mastrianni J, Gabizon R, Torchia M, Cohen FE, DeArmond SJ, and Prusiner SG. 1995. Prion propagation in mice expressing human and chimeric PrP transgenes implicates the interaction of cellular PrP with another protein. Cell 83, 79-90.

Terry LA, Marsh S, Ryder SJ, Hawkins SA, Wells GA, Spenser YI. 2003. Detection of disease-specific PrP in the distal ileum of cattle exposed orally to the agent of bovine spongiform encephalopathy. Vet Rec 152, 387-392.

Tremblay P, Bauzamondo-Bernstein E, Heinrich C, Prusiner SB, DeArmond SJ. 2007. Developmental expression of PrP in the post-implantation embryo. Brain Res 30, 60-67.

United States Department of Agriculture (USDA). 2005. Animal and Plant Health Inspection Service. Factsheet, BSE Confirmatory Tests.

Vassallo N, Herms J. 2003. Cellular prion protein function in copper homeostasis and redox signaling at the synapse. J Neurochem. 86, 538-544.

Wechselberger C, Wurm S, Pfarr W, Hoglinger O. 2002. The physiological functions of prion protein Exp Cell Res 281, 1-8.

Wells GA, Scott AC, Johnson CT, Gunning RF, Hancock M, Jeffrey M, Dawson M, Bradley R. 1987. A novel progressive spongiform encephalopathy in cattle. Vet Rec 121, 419-420.

Wells GAH, Hancock RD, Cooley WA, Richards MS. 1989. Bovine spongiform encephalopathy: diagnostic significance of vacuolar changes in selected nuclei of the medulla oblongata. Vet Rec 125, 521-524.

Wells GAH, Wilesmith JW. 1995. The neuropathology and epidemiology of bovine spongiform encephalopathy. Brain Pathol 5, 91-103.

Westaway D, Zuliani V, Cooper CM, Da Costa M, Neuman S, Jenny AL, Detwiler L, Prusiner SB. 1994. Homozygosity for prion protein alleles encoding glutamine-171 renders sheep susceptible to natural scrapie. Genes Dev 8, 959-969.

Westergard L, Christensen HM, Harris DA. 2007. The cellular prion protein (PrPC): Its physiological function and role in disease. Biochim. Biophys. Acta. Doi: 10 1016/ibbadis 2007 02 011.

Wong BS, Liu T, Li R, Pan T, Petersen RB, Smith MA, Gambetti P, Perry G, Manson JC,Brown DR, Sy MS. 2001. Increased levels of oxidative stress markers detected in the brains of mice devoid of prion protein. J Neurochem 76, 565-572.

Zanata SM, Lopes MH, Mercadante AF, Hajj GN, Chiarini LB, Nomizo R, Freitas AR, Cabral AL, Lee KS, Juliano MA, de Oliveira E, Jachieri SG, Burlingame A, Huang L, Linden R, Brentani RR, Martins VR. 2002. Stress-inducible protein 1 is a cell surface ligand for cellular prion that triggers neuroprotection EMBO J 21, 3307-3316.

Zhang CC, Steele AD, Lindquist S, Lodish HF. 2006. Prion protein is expressed on long-term repopulating hematopoietic stem cells and is important for their self-renewal. Proc Natl Acad Sci USA 103, 3416-3421.

Zou WQ, Zheng J, Gray DM, Gambetti P, Chen SG. 2004. Antibody to DNA detects scrapie but not normal prion protein. Proc Natl Acad Sci USA 101, 1380-1385.

CHAPTER II

COMPARATIVE ANALYSIS OF THE EXPRESSION OF THE CELLULAR PRION PROTEIN (PrP^C) IN SOMATIC TISSUES OF THE BOVINE ADULT

INTRODUCTION

The cellular prion protein (PrP^C) is a 250-amino acid glycoprotein commonly found attached by a glycosylphosphotidylinositol (GPI) anchor to lipid rafts in the plasma membrane. Through a poorly understood process, PrP^C is post-transcriptionally converted from a predominantly α-helical structure to a mainly β-sheet isoform (PrP^{Sc}). Substantial evidence indicates that PrP^{Sc} is the principal if not the only component of the agent causing transmissible spongiform encephalopathies (TSEs). This neurodegenerative and infectious group of diseases affects several mammalian species including human (Creutzfeldt-Jakob disease), bovine (spongiform encephalopathy) sheep (scrapie), mink (transmissible encephalopathy) and cervids (chronic wasting disease). Although much is known about the role of PrP^{Sc} in prion diseases, the normal function of PrP^C is poorly understood. One line of investigation proposes that PrP^C is an antioxidant factor that directly or indirectly promotes detoxification of reactive oxygen species (ROS) (Milhavet et al., 2002). Another hypothesis has associated this molecule with cytoprotective activity by blocking the internal or environmental stresses that initiate the apoptotic program (Roucou et al., 2004 and 2005). Furthermore, several authors have recently proposed that PrP^C participate in transmembrane signaling processes associated with cellular survival, replication and differentiation (Mouillet-Richard et al., 2000; Schneider et al., 2003).

Mice devoid of PrP^C have showed resistance to scrapie infection indicating that PrP^C expression is required for the infection process (Bueler et al., 1993). Thus, understanding the tissue-specific expression of PrP^C is crucial considering that cells expressing high levels of PrP^C bear a risk for conversion and accumulation of PrP^{Sc}. Paradoxically, there is a lack of information about the distribution of PrP^C protein in bovine tissues, which are regarded as a source of variant CJD. Tissue-specific analyses in mice and hamsters have demonstrated a ubiquitous presence of PrP^C with intense expression in murine neurons and lymphoreticular cells (Ford et al., 2002a,b; Bailly et al., 2004; Ning et al., 2005). PrP^C has also been localized in human, mouse and bovine digestive cells (Pammer et al., 2000; Marcos et al., 2004, 2005; Amselgruber et al., 2006) and bovine renal cells (Amselgruber et al., 2005). Moreover, reproductive tissues in mice (Ford et al., 2002a) and skin in human (Pammer et al., 1998) have shown cellular-specific immunoreactivity for PrP^C. Lymphoreticular and neural cells actively participate in the pathogenesis of TSEs through the transport, replication and accumulation of PrP^{Sc}. Immune cells are believed to be responsible for the transport of PrP^{Sc} from the intestinal lumen through the enteric wall after oral inoculation. Thereafter, PrP^{Sc} is transported to lymphatic tissues where it replicates and initiates

colonization of the nervous system. After a long period of incubation that ranges from one to five years in cattle, PrP^{Sc} is able to infect the CNS inducing the characteristic spongiform degeneration and neuropathological symptoms.

In the present study, we sought to analyze and compare PrP^{C} expression in fifteen different somatic bovine tissues by western blot and immunohistochemistry. Computerized quantification of western blot bands showed that PrP^{C} was expressed in all tissues analyzed. However, PrP^{C} is differentially expressed, showing intense levels in neural tissues and reduced levels in muscle and liver. Specific antibody staining revealed that PrP^{C} was expressed in cell-specific manner in a wide range of organs including brain, thymus, intestine, lung, and skin. The wide-spread expression of PrP^{C} in bovine tissues suggests that this protein may have important biological functions for this molecule. High levels of PrP^{C} expression in organs not commonly involved in TSE pathogenesis suggest that a higher number of tissues may be at potential risk for PrP^{Sc} infection and transmission.

MATERIAL AND METHODS

Tissue collection

Bovine tissues were obtained from three, 13 month old, healthy Angus steers. Animals were slaughtered at an abattoir located on campus. Samples of the following tissue were collected within 20 min of slaughter: cerebellum, obex, spinal cord (Pars thoracalis), sciatic nerve, mesenteric lymph node, thymus, spleen, liver, pancreas, ileum, kidney, heart, skin and skeletal muscle. Samples for western blot were placed in a glass container and frozen on dry ice. For immunohistochemistry, samples were fixed in 10% formalin.

Western blot

Frozen tissue samples of < 700 mg were thawed and homogenized (10 w/v) in lysis buffer (10 mM Tris, pH 7.4, 150 mM NaCl, 1% Triton-X-100, 1% deoxycholate, 0.1% SDS) using a pestle homogenizer (Fisher Scientific, Hampton, NH, USA). Homogenates were centrifuged at 13,500 rpm for 5 min and the supernatants transferred into a new tube. Total protein concentrations were

determined using a Bicinchoninic acid (BCA) kit (Pierce; Rockford, IL) according to the manufacturer's instructions. For protein denaturation, 50 µl of each homogenized sample was mixed with 50 µl of Laemmli buffer (BioRad Laboratories, Hercules, CA, USA) and heated at 98° C for 5 min. Aliquots containing 20 µg of total protein were added to each lane and separated by SDS-PAGE in 12% gels (BioRad). Electrophoresis was performed at 125V for 60 min. Proteins were then transferred onto PVDF membranes by electroblotting at 100 V for 1h. Membranes were immersed in blocking buffer (LI-COR Corp., Lincoln, NE, USA) for 1 h with shaking. PrP^C was detected by incubation for 1 h in SAF-32 mouse monoclonal anti-PrP (1:400; Cayman Chemical Company, Ann Arbor, MI, USA) directed against amino acid sequence 59-89 located in the N-terminal octapeptide repeat region of the protein. For reference, membranes were co-incubated in rabbit anti-GAPDH (1:1000; Santa Cruz Biotechnology, Santa Cruz, CA, USA). Both primary antibodies were diluted in 0.1% Tween-20 in blocking buffer. After four washes in 0.1% Tween-20 in phosphate-buffered saline (PBS) for 5 min each, membranes were incubated in secondary IgG fluorescent anti-mouse and anti-rabbit antibodies (1:5000; LI-COR) diluted in 0.1% Tween-20 in blocking buffer for 30 min with shaking. Immunoreactive bands for PrP^C were quantified and added as integrated intensity values using an Odyssey infrared imaging system (LI-COR). Relative expression of PrP^C was corrected by GAPDH expression and standardized to the highest expression value (cerebellum).

Immunohistochemistry

Formalin-fixed tissues were embedded in paraffin and sectioned at 5-7 µm using a microtome (Historange, LKB Bromma, Sweden). Tissue sections were mounted on adhesive coated slides (Newcomer supply; Middleton, Wisconsin) and incubated overnight at 37 °C. Mounted tissues were deparaffinized in xylene and dehydrated in serial alcohol solutions. Slides were subjected to an unmasking protocol that employed unmasking solution (Vector Laboratories., Burlingame, CA, USA) and autoclaving at 120°C for 5 min. Endogenous peroxidase was blocked by incubation in 3% hydrogen peroxide diluted in 0.1 M PBS (pH 7.4) for 30 min. Tissues were then rinsed two times in 0.1 M PBS and blocked in 2.5% horse serum for 15 min. PrP^C was specifically detected by overnight incubation at room temperature with primary antibody SAF-32 (1:400) diluted in 1.5 % equine serum solution (Vector Laboratories). After two washes in 0.1 M PBS (pH 7.4), bound primary antibody was detected using horse anti-mouse secondary antibody complexed to horseradish-peroxidase for 10 min at room temperature (Vector Lab). Immune

complexes were visualized using 3,3'-diaminobenzidine (DAB) substrate for 5 min or until the signal became visible. Probed sections were then counterstained with hematoxilyn and rehydrated in serial alcohol solutions. Sections were mounted with Permount mounting medium (Fisher Scientific) and coverslides. Neighboring sections processed identically using horse serum instead of primary antibody, served as controls. Digital photos of tissue sections were obtained using bright microscopy (Olympus Vanox-T, Tokyo, Japan).

Data Analysis

Statistical analyses for quantitative western blot were performed using SAS software (version 9.3.1, SAS Institute Inc., Cary, North Carolina, USA). Analyses were repeated at least three times for statistical significance. Analyses of significance ($P < 0.05$) were performed using One-way ANOVA. Expression values for individual tissues were compared to the highest expression (cerebellum) using Dunnet's t-test; whereas, significant differences between tissues were analyzed using Duncan's multiple comparison test.

RESULTS

Western blot

Independent assays comparing the relative levels of PrP^C expression were performed on tissues from three different animals by western blot. PrP^C was detected in all tissue samples in this study. PrP^C showed three distinct migration bands corresponding to molecular weights of 35, 28 and 25 kDa (Fig. 1a). Although we did not specifically analyze bands for glycosylation, each band is likely associated with the di-, mono- and un-glycosylated isoforms of PrP^C (Priola and Vorberg, 2006). The di-glycosylated isoform was predominant form across all tissues; whereas the mono- and un-glycosylated bands showed more variable intensities. Di-glycosylated PrP^C displayed strong bands in CNS tissues and thymus, whereas, immunoreactivity for the same isoform was low in pancreas and liver. In peripheral nerve, intestine, lung and heart the di-glycosylated PrP^C was observed as a doublet. Un-glycosylated PrP^C was undetectable in sciatic nerve and lymphatic tissues. Computerized quantification of PrP^C bands showed the highest ($P<0.05$) PrP^C relative

value in the cerebellum (Fig. 1b). Lowest PrP^C levels were found in liver and pancreas. Expression of PrP^C was higher in neural tissues compared with non-neural tissues with the exception of the thymus, which showed the highest ($P<0.05$) levels of PrP^C among non-neural tissues.

Immunohistochemistry

In order to establish the precise cellular localization of PrP^C within the tissues analyzed, we performed immunohistochemistry using anti-PrP SAF-32 monoclonal antibody. All results are typical for multiple experiments and were in general congruent with the western blot analysis. No staining was observed in the negative control sections incubated with normal horse serum instead of SAF-32 antibody.

Nervous system. Among tissues analyzed, the most intense and wide distribution of PrP^C immunostaining was observed in the nervous system. PrP^C labeling in the cerebellum was confined to the gray matter and appeared homogenous and diffuse on neuron bodies and the neuropil (Fig 2a). At the cellular level, PrP^C immunoreactivity was present in unmyelinated fibers, granule cells, and stellate and basket cells of the molecular layer. Purkinje cells observed in all the extensions of the central layer showed intense PrP^C staining (Fig. 2c). Similarly, PrP^C immunoreactivity was intense in neuronal bodies of the solitary tract nucleus in the obex (Fig. 3a, c). Astrocytes and oligodendrocytes observed around neurons showed moderate levels of PrP^C labeling (Fig. 3c). Immunoreactivity for PrP^C was analyzed in the thoracic portion (Pars thoracalis) of the spinal cord. In this tissue, the pattern of staining was confined to the gray matter (Fig. 4a). PrP^C labeling was also observed in neuronal tracts emerging from the gray matter into the white matter of the spinal cord. Analysis of PrP^C distribution in peripheral nerves was performed in transverse tissue sections obtained from the sciatic nerve. PrP^C labeling was restricted to the neural fibers contained in nerve fascicles (Fig. 5a). No PrP^C reactivity was observed in the connective tissue forming the perineurium or the epineurium.

Lymphoreticular system. Lobules in the cortex of the thymus were intensely labeled for PrP^C (Fig 6a). Observation with higher magnification evidenced a cell-specific staining associated with stromal cells with the appearance of lymphocytes of the T cell lineage (Fig 6c,e). Less intense PrP^C immunoreactivity was detected in epithelial cells located in the medulla. The intense and

wide immunoreactivity observed in the thymus contrasted with a scattered staining detected in the spleen. PrP^C-positive cells with the appearance of myeloid dendritic cells were located in the perilymphoid zones of the red pulp immediately adjacent to nodules of white pulp (Fig. 7a,c,e,f). Mesenteric lymph nodes showed cellular PrP^C staining associated with germinal centers and surrounding areas of secondary lymphoid follicles in the cortex (Fig. 8a). PrP^C-positive cells had the morphology and location of B lymphocytes and follicular dendritic cells (FDCs) (Fig. 8c,e).

Gastrointestinal system. PrP^C immunohistochemical analysis was performed in the ileum section of the intestine. Staining was intense and restricted to enteric neural cells present in the intestinal wall. PrP^C-positive neural cells were observed in the lamina propia within intestinal crypts (Fig. 9a,c). Labeling was also present in neural fibers located in parallel to muscle fibers in the inner circular muscular layer. Between the inner and outer layers of the muscularis, clusters of parasympathetic ganglion cells associated to the myenteric plexus showed intense PrP^C staining throughout the extension of the sections (Fig. 9c,d). In pancreas, PrP^C labeling was restricted to the endocrine tissue conformed by the islets of Langerhans (Fig. 10a,c). No staining was observed in the exocrine pancreatic tissue. Liver tissue showed a weak immunoreactivity PrP^C (Fig 11a).

Skeletal, smooth and cardiac muscle. Skeletal muscle samples were obtained for the gluteus muscle. PrP^C immunoreactivity was not observed in all the extension of the skeletal muscle sections (Fig. 12a). In contrast, neural fibers innervating smooth muscle fibers in the enteric muscularis layers showed strong immunoreaction for anti-PrP antibody (Fig. 9a). Similarly, a homogeneous PrP^C labeling was observed associated with cardiac muscle cells in the myocardium (Figure 13a,c).

Miscellaneous tissues. PrP^C labeling in the lung was mainly associated to the alveolar wall (Fig. 14a). At the cellular level, PrP^C staining appeared to be present in all cells forming the alveolar sacs including pneumocites (Fig. 14c). In the kidney, PrP^C positive staining was observed in cortical convoluted tubules and collective ducts located in the medulla (Fig. 15a). Renal glomeruli showed strong PrP^C labeling associated to extraglomerular mesangial cells, podocytes and endothelial cells (Fig. 15c). The skin tissue sample obtained from the flank area displayed PrP^C labeling in keratinocytes localized in the epidermis and outer sheaths of the hair follicle (Fig. 16a,c). Furthermore, horizontal sections at the level of the dermis allowed the detection of PrP^C immunoreactivity in sebaceous glands (Fig. 16e).

DISCUSSION

Neuropathological findings in animals and humans affected with prions indicate a correlation between PrP^{C} expression and accumulation of PrP^{Sc}. Moreover, the mechanism of the PrP^{C} to PrP^{Sc} conversion does not occur in scrapie-infected *Prnp*$^{0/0}$ mice, indicating the necessity for the infected host cells to express PrP^{C} in order to support conversion or replication (Bueler et al., 1993). Identification of cell types expressing PrP^{C} is necessary to better understand how the agent replicates and spreads from the periphery to the CNS. Furthermore, a spatial localization analysis of PrP^{C} expression may help in the understanding of its cellular function.

The tissue-specific comparative western blot analysis performed in our study is the first reported in the bovine specie. Different PrP^{C} glycosylation patterns were observed among tissues analyzed. Implication for this variability is not completely understood; however, variations in PrP^{C} glycosylation have been shown to affect susceptibility to PrP^{Sc} infection in mouse brain (DeArmond et al., 1999). In our study, the un-glycosylated isoform of PrP^{C} showed undetectable levels in lymphatic tissues. Some authors have proposed that variations in PrP^{C} molecular features could be related to the absence of detectable infectivity in peripheral lymph organs in BSE-affected cattle (Thielen et al., 2001). A significantly higher PrP^{C} expression was observed in neural tissues versus non-neural tissues. We performed a parallel tissue-specific analysis of PrP^{C} mRNA expression using the same tissue samples analyzed by western blot (data not shown). Higher PrP^{C} mRNA expression levels were observed also in neural tissues. However, we found no full correlation when mRNA expression was compared to the protein level. Previous reports of PrP^{C} mRNA using quantitative-PCR analysis in the bovine (Tichopad et al., 2003), hamster (Ning et al., 2005) and sheep (Han et al., 2006) have also shown discordance with western blot analysis. Disparity between PrP^{C} transcription and translation may explain the differences in the efficiency of message and/or protein expression and degradation among tissues.

Computerized quantification of western blot bands showed higher levels of PrP^{C} expression in the cerebellum compared to the spinal cord and peripheral nerves. PrP^{C} expression seems to be more intense in organs with higher proportion of gray matter (e.g. cerebellum) than in those with predominantly white matter structures (e.g. spinal cord). Lower levels of PrP^{C} in peripheral

nerves may be explained by the heterogeneous conformation of this tissue, consisting of a high proportion of collagen and myelin.

Western blot analysis of PrP^C in bovine somatic tissues showed the most intense immunoreactivity in the nervous system. Strong bands associated to PrP^C in lymphoid tissues, especially thymus, indicate that the second major source of PrP^C is located in the lymphoreticular compartment. The remaining organs displayed bands of weak intensity suggesting either low expression of PrP^C in the tissue or cellular-specific immunoreactivity.

PrP^C is mainly found attached to the plasma membrane as a GPI-anchored glycoprotein; however, our immunohistochemical protocol displayed a diffuse PrP^C staining not limited to the plasma membrane but covering the neuronal cytoplasm. Although a proportion of PrPC is located in the cytoplasm, this phenomenon may also be explained by the diffusion of the marker present in the immunoperoxidase method that can create an even distribution of the immunostaining throughout the tissue. Similarly to previous studies, our immunohistochemical analysis detected more intense PrP^C staining in gray matter areas compared to white matter regions of the CNS (Ford et al., 2002b; Diaz-San Segundo et al., 2006). PrP^C signal in the gray matter is mainly associated with the neuropil, defined as the region containing the dendritic tree of neurons, axons terminals and synapses (Taraboulos et al., 1992). Neuropil expression of PrP^C predisposes the accumulation of PrP^{Sc} and correlates with vacuolization observed in histological findings of cattle affected by BSE. Bilaterally symmetric vacuolization of the gray matter neuropil (spongiosis) is considered the most characteristic histological change in BSE (Gavier-Widen et al., 2005). Furthermore, PrP^{Sc} immunoreactivity has revealed that this agent is present in the neuropil but in some cases can spread to neural bodies (Wells and Wilesmith, 1995). Some authors have explained the weak PrP^C immunoreaction in white areas of the CNS by the resistance of myelin-coated pits to protein blotting or penetration by specific PrP antibodies (Taraboulos et al., 1992; Moleres and Velayos, 2007). However, PrP^C labeling has been co-localized with specific markers of astrocytes and oligodendrocytes present in the rat white matter and was detected in glia and axons in the cerebellum of mice (Moleres and Velayos, 2007; Taraboulos et al., 1992). These data may explain the presence of PrP^{Sc} in the white matter of infected brains and support the hypothesis that PrP^{Sc} is axonally transported to the CNS.

Similar to our results, immunoreactivity for PrP^C in mice cerebellum has been described previously in Purkinge, granular cells, and stellate and basket cells of the molecular layer (Ford et

al., 2002b). In Purkinge and granular cells, PrP^C expression has been confirmed by immunogold and GFP-labeling (Lemaire-Vieille et al., 2000; Bailly et al., 2004). Intense PrP^C expression in these cells may explain the specific accumulation of PrP^{Sc} plaques or fine depositions in the molecular and granular layers. These findings have been observed in patients suffering from TSEs that target the cerebellum including Creutzfeldt-Jakob, Gerstmann-Straussler-Scheinker and kuru (Bell and Ironside, 1993).

Consistent early accumulation of PrP^{Sc} in the bovine medulla oblongata at the obex level makes this area of the brain an optimal site for BSE diagnosis. Our analysis in the solitary tract nucleus of the obex detected intense PrP^C immunoreaction in the neuropil, neuroglia and in all neuronal bodies present. In the bovine, areas most consistently and severely affected in the obex are the solitary tract nucleus and spinal tract nucleus of the trigeminal nerve, which vacuolization is considered to be pathognomonic for BSE (Wells et al., 1989). Intense immunoreactivity in neurons of the obex, may explain neuronal degeneration during PrP^{Sc} infection, since neuronal bodies expressing high levels of PrP^C appeared to be particularly sensitive to PrP^{Sc} neurotoxicity (Guentchev et al., 1998; Ford et al., 2002).

Despite the large number of reports, the role of PrP^C in the nervous system has not been completely clarified. Cellular localization of PrP^C along axons and in proximity to presynaptic membrane domains suggest that PrP^C could be involved in synapse formation or transmission (Collinge et al., 1994). Incubation of cultured hippocampal neurons with recombinant PrP^C has been shown to induce rapid elaboration of axons and dendrites, and increase the number of synaptic contacts (Kanaani et al., 2005). Moreover, *Prnp* null mice have been reported to display neurobiological abnormalities related to synapse function such as circadian rhythm (Tobler et al., 1996) and spatial learning (Criado et al., 2005). However, several reports have also described a role for PrP^C against oxidative stress in neurons. Cerebellar granular and neocortical cells cultured from *Prnp* null mice are more susceptible than wild-type counterparts to treatments with agents that induce oxidative stress, including hydrogen peroxide, xanthine oxidase and copper ions (Brown et al., 1997 and 2002). Consistent with these results, brain tissue from *Prnp* null mice exhibits increased levels of protein carbonyls and lipid peroxidation products, which are indications of intense oxidative stress (Wong et al., 2001). Recently PrP^C has also been involved in neurogenesis and differentiation *in vitro* and *in vivo*. Loss- and gain-of-function experiments demonstrate that PrP^C levels correlate with differentiation of multipotent neural precursors into mature neurons *in vitro*. Moreover, PrPC overexpresser mice showed higher cellular proliferation

in the subventricular zone of the nervous system compared to wild-type and knockout mice (Steele et al., 2006).

The thymus showed the highest levels of PrP^C expression among non-neural tissues analyzed. Previous studies have described PrP^C expression in epithelial cells of the medulla and cortex in mice thymus; however, with lower distribution as reported here (Lemaire-Vieille et al., 2000; Ford et al., 2002a). Our analysis showed intense PrP^C labeling in the cortex associated to epithelial cells with the morphology of lymphocytes from the T lineage. Thymus function consists on the development of immunocompetent T lymphocytes derived from the bone marrow (Wheater et al., 1993). PrP^C expression is regulated during lymphocyte development in both thymus and bone marrow (Kubosaki et al., 2001; Liu et al., 2001). Moreover, in mice, PrP^C is believed to be a surface molecule that participates in T lymphocyte activation (Mabbot et al., 1997). All these data suggest that PrP^C participates as a T lymphocyte inducing factor and that this action is initiated at early stages of maturation in the thymus. As part of the lymphoreticular system, the thymus has also been shown to participate in TSEs infection. Studies in mice described a rapid accumulation of PrP^{Sc} in the thymus after inoculation, suggesting that this organ has an active role in replication of the agent (Fraser and Dickinson, 1978; Muramoto et al., 1992).

Despite its known involvement in TSE pathogenesis, the spleen displayed low levels of PrP^C expression in both western blot and immunohistochemical analyses. Most cell types and stromal elements were not reactive to SAF-32 antibody and the staining was restricted to scattered cells concentrated adjacent to the marginal zone of the white pulp. Similar results were reported in the human spleen, where PrP^C was co-localized with MHC class II lineage-defining antigens consistent with the distribution and phenotype of myeloid dendritic cells (DCs) (Burthem et al., 2001). The same study showed that PrP^C was specifically expressed in myeloid DCs and not in follicular dendritic cells (FDCs), B cells and macrophages of the spleen. Myeloid DCs are derived from bone marrow precursor cells or from monocytes and migrate into lymphoid areas after receiving maturation stimulus (Burthem et al., 2001). Migratory myeloid DCs are able to enter the intestinal wall from the bloodstream and sample antigens from the gut lumen providing a potential cellular bridge to lymphoid tissues that serve for PrP^{Sc} replication (Huang et al., 2002). The spleen has an important participation in PrP^{Sc} pathogenesis evidenced by the high titers of infectivity exhibited in mice during early stages of PrP^{Sc} infection. Sheep orally inoculated with BSE agent showed PrP^{Sc} deposition in the same marginal zone of the white pulp where myeloid

DCs PrP^{C}-positive cells were observed in our study (Andreoletti et al., 2006). Nevertheless, some reports have showed that PrP^{Sc} deposition does not occur in the spleen of BSE-infected cattle (Somerville et al., 1997; Buschmann and Groschup, 2005).

Our analysis in the mesenteric lymph node showed PrP^{C}-positive cells in germinal centers and surrounding areas of lymphoid follicles. The location indicates that these cells may be FDCs or/and B lymphocytes (Klein et al., 1998; Thielen et al., 2001). In addition to myeloid DCs, both FDCs and B lymphocytes have direct and indirect participation in PrP^{Sc} pathogenesis. FDCs are critical for PrP^{Sc} replication and accumulation in mice lymphoid tissues and have participation in neuroinvasion (Brown et al., 1999; Mabbot et al., 2000). B lymphocytes have not been directly involved in PrP^{Sc} delivery but are essential for FDCs maturation (Kosco-Vilbois et al., 1997; Chaplin and Fu, 1998). In mice, PrP^{C} is highly express in FDCs, which mediate accumulation of PrP^{Sc} in lymph nodes (Bruce et al., 2000; Schreuder et al., 1998). PrP^{C} is also expressed in bovine FDCs; however, BSE infectivity has been detected only in lymph nodes from experimentally inoculated cows (Wells et al., 1994; Terry et al., 2003) but not from naturally affected cattle (Iwata et al., 2006; Terry et al., 2003). Contrary to our results, Thielen et al, (2001) previously reported undetectable levels of PrP^{C} expression inside the bovine lymphoyd tissue using SAF-32 antibody. Differences in results may be related to the requirement of an epitope unmasking step for the immunoreaction of PrP^{C} in the lymph node. Furthermore, PrP^{C} immunoreactivity may be critically affected by the fixatives used.

Localization of PrP^{C} in the intestine is of considerable importance due to its role as a major route for entry of TSEs agents. Previous reports in hamster, mouse, human, rat, bovine and monkey have described intense PrP^{C} expression in the epithelium of the intestinal wall (Fournier et al., 1998; Ford et al., 2002a; Pammer et al., 2000; Marcos et al., 2004, 2005). In mouse, rat and human, PrP^{C} immunoreactivity was detected in enteroendocrine cells (Ford et al., 2002a; Marcos et al., 2004; Pammer et al., 2000). Other authors have described PrP^{C} immunolabeling in mucous and parietal cells in humans (Fournier et al., 1998; Pammer et al., 2000), in mucous, parietal and goblet cells in hamsters (Fournier et al., 1998, 2000) and in DCs in rat intestine (Miyazawa et al., 2007). In our study, absence of PrP^{C}-specific labeling in the enteric epithelium maybe related to differences in the antibody used. However, we detected intense PrP^{C} staining in neurons located within enteric crypts and inserted in parallel to muscularis fibers. Furthermore, strong PrP^{C} immunoreactivity was observed in the myenteric plexus. Whether enteric neurons participate in PrP^{Sc} transport from intestinal lumen is unknown. Parasympathetic pre-ganglionic neurons in the

vagal trunks derived from the dorsal motor nucleus innervate the mucosa and submucosa of the gastrointestinal tract, via the myenteric plexuses. These motor neurons of the vagus nerves represent a potential route for PrP^{Sc} transport after oral inoculation. This hypothesis is supported by reports of PrP^{Sc} accumulation in the enteric nervous system, especially in the myenteric plexus of BSE-affected cattle and scrapie-affected sheep (Iwata et al., 2006; Terry et al., 2003; van Keulen et al., 1999; Ersdal et al., 2003). However, enteric neurons have also close proximity with other cells types, such as DCs and intraepithelial lymphocytes, which are known to deliver PrP^{Sc} to secondary lymphatic tissue. Therefore, the oral route of transmission seems to be a flexible way to transport PrP^{Sc} to the CNS, either by nervous tissue innervating the intestine or by migratory cells colonizing lymphatic tissue or both.

Previous studies have reported expression of PrP^{C} in mice and bovine pancreatic tissue restricted to a subset of cells in the islets of Langerhans (Ford et al., 2002a; Amselgruber et al., 2006). Mice inoculated with scrapie showed an inflammatory reaction in the endocrine pancreas, which may be associated with PrP^{Sc} accumulation (Ye et al., 1997). PrP^{Sc} deposits have also been described in the pancreas of cervids infected with chronic wasting disease (Sigurdson et al., 2001). Using a panel of antibodies in bovine pancreas, PrP^{C}-specific labeling was co-localized with glucagon producing α-cells (Amselgruber et al., 2006). Nevertheless, a recent study in rat pancreas described co-localization of PrP^{C} inclusions exclusively in insulin producing β-cells (Strom et al., 2007). These authors observed that inclusions of PrP^{C} increased with age and under hyperglycemic conditions suggesting a novel physiological role of PrP^{C} in glucose homeostasis.

As previously described (Ford et al., 2002a), our analysis showed undetectable levels of PrP^{C} in the liver tissue. Low PrP^{C} expression in liver cells may explain the reduced PrP^{Sc} infectivity reported *in vitro* (Bosque et al., 2001). Evidence of PrP^{C} expression in bovine skeletal muscle has important implications for the potential transmission of BSE through the consumption of beef products. Low levels of PrP^{C} expression in bovine skeletal muscle support the idea of a reduced potential for PrP^{Sc} infection in meat. However, PrP^{C} expression in mouse muscle was reported to be 5-10% of that in brain and still sufficient to induce PrP^{Sc} accumulation (Bosque et al., 2001). In our study, we found a similar ratio of PrP^{C} in skeletal muscle in comparison to the brain (4.22%; Fig. 1), which may potentially be sufficient for PrP^{Sc} accumulation. PrP^{Sc} has been detected in skeletal muscle after experimental inoculation of several species including mouse, hamster, goat and sheep (Bosque et al., 2001; Thomzig et al., 2003; Pattison and Millson, 1962; Casalone et al., 2005). Bosque et al, (2001) reported that PrP^{Sc} was accumulated in muscle of

mice after intracerebral inoculation and that muscle and not neural or lymphatic PrP^{C} was the substrate for PrP^{Sc} conversion. These authors also discussed a number of variables that may affect PrP^{Sc} production in muscle including muscle type, prion strain, host species and inoculation route. One or more of these variables may be responsible for the lack of PrP^{Sc} detection in the skeletal muscle from experimentally inoculated cattle (Hamir et al., 2004). Despite the reduced levels of PrP^{C} in skeletal muscle, this protein may play a role in muscle physiology. Studies *in vitro* have implicated PrP^{C} in myocyte differentiation as well as protection against oxidative stress (Brown et al., 1998; Massimino et al., 2006). PrP^{C} expression is up-regulated in regenerating muscle fibers (Sarkozi et al., 1994) and may have a general stress-response effect in various neuromuscular disorders (Kovacs et al., 2004).

Detection of PrP^{C} staining was previously reported in pneumocytes of mice lung tissue (Ford et al., 2002a). Considering the respiratory system as a route for entry in several diseases, the expression of PrP^{C} in the lung may lead to think that there is a potential respiratory transmission route for TSEs. However, this passage of prion pathogenesis has not been clarified. In a previous study in the bovine kidney, PrP^{C} labeling was reported to be restricted to the renal glomeruli (Amselgruber et al., 2005). However, our analysis detected PrP^{C} staining also associated to cortical and convoluted tubules, and collective ducts in the medulla. Disparity in the pattern of staining may be associated to different antibodies used. Expression of PrP^{C} in the kidney can potentially predispose PrP^{Sc} conversion and accumulation in the urinary system. This idea is supported by reports of scrapie-infected hamsters and CJD patients showing PrP^{Sc} urinary excretion (Shaked et al., 2001). Moreover, a study in mice suffering from chronic nephritis showed that urinary inflammation was able to trigger excretion of prion infectivity into urine, which may potentially constitute a vector for horizontal TSEs transmission (Seeger et al., 2005).

A previous report and our study showed intense PrP^{C} expression in epidermal keratinocytes (Pammer et al., 1998). Additionally, we observed intense PrP^{C} staining in sebaceous glands located in horizontal tissue sections of the skin at the level of the dermis. PrP^{C} expression was also detected in cells surrounding the inner and the outer root sheet of the hair follicle. Interestingly, this group of cells in the hair follicle, including the sebaceous gland, has been described as stem cells responsible for hair follicle regeneration (Levy et al., 2005). This finding supports the idea that PrP^{C} may play a role in induction of cellular differentiation. Intense and specific expression of PrP^{C} in the skin may explain the detection of PrP^{Sc} in the dermis of mice and sheep after oral inoculation (Thomzig et al., 2007). Despite intense expression of PrP^{C} in

keratinocytes and sebaceous cells, deposition of PrP^{Sc} has showed to occur exclusively on peripheral nerve fibers, indicating that PrP^{Sc} is transported by neurons and centrifugally spread to the skin. (Thomzig et al., 2007).

The wide-spread expression and the evolutionary conservation among mammals suggest that PrP^{C} has an important biological function. Several studies have showed roles for PrP^{C} associated with cytoprotection through anti-oxidant and anti-apoptotic effects. These properties have been observed in specialized and mitotically inactive cells such as neurons (Brown et al., 1997 and 2002) and myocytes (Sarkozi et al., 1994; Kovacs et al., 2004). PrP^{C} may be exerting a similar role in other specialized cells where our analysis found intense PrP^{C} expression such as FDCs, podocytes, keratinocytes and pneumocytes. However, in developing cells PrP^{C} expression has been correlated with differentiating and mitogenic processes as showed by studies in neuronal precursors (Steele et al., 2006), myoblasts (Massimino et al., 2006), thymocytes (Kubosaki et al., 2001), lymphocytes (Bainbridge et al., 2005) and hematopoietic cells (Liu et al., 2001). Moreover, several reports have demonstrated that PrP^{C} expression is increased during inflammation in the skin (Pammer et al., 1998), gastric mucosa (Konturek et al., 2005), kidney (Seeger et al., 2005), pancreas and liver (Heikenwalder et al., 2005). All these data suggest that PrP^{C} may have a dual role in damaged tissues that involve protecting cells affected by acute or chronic oxidative stress and also inducing differentiation of immature cells into specialized and functional cells that can serve in tissue regeneration.

Our study presented the first comparative analysis of PrP^{C} expression in bovine tissues. The importance of this study is to lay the foundation for understanding the tissue-specific PrP^{C} expression and to consider the potential participation of more bovine tissues in transmission of BSE infection. Moreover, the wide-spread expression of PrP^{C} in bovine tissues opens the spectrum of possibilities to new cell models for the study of PrP^{C} elusive function.

a

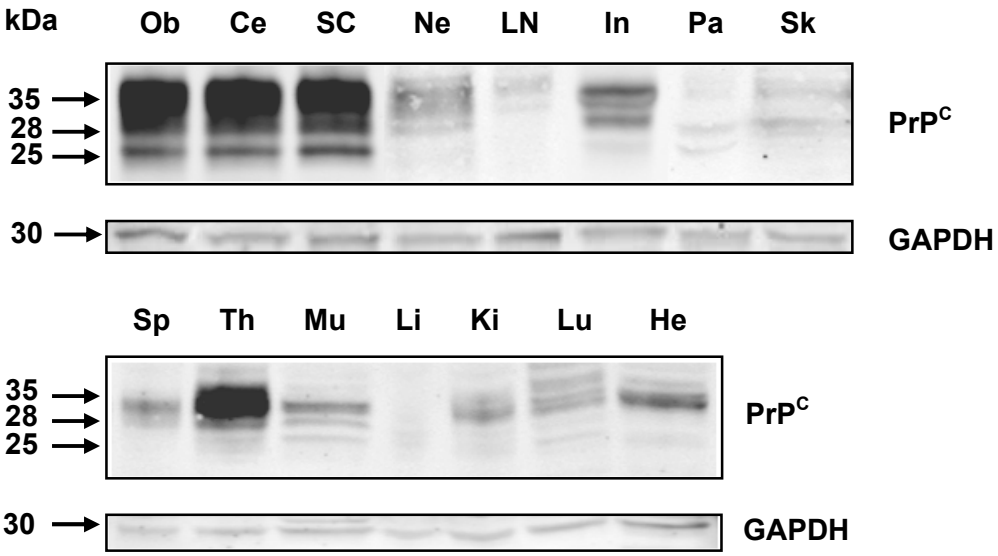
kDa
Ob
Ce
SC
Ne
LN
In
Pa
Sk
35
28
25
PrP^C
30
GAPDH
Sp
Th
Mu
Li
Ki
Lu
He
35
28
25
PrP^C
30
GAPDH

b

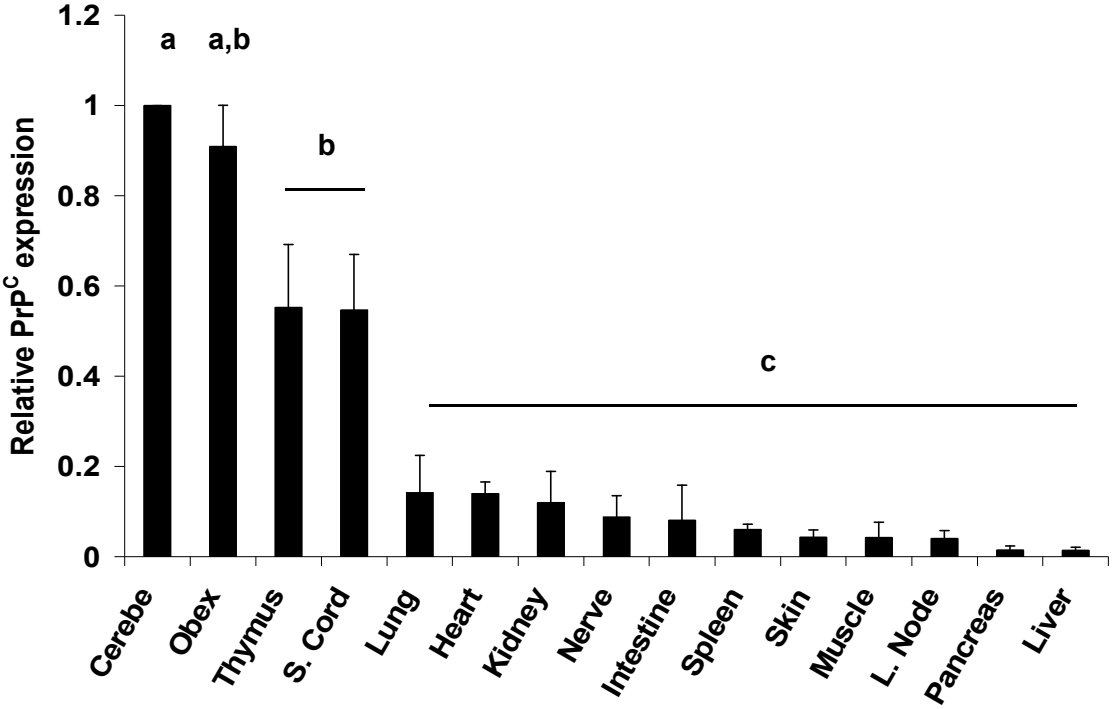

Fig. 1 Western blot analysis of relative PrP^C expression in bovine tissues. (A) PrP^C displayed three distinct migration bands corresponding to molecular weights of 35 kDa (di-), 28 kDa (mono-) and 25 kDa (un-glycosylated). PrP^C was detected in all tissues with higher intensity in neural tissues and thymus. GAPDH was used as control protein (30 kDa). (B) Cerebellum showed the highest ($P<0.05$) levels of PrP^C expression. Among non-neural tissues, the thymus expressed the highest ($P<0.05$) levels of PrPC. Different superscripts indicate significant differences ($P<0.05$). Ob, Obex; Ce, Cerebellum; SC, Spinal Cord; Ne, Nerve; LN, Lymph node; In, Intestine; Pa, Pancreas; Sk, Skin; Sp, Spleen; Th, Thymus; Mu, Muscle; Li, Liver; Ki, Kidney; Lu, Lung; He, Heart.

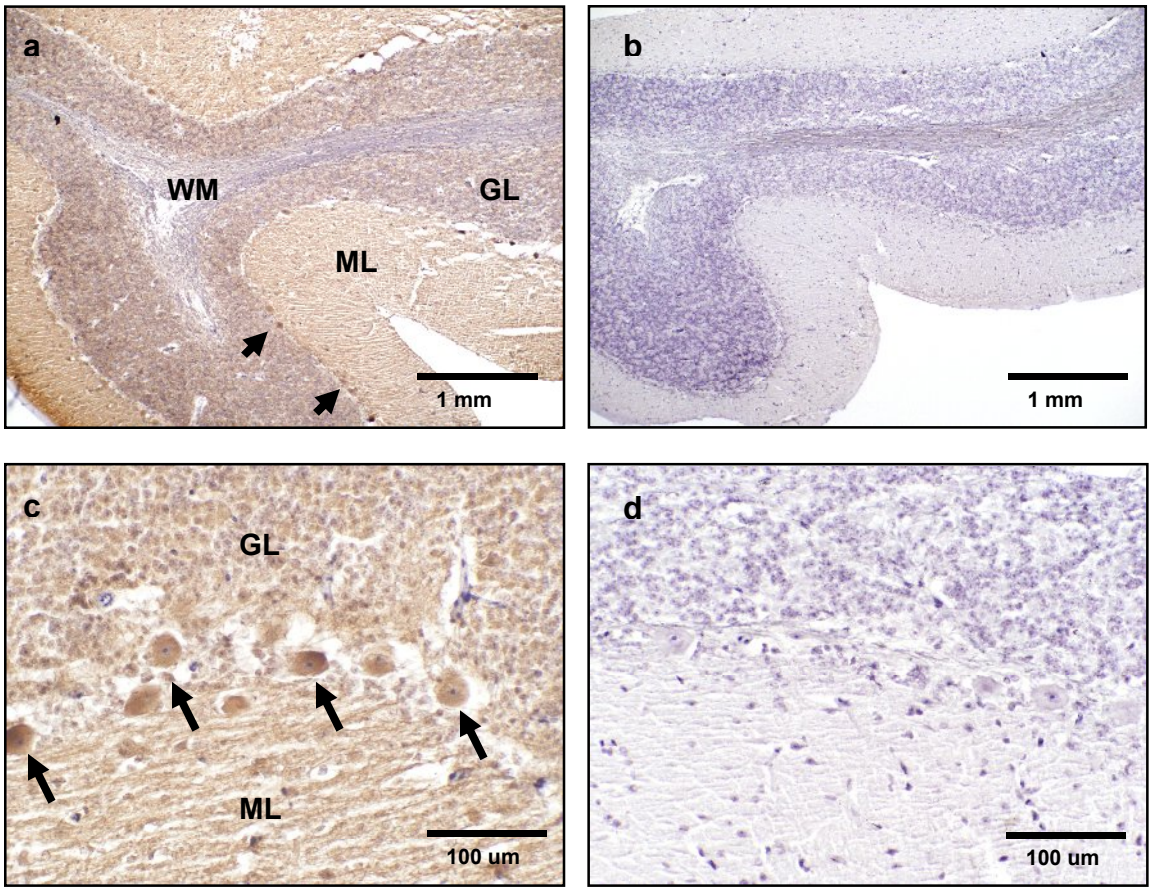

Figure 2. Expression of PrP^C in the bovine cerebellum. (a) Transverse tissue section incubated with SAF-32 antibody and stained using peroxidase. PrP^C staining was confined to the molecular layer (ML), granular layer (GL) and Purkinje cells (*arrows*) located in the gray matter. No staining was observed in the white matter (WM). (c) Higher magnification shows intense PrP^C expression in fibers of the ML, Purkinje cells (*arrows*) and neurons of the GL. (b,d) Serial section incubated with non-immune horse serum instead of SAF-32 antibody shows no staining (negative control).

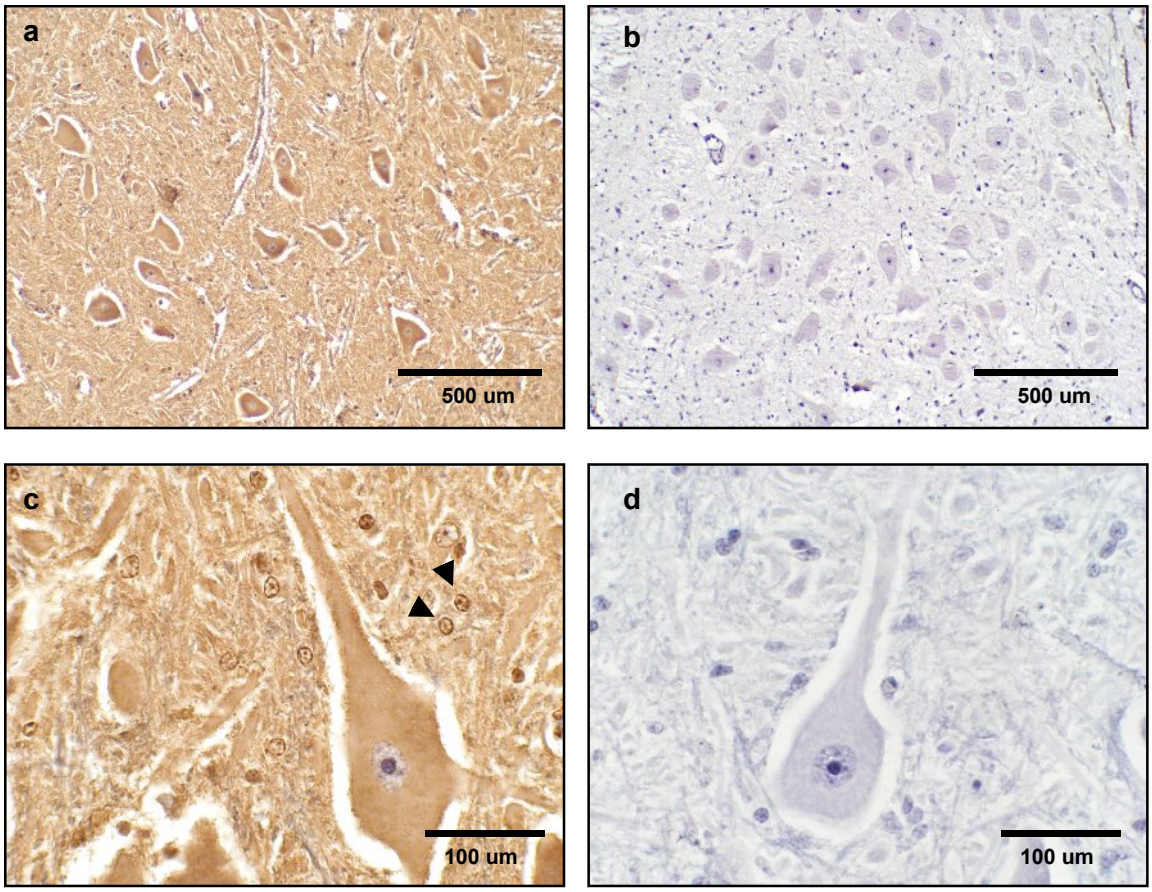

Figure 3. Expression of PrP^C in the bovine obex. (a) PrP^C expression is associated to neuronal bodies, neuropil and neuroglia of the solitary tract nucleus. (c) Higher magnification shows PrP^C labeling in neuronal bodies, appendixes and glial cells (*arrow-heads*). (b,d) Serial section incubated with non-immune horse serum instead of SAF-32 antibody shows no staining (negative control).

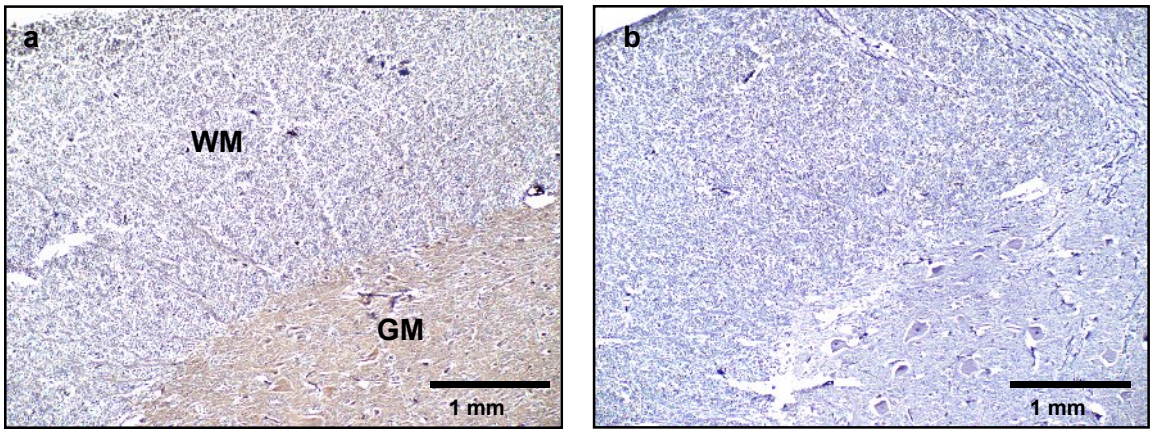

Figure 4. Expression of PrP^C in the bovine spinal cord. (a) Sagittal section showing PrP^C-specific labeling using SAF-32 antibody and peroxidase staining. PrP^C immunoreactivity was restricted to the gray matter. (b) Serial section of the spinal cord incubated with non-immune horse serum instead of SAF-32 (negative control).

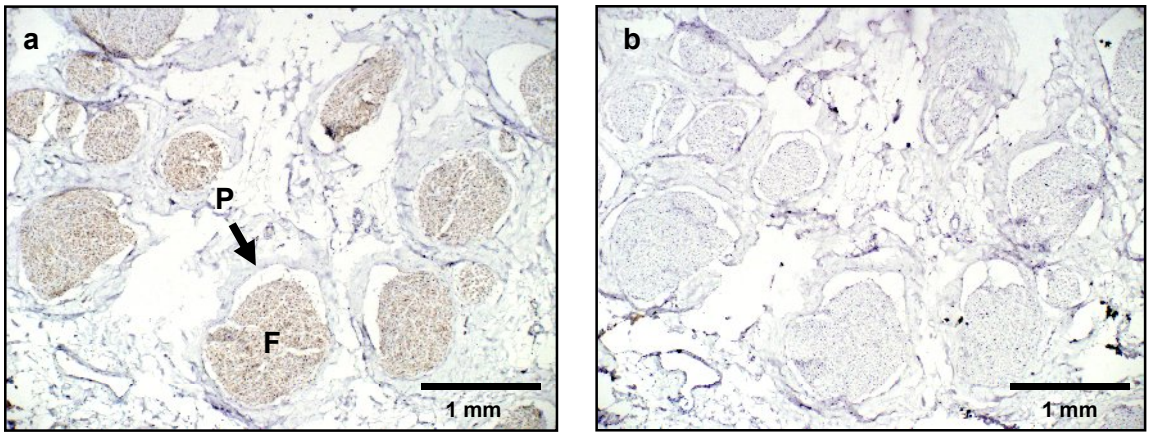

Figure 5. Expression of PrP^C in the bovine syatic nerve. (a) Transverse tissue section incubated with SAF-32 antibody and stained with peroxidase. PrP^C staining is confined to neural fibers associated in fascicles (F). No PrP^C labeling was observed in the perineurum (P). (b) Serial section incubated with non-immune horse serum instead of SAF-32 antibody (Negative control).

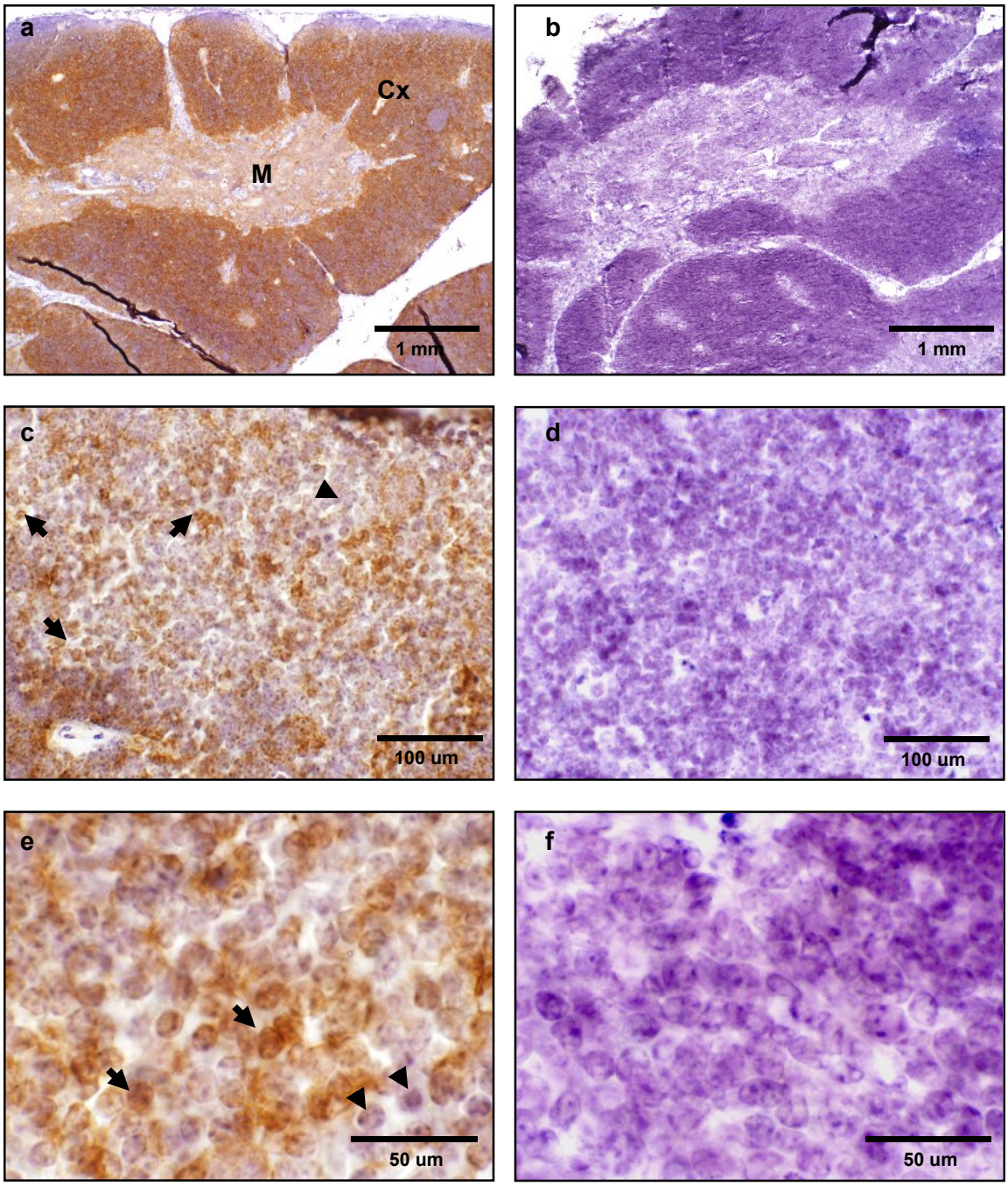

Figure 6. Expression of PrP^C in the bovine thymus. (a). Intense PrP^C-specific labeling is observed in the cortex (Cx) of the thymus. (c,e) Higher magnification in the cortex area shows PrP^C positive (*arrows*) and negative (arrow-heads) stromal cells. (b,d,f) Serial section incubated with non-immune horse serum instead of SAF-32 antibody (Negative control).

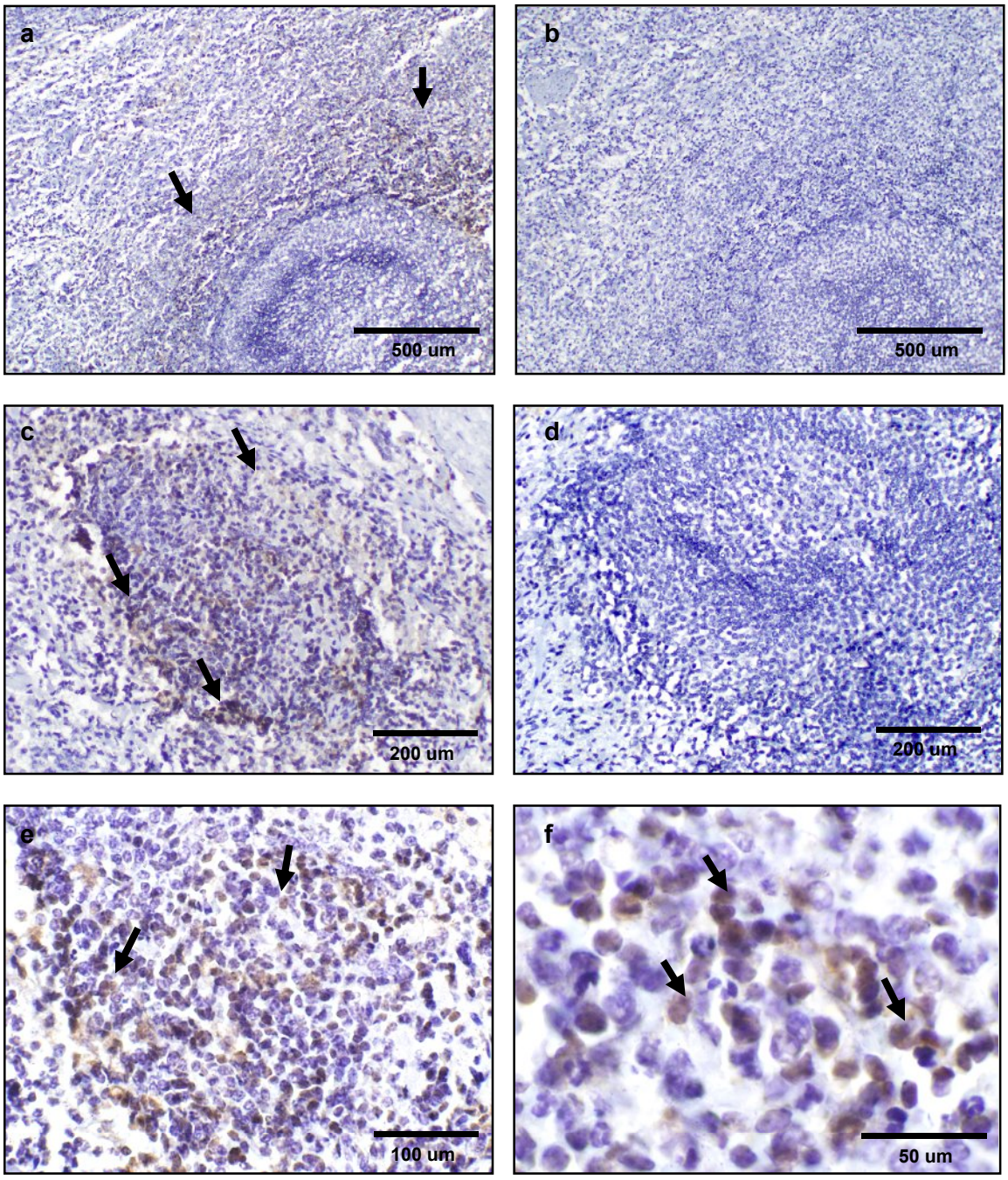

Figure 7. Expression of PrP^C in the bovine spleen. (a,c,e,f) PrP^C staining was associated with cells with the appearance of myeloid dendritic cells (*arrow*) in perilymphoid zones surrounding nodules of white pulp. (b,d) Serial section incubated with non-immune horse serum instead of SAF-32 antibody (Negative control).

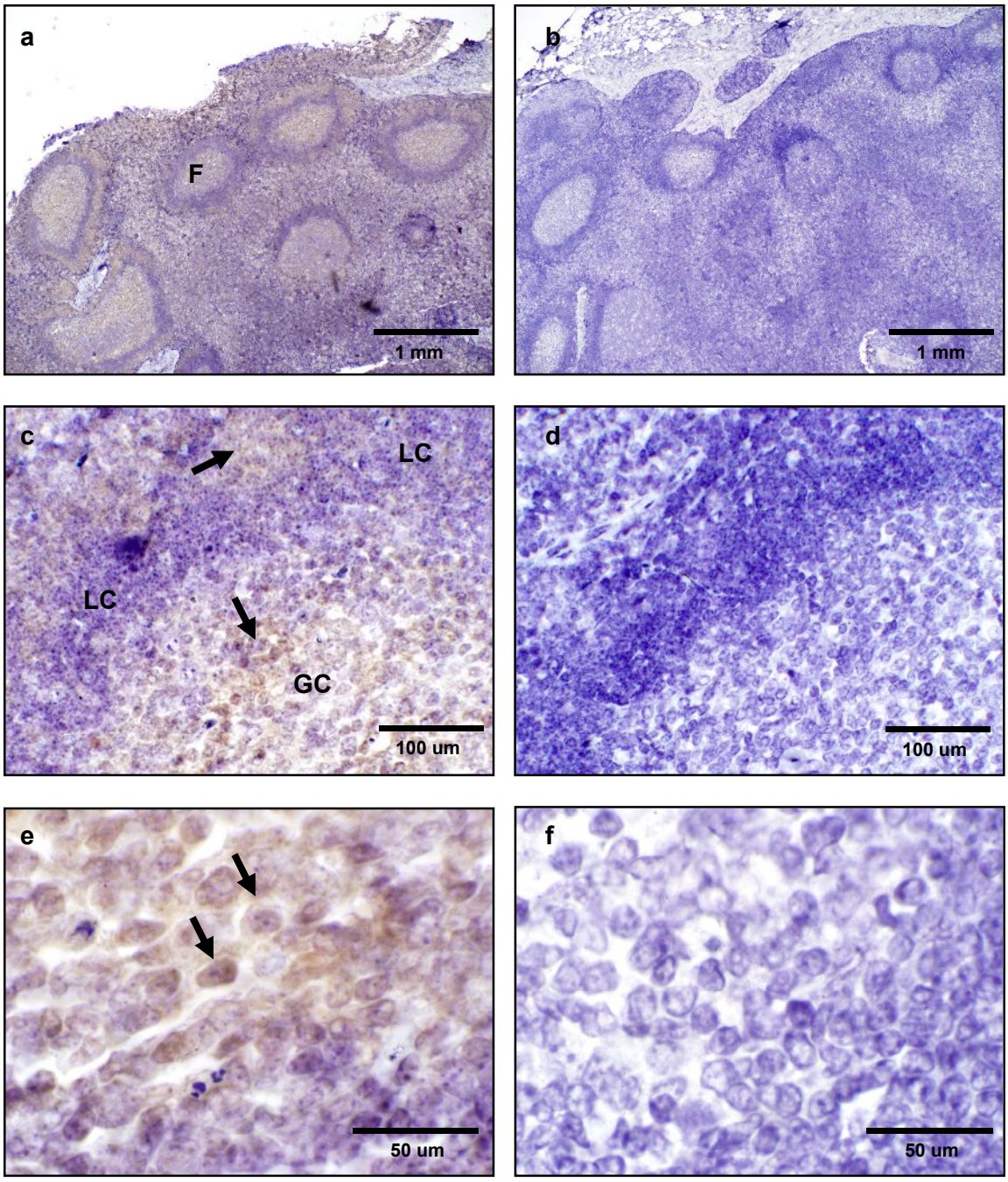

Figure 8. Expression PrP^C in the bovine lymph node. (a) Tissue section shows PrP^C-specific labeling associated with lymphoid follicles in the cortex area. (c,e) Higher magnification evidence of specific PrP^C staining associated with lymphocytes (*arrow*) surrounding the lymphocyte corona (LC) and germinal centers (GC). (b,d,f) Serial section incubated with non-immune horse serum instead of SAF-32 antibody (Negative controls).

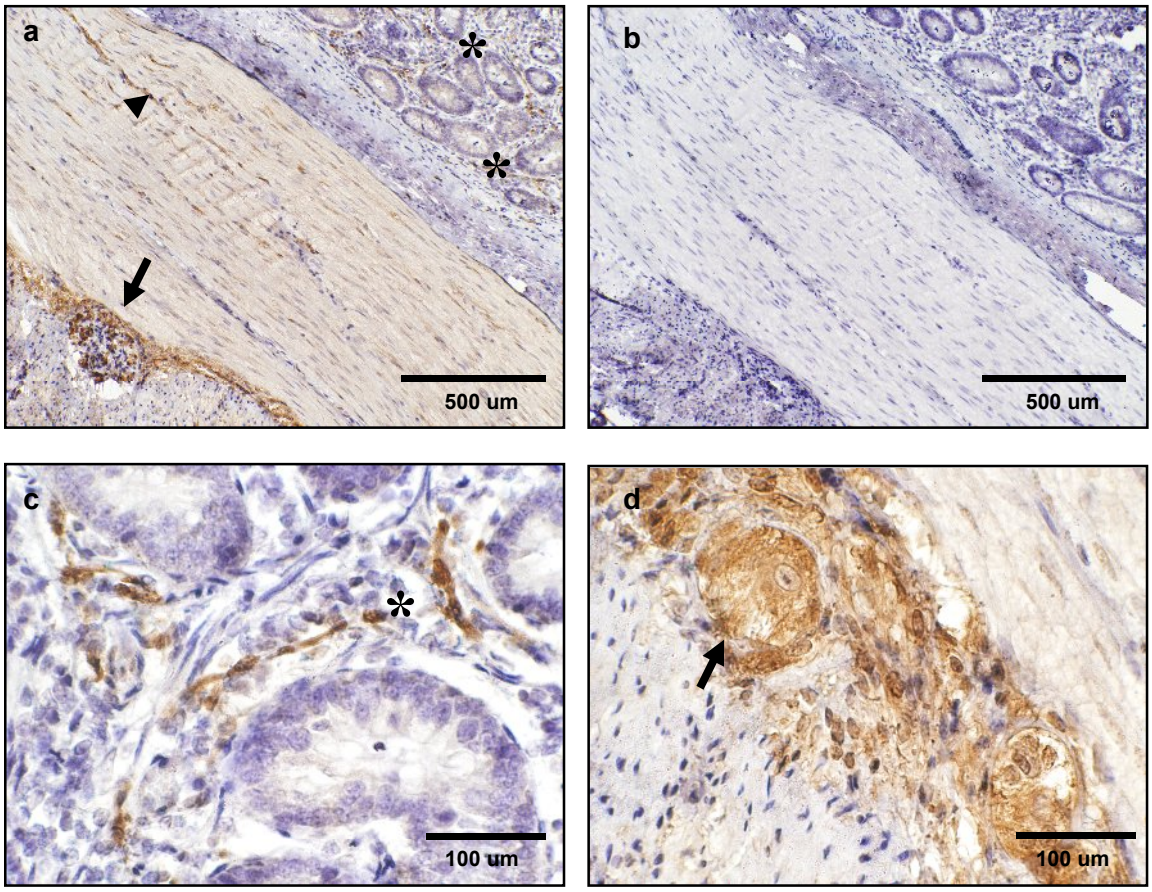

Figure 9. Expression of PrP^C in the bovine ileum. (a) Sagittal tissue section showing PrP^C-specific labeling in enteric mucosa (*), muscularis (*arrowhead*) and myenteric plexus (*arrow*). (c) Higher magnification evidence PrP^C-positive neurons in the lamina propia. (d) PrP^C is highly expressed in parasympathetic ganglion cells forming the myenteric plexus. (b) Serial section incubated with non-immune horse serum instead of SAF-32 antibody (Negative control).

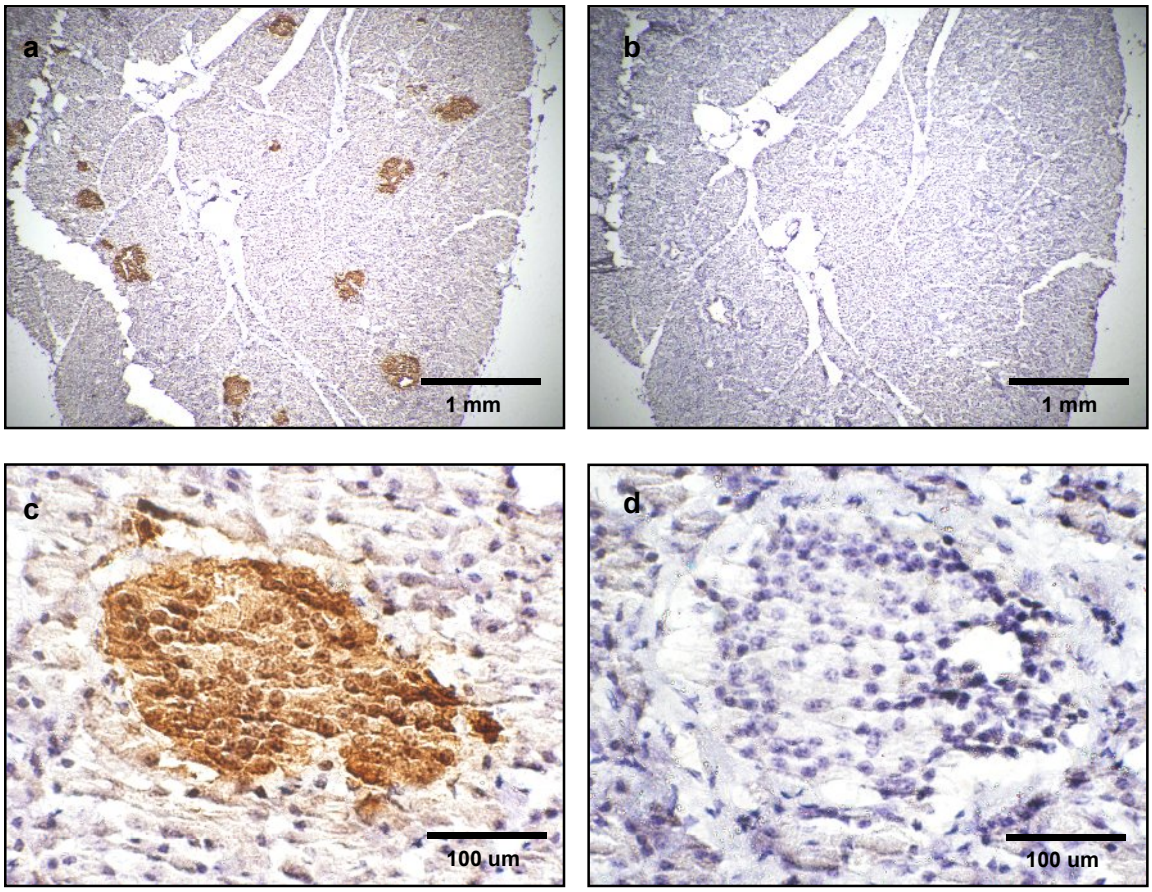

Figure 10. Expression of PrP^C in the bovine pancreas. (a) PrP^C positive staining is restricted to the endocrine pancreas in the islets of langerhans. (c) Higher magnification shows specific PrP^C-positive endocrine cells. (b,d) Serial section incubated with non-immune horse serum instead of SAF-32 antibody (Negative control).

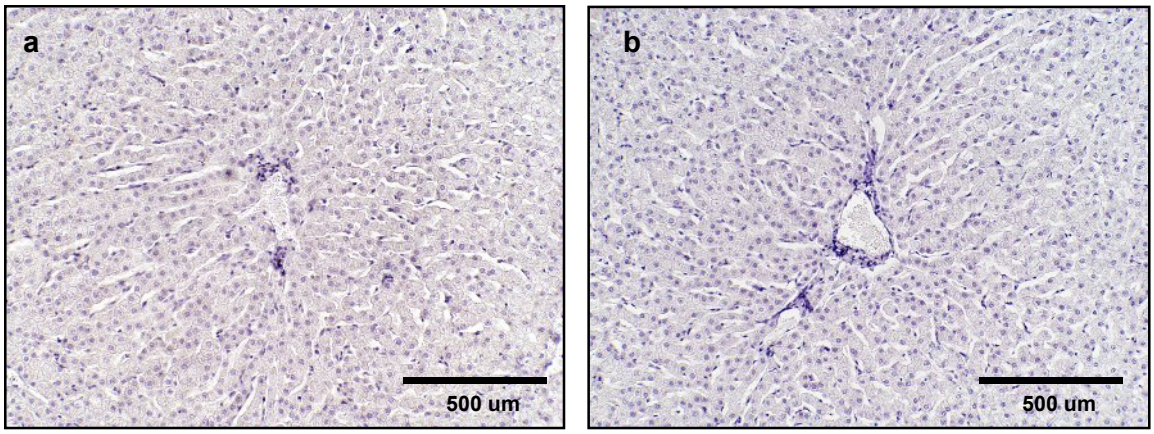

Figure 11. Expression of PrP^C in the bovine liver. (a). No PrP^C staining was observed in the liver tissue after incubation with SAF-32 antibody. (b) Negative control.

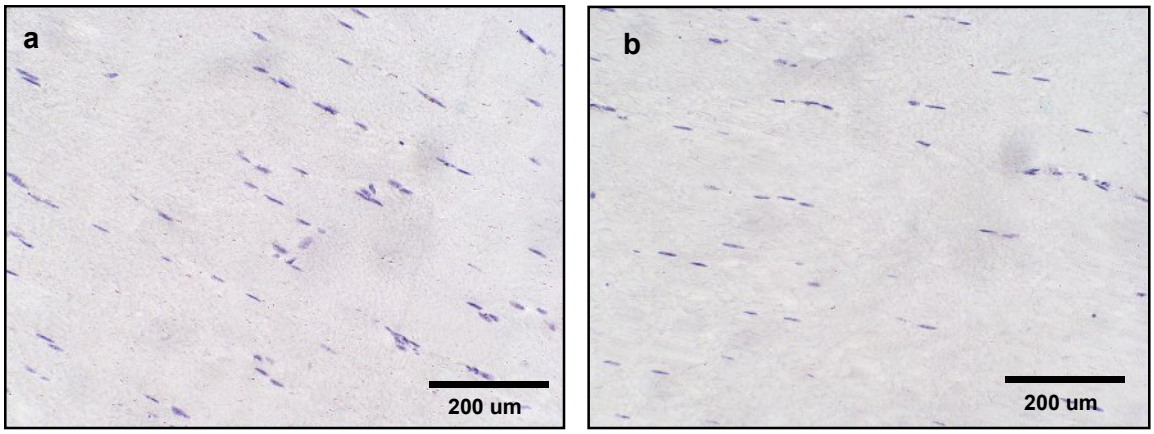

Figure 12. Expression of PrP^C in the bovine skeletal muscle. (a) Tissue section incubated with SAF-32 antibody. No detectable PrP^C expression was observed in the skeletal muscle. (b) Serial section incubated with non-immune horse serum instead of SAF-32 antibody (Negative control).

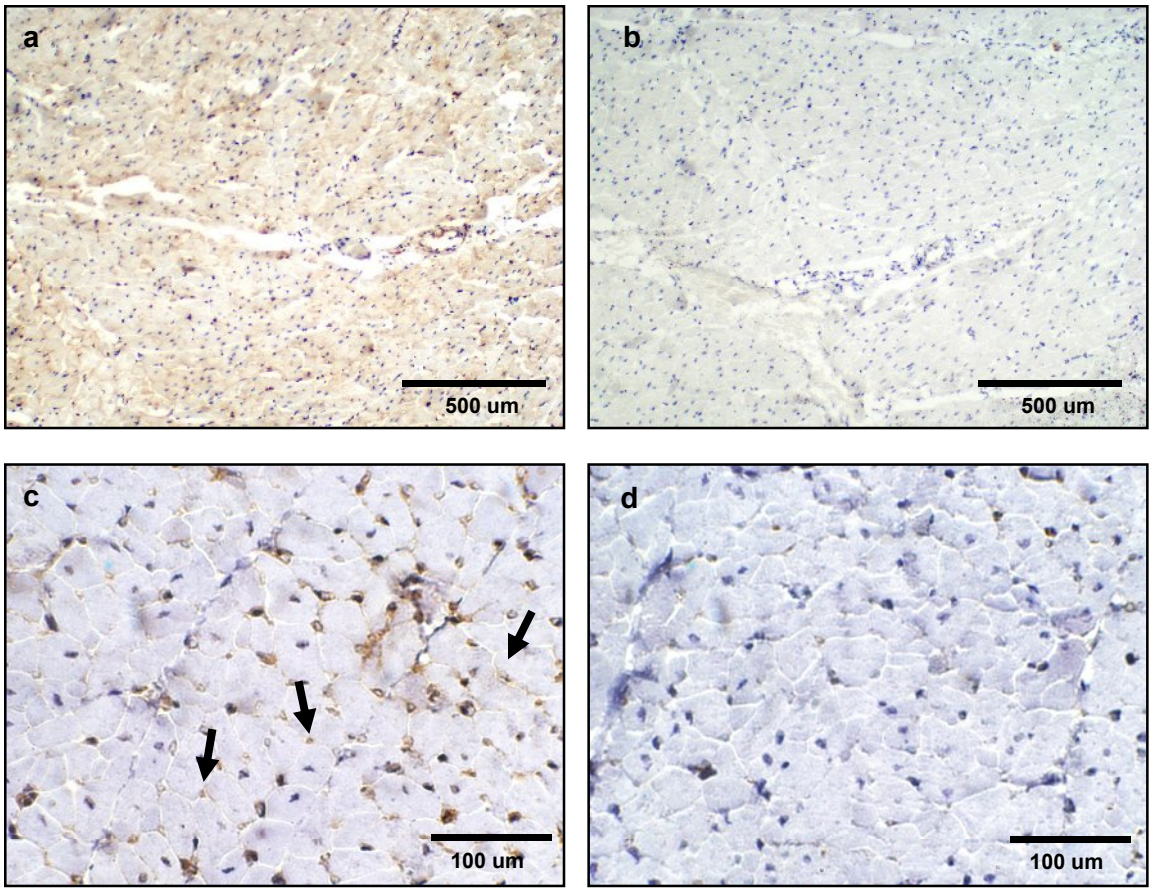

Figure 13. Expression of PrP^C in the bovine cardiac muscle. (a) PrP^C labeling was observed in cardiac muscle cells located in the myocardium. (c) Higher magnification shows PrP^C staining associated with cardiac muscle cells. (b,d) Serial section incubated with non-immune horse serum instead of SAF-32 antibody (Negative control).

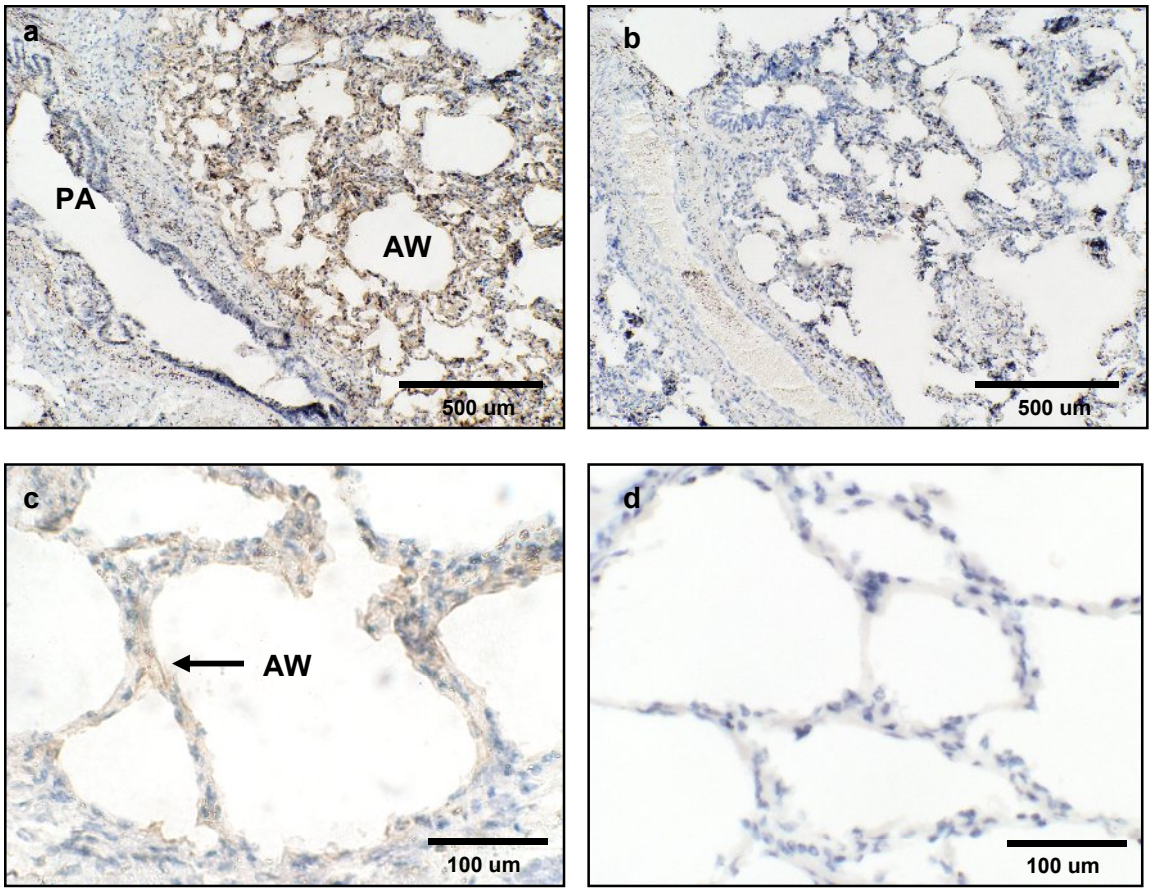

Figure 14. Expression of PrP^C in the bovine lung. (a). PrP^C-specific labeling was observed associated with the alveolar wall (AW). (c) Higher magnification shows PrP^C-specific labeling associated with pneumocites (*arrow*). (b,d) Serial section incubated with non-immune horse serum instead of SAF-32 antibody (Negative control). (PA) Pulmonary artery.

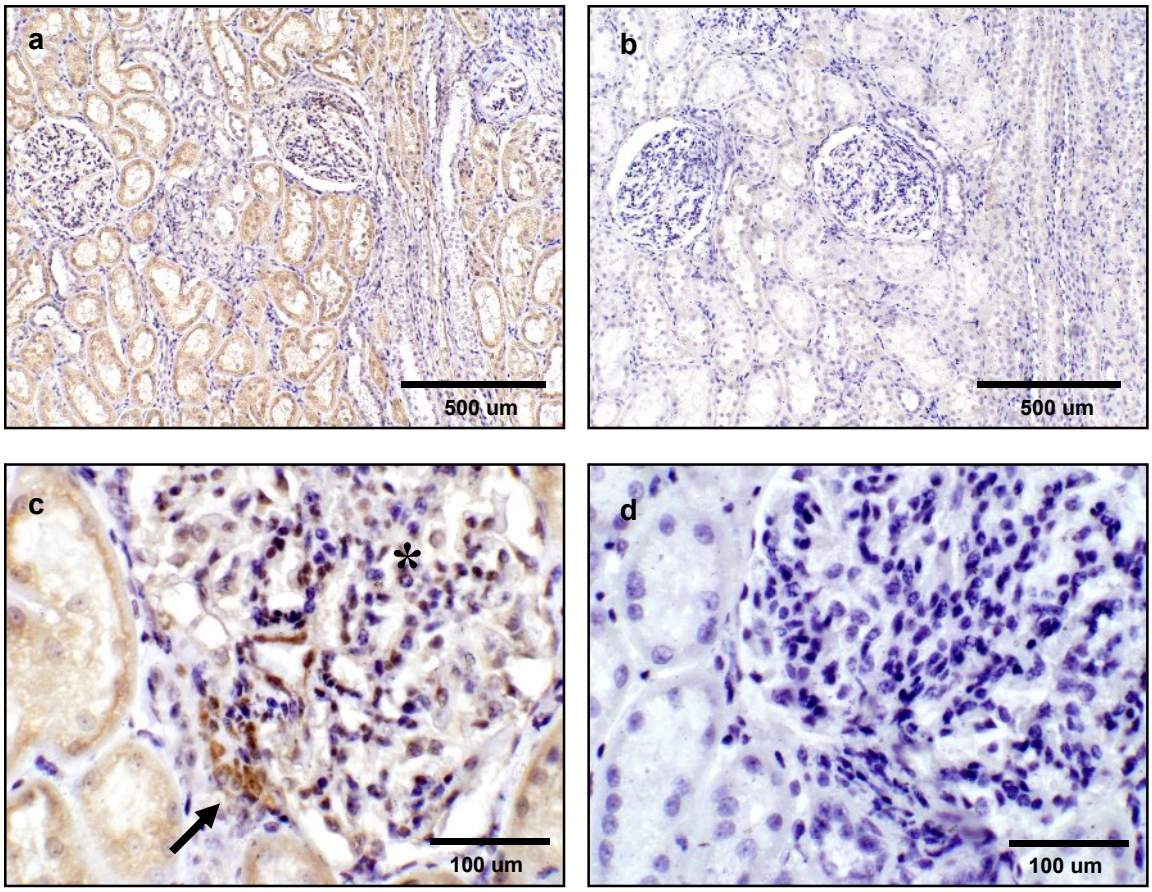

Figure 15. Expression of PrP^C in the bovine kidney. (a) PrP^C expression is associated with cortical convoluted tubules and collective ducts in the medulla. (c) Higher magnification of renal glomerulus shows strong PrP^C staining in extraglomerular mesangial cells (*arrow*). (b,d) Serial section incubated with non-immune horse serum instead of SAF-32 antibody (Negative control). Moderate labeling was detected in podocytes and endothelial cells (*).

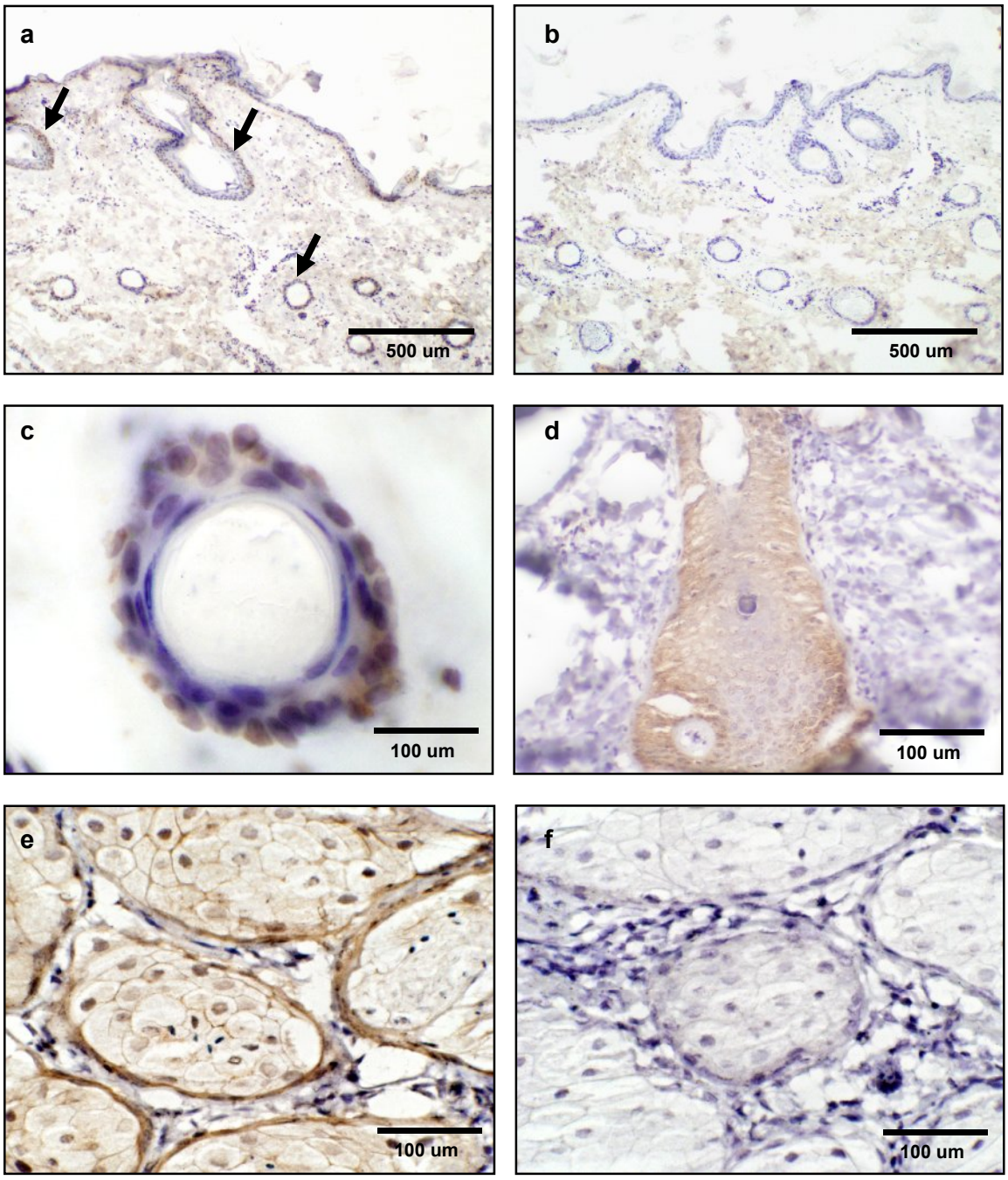

Figure 16. Expression of PrP^C in the bovine skin. (a) PrP^C expression is associated with keratinocytes in the epidermis and hair follicles (*black arrows*). (c) Higher magnification shows that PrP^C is expressed in cells surrounding the hair follicle. (d,e) PrP^C staining was also present in sebaceous glands located in the dermis. (b,f) Serial section incubated with non-immune horse serum instead of SAF-32 antibody (Negative control).

LITERATURE CITED

Amselgruber WM, Steffl M, Didier A, Martbauer E, Pfaff E, Buttner M. 2005. Prion protein expression in bovine podocytes and extraglomerular mesangial cells. Cell Tissue Res. DOI 10.1007/s00441-005-0128-6.

Amselgruber WM, Buttner M, Schlegel T, Schweiger M, Pfaff E. 2006. The normal cellular prion protein (PrPC) is strongly expressed in bovine endocrine pancreas. Histochem Cell Biol 125, 441-448.

Andreoletti O, Morel N, Lacroux C, Rouillon V, Barc C, Tabouret G, Sarradin P, Berthon P, Bernardet P, Mathey J, Lugan S, Costes P, Corbiere F, Espinosa J-C, Torres JM, Grassi J, Schelcher F, Lantier F. 2006. Bovine spongiform encephalopathy agent in spleen from an ARR/ARR orally exposed sheep. J Gen Virol 87, 1043-1046.

Bailly Y, Haeberle A-M, Blanquet-Grossard F, Chasserot-Golaz S, Grant N, Schulze T, Bombarde G, Grassi J, Cesbron J-Y, Lemaire-Vieille C. 2004. Prion protein (PrPC) immunocytochemistry and expression of the green fluorescent protein reporter gene under control of the bovine PrP gene promoter in the mouse brain. J Comp Neurol 473, 244-269.

Bainbridge J, Walker KB. 2005 The normal cellular form of prion protein modulates T cell responses. Immunol Lett 15, 147-150

Bell JE, Ironside JW. 1993. Neuropathology of spongiform encephalopathies in humans. Br Med Bull 49, 738-777.

Bosque PJ, Ryou C, Telling G, Peretz D, Legname G, DeArmond SJ, Prusiner SB. 2001. Prions in skeletal muscle. Proc Natl Acad Sci USA 99, 3812-3817.

Brown DR, Schulzschaeffer WJ, Schmidt B, Kretzschmar HA. 1997. Prion protein-deficient cells show altered response to oxidative stress due to decreased SOD-1 activity. Exp Neurol 146, 104-112.

Brown DR, Schmidt B, Groschup MH, Kretzschmar HA. 1998. Prion protein expression in muscle cells and toxicity of a prion protein fragment. Eur J Cell Biol 75, 29-37.

Brown, KL, Stewart K, Ritchie DL, Mabbot NA, Williams A, Fraser H, Morrison WI, Bruce ME. 1999. Scrapie replication in lymphoid tissues depends on prion protein-expressing follicular dendritic cells. Nat Med 5, 1308-1312.

Brown DR, Nicholas RS, Canevari L. 2002. Lack of prion protein expression results in a neuronal phenotype sensitive to stress. J Neurosci Res 67, 211-224.

Bruce ME, Brown KL, Mabbot NA, Farquar CF, Martin J. 2000. Follicular dendritic cells in TSE pathogenesis. Immunol Today 21, 442-446.

Bueler H, Aguzzi A, Sailer A, Greiner RA, Autenried P, Aguet M and Weissman C. 1993. Mice devoid of PrP are resistant to scrapie. Cell 73, 1339-1347.

Burthem J, Urban B, Pain A, Roberts DJ. 2001. The normal cellular prion protein is strongly expressed by myeloid dendritic cells. Blood 98, 3733-3738.

Buschmann A, Groschup MH. 2005. Highly bovine spongiform encephalopathy-sensitive transgenic mice confirm the essential restriction of infectivity to the nervous system in clinically diseased cattle. J Infect Dis 192, 934-942.

Casalone C, Corona C, Crescio MI, Martucci F, Mazza M, Ru G, Bozzetta E, Acutis PL Caramelli M. 2005. Pathological prion protein in the tongues of sheep infected with naturally occurring scrapie. J Virol 79, 5847–5849.

Chaplin DD, Fu Y-X. 1998. Cytokine regulation of secondary lymphoid organ development. Curr Opin Immunol 10, 289-297.

Collinge J, Whittington MA, Slide KCL, Smith CJ, Palmer MS, Clarke AR, Jefferys JGR. 1994. Prion protein is necessary for normal synaptic function. Nature 370, 295-297.

Criado JR, Sanchez-Alavez M, Conti B, Giacchino JL, Wills DN, Henriksen SJ, Race R, Manson JC, Chesebro B, Oldstone MB. 2005. Mice devoid of prion protein have cognitive deficits that are rescued by reconstitution of PrP in neurons. Neurobiol Dis 19, 255-265.

DeArmond SJ, Qiu Y, Sanchez H, Spilman PR, Ninchak-Casey A, Alonso D, Daggett V. 1999. PrPC glycoform heterogeneity as a function of brain region: implication for selective targeting of neurons by prion strains. J Neuropathol Exp Neurol 58, 1000-1009.

Diaz-San Segundo F, Salguero FJ, de Avila A, Espinosa JC, Torres JM, Brun A. 2006. Distribution of the cellular prion protein (PrP^{C}) in brains of livestock and domesticated species. Acta Neuropathol 112, 587-595.

Ersdal C, Ulvund MJ, Benestad SL, Tranulis MA. 2003. Accumulation of pathogenic prion protein (PrPSc) in nervous and lymphoid tissues of sheep with subclinical scrapie. Vet Pathol 40, 164-174.

Ford MJ, Burton LJ, Morris RJ, Hall SM. 2002a. Selective expression of prion protein in peripheral tissues of the adult mouse. Neuroscience 113, 177-192

Ford M, Burton L, Graham C, Frobert Y, Grassi J, Hall S, Morris R. 2002b. A marked disparity between the expression of prion protein and its message by neurons of the CNS. Neuroscience 111, 5333-551.

Fournier J-G, Escaig-Haye F, Billette de Villemeur T, Robain O, Lasmezas C, Deslys J-P, Dormont D, Brown P. 1998. Distribution and submicroscopic immunogold localization of cellular prion protein (PrPC) in extracerebral tissues. Cell Tissue Res 292, 77-84.

Fournier J-G, Escaig-Haye F, Grigoriev V. 2000. Ultrastructural localization of prion proteins : Physiological and pathological implications. Microscopy Res Tech 50, 76-88.

Fraser H, Dickinson AG. 1978. Studies on the lymphoreticular system in the pathogenesis of scrapie: the role of spleen and thymus. Journal of Comparative Pathology 88, 563-573.

Gavier-Widen D, Stack MJ, Thierry B, Balachandran A, Simmons M. 2005. Diagnosis of transmissible spongiform encephalopathies in animals: a review. J Vet Diagn Invest 17, 508-527.

Guentchev M, Groschup MH, Kordek R, Liberski PP, Budka H. 1998. Severe, early and selective loss of a subpopulation of GABAergic inhibitory neurons in experimental transmissible spongiform encephalopathies. Brain Pathol 8, 615-623.

Halliday S, Houston F, Hunter N. 2005. Expression of PrPC on cellular components of sheep blood. J Gen Virol 86, 1571-1579.

Hamir AN, Miller JM, Cutlip RC. 2004. Failure to detect prion protein (PrPres) by immunohistochemistry in striated muscle tissues of animals experimentally inoculated with agents of transmissible spongiform encephalopathy. Vet Pathol 41, 78-81.

Han C-X, Liu H-X, Zhao D-M. 2006. The quantification of prion gene expression in sheep using real-time RT-PCR. Virus Genes 33, 359-364.

Heikenwalder M, Zeller N, Seeger H, Prinz M, Klohn P-C, Schwarz P, Ruddle NH, Wissmann C, Aguzzi A. 2005. Chronic lymphocytic inflammation specifies the organ tropism of prions. Science 307, 1107-1110.

Huang F-P, Farquhar CF, Mabbot NA, Bruce ME, MacPherson GG. 2002. Migrating intestinal dendritic cells transport PrPSc from the gut. J Gen Virol 83, 267-271.

Iwata N, Sato Y, Higuchi Y, Nohtomi K, Nagata N, Hasegawa H, Tobiume M, Nakamura Y, Hagiwara K, Furuoka H, Horiuchi M, Yamakawa Y, Sat T. 2006. Distribution of PrPSc in cattle with bovine spongiform encephalopathy slaughtered at abattoirs in Japan. Jpn J Infect Dis 59, 100-107.

Kanaani J, Prusiner SB, Diacovo J, Baekkeskov S, Legname G. 2005. Recombinant prion protein induces rapid polarization and development of synapses in embryonic rat hippocampal neurons in vitro. J Neurochem 95, 1373-1386.

Klein MA, Frigg R, Raeber AJ, Flechsig E, Hegyi I, Zinkernagel RM, Wissmann C, Agguzzi A. 1998. PrP expression in B lymphocytes is not required for prion neuroinvasion. Nature Medicine 4, 1429-1433.

Konturek PC, Bazela K, Kukharskyy V, Bauer M, Hahn EG, Schuppan D. 2005. Helicobacter pylori upregulates prion protein expression in gastric mucosa: A possible link to prion disease. World J Gastroenterol 11, 48, 7651-7656.

Kosco-Vilbois MH, Zentgraf H, Gerde J, Bonnefoy JY. 1997. To 'B' or not to 'B' a germinal center? Immunol Today 18, 225-230.

Kovacs GG, Kalev O, Gelpi E, Haberler C, Wanschitz J, Strohscneider M, Molnar MJ, Laszlo L, Budka H. 2004. The prion protein in human neuromuscular diseases. 204, 241-247.

Kubosaki A, Ueno A, Matsumoto Y, Kunio D, Saeki K, Matsumoto Y and Onodera T. Analysis of prion mRNA by in situ hybridization in brain and placenta of sheep. 2000. Biochem and Biophy Res Comm 273, 890-893.

Kubosaki A, Yusa S, Nasu Y, Nishimura T, Nakamura Y, Saeki K, Matsumoto Y, Itohara S, Onodera T. 2001. Distribution of cellular isoform of prion protein in T lymphocytes and bone marrow, analyzed by wild-type and prion protein gene-deficient mice. Biochemical and Biophysical Research Communications 282, 103-107.

Lemaire-Vieille C, Schulze Tobias, Podevin-Dimster V, Follet J, Bailly Y. Blanquet-Grossard F, Decavel J-P, Heinen E, Cesbron J-Y. 2000. Epithelial and endothelial expression of the green fluorescent protein reporter gene under the control of bovine prion protein (PrP) gene regulatory sequences in transgenic mice. PNAS 97, 5422-5427.

Levy V, Lindon C, Harfe BD, Morgan BA. 2005. Distinct stem cell populations regenerate the follicle and interfollicular epidermis. Dev Cell 9, 855-861.

Liu T, Li R, Wong B, Liu D, Pan T, Petersen R, Gambetti P, Sy, MS. 2001. Normal cellular prion protein is preferentially expressed on subpopulations of murine hemopoietic cells. Journal of Immunology. 166, 3733-3742.

Mabbot NA, Brown KL, Manson J, Bruce ME. 1997. T-lymphocyte activation and the cellular form of the prion protein. Immunology 92, 161-165.

Mabbot NA, Mackay F, Minns F, Bruce ME. 2000. Temporary inactivation of follicular dendritic cells delays neuroinvasion of scrapie. Nature Med 6, 719-720.

Marcos Z, Pffeifer K, Bodegas ME, Sesma MP, Guembe L. 2004. Cellular prion protein is expressed in a subset of neuroendocrine cells of the rat gastrointestinal tract. J Histochem Cytochem 52, 1357-1365.

Marcos Z, Bodegas ME, Sesma MP, Guembe L. 2005. Comparative study of PrP^{C} expression in rat, monkey, and cow intestinal tract. Ann NY Acad Sci 1040, 391-394.

Massimino ML, Ferrari J, Sorgato MC, Bertoli A. 2006. Heterogeneous PrPC metabolism in skeletal muscle cells. FEBS Letters 580, 878-884.

McLennan NF, Rennison KA, Bell JE and Ironside JW. 2001. In situ hybridization analysis of PrP mRNA in human CNS tissues. Neuropath and Applied Neurobiol. 27, 373-383.

Milhavet O, Lehmann S. 2002. Oxidative stress and the prion protein in transmissible spongiform encephalopathies. Brain Res Rev 38, 328-339.

Miyazawa K, Kanaya T, Tanaka S, Takakura I, Watanabe K, Ohwada S, Kitazawa H, Rose MT, Sakaguchi S, Katamine S, Yamaguchi T, Aso H. 2007. Immunohistochemical characterization of cell types expressing the cellular prion protein in the small intestine of cattle and mice. Histochem Cell Biol 127, 291-301.

Moleres FJ and Velayos JL. 2007. Expression of PrPC in the rat brain and characterization of a subset of cortical neurons. Brain Res 1174, 143-151.

Mouillet-Richard S, Ermonval M, Chebassier C, Laplanche JL, Lehmann S, Launay JM, Kellermann O. 2000. Signal transduction through prion protein. Science 289, 1925-1928.

Muramoto T, Kitamoto T, Tateishi J, Goto I. 1992. The sequential development of abnormal prion protein accumulation in mice with Creutzfeldt-Jakob disease. Am J Pathol 140, 1411-1420.

Ning ZY, Zhao DM, Liu HX, Yang JM, Cui YL, Meng LP, Wu CD. 2005. Quantification of prion gene expression in brain and peripheral organs of golden hamster by real-time RT-PCR. Animal biotechnol. 16, 55-65.

Pammer J, Weninger W, Tschachler E. 1998. Human keratinocytes express cellular prion-related protein in vitro and during inflammatory skin diseases A J Pathol 153, 1353-1358.

Pammer J, Cross HS, Frobert Y, Tschachler E, Oberhuber G. 2000. The pattern of prion-related protein expression in the gastrointestinal tract. Virchows Arch 436, 466-472.

Pattison IH, Millson GC. 1962. Distribution of the scrapie agent in the tissues of experimentally inoculated goats. J Comp Pathol 72, 233-244.

Priola SA, Vorberg I. 2006. Molecular aspects of disease pathogenesis in the transmissible spongiform encephalopathies. Mol Biotech 33, 71-88.

Roucou X, Gains M, LeBlanc AC. 2004. Neuroprotective functions of prion protein. J Neurosci Res 75, 153-161.

Roucou X, Giannopoulos PN, Zhang Y, Jodoin J, Goodyer CG, LeBlanc A. 2005. Cellular prion protein inhibits proapoptotic Bax conformational change in human neurons and in breast carcinoma MCF-7 cells. Cell Death Differ 12, 783-795.

Sarkozi E, Askanas V, Engel WK. 1994. Abnormal accumulation of prion protein mRNA in muscle fibers of patients with sporadic inclusion-body myositis and hereditary inclusion-body myopathy. Am J Pathol 145, 1280-1284.

Schneider B, Mutel V, Pietri M, Ermonval M, Mouillet-Richard S, Kellermann O. 2003. NADPH oxidase and extracellular regulated kinases ½ are targets of prion protein signaling in neuronal and nonneuronal cells. Proc Natl Acad Sci USA 100, 13326-13331.

Schreuder BE, van Keulen LJ, Vromans ME, Langeveld JP, Smits MA. 1998. Tonsillar biopsy and PrPSc detection in the preclinical diagnosis of scrapie. Vet Rec 142, 564-568.

Seeger H, Heikenwalder M, Zeller N, Kranich J, Schwarz P, Gaspert A, Seifert B, Miele G, Aguzzi A. 2005. Coincident scrapie infection and nephritis lead to urinary prion excretion 310, 324-326.

Shaked GM, Shaked Y, Kariv-Inbal Z, Halimi M, Avraham I, Gabizon R. 2001. A protease-resistant prion protein isoform is present in urine of animals and humans affected with prion disease. J Biol Chem 276, 34, 31479-31482.

Sigurdson CJ, Spraker TR, Miller MW, Oesch B, Hoover EA. 2001. PrP (CWD) in the myenteric plexus, vagosympathetic trunk and endocrine glands of deer with chronic wasting disease. J Gen Virol 82, 2327-2334.

Somerville RA, Birkett CR, Farquhar CF, Hunter N, Goldmann W, Dornan J, Grover D, Hennion RM, Percy C, Foster J, Jeffrey M. 1997. Immunodetection of PrPSc in spleens of some scrapie-infected sheep but not BSE-infected cows. J Gen Virol 78, 2389-2396.

Steele AD, Emsley JG, Ozdinler PH, Lindquist S, and Macklis J. 2006. Prion protein (PrPC) positively regulates neural precursor proliferation during developmental and adult mammalian neurogenesis. PNAS, 103, 3416-3421.

Strom A, Wang G-S, Reimer R, Finegood DT, Scott FW. 2007. Pronounced cytosolic aggregation of cellular prion protein in pancreatic β-cells in response to hyperglycemia. Lab Invest 87, 139-149.

Taraboulos A, Jendroska K, Serban D, Yang SL, DeArmond SJ, Prusiner SB. 1992. Regional mapping of prion proteins in brain. Proc Natl Acad Sci USA 89, 7620-7624.

Terry LA, Marsh S, Ryder SJ, Hawkins SA, Wells GA, Spencer YI. 2003. Detection of disease-specific PRP in the distal ileum of cattle exposed orally to the agent of bovine spongiform encephalopathy. Vet Rec 152, 387-392.

Thielen C, Melot F, Jolois O, Leclercq F, Tsunoda R, Frobert Y, Heinen E, Antoine N. 2001. Isolation of bovine follicular dendritic cells allows the demonstration of a particular cellular prion protein. Cell Tissue Res 306, 49-55.

Thomzig A, Kratzal C, Lenz G, Kruger D, Beekes M. 2003. Widespread PrPSc accumulation in muscles of hamsters orally infected with scrapie. EMBO Rep 4, 530-533.

Thomzig A, Schulz-Schaeffer W, Wrede A, Wemheuer W, Brenig B, Kratzel C, Lemmer K, Beekes. 2007. Accumulation of pathological prion protein PrPSc in the skin of animals with experimental and natural scrapie. PLoS Pathog 3, 5, e66. doi:10.1371/journal.ppat.0030066.

Tichopad A, Pfaffl MW, Didier A. 2003. Tissue-specific expression pattern of bovine prion gene: quantification using real-time RT-PCR. Mol Cell Probes 17, 5-10.

Tobler I, Gaus SE, Deboer T, Achermann P, Fischer M, Rulicke T, Moser M, Oesch B, McBride PA, Manson JC. 1996. Altered circadian activity rhythms and sleep in mice devoid of prion protein. Nature 380, 639-642.

van Keulen LJ, Schreuder BE, Vromans ME, Langeveld JP, Smits MA. 1999. Scrapie-associated prion protein in the gastrointestinal tract of sheep with scrapie. J Comp Pathol 121, 55-63.

Wells GAH, Hancock RD, Cooley WA, Richards MS. 1989. Bovine spongiform encephalopathy: diagnostic significance of vacuolar changes in selected nuclei of the medulla oblongata. Vet Rec 125, 521-524.

Wells GA, Dawson M, Hawkins SA, Green RB, Dexter I, Francis ME, Simmons MM, Austin AR, Horigan MW. 1994. Infectivity in the ileum of cattle challenged orally with bovine spongiform encephalopathy. Vet Rec 135, 40-41.

Wells GAH, Wilesmith JW. 1995. The neuropathology and epidemiology of bovine spongiform encephalopathy. Brain Pathol 5, 91-103.

Wheater PR, Burkitt HG, Young B, Heath JW. 1993. Wheater's functional histology third edition. Churchill Livingstone.

Wong BS, Liu T, Li R, Pan T, Petersen RB, Smith MA, Gambetti P, Perry G, Manson JC,Brown DR, Sy MS. 2001. Increased levels of oxidative stress markers detected in the brains of mice devoid of prion protein. J Neurochem 76, 565-572.

Ye X., Scallet AC., Carp RI. 1997. The 139H scrapie agent produces hypothalamic neurotoxicity and pancreatic islet histopathology: electron microscopic studies. Neurotoxicology 18, 533-545.

CHAPTER III

COMPARATIVE ANALYSIS OF THE EXPRESSION OF THE CELLULAR PRION PROTEIN (PrP^C) IN RUMINANT REPRODUCTIVE TISSUES

INTRODUCTION

The cellular prion protein (PrP^C) is a highly conserved glycoprotein commonly attached by a glycophosphatidylinositol (GPI) anchor to lipid rafts in the plasma membrane. The structure of PrP^C includes two glycosylation sites an octapeptide repeat region is composed of a predominantly α-helicoidal secondary configuration. Our data (see Chapter II) and those of others (Fournier et al., 1998; Brown et al., 2000; Ford et al., 2000) have showed that PrP^C is expressed in a wide variety of tissues including the nervous system, lymph nodes, thymus, intestine, pancreas, and kidney. This widespread expression pattern suggests that PrP^C may have important biological roles; however, its specific function remains unknown. Several lines of *Prnp* null mice have been generated in order to gain insight into the still unknown physiological function of PrP^C. These mice apparently develop and reproduce normally and are resistance to TSE infection (Bueler et al., 1992, 1993). Some studies have reported that PrP^C is able to block some of the signals that initiate apoptosis, suggesting a cell protective function (Roucou et al., 2004 and 2005). Other studies have showed that the histidine-containing octapeptide repeats present in the PrP^C amino acid sequence are able to bind copper ions in a pH-dependent manner (Brown et al., 1997; Walter et al., 2006). The capacity for copper binding suggests that PrP^C may participate as an antioxidant factor that controls the formation of reactive oxygen species catalyzed by copper (Martins et al., 2001). Furthermore, considering its location in the plasma membrane, some researchers have postulated that PrP^C may be involved in transmembrane signaling (Mouillet-Richard et al., 2000; Westergard et al., 2007). PrP^C acting independently or with specific ligands is able to activate several transmembrane signaling pathways including neuronal survival, replication and neurite outgrowth (Graner et al., 2000; Santuccione et al., 2005; Steele et al., 2005).

Among the hypothetical roles for PrP^C there is no indication of a specific function in reproductive physiology. Lines of mice and cattle in which PrP^C has been ablated have shown no evident physiological defects suggesting that PrP^C does not have a critical role in reproduction (Bueler et al., 1992; Richt et al., 2006). However, intense PrP^C expression has been reported in various reproductive tissues in several species. PrP^C expression was strongly detected during spermatogenesis in the mouse testes (Fujisawa et al., 2004), in the epididymis (Ford et al., 2002) and after maturation in human ejaculated sperm (Peoc'h et al., 2002). In the ram genital tract, PrP^C is thought to be synthesized and released in soluble form into the epididymal fluid and processed enzymatically during the epididymal transit (Gatti et al., 2002). In female reproductive

tissues, PrP^C immunodetection showed variable levels of expression in the ovary, oviduct, and uterine endometrium and myometrium in the sheep (Tuo et al., 2001) and the cow (Thumdee et al., 2007). In pregnant ewes, high levels of PrP^C were observed in cotyledons of the chorioallantois, allantoic fluid, and caruncular endometrium, but not in the intercotyledonary chorioallantois and amnion (Tuo et al., 2001). Overall, these studies indicated that PrP^C has a tissue specific pattern of expression in the reproductive system, which suggest a potential role in gamete development, storage or survival.

Under certain circumstances, PrP^C can adopt a pathogenic conformation known as PrP^{Sc} which plays a crucial role in neurodegenerative disorders known as transmissible spongiform encephalopathies (TSEs). Several species are affected by TSEs including human (Creutzfeldt-Jakob disease), bovine (spongiform encephalopathy), cervids (chronic wasting disease) and sheep (scrapie). Because PrP^C can be converted into PrP^{Sc}, tissues expressing high levels of PrP^C bear some risk for conversion and accumulation of PrP^{Sc}. Several studies in TSE-infected ruminants have shown that PrP^{Sc} is accumulated in the CNS (Wells and Wilesmith, 1995), spleen (Andreoletti et al., 2006), intestine (Iwata et al., 2006), Peyer's patches (Terry et al., 2003) and skin (Thomzig et al., 2007). However, in BSE-affected cattle, analyses in reproductive tissues including testis, accessory glands, ovary and uterus showed accumulation of PrP^{Sc} (Wrathall, 2000). Moreover, experimental studies have showed that PrP^{Sc} is not transmitted in cattle by gamete or embryo transfer, indicating that the risk of transmission of PrP^{Sc} through reproductive contact is very low (Wrathall, 2000; Wrathall et al., 2002). Nevertheless, under natural conditions, reproductive tissues such as fetal membranes and placenta expelled after parturition can carry PrP^{Sc} and are believed to be responsible for vertical transmission of scrapie to lambs as well as horizontal transmission to adult sheep (Tuo et al., 2001).

In the present study, we investigated the cellular distribution of PrP^C in bovine and ovine reproductive tissues. Immunohistochemical analyses showed that PrP^C is widely expressed both in male and female reproductive system. Computerized quantification of migration bands in western blot detected higher levels of PrP^C in male compared to female reproductive tissues. In cattle, highest levels of PrP^C were detected in the epididymis, whereas, in the ovine the most intense expression was observed in the testes. Specific antibody staining revealed that PrP^C is expressed in a cell-specific fashion during spermatogenesis and in the epithelium of epididymis, ductus deferens and accessory glands. Intense expression of PrP^C in testis, epithelium and vas deferens suggests a potential role for PrP^C in gamete protection or/and development.

MATERIAL AND METHODS

Tissue collection

All tissue samples were collected from clinically healthy animals slaughtered at a local abattoir. Animals included three Holstein cows (n=3) and three Angus bulls (n=3) ranging from 2 to 6 years. Ovine tissues were obtained from three Merino ewes and three Katahdin rams ranging from 1 to 3 years old. Bovine tissue samples were collected from ovary, uterus, vagina, oviduct, mammary gland, testis, penis, glans, prepuce, vas deferens, vesicular gland and prostate. Ovine tissues samples included ovary, uterus, testis and epididymis. Samples were either frozen at -70° C for western blot or fixed in 10 % formaldehyde for immunohistochemistry.

Western blot

Frozen tissue samples of < 700 mg were thawed and homogenized in lysis buffer (10% w/v; 10 mM Tris, pH 7.4, 150 mM NaCl, 1% Triton-X-100, 1% deoxycholate, 0.1% SDS) using a pestle homogenizer (Fisher Scientific, Hampton, NH, USA). Homogenates were centrifuged at 13,500 rpm for 5 min and the supernatants transferred into a new tube. Total protein concentrations were determined using a Bicinchoninic acid (BCA) kit (Pierce; Rockford, IL) according to the manufacturer's instructions. For protein denaturation, 50 µl of each homogenized sample was mixed with 50 µl of Laemmli buffer (BioRad Laboratories, Hercules, CA, USA) and heated at 98° C for 5 min. Aliquots containing 20 µg of total protein were added to each lane and separated by SDS-PAGE in 12% gels (BioRad). Electrophoresis was performed at 125V for ~60 min. Proteins were then transferred onto PDVF membranes by electroblotting at 100 V for 60 min. Membranes were immersed in blocking buffer (LI-COR Corp., Lincoln, NE, USA) for 1 h with shaking. PrP^C was detected by incubation for 1 h in SAF-32 mouse monoclonal anti-PrP (1:400; Cayman Chemical Company, Ann Arbor, MI, USA) directed against amino acid sequence 59-89 located in the N-terminal octapeptide repeat region of the protein. For reference, membranes were co-incubated in rabbit anti-GAPDH (1:1000; Santa Cruz Biotechnology, Santa Cruz, CA, USA). Both primary antibodies were diluted in 0.1% Tween-20 in blocking buffer. After four washes in

0.1% Tween-20 in phosphate-buffered saline (PBS) for 5 min each, membranes were incubated in secondary IgG fluorescent anti-mouse and anti-rabbit antibodies (1:5000; LI-COR) diluted in 0.1% Tween-20 in blocking buffer for 30 min with shaking. Immunoreactive band intensities of PrP^C were detected and added as integrated intensity values using an Odyssey infrared imaging system (LI-COR). Relative expression of PrP^C was corrected by GAPDH expression and standardized to the highest expression value (obex).

Immunohistochemistry

Formalin-fixed tissues were embedded in paraffin and sectioned at 5-7 µm using a microtome (Historange, LKB Bromma, Sweden). Tissue sections were mounted on adhesive coated slides (Newcomer supply; Middleton, Wisconsin) and incubated overnight at 37 °C. Mounted tissues were deparaffinized in xylene and dehydrated in serial alcohol solutions. Slides were subjected to an unmasking protocol that employed unmasking solution (Vector Laboratories., Burlingame, CA, USA) and autoclaving at 120°C for 1 min. Endogenous peroxidase was blocked by incubation in 3% hydrogen peroxide diluted in 0.1 M PBS (pH 7.4) for 30 min. Tissues were then rinsed two times in PBS and blocked in 2.5% horse serum for 15 min. PrP^C was specifically detected by overnight incubation at room temperature with primary antibody SAF-32 (1:400) diluted in 1.5 % equine serum solution (Vector Laboratories). After two washes in PBS, bound primary antibody was detected using a biotinylated horse anti-mouse secondary antibody complexed to horseradish-peroxidase for 10 min at room temperature (Vector Labs). Immune complexes were visualized using 3,3'-diaminobenzidine (DAB) substrate for 5 min or until the signal became visible. Probed sections were then counterstained with hematoxolin and rehydrated in serial alcohol solutions. Sections were mounted with Permount mounting medium (Fisher Scientific) and coverslides. Neighboring sections processed identically but using horse serum instead of primary antibody, served as negative controls. Digital photos of tissue sections were obtained using bright microscopy (Olympus Vanox-T, Tokyo, Japan).

Immunofluorescence

Semen was collected from two Black Angus bulls and two Suffolk rams proven fertility by electroejaculation. Spermatozoa were washed three times in 8 ml of PBS, spun down at 500 *g* and

resuspended in 1 ml PBS. Smears were prepared by depositing approximately 1.5 x 10^6 of spermatozoa in each glass slide. Air dried smears were fixed with 4% paraformaldehyde for 10 min at room temperature and washed with PBS three times for 10 min each. Slides were dipped in unmasking solution (Vector Labs) at 120° in a pressure cooker for 10 min and washed three times in PBS. Sperm smears were incubated in 3% BSA in PBS for 30 min followed by incubation in SAF-32 primary antibody diluted 1:25 in 1% BSA in PBS overnight at 4°C. The next day, slides were washed three times for 10 min each in PBS followed by incubation for 3 h in Alexa fluor 488 rabbit anti-mouse antibody (Invitrogen Corporation, California, USA) diluted 1:100 in 1% BSA in PBS. After several washes in 0.1 M PBS, the slides were mounted using mounting solution with DAPI (Vector Labs) and visualized under a fluorescent microscope (Olympus, Japan).

Immunofluorescence of paraffinized-embeded ovine testis was performed following the same protocol described for immunohistochemistry. However, the peroxidase inhibition step was omitted and after detection with SAF-32, slides were incubated in Alexa-fluor 594 conjugated rabbit anti-mouse antibody (Invitrogen). Slides were coverslipped using mounting solution with 4', 6-diamidino-2-phenylindole (DAPI) for nuclei visualization and examined under the fluorescent microscope.

Data Analysis

Statistical analyses for quantitative western blot were performed using SAS software (version 9.3.1, SAS Institute Inc., Cary, North Carolina, USA). Tissue samples from each animal was subjected to quantitative western blot in triplicate. Analyses of significance ($P < 0.05$) were performed using One-way ANOVA. Expression values for individual reproductive tissues were compared to expression of PrP^C in the obex using Dunnet's t-test. Significant differences between reproductive tissues were analyzed using Duncan's multiple comparison test.

RESULTS

Analysis of PrP^C by Western blot

Western blot analysis of tissue homogenates revealed the presence of PrP^C in both the bovine and ovine reproductive system. PrP^C showed three main immunoreactive bands corresponding to the di-, mono- and un-glycosylated isoforms of PrP^C (~35, 31 and 29 kDa, respectively; Fig. 1a, 2a, 3a, 4a). The more distinct band was observed at about 35 kDa, with other weakly detected bands at 31 kDa and at 27 kDa. The 35 kDa band showed variable intensities between tissues with some displaying strong immunoreactivity and others lower levels. The 31 kDa and 27 kDa band were weakly immunodetected but showed more consistent intensity among tissues. Computerized quantification of immunoreactive bands detected lower ($P < 0.05$) PrP^C levels in bovine reproductive tissues compared to the bovine obex (Fig. 1b). However, the ovine testes showed statistically similar PrP^C levels compared to the ovine obex (Fig. 2b). Among male tissues, testis and epididymis showed the highest ($P < 0.05$) levels of PrP^C. Intermediate levels were detected in the bovine and ovine ductus deferens and seminal vesicles. All female tissues showed lower ($P < 0.05$) levels of PrP^C expression compared to the obex (3c and 4c). Among female reproductive tissues, the bovine ovary showed the highest ($P < 0.05$) levels of PrP^C. Levels of PrP^C expression were in general higher in male compared to female tissues.

Analysis of PrP^C by Immunohistochemistry

In order to establish the precise cellular localization of PrP^C within the tissues analyzed, we performed immunohistochemistry with anti-PrP SAF-32 antibody. Results are typical for three experimental repetitions. Immunohistochemical results were generally in agreement with the western blot analysis. No staining was observed in the negative control sections incubated with normal horse serum or BSA instead of anti-PrP antibody.

Male reproductive system. At low magnification, staining for PrP^C using antibody SAF-32 was observed in all seminiferous tubules in both the ovine and bovine testicular sections (Fig. 5a and 6a). Inside seminiferous epithelium the staining appeared to be more intensely associated with later stages of spermatogenesis. At higher magnification, weak PrP^C staining was observed in the cytoplasm of spermatogonia, spermatocytes and Sertoli cells (Fig. 5c and 6c). However, an intense staining was observed in the cytoplasmic lobes of spermatids (Fig. 5e,f and 6e,f). Diffusion of the DAB marker present in the immunoperoxidase method can create an even distribution and a false impression of the immunoreactivity throughout the seminiferous tubule.

Therefore, we performed immunofluorescence for specific PrP^C detection using Alexa fluor secondary antibody and DAPI counterstaining (Fig. 7a,b). The pattern of PrP^C fluorescence observed using this method was consistent with the immunoperoxidase staining. PrP^C labeling was intensely associated to spermatids but also appeared to be present in Sertoli cells and spermatocytes.

Observation of the ovine and bovine epididymis at low magnification indicated an intense PrP^C staining associated to the epididymal duct (Fig. 8a and 9a). At higher magnification, the labeling was restricted to the pseudostratified epithelium with stereocilia lining the epididymis duct (8c and 9c). No PrP^C staining was detected in individual spermatozoa observed in the epididymal lumen (Fig. 8d and 9c,d). Weak staining was observed in aggregates of spermatozoa in the epididymal duct lumen probably associated with spermatid residual bodies (Fig. 8c). However, immunofluorescence analysis of bovine and ovine sperm confirmed that PrP^C is present in the mature sperm. PrP^C immunolabeling was intensely detected in the equatorial area in the bovine sperm (Fig. 10 a,c,e). PrP^C labeling in the ovine sperm was different from the bovine, showing specific fluorescence in the acrosome area (Fig. 11 a,c,e). The pseudostratified epididymal epithelium has anatomical continuity and histological similarity with the epithelium of the ductus deferens. PrP^C staining was intense in the pseudostratified epithelia with stereocilia of the ductus deferens showing a similar pattern of staining observed in the epididymis (Fig. 12a). The secretory epithelia of the bovine seminal vesicles displayed moderate intensity of PrP^C staining (Fig. 13a). Seminal fluid observed in glandular acini also showed immunoreactivity for PrP^C (Fig. 13c,d). A similar pattern of staining was observed in the prostate; however, the intensity of the labeling was weaker both in the glandular epithelium and in the secretory fluid compared to the seminal vesicles (Fig. 14a,c,d).

Female reproductive system. Scattered PrP^C immunoreactivity, probably associated with the neural tracts located in the mesovarium was observed in the bovine ovary (Fig. 15a). No PrP^C labeling was present in cells associated with large follicles; however, a weak PrP^C staining was observed in granulosa cells of small follicles (Fig. 15c). Several blood vessels present in the corpus luteum were positive for PrP^C (Fig. 15d).

A more diffuse PrP^C staining was observed in the medulla of the ovine ovary compared to the bovine (Fig. 16a). No signal was detected either in the ovine corpus luteum (Fig. 16 c,d). No immunoreactivity was observed in follicular and theca cells. The oviduct showed undetectable

levels of PrP^C (Fig. 17a). At low magnification, no PrP^C staining was evident in the uterus sections of both species (Fig. 18a and 19a). However, at high magnification, PrP^C immunoreactivity was observed in secretory glands located in the endometrium (Fig. 18c and 19c). PrP^C staining was undetectable in the bovine mammary gland using SAF-32 antibody (Fig. 20a).

DISCUSSION

Previous reports have analyzed expression of PrP^C in various species and organs and showed that PrP^C is not only present in the nervous system but also in several non-neuronal tissues (Fournier et al., 1998; Brown et al., 2000; Ford et al., 2002). Systematic studies of PrP^C expression in bovine tissues are lacking, which is surprising since BSE-infected cattle have been implicated as the source of new variant CJD transmission to humans. In the present study, we investigated the level and the cell-type-specific localization of PrP^C in bovine and ovine reproductive tissues. Our analyses detected a tissue-specific pattern of PrP^C expression throughout the ruminant reproductive system. PrP^C levels were higher in male compared to female tissues. Intense PrP^C staining was detected in seminiferous tubules of the testes and epithelia of the epididymis, ductus deferens and accessory glands.

Previous analysis of mRNA expression by *in situ* hybridization in mice testes indicated that PrP^C is expressed in spermatocytes and round spermatids but not in elongate spermatids and spermatozoa (Fujisawa et al., 2004). However, at the protein level, our study and others have showed that PrP^C is intensely expressed in elongated spermatids (Ford et al., 2002; Peoc'h et al., 2002). The reason for discordance between PrP^C mRNA and protein expression is not clear; however, may be related to protein trafficking or degradation (Ford et al., 2002). During maturation, spermatids shed a large portion of their still interconnected cytoplasm, namely the cytoplasmic lobe, which is released as residual bodies upon spermiation (Sprando and Russell, 1987). PrP^C is highly expressed in the spermatid cytoplasmic lobes and residual bodies, suggesting a role for this protein during the final remodeling and maturation of elongated spermatids.

Our immunofluorescence analyses showed positive reactivity for the PrP^C isoform present in the ejaculated sperm using the MAb SAF-32. This antibody binds the 59-89 amino acid sequence

located in the N-terminal region of PrP^C. Our previous attempts to detect PrP^C in sperm using antibodies SAF-70 and 12F10, designed to bind sequence 142-160 in the C-terminus, were unsuccessful (data not shown). Thus, our data suggest that the PrP^C isoform present in the ejaculated sperm is C-terminally truncated. In agreement with this observation, a previous study characterized the PrP^C present in the mature ovine sperm as a glycosylated 25 kDa isoform, which was C-terminally truncated and therefore only able to react to N-terminal binding antibodies (Ecroyd et al., 2004). This report indicated that sperm PrP^C was associated to membrane lipid rafts predominantly in spermatozoa obtained from testes, cauda epididymis, semen and cytoplasmic droplets. A similar isoform of PrP^C was also characterized in sperm from mouse, hamster, human and bovine (Shaked et al., 1999). Surprisingly, our immunofluorescence analyses indicated that the location of PrP^C in the head of the sperm showed species-specific differences. PrP^C was detected in the equatorial area in the bovine sperm in contrast to the acrosomal location in the ovine. The intense PrP^C-associated fluorescence observed in the acrosomal area of the mature ovine sperm suggests a potential role for this molecule during fertilization. However, a recent study reported that sperm obtained from null PrP^C bulls were morphologically normal and capable of generating embryos after *in vitro* fertilization, suggesting that this potential function of PrP^C is not fundamental for fertilization (Richt et al., 2006).

Previous studies detected the presence of PrP^C in both epididymal fluid and seminal plasma (Gatti et al., 2002; Ecroyd et al., 2004). Interestingly, genital tract fluid is the only location where PrP^C is secreted as a soluble protein and not attached to membranes. PrP^C appeared to be synthesized and secreted inside the epididymis forming a pool of complete protein and also both N- and C-terminally truncated isoforms (Gatti et al., 2002). Our immunohistochemical analysis showed that PrP^C expression occurs in the epididymal epithelium, which is the most probable source for secreted PrP^C. Considering the strong expression of PrP^C that we observed in the epithelium of the ductus deferens and seminal vesicles, we hypothesized that these organs may also participate in PrP^C secretion into the seminal plasma. However, analyses of PrP^C in seminal plasma obtained from vasectomized rams showed that PrP^C is only originated in the epididymis (Gatti et al., 2002). The proteolytic process occurring inside the epididymis may be partially responsible for the different isoforms of PrP^C present in the male reproductive fluid. However, the epididymal epithelium may also influence this phenomenon by secreting different isoforms of PrP^C. The C-terminally truncated isoform present in the sperm membrane may also be transferred from PrP^C secreted by the epididymal epithelium into the seminal plasma.

The intense pattern of PrP^C expression observed in the epididymal epithelium was continuous through the pseudostratified epithelium of the ductus deferens and seminal gland. Interestingly, the epididymis and the ductus deferens have the same embryological origin in the mesonephric duct. The mesonephros is a bilaterally paired structure that serves as a fetal kidney producing urine which is drained by the mesonephric ducts. As part of parallel study, our immunohistochemical analysis for PrP^C in bovine fetuses showed a strong reactivity in the mesonephric epithelium (see Chapter IV). These analyses suggest that the pattern of PrP^C expression in the mesonephros is continued after fetal differentiation and until formation of the adult epididymis and ductus deferens.

The physiological function of PrP^C remains largely unknown. Reports on *Prnp* knockout mice and cattle have revealed no specific phenotypes to suggest a function for PrP^C and indicate that PrP^C may not play a role in normal physiology or reproductive function (Bueler et al., 1992; Richt et al., 2006). It has been hypothesized that the PrP-like protein Doppel (Dpl) may have a compensatory effect for the loss of PrP^C function in several mouse lines thus preventing the manifestation of a clear phenotype. *Dpl* null mice develop normally and have a normal behavior but males are infertile (Genoud et al., 2003; Paisley et al., 2004). The potential functional link between these two proteins appeared when reintroduction of PrP^C in mice lines restored the infertility induced by the *Dpl* knockout (Nishida et al., 1999). However, double-mutant mice lacking both *Prnp* and *Dpl* showed no additional phenotype that could indicate *Dpl* compensation for the absence of PrP^C (Genoud et al., 2003; Paisley et al., 2004). Thus, attempts to deduce the function of PrP^C from the phenotypes of PrP-null mice have been uninformative. However, experiments utilizing cells obtained from PrP-null mice suggest the involvement of PrP^C in diverse cellular functions including protection from oxidative stress (Milhavet and Lehmann, 2002), suppression of apoptosis (Yuan and Yanker, 2000) and cellular differentiation (Steele et al., 2006). A potential protective function of PrP^C in the mature sperm against copper toxicity was reported after copper addition caused a toxic effect in sperm obtained from *Prnp* null mice (Shaked et al., 1999). The C-terminal truncated isoform of PrP^C present in the mature sperm is probably the result of proteolytic cleavages occurring in PrP^C during epididymal transit and especially during the ejaculation process (Blobel, 2000). The remaining N-terminal section contains octapeptide repeats reported as copper-binding sites (Hornshaw et al., 1995). Copper binds specifically to this histidine-containing octapeptide repeats in a pH-dependent and negatively cooperative manner, which may result in a reduced availability for copper toxicity (Walter et al., 2006). However, some studies have questioned the potential role of PrP^C in

controlling copper levels due to the over-physiological concentrations required to activate this property (Westergard et al., 2007). A putative role for PrP^C as a cytoprotective factor against specific stress situations such as high copper concentrations, may explain the requirement of a hyper-physiological stimulus to activate this function. Moreover, a potential cytoprotective role of PrP^C only under specific stress situations is also consistent with the apparent lack of abnormality in PrP^C knockout mice under a normal environment.

Experiments have shown that PrP^C is able to exert a cytoprotective activity against internal or environmental stresses that initiate apoptosis (Roucou and LeBlanc, 2005). This activity has been demonstrated in a variety of cells, including fetal neurons (Yuan and Yanker, 2000), mammary adenocarcinoma cells (Diarra-Mehrpour et al., 2004) and neuroblastoma cells (Qin et al., 2006). The exact mechanism for apoptosis suppression is not clearly understood; however, may be mediated by PrP^C inhibition of Bax pro-apoptotic effect. The capacity of PrP^C to bind copper ions may also contribute to suppress apoptosis initiated by reactive oxygen species (ROS) catalyzed by copper. Several studies have showed that apoptosis is the underlying mechanism of germ cell death during normal spermatogenesis, and it is a major mechanism in regulating spermatogenesis in various mammalian species (Sinha Hikim et al., 1999; Print and Loveland, 2000). A large portion of granulosa cells undergoes apoptosis due to the intense steroidogenic activity which results in a high output of ROS (Tilly, 1996). As such, one could speculate that the presence of PrP^C in these cells may be associated with the control of apoptosis both during spermatogenesis and granulosa steroidogenic function.

Histopathological changes in animals and humans affected by TSEs indicate a high correlation between PrP^C expression and infectivity for PrP^{Sc}. Moreover, conversion of PrP^C into PrP^{Sc} does not occur in PrP^C null mice inoculated with scrapie, indicating the necessity of PrP^C expression in host cells in order to support conversion and replication of PrP^{Sc} (Bueler et al., 1993). Despite the intense expression of PrP^C that we observed in several male reproductive tissues, previous analyses in TSEs-affected animals have not detected PrPSc infectivity in the same tissues. Immunodetection of PrP^{Sc} in testis, epididymis, prostate, seminal vesicles and semen obtained from TSE-infected rams, bucks and bulls was negative (Wrathall, 2000). An early study reported that inoculation of semen obtained from a scrapie-affected ram into lambs resulted in no transmission of scrapie infection (Palmer, 1959). Moreover, an epidemiological report showed that the incidence of BSE among the offspring of infected AI bulls was not statistically different from that in the offspring of unaffected bulls (Wilesmith, 1994). However, some of these studies

have been questioned due to the lack of consideration of variables such as PrP genotype, stage of infection, breed and species.

Our analysis and previous studies evidenced expression of PrP^C in a wide range of tissues in the female reproductive system (Tuo et al., 2001; Thumdee et al., 2007). PrP^C is expressed in the ovary, endometrium and myometrium in sheep and cows. However, as in the male, the distribution of PrP^C expression in female reproductive tissues does not correlate with the accumulation of PrP^{Sc} during infection. Analyses in scrapie-infected pregnant sheep have showed that PrP^{Sc} deposition is restricted to the caruncular endometrium and cotyledonary chorioallantois (Tuo et al., 2001). Placenta and fetal fluids are believed to be source of scrapie transmission under natural conditions from the dam to the lamb by contamination of the wool, mammary gland and lambing area. However, the lack of apparent vertical transmission of TSE infectivity to the embryo/fetus *in utero* has been associated with the undetectable levels of PrP^C expressed in the amnion, which may serve as a barrier that block PrP^{Sc} infectivity originated in the chorioallantois (Tuo et al., 2001). Embryos generated from bulls and cows infected with BSE did not infect cows or calves they produced (Wrathall et al., 2002). There are few studies on the potential of TSE-transmission through sexual contact or reproductive technologies. However, the lack of PrP^{Sc} infectivity observed in reproductive tissues including gametes and embryos suggest that the risk of transmission by reproductive contact is probably low.

In conclusion, our study demonstrated that PrP^C is express in tissue-specific pattern in the ruminant reproductive system and is intensely expressed in male tissues. Intense expression of PrP^C during spermatogenesis suggests the participation of this protein in sperm development and maturation. PrP^C expression in the epithelium of epididymis, ductus deferens, seminal vesicles and prostate suggest that PrP^C may be involved in a protective function of sperm after spermiation and during transit in the reproductive system. In this study we reported for the first time the specific location of PrP^C in the mature bovine and ovine sperm.

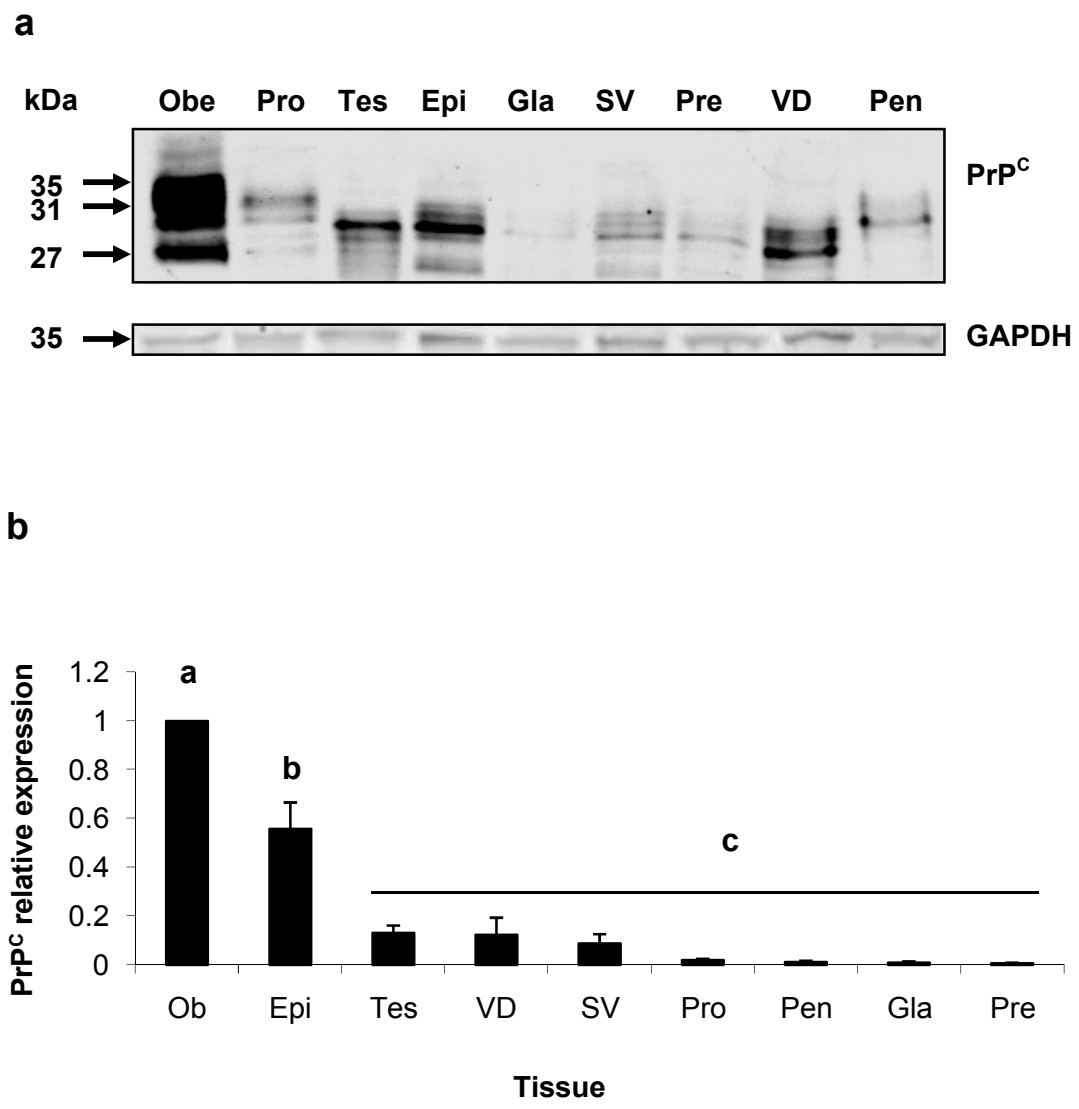

Figure 1. Relative expression of PrP^C in the bovine male reproductive system. (a) PrP^C was detected by SAF-32 antibody using western blot analysis. Migratory bands showed variable intensities and molecular weights of ~35, 31, and 27 kDa for PrP^C isoforms. (b) Reproductive tissues showed lower ($P < 0.05$) levels of PrP^C compared to the obex. Epididymis showed the highest PrP^C expression among reproductive tissues ($P < 0.05$). (a,b,c) Different subscripts indicate significant difference ($P < 0.05$). Ob, Obex; Pro, Prostate; Tes, Testis, Epi, Epididymis; Gla, Glans; SV, Seminal vesicles ; Pre, Prepuce ; VD, Vas deferens ; Pen, Penis.

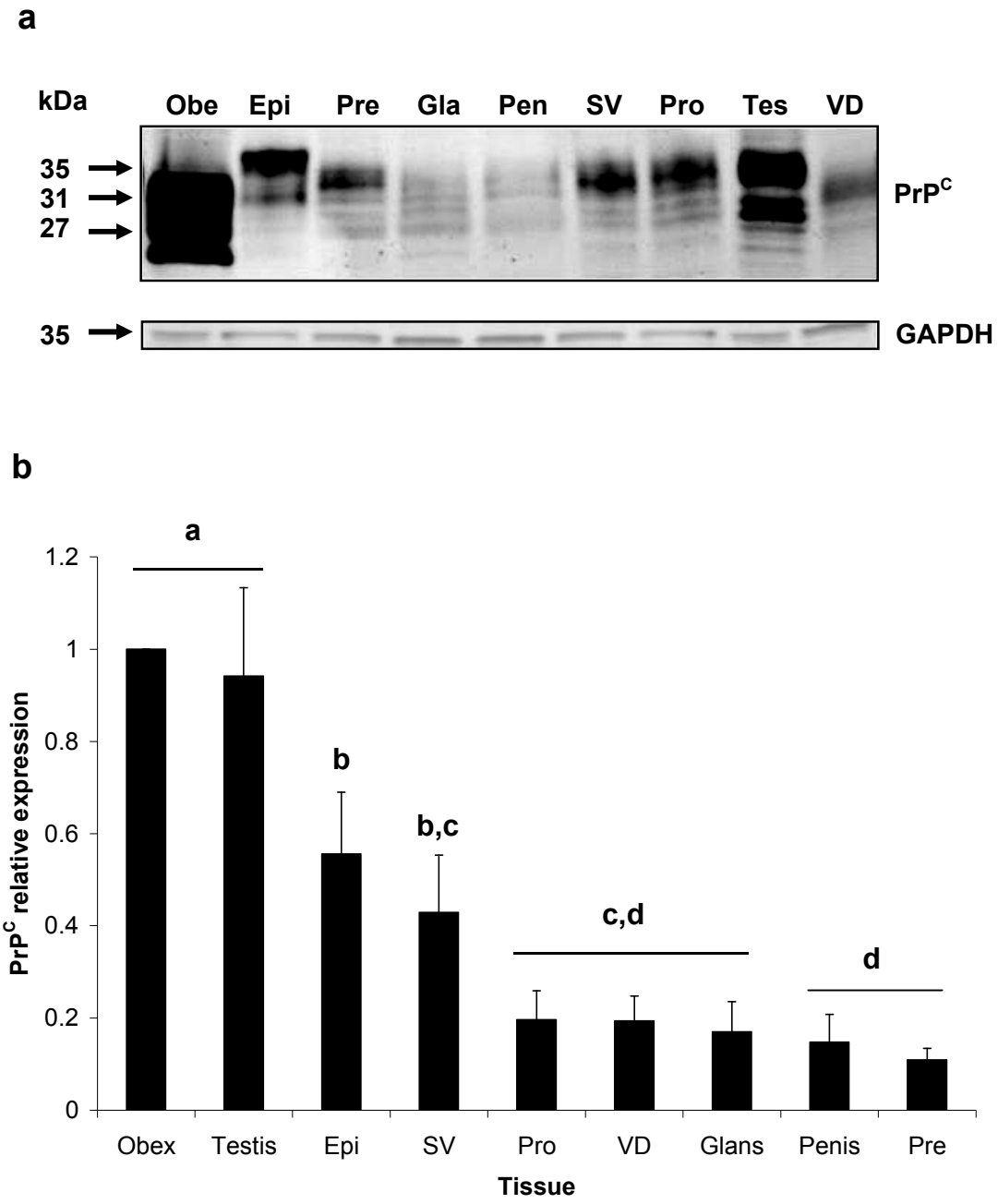

Figure 2. Relative expression of PrP^C in the ovine male reproductive system. Migratory bands showed variable intensities and molecular weights of ~35, 31, and 27 kDa for PrP^C isoforms. Testis showed no difference ($P < 0.05$) in PrP^C expression compared to obex and showed highest levels among reproductive tissues. (a,b,c,d) Different subscripts indicate significant difference ($P < 0.05$). Ob, Obex; Pro, Prostate; Tes, Testis, Epi, Epididymus; Gla, Glans; SV, Seminal vesicles ; Pre, Prepuce ; VD, Vas deferens ; Pen, Penis.

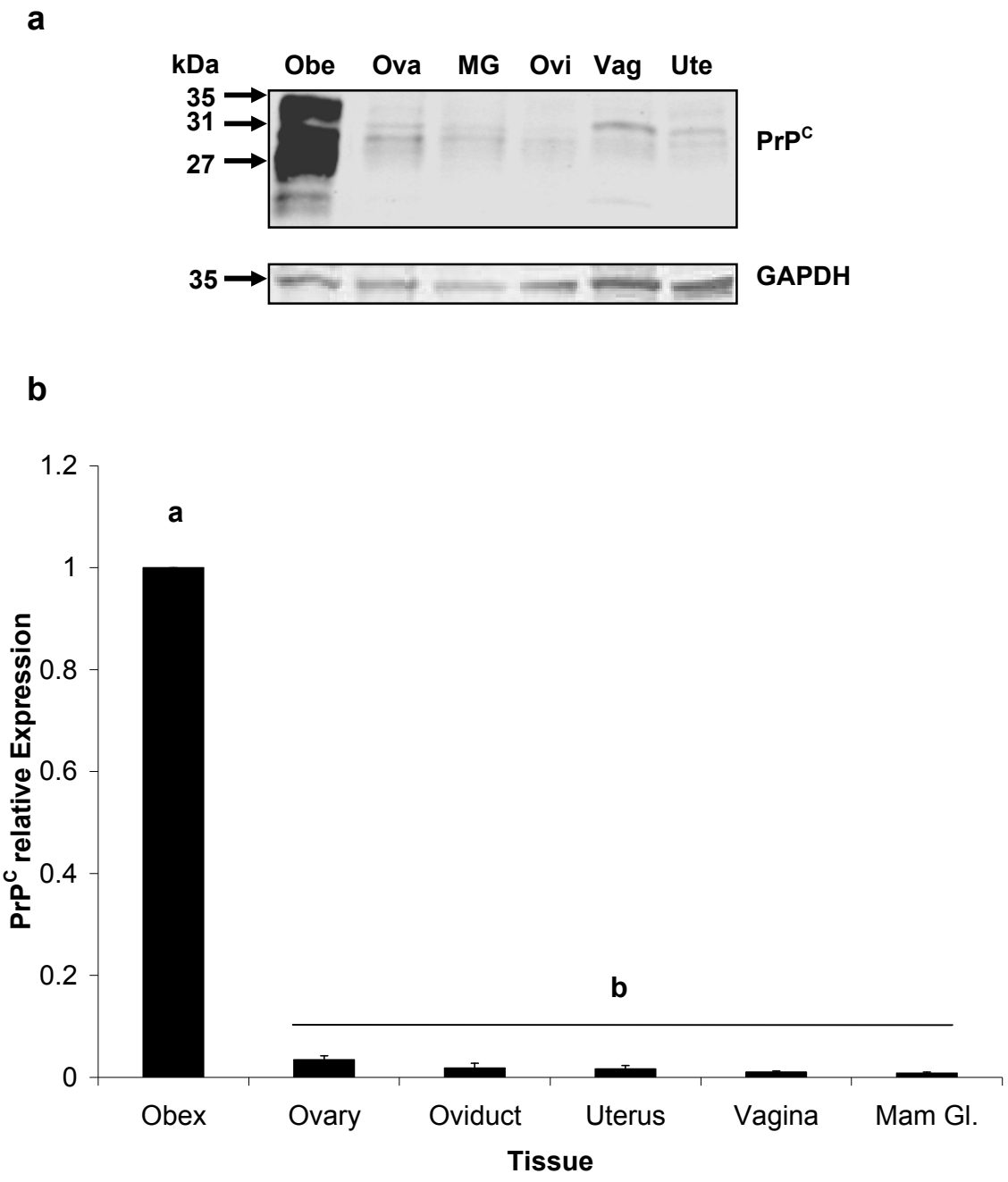

Figure 3. Relative expression of PrP^C in the bovine female reproductive system. (a) PrP^C was detected by SAF-32 antibody using western blot analysis. Migratory bands showed variable intensities and molecular weights of ~35, 31, and 27 kDa for PrP^C isoforms. (b) Reproductive tissues showed lower ($P < 0.05$) levels of PrP^C compared to the obex. (a,b,c,d) Different subscripts indicate significant difference ($P < 0.05$). Obe, Obex; Ova, Ovary; MG, Mammary gland; Ovi, Oviduct; Vag, Vagina; Ute, Uterus.

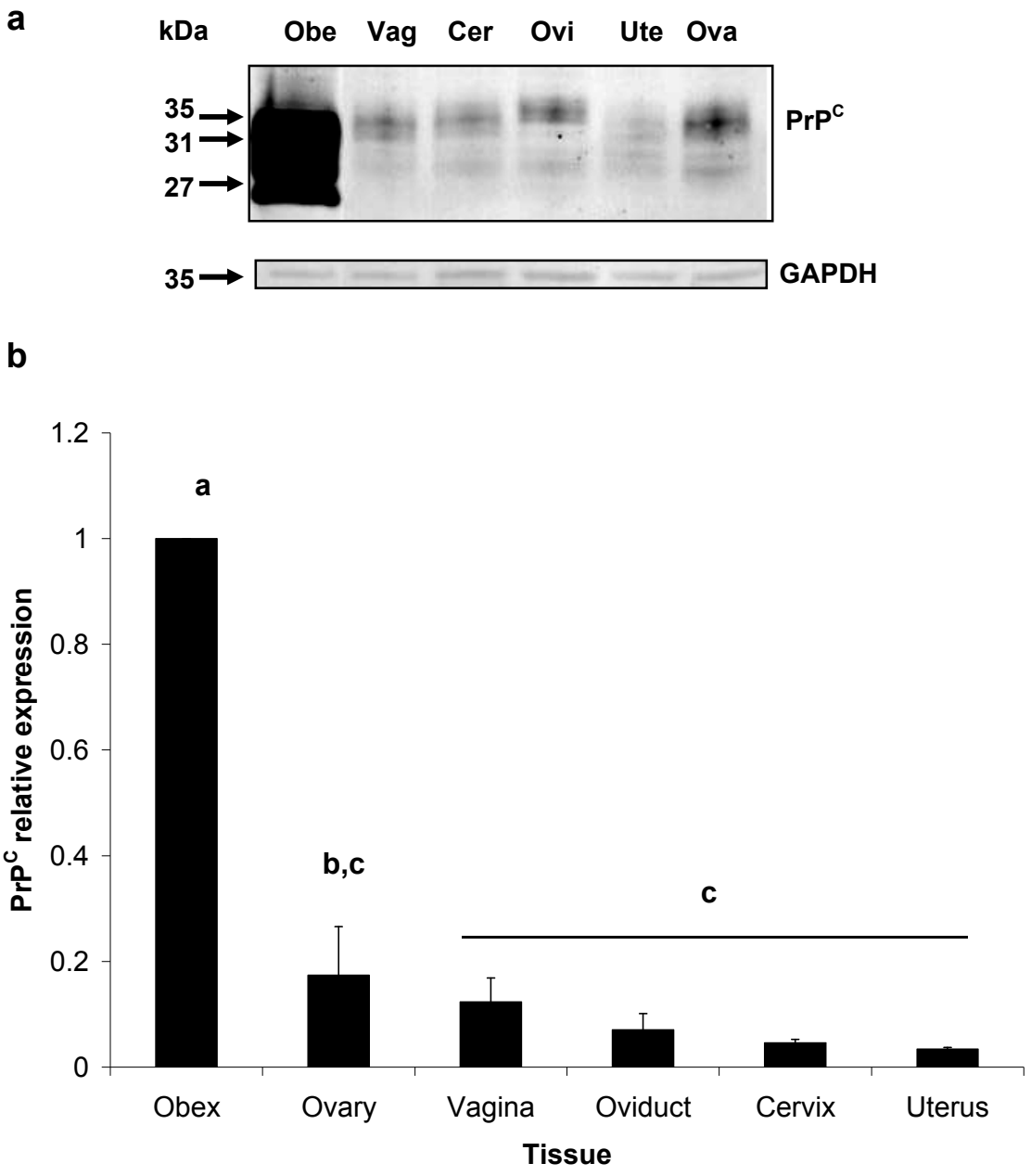

Figure 4. Relative expression of PrP^C in the ovine female reproductive system. Migratory bands showed variable intensities and molecular weights of ~35, 31, and 27 kDa for PrP^C isoforms. Reproductive tissues showed lower ($P < 0.05$) levels of PrP^C expression compared to obex. Ovary showed the highest levels of PrP^C expression among reproductive tissues ($P<0.05$). (a,b,c,d) Different subscripts indicate significant difference ($P < 0.05$). Obe, Obex; Ova, Ovary; MG, Mammary gland; Ovi, Oviduct; Vag, Vagina; Ute, Uterus.

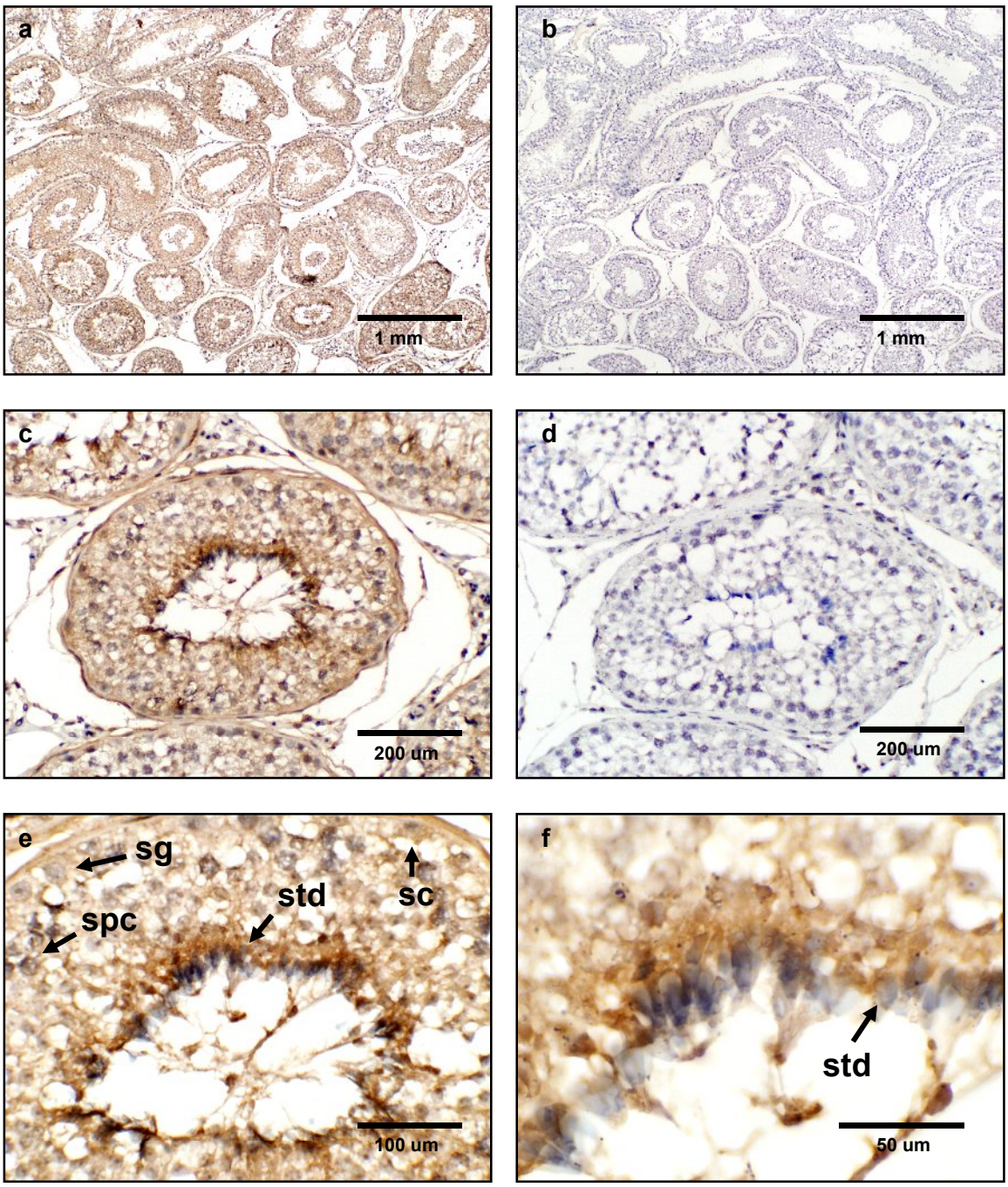

Figure 5. Expression of PrP^C in the bovine testis. (a) Tissue sections were incubated with SAF-32 monoclonal antibody and labeled with peroxidase. PrP^C staining was observed associated with seminiferous tubules. (c,e,f) Spermatids showed intense PrP^C labeling in the cytoplasm. Spermatogonia, spermatocytes and sertoli cells showed weak. (b,d) Tissue sections were incubated with non-immune horse serum instead of SAF-32 as a negative control. Abbreviations: sc, Sertolli cell; sg, spermatogonia; spc, spermatocyte; std, spermatid.

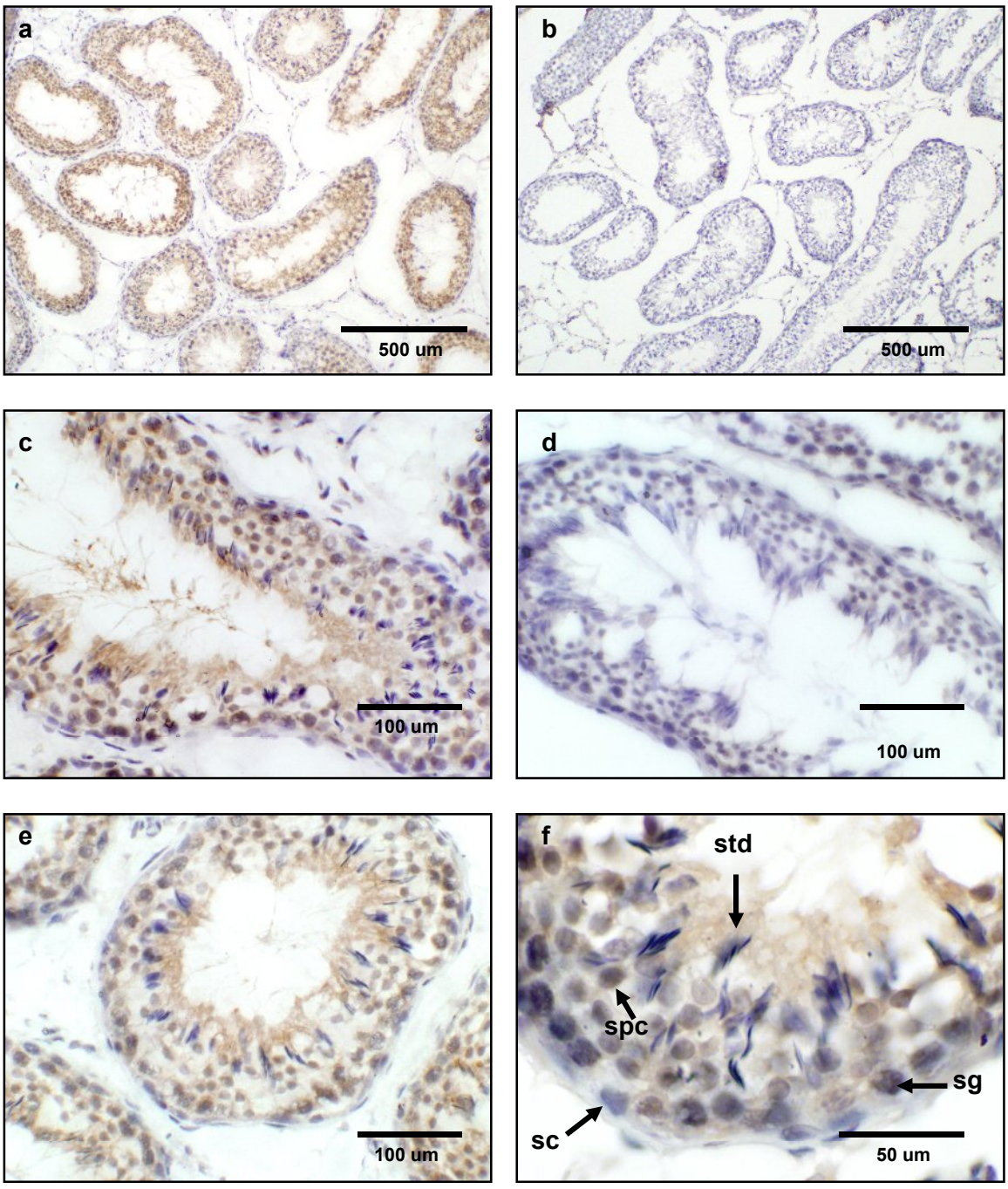

Figure 6. Expression of PrP^C in the ovine testis. (a) PrP^C staining was observed associated to seminiferous tubules. (c,e) Inside seminiferous tubules, spermatocytes and spermatids immunoreacted for PrP^C. (f) Spermatogonia and sertoli cells showed weak PrP^C labeling. Tissue sections were incubated with non-immune horse serum instead of SAF-32 as a negative control (b,d). Abbreviations: sc, Sertolli cell; sg, spermatogonia; spc, spermatocyte; std, spermatid.

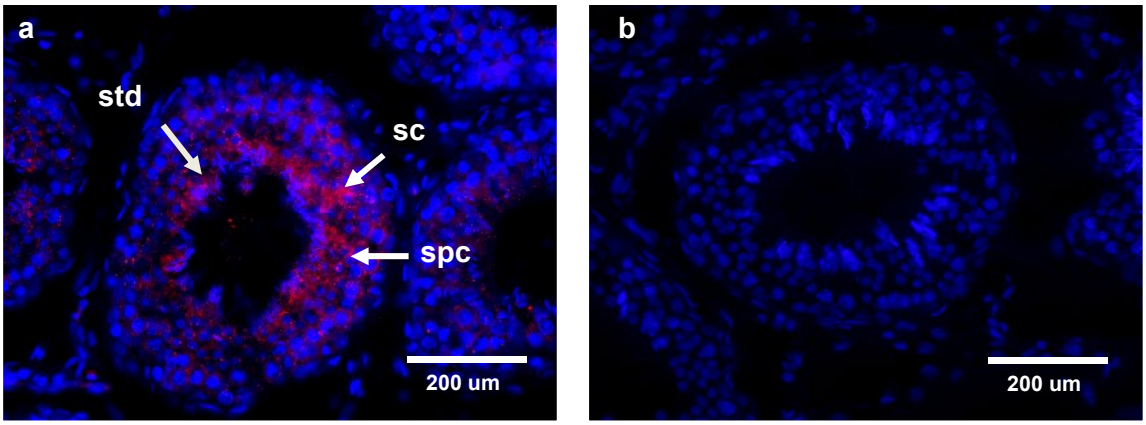

Figure 7. Expression of PrP^C in the bovine testis. (a) Tissue sections were incubated with SAF-32 monoclonal antibody followed by Alexa-fluor 594. PrP^C labeling was observed associated with sertoli cells, spermatocytes and spermatids in the seminiferous tubules. (b) Tissue sections were incubated with non-immune horse serum instead of SAF-32 as a negative control. Abbreviations: sc, Sertoli cell; sg, spermatogonia; spc, spermatocyte; std, spermatid.

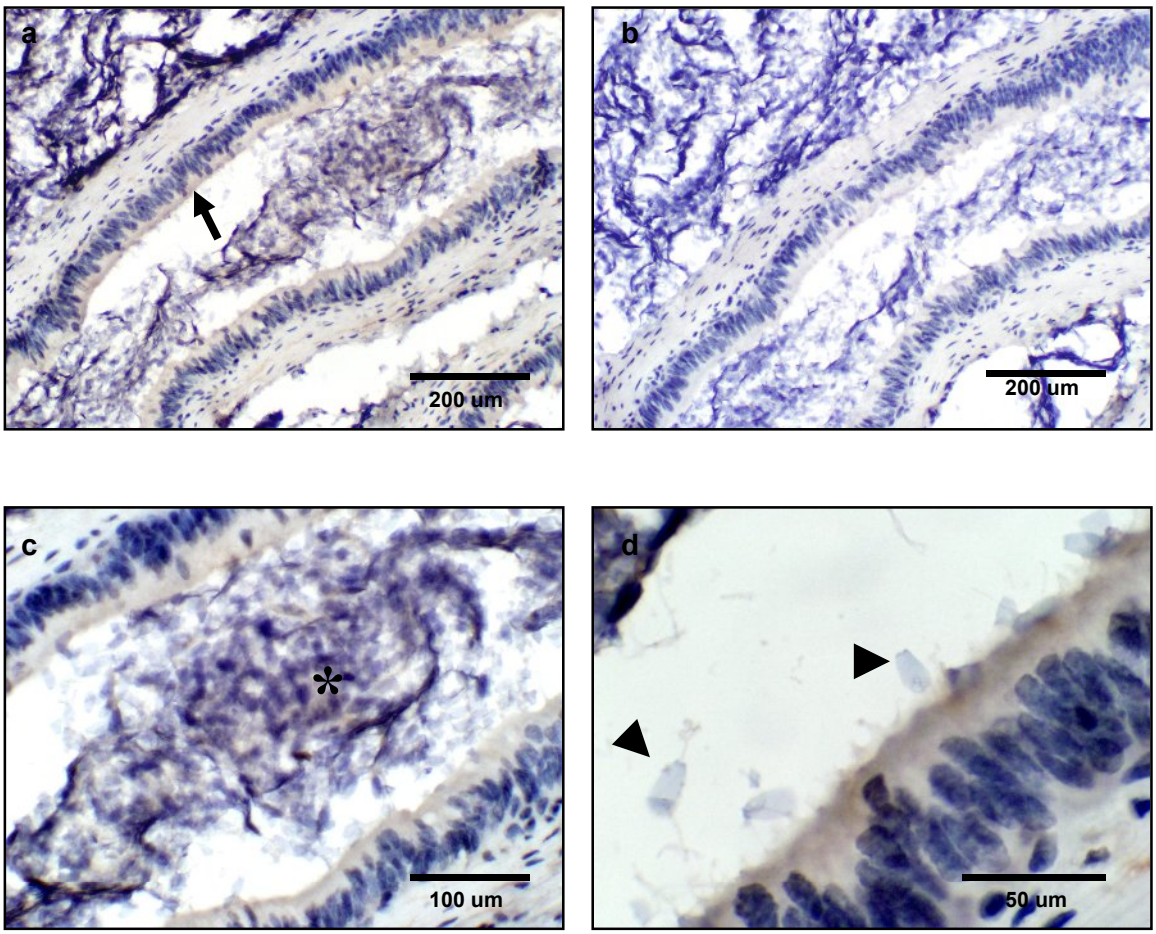

Figure 8. Expression of PrP^C in the bovine epididymis. (a,c,d) PrP^C staining was restricted to the pseudostratified epithelium lining the epididymal duct (*black arrow*). Weak immunoreactivity for PrP^C was observed in residual bodies of speramtids in the epididymis (*). (d) Spermatozoa showed no PrP^C immunoreactivity (*arrow head*). (b)Sections incubated with non-immune horse serum instead of SAF-32 were used as negative controls.

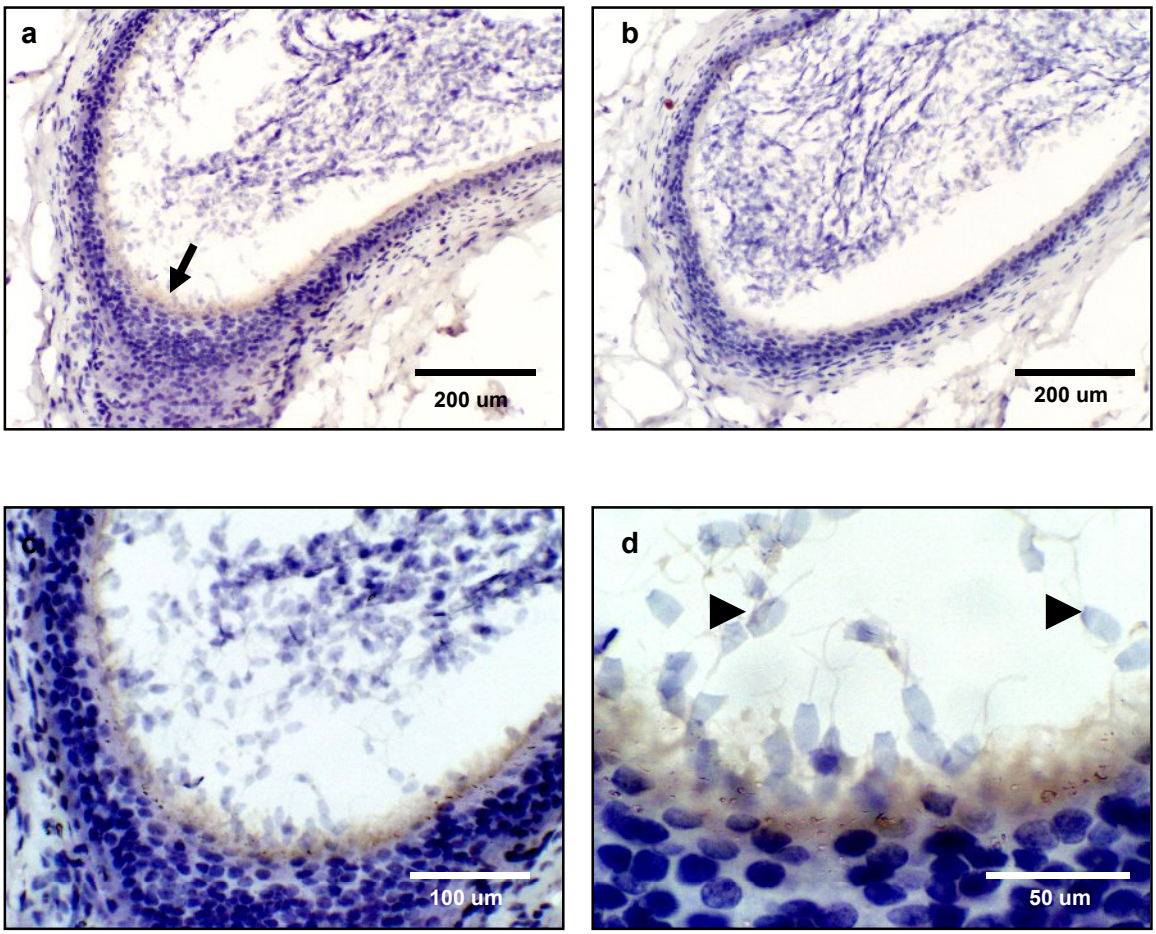

Figure 9. Expression of PrP^C in the ovine epididymis. (a) PrP^C staining was detected in the pseudostratified epithelium lining the epididymal duct (*black arrow*). (c,d) No staining was detected in spermatozoa located in the lumen (*arrow head*). (b) Serial sections were incubated with non-immune horse serum instead of SAF-32 as a negative control.

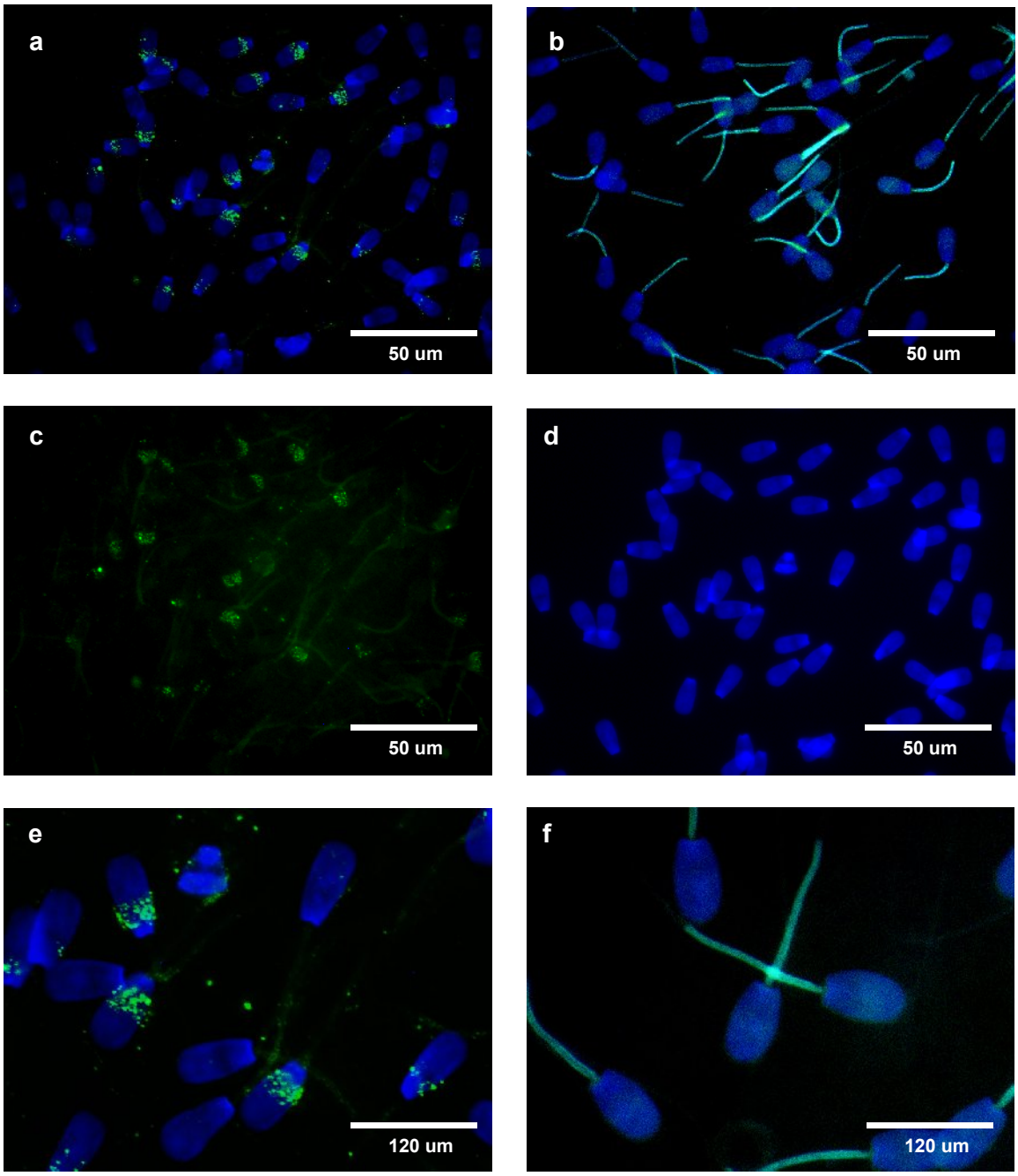

Figure 10. Expression of PrP^C in the bovine sperm. Sperm smears were incubated with SAF-32 monoclonal antibody followed by Alexa-fluor 488 secondary antibody and counterstained with DAPI. (a,c,e) PrP^C immunofluorescence was observed in the equatorial area of the spermatozoa. (b,d,f) Sections were incubated with non-immune horse serum instead of SAF-32 as a negative control.

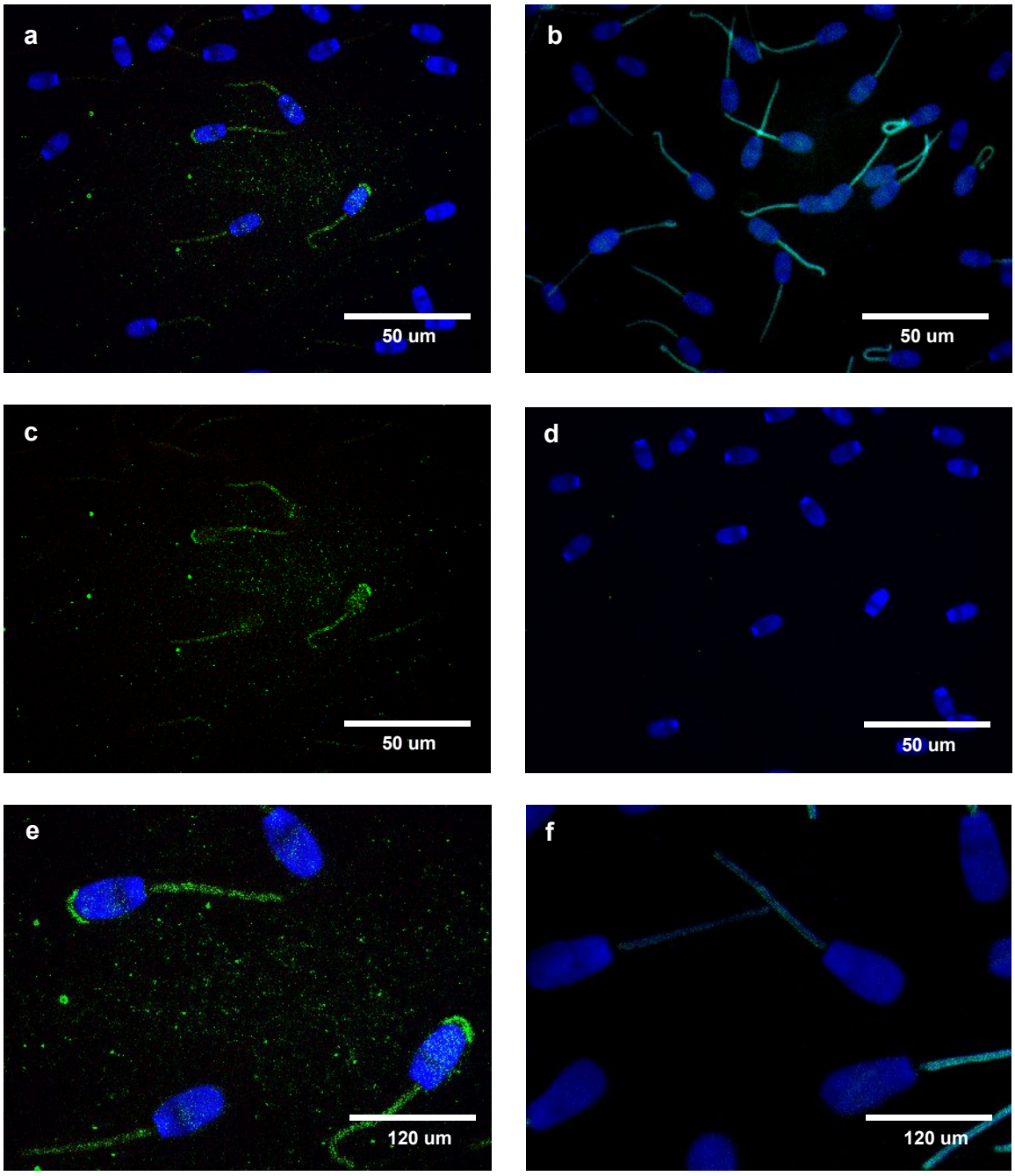

Figure 11. Expression of PrP^C in the ovine sperm. Sperm smears were incubated with SAF-32 monoclonal antibody followed by Alexa-fluor 594 secondary antibody and counterstained with DAPI. (a,c,e) PrP^C immunofluorescence was observed in the acrosome area of the spermatozoa. (b,d,f) Sections were incubated with non-immune horse serum instead of SAF-32 as a negative control.

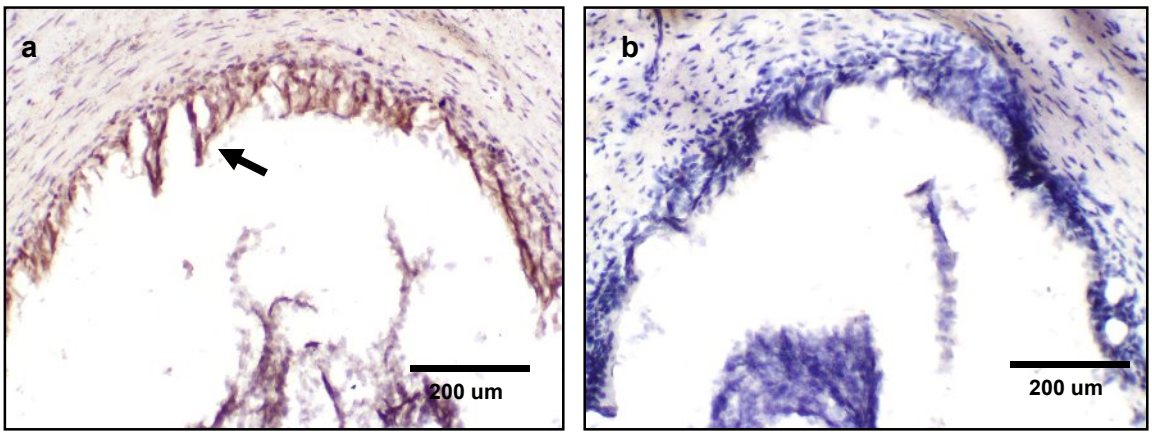

Figure 12. Expression of PrP^C on the bovine ductus deferens. Sections (a) PrP^C staining was detected in the pseudostratified epithelium and stereocilia lining the ductus deferens (*black arrow*). (b) Serial sections were incubated with non-immune horse serum instead of SAF-32 as a negative control.

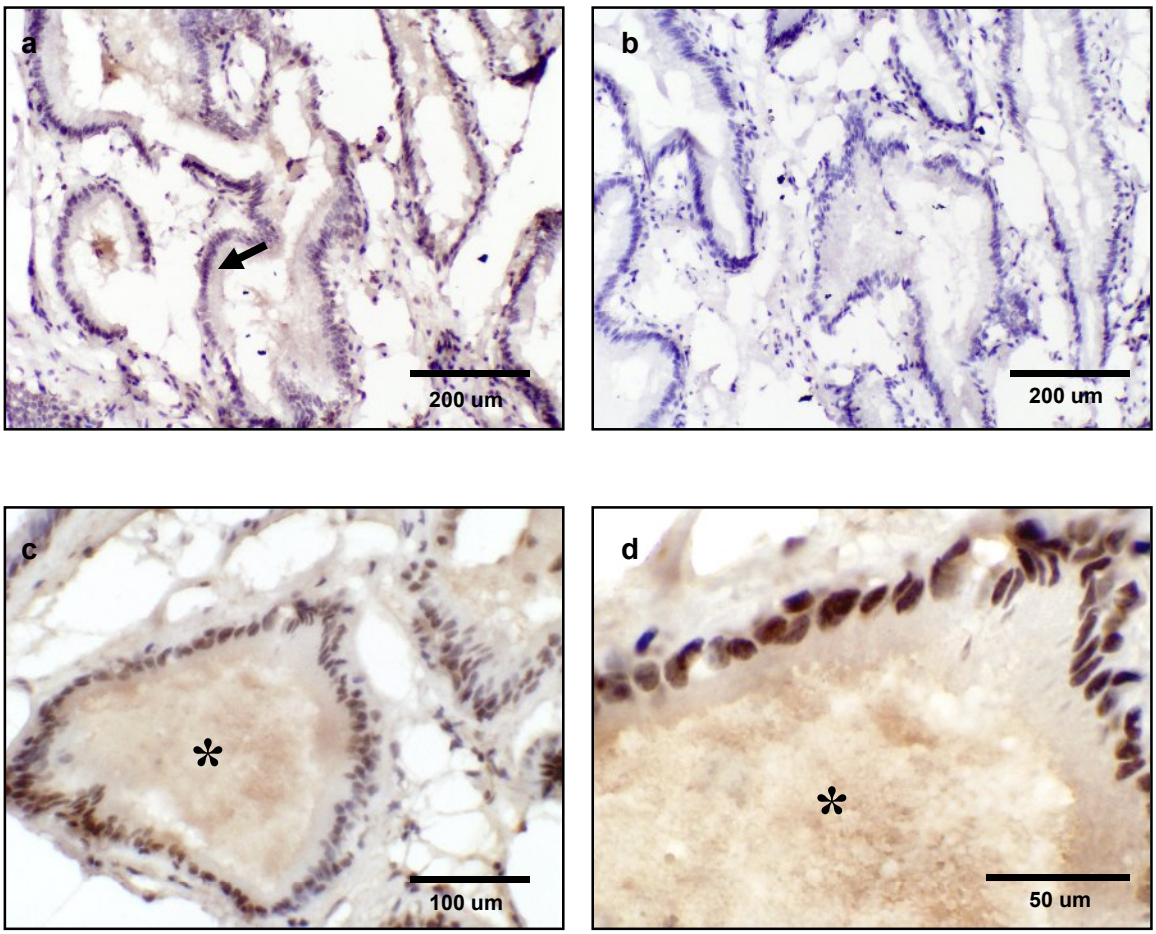

Figure 13. Expression of PrP^C in the bovine seminal glands. (a) PrP^C staining was observed in the secretory epithelium (*black arrow*). (c,d) Seminal fluid also immunoreacted for PrP^C (*). (b) Sections were incubated with non-immune horse serum instead of SAF-32 as a negative control.

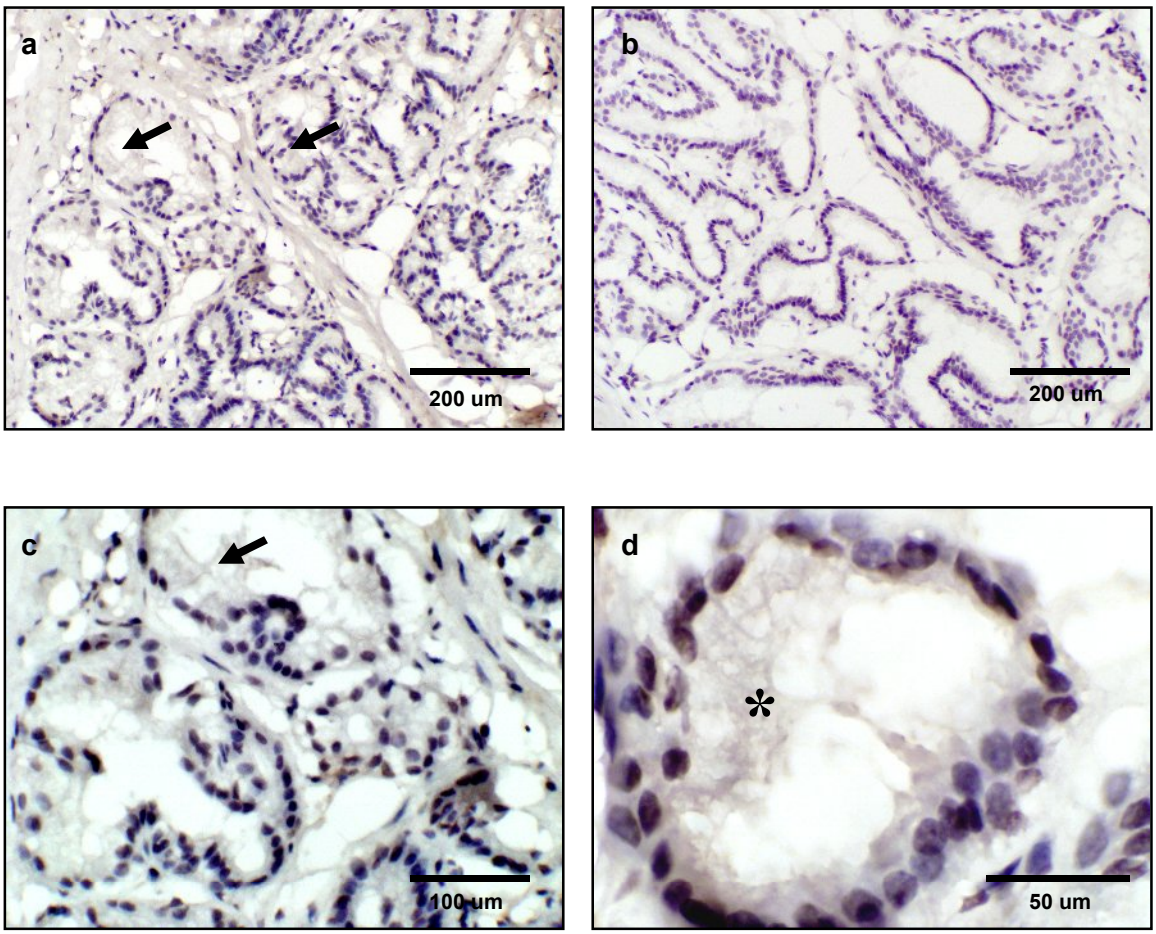

Figure 14. Expression of PrP^C in the bovine prostate. (a,c) PrP^C staining was observed in the secretory epithelium (black arrow). (d) Prostate fluid immunoreacted weakly to PrP^C (*). (b) Sections were incubated with non-immune horse serum instead of SAF-32 as a negative control.

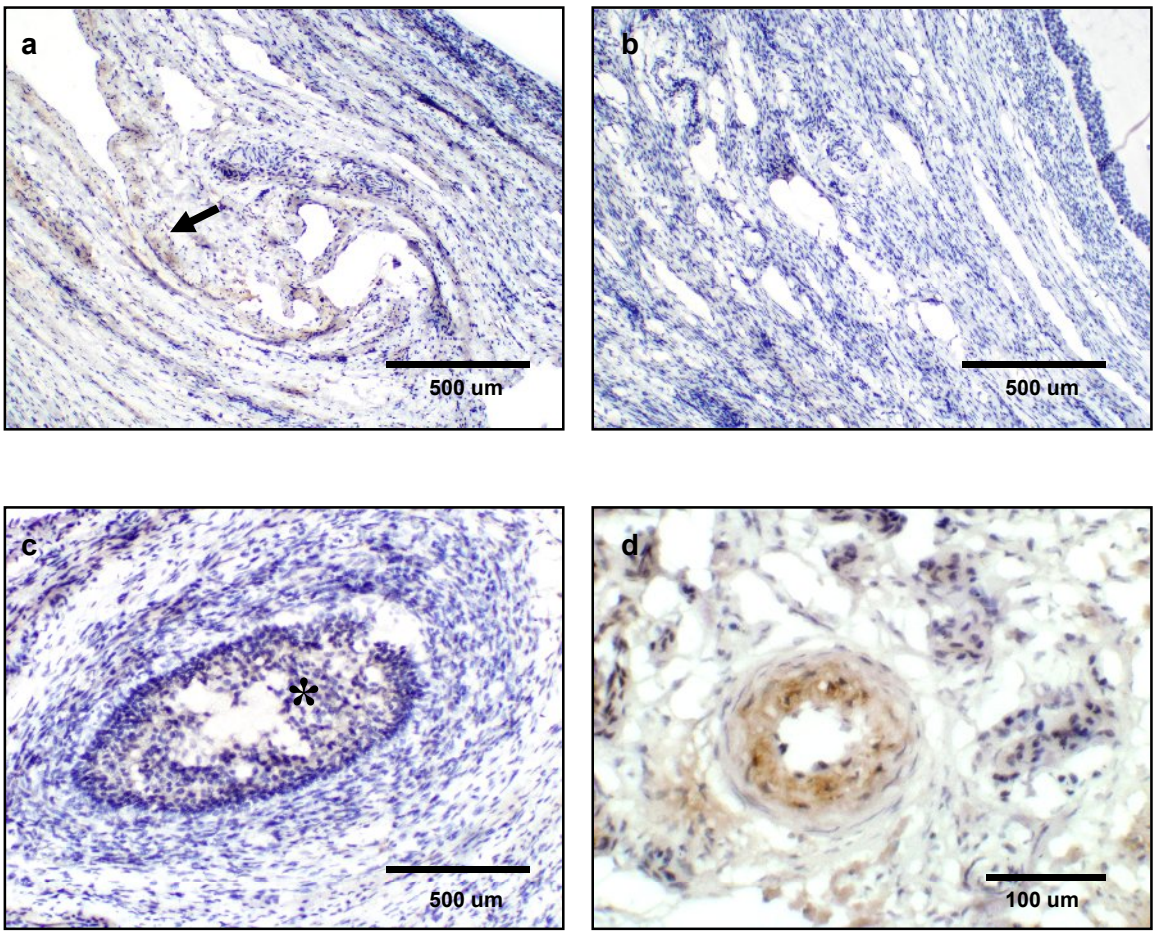

Figure 15. Expression of PrP^C in the bovine ovary. (a) PrP^C staining was observed associated to the mesovarium (*black arrow*). (c) Granulosa cells showed weak immunoreactivity for PrP^C (*). (d) Blood vessels in the corpus luteum showed PrP^C labeling. (b) Sections were incubated with non-immune horse serum instead of SAF-32 as a negative control.

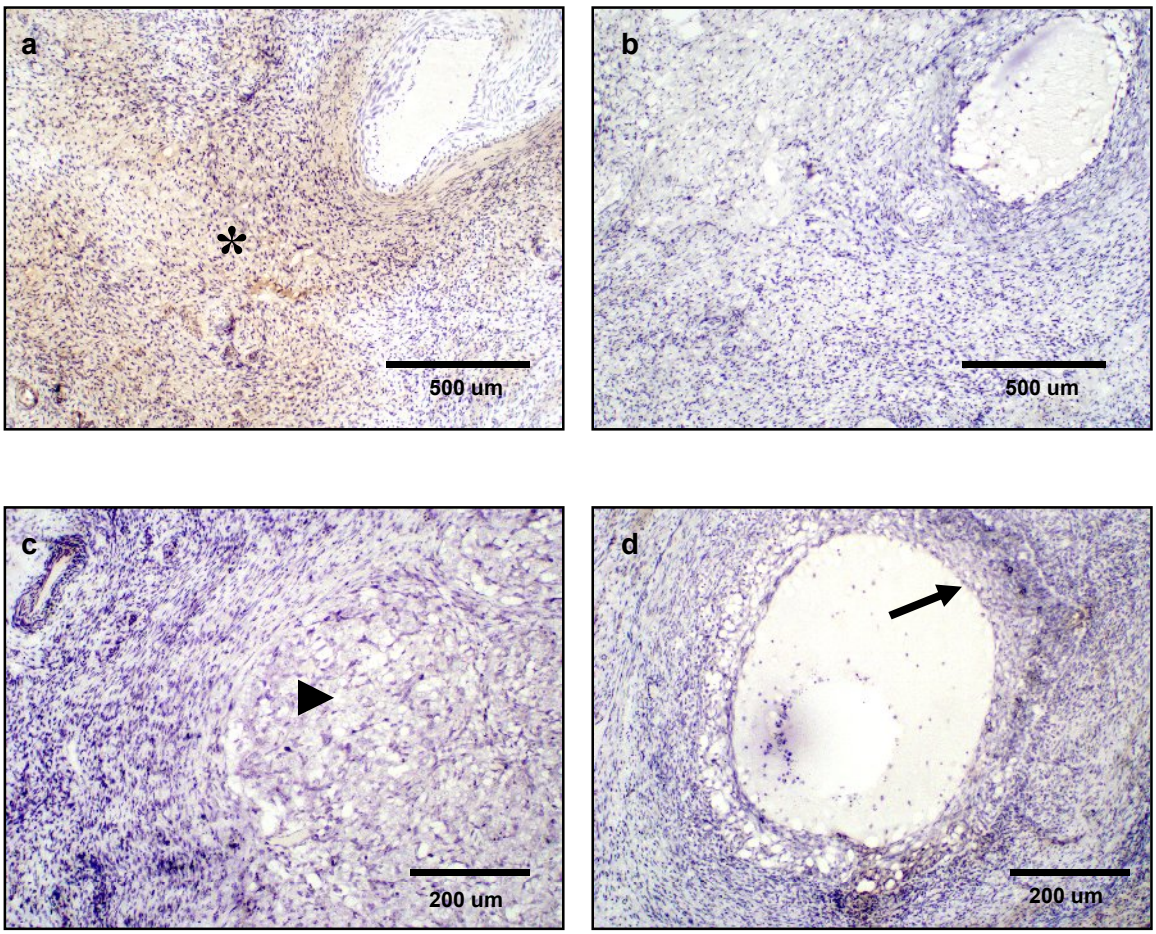

Figure 16. Expression of PrP^C in the ovine ovary. (a) PrP^C staining was observed in the mesovarium (*). (c) No staining was detected in the corpus luteum (*arrow head*). (d) Follicular and theca cells were also immunonegative for PrP^C (*black arrow*). (b) Sections were incubated with non-immune horse serum instead of SAF-32 as a negative control.

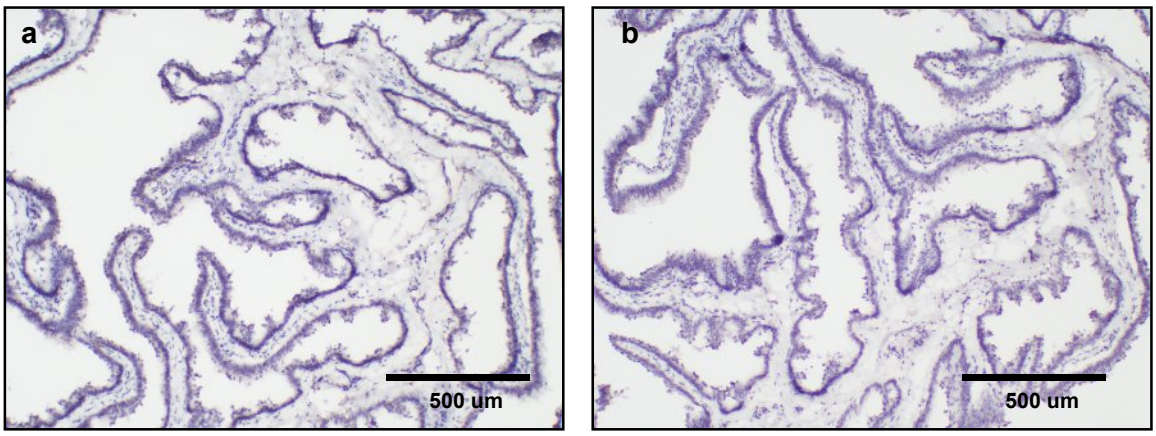

Figure 17. Expression of PrP^C on the bovine oviduct. (a) PrP^C showed undetectable levels of expression in the bovine oviduct. (b) Sections were incubated with non-immune horse serum instead of SAF-32 as a negative control.

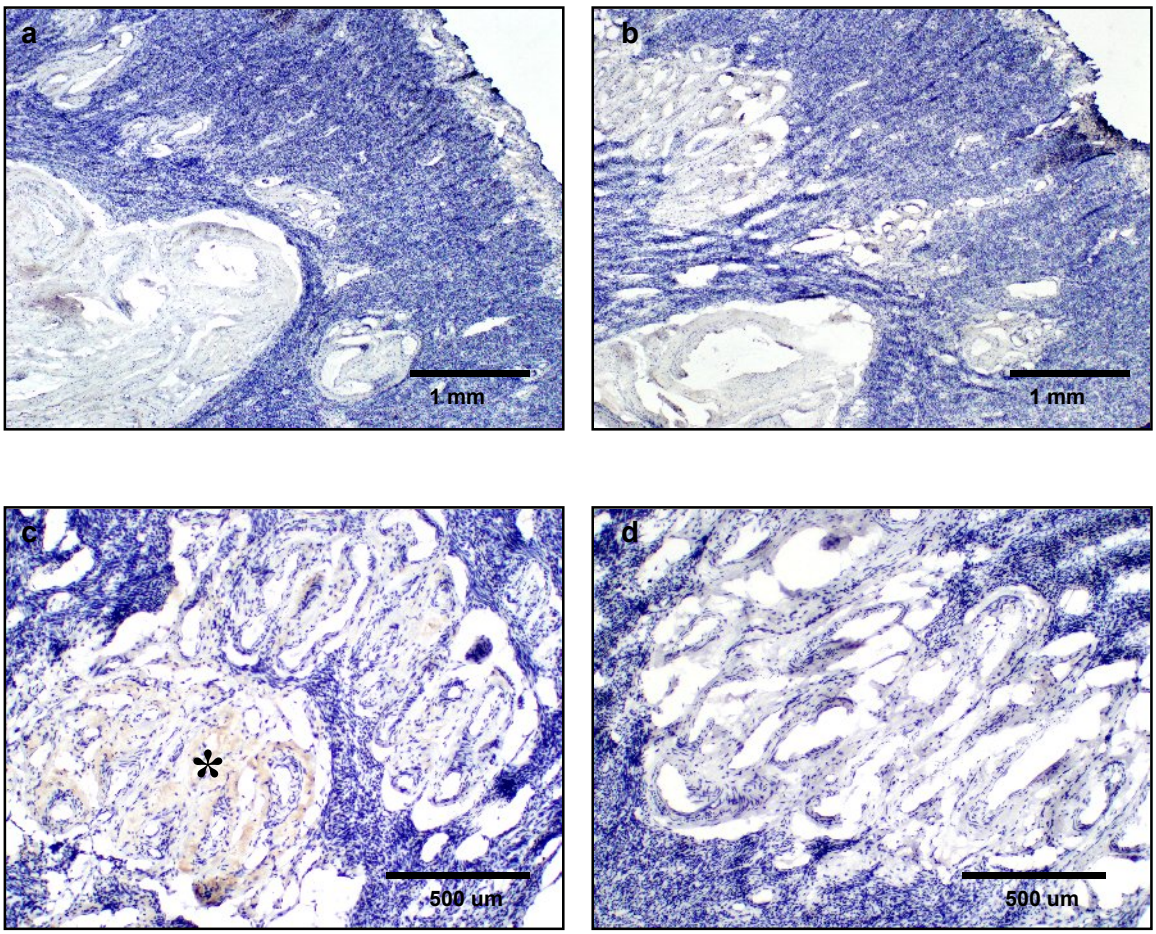

Figure 18. Expression of PrP^C on the bovine uterus. (a) No PrP^C staining was observed at low magnification. (c) At high magnification, PrP^C labeling was detected in glandular tissue in the endometrium (*). (b,d) Sections were incubated with non-immune horse serum instead of SAF-32 as a negative control.

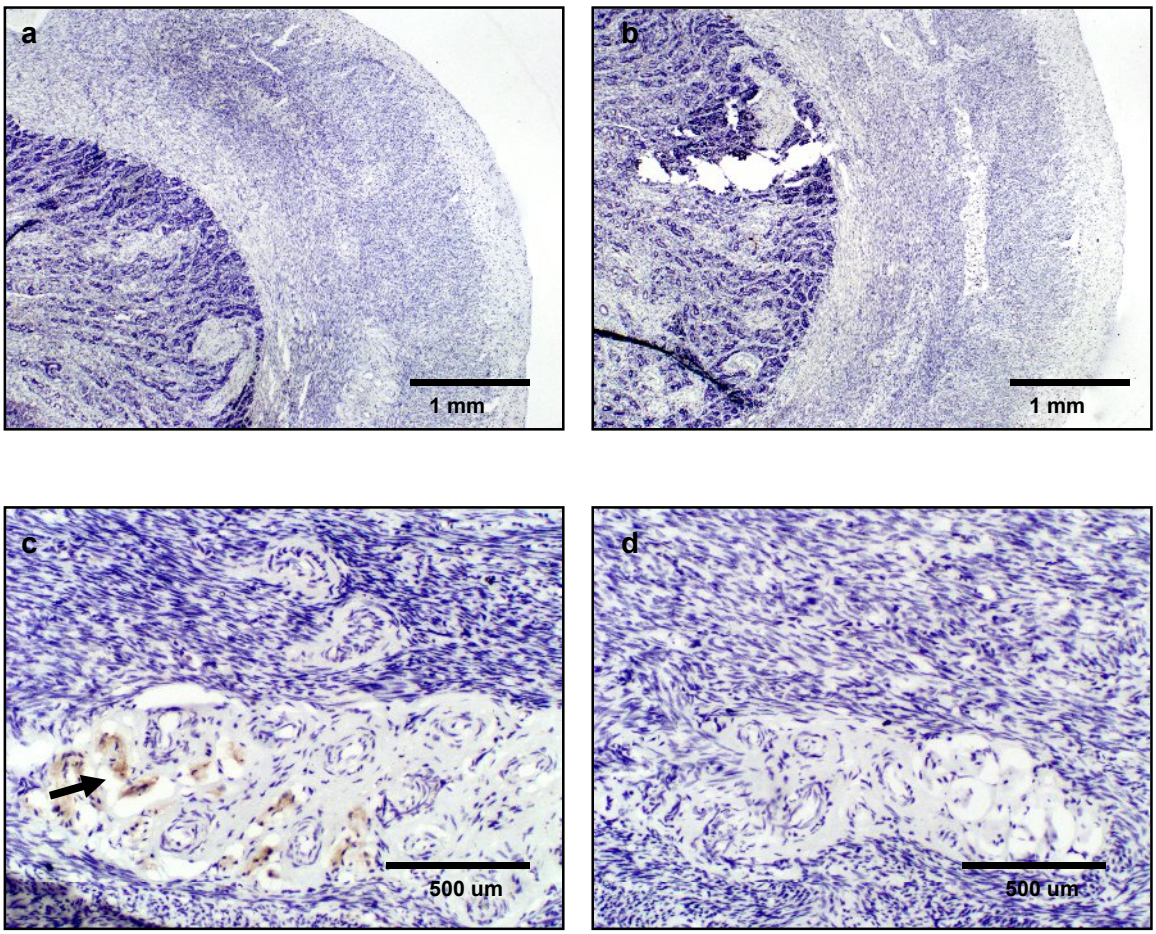

Figure 19. Expression of PrP^C on the ovine uterus. (a) No PrP^C staining was observed at low magnification. At high magnification, PrP^C labeling was detected in glandular tissue located in the endometrium (*black arrow*). (b,d) Sections were incubated with non-immune horse serum instead of SAF-32 as a negative control.

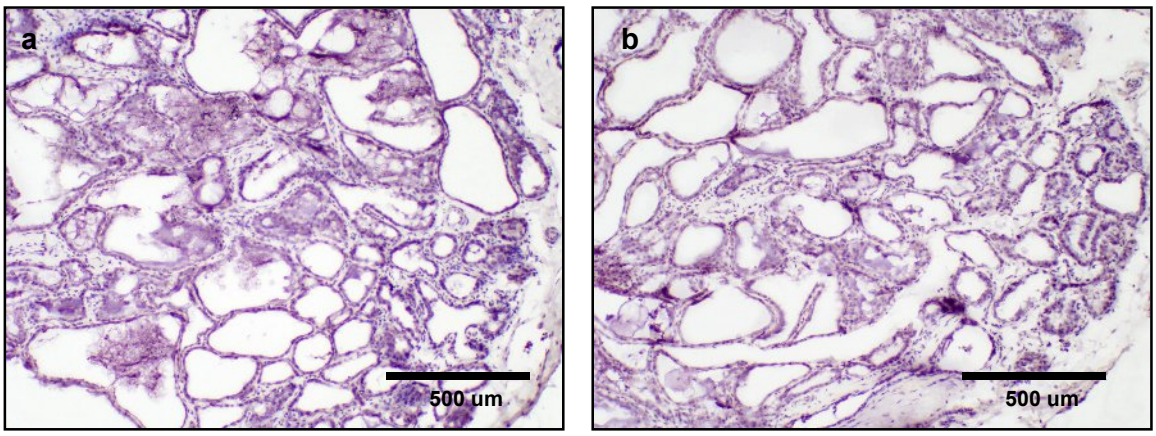

Figure 20. Expression of PrP^C on the bovine mammary gland. (a) No PrP^C staining was observed in tissue sections of the bovine mammary gland incubated with SAF-32 monoclonal antibody. (b) Sections were incubated with non-immune horse serum instead of SAF-32 as a negative control.

LITERATURE CITED

Andreoletti O, Lacroux C, Chabert A, Monnereau L, Tabouret G, Lantier F, Berthon P, Eychenne F, Lafond-Benestad S, Elsen J-M, Schelcher F. 2002. PrPSc accumulation in placentas of ewes exposed to natural scrapie: influence of foetal PrP genotype and effect on ewe-to-lamb transmission. J Gen Virol 83, 2607-2616.

Bainbridge J, Walker KB. 2005. The normal cellular form of prion protein modulates T cell responses. Immunol Lett 96, 147-150.

Blobel CP. 2000. Functional processing of fertilin: evidence for a critical role of proteolysis in sperm maturation and activation. Rev Reprod 5, 75-83.

Brown DR, Qin KF, Herms JW, Madlung A, Manson J, Strome R, Fraser PE, Kruck T, Vonbohlen A, Schulzschaeffer W, Giese A, Westaway D, Kretzschmar H. 1997. The cellular prion protein binds copper in vivo. Nature 390, 684-687.

Brown KL, Ritchie DL, McBride PA, Bruce ME. 2000. Detection of PrP in extraneural tissues. Microsc Res Tech 50, 40-45.

Bueler H, Fischer M, Lang Y, Bluethmann H, Lipp HP, DeArmond SJ, Prusiner SB, Aguet M, Weissmann C. 1992. Normal development and behavior of mice lacking the neuronal cell-surface PrP protein. Nature 16, 356, 6370, 577-582.

Bueler H, Aguzzi A, Sailer A, Greiner RA, Autenried P, Aguet M, Weissmann C. 1993. Mice devoid of PrP are resistant to scrapie. Cell 73, 7, 1339-1347.

Diarra-Mehrpour M, Arrabal S, Jalil A, Pinson X, Gaudin C, Pietu G, Pitaval A, Ripoche H, Eloit M, Dormont D, Chouaib S. 2004. Prion protein prevents human breast carcinoma cell line from tumor necrosis factor alpha-induced cell death. Cancer Res 64, 719-727.

Ecroyd H, Sarradin P, Dacheux J-L, Gatti J-L. 2004. Compartmentalization of prion isoforms within the reproductive tract of the ram. Biol Reprod 71, 993-1001.

Ford MJ, Burton LJ, Morris RJ, Hall SM. 2002. Selective expression of prion protein in peripheral tissues of the adult mouse. Neuroscience 113, 1, 177-192.

Fournier JG, Escaig-Haye F, Billette de Villemeur T, Robain O, Lasmezas CI, Deslys JP, Dormont D, Brown P. 1998. Distribution and submicroscopic immunogold localization of cellular prion protein (PrPc) in extracerebral tissues. Cell Tissue Res 292, 1, 77-84.

Fujisawa M, Kanai Y, Nam S-Y, Maeda S, Nakamuta N, Kano K, Kurohmaru M, Hayashi Y. 2004. Expression of *Prnp* mRNA (Prion protein gene) in mouse spermatogenic cells. J Reprod Dev 50, 5, 565-570.

Gatti J-L, Metayer S, Moudjou M, Andreoletti O, Lantier F, Dacheux J-L, Sarradin P. 2002. Prion protein is secreted in soluble forms in the epididymal fluid and proteolytically processed and transported in seminal plasma. Biol Reprod 67, 393-400.

Genoud N, Behrens A, Arrighi I, Aguzzi A. 2003. Prion proteins and infertility: insight from mouse models. Cytogenet Genome Res 103, 285-289.

Graner E, Mercandante AF, Zanata SM, Forlenza OV, Cabral AL. Veiga SS, Juliano MA, Roesler R, Walz A, Minetti A, Izquierdo I, Martins VR, Brentani RR. 2000. Cellular prion protein binds laminin and mediates neuritogenesis. Mol Brain Res 76, 85-92.

Hornshaw MP, McDermott JR, Candy JM, Lakey JH. 1995. Copper binding to the N-terminal tandem repeat region of mammalian and avian prion protein: structural studies using synthetic peptides. Biochem Biophys Res Commun 25, 214, 3, 993-999.

Iwata N, Sato Y, Higuchi Y, Nohtomi K, Nagata N, Hasegawa H, Tobiume M, Nakamura Y, Hagiwara K, Furuoka H, Horiuchi M, Yamakawa Y, Sata T. 2006. Distribution of PrP(Sc) in cattle with bovine spongiform encephalopathy slaughtered at abattoirs in Japan. Jpn J Infect Dis 59, 2, 100-107.

Kubosaki A, Yusa S, Nasu Y, Nishimura T, Nakamura Y, Saeki K, Matsumoto Y, Itohara S, Onodera T. 2001. Distribution of cellular isoform of prion protein in T lymphocytes and bone

marrow, analyzed by wild-type and prion protein gene-deficient mice. Biochem Biophys Res Commun 282, 1, 103-107.

Liu T, Li R, Wong BS, Liu D, Pan T, Petersen RB, Gambetti P, Sy MS. 2001. Normal cellular prion protein is preferentially expressed on subpopulations of murine hemopoietic cells. J Immunol 166, 6, 3733-3742.

Martins VR, Mercandante AF, Cabral AL, Freitas AR, Castro RM. 2001. Insights into the physiological function of cellular prion protein. Braz J Med Biol Res. 34, 5, 585-595.

Massimino ML, Ferrari J, Sorgato MC, Bertoli A. 2006. Heterogeneous PrPC metabolism in skeletal muscle cells. FEBS Lett 580, 3, 878-84.

Milhavet O, Lehmann S. 2002. Oxidative stress and the prion protein in transmissible spongiform encephalopathies. Brain Res Rev 38, 3, 328-339.

Nishida N, Tremblay P, Sugimoto T, Shigematsu K, Shirabe S, Petromilli C, Erpel SP, Nakaoke R, Atarashi R, Houtani T, Torchia M, Sakaguchi S, DeArmond SJ, Prusiner SB, Katamine S. 1999. A mouse prion protein transgene rescues mice deficient for the prion protein gene from Purkinje cell degeneration and demyelination. Lab Invest 79, 6, 689-697.

Qin K, Zhao L, Tang Y, Bhatta S, Simard JM, Zhao RY. 2006. Doppel-induced apoptosis and counteraction by cellular prion protein in neuroblastoma cells and astrocytes. Neuroscience 141, 1375-1388.

Paisley D, Banks S, Selfridge J, McLennan NF, Ritchie A-N, McEwan C, Irvine DS, Saunders PTK, Manson JC, Melton DW. 2004. Male infertility and DNA damage in Doppel knockout and Prion protein/Doppel double knockout mice. Am J Pathol, 164, 6, 2279-2288.

Palmer AC. 1959. Attempt to transmit scrapie by injection of semen from an affected ram. Vet Rec 71, 664.

Peoc'h K, Serres C, Frobert Y, Martin C, Lehmann S, Chasseigneaux S, Sazdovitch V, Grassi J, Jouannet P, Launay J-M, Laplanche J-L. 2002. The human "prion like" protein Doppel is expressed in both sertolli and spermatozoa. J Biol Chem 277, 45, 43071-43078.

Print CG, Loveland KL. 2000. Germ cell suicide: new inside into apoptosis during spermatogenesis Bio Essays 22, 423-430.

Richt JA, Kasinathan P, Hamir AN, Castilla J, Sathiyaseelan T, Vargas F, Sathiyaseelan J, Wu H, Matsushita H, Koster J, Kato S, Ishida I, Soto C, Robl JM, Kuroiwa Y. 2006. Production of cattle lacking prion protein. Nature Biotech 25, 132-138.

Roucou X, Gains M, LeBlanc AC. 2004. Neuroprotective functions of prion protein. J Neurosci Res 75, 153-161.

Roucou X, LeBlanc AC. 2005. Cellular prion protein neuroprotective function: implications in prion diseases. J Mol Med 83, 3-11.

Santuccione A, Sytnyk V, Leshchyns'ka I, Schachner M. 2005. Prion protein recruits its neuronal receptor NCAM to lipid rafts to activate p59fyn and to enhance neurite outgrowth. J Cell Biol 169, 341-354.

Shaked Y, Rosenmann H, Talmor G, Gabizon R. 1999. A C-terminal-truncated PrP isoform is present in mature sperm. J Biol Chem 274, 45, 32153-32158.

Sinha Hikim AP, Swerdloff RS. 1999. Hormonal and genetic control of germ cell apoptosis in the testis. Rev Reprod 4, 38-47.

Sprando R, Russell. 1987. Comparative study of cytoplasmic elimination in spermatids of selected mammalian species. Am J Anat 178, 72-80.

Steele AD, Emsley JG, Ozdinler PH, Lindquist S, Macklis JD. 2005. Prion protein (PrPC) positively regulates neural precursor proliferation during developmental and adult mammalian neurogenesis. PNAS 103, 9, 3416-3421.

Terry LA, Marsh S, Ryder SJ, Hawkins SA, Wells GA, Spencer YI. 2003. Detection of disease-specific PrP in the distal ileum of cattle exposed orally to the agent of bovine spongiform encephalopathy. Vet Rec 29, 152, 13, 387-392.

Thomzig A, Schulz-Schaeffer W, Wrede A, Wemheuer W, Brenig B, Kratzel C, Lemmer K, Beekes M. 2007. Accumulation of pathological prion protein PrPSc in the skin of animals with experimental and natural scrapie. PLoS Pathog 3, 5: e66. doi:10.1371/journal.ppat.0030066.

Thumdee P, Ponsuksili S, Murani E, Nganvongpanit K, Gehrig B, Tesfaye D, Gilles M, Hoelker M, Jennen D, Griese J, Schellander K, Wimmers K. 2007. Expression of the prion protein gene (PRNP) and cellular prion protein (PrPc) in cattle and sheep fetuses and maternal tissues during pregnancy. Gene Exp 13, 283-297.

Tilly JL. 1996. Apoptosis and ovarian function. Rev Reprod 1:162-172.

Tuo W, Zhuang D, Knowles DP, Cheevers WP, Sy M-S, O'Rourke KI. 2001. PrP-C and PrP-Sc at the fetal-maternal interface. J Biol Chem 276, 21, 18229-18234.

Yuan J, Yankner BA. 2000. Apoptosis in the nervous system. Nature 407. 802-809.

Walter ED, Chattopadhyay M, Millhauser GL. 2006. The affinity of copper binding to the prion protein octarepeat domain: evidence for negative cooperativity. Biochem 45, 13083-13092.

Wells GAH, Wilesmith JW. 1995. The neuropathology and epidemiology of bovine spongiform encephalopathy. Brain Pathol 5, 91-103.

Westergard L, Christensen HM, Harris DA. 2007. The cellular prion protein (PrPC): Its physiological function and role in disease. Biochim Biophys Acta 1772, 6, 629-644.

Wilesmith JW. 1994. Bovine spongiform encephalopathy and related diseases: an epidemiological overview. NZ Vet J 42, 1-8.

Wrathall AE. 2000. Risks of transmission of spongiform encephalopathies by reproductive technologies in domesticated ruminants. Livestock Prod Sci 62, 287-316.

Wrathall AE, Brown KFD, Sayers AR, Wells GAH, Simmons MM, Farrelly SSJ, Bellerby P, Squirrell J, Spencer YI, Wells M, Stack MJ, Bastiman B, Pullar D, Scatcherd J, Heasman L, Parker J, Hannam DAR, Helliwell DW, Chree A, Fraser H. 2002. Studies of embryo transfer from cattle clinically affected by bovine spongiform encephalopathy (BSE). Vet Rec 150, 365-378.

CHAPTER IV

ANALYSIS OF THE PRION EXPRESSION DURING BOVINE EMBRYONIC DEVELOPMENT

INTRODUCTION

The cellular prion protein (PrP^C) is a host-encoded glycoprotein best known for its role in prion diseases or transmissible spongiform encephalopathies (TSEs). Through a poorly understood process, PrP^C is post-transcriptionaly converted into a protease resistant and pathogenic isoform (PrP^{Sc}). Although substantial evidence indicates that PrP^{Sc} is the principal if not the only component of the TSE agent, additional and still unknown conversion factors may be required in the host to sustain proper PrP^{Sc} replication (Prusiner, 1998; Collinge, 2001; Abid and Soto, 2006).

Before post-translational modification, PrP^C has a sequence of 253 amino acids with a slight variation between species depending on the number of octapeptide repeats located near the N-terminus (Prusiner and Scott, 1997). PrP^C is usually found attached by a glycosylphosphotidylinositol (GPI) anchor to lipid rafts in the plasma membrane (Martins et al., 2002, DeMarco et al., 2005). The PrP^C gene (*Prnp*) consists in a structure of three exons in the bovine; with the third exon responsible for protein coding (Chesebro et al., 1985; Oesch et al., 1985; Inoue et al., 1997). Expression of *Prnp* is high in the central nervous system (CNS) and lymphatic tissues but has also been described in skin, testes, kidney and pancreas (Chapter II and III; Fournier et al., 1998; Ford et al., 2002; Bailly et al., 2004). In the CNS, PrP^C is expressed primarily in neurons and astrocytes and at low levels in oligodendrocytes (Moser et al., 1995). During development, the earliest expression of *Prnp* has been reported at day 6.5 in extra-embryonic membranes of the mouse. After day 8.5, *Prnp* is intensely expressed in the developing nervous system throughout gestation (Manson et al., 1992; Miele et al., 2003; Tremblay et al., 2007; Tremblay et al., 2007).

Several lines of *Prnp* null mice have been generated in order to gain insight into the still unknown physiological function of PrP^C. These mice apparently develop and reproduce normally, although they show resistance to TSE infection (Bueler et al., 1992, 1993). Some phenotypes associated with *Prnp* null mice have provided clues to the potential function of PrP^C including a marked reduction in hippocampal and myocardial mitochondrial numbers (Miele et al., 2002) and abnormal hippocampal synaptic plasticity (Collinge et al., 1994). Furthermore, studies *in vitro* have provided evidence for the action of PrP^C in activation of signal transduction pathways involved in neuronal adhesion, proliferation and differentiation (Westergard et al., 2007). Binding of PrP^C to the neural cell adhesion molecule (N-CAM) results in axonal outgrowth in hippocampal neurons through phosphorylation of the cytoplasmic tyrosine Fyn

kinase (Santuccione et al., 2005). Laminin, a major protein of the extracellular matrix has also been shown to interact with PrP^C enhancing neuronal proliferation, migration and neurite outgrowth (Graner et al., 2000). Recently, experiments with *Prnp* knockout and overexpressor mice demonstrated that PrP^C levels correlate with neuronal differentiation and increases cellular proliferation in neurogenic regions of the CNS (Steele et al., 2005).

Although several studies have been reported on the developmental expression of PrP^C in mice, little data is available in the bovine. Identification of the tissues involved in PrP^C expression may provide crucial information about the potential susceptibility of various tissues to BSE infection. Moreover, identification of PrP^C expressing cells and tissues may provide some clues about the potential function of this protein. In the present study, we investigated the expression of the *Prnp* gene and PrP^C protein during pre-implantation and post-implantation stages of bovine embryonic development. Our data describes a close relation between expression of PrP^C and important stages of bovine development including embryo attachment and nervous system development.

MATERIAL AND METHODS

Oocytes and semen

Ovaries were obtained from cattle at a commercial abattoir within 30 min of slaughter, packed in insulated containers and transported to the laboratory at 27 °C. Cumulus-oocyte complexes (COCs) were aspirated from antral follicles (> 3mm diam.) using and 18g-needle connected to a 12 ml syringe and washed three times in 5 ml of HEPES-buffered synthetic oviduct fluid (SOFH). Spermatozoa used for IVF was obtained from frozen-thawed semen collected from fertile bulls (ABS, American Breeders Service, DeForest, WI, USA). Immature oocytes and sperm were used for *in vitro* fertilization (IVF) and for Q-PCR analyses.

Production, collection and fixation of embryos and fetuses

Pre-attachment embryos

Days 2-8 post-insemination. Bovine pre-implantation embryos were produced by standard procedures from oocytes using *in vitro* maturation (IVM), fertilization (IVF) and culture (IVC) techniques (Eyestone, 1999), (IVF; Bracket et al., 1982) and *in vitro* culture (IVC; Kaine, 1987) techniques. After isolation, COCs were matured in 3 ml of synthetic oviduct fluid (SOF) media supplemented with 5 μg/ml of FSH and 10% of FCS for 22 h at 38.5 °C in a humidified atmosphere of 5% CO_2 in air. After maturation COCs were washed three times in synthetic oviduct fluid Hepes (SOFH) and placed in 48-μl fertilization droplets of IVF medium without glucose and supplemented with 10 μg/ ml of heparin (Sigma, St. Louis, MO, USA). Live spermatozoa were selected using the swim-up method. Briefly, 0.25 ml of frozen-thawed semen was layered under 1 ml of IVF medium in a 15-ml clinical tube and incubated for 30 min at 38.5°C. The supernatant was then aspirated and centrifuged at 120-g for 20 min. Pelleted spermatozoa were the counted and diluted with IVF medium to a concentration of 25 x 10^6 per ml and 2 μl of this stock was added to fertilization droplets and incubated for ~18 h. COCs were then stripped of cumulus cells by vortex agitation for 5 min and washed three times in SOFH. Aliquots of 30 inseminated oocytes were transferred to 10 μl droplets of FCS-supplemented SOF media under oil for IVC in an atmosphere containing 5 % CO_2, 5 % O_2 and 90 % N_2 in a modular incubator chamber (Billups-Rothenberger, Del Mar, CA, USA). Cumulus cells were expanded in SOF media under the same atmosphere used for IVM for 2 weeks to obtain sufficient cells for mRNA extraction. Immature oocytes (n = 415), day 4 (n = 293), day 8 (n = 283), spermatozoa (~75 x 10^5), and cumulus cells (~9 x 10^4) were collected and immediately fixed in RLT buffer.

Days 14-18 of gestation. Embryos at 14 days (n=18) and 18 days (n=8) after fertilization were collected from thirty two single-ovulated and four super-ovulated Angus cows. Estrus was synchronized in group of cows by administration of 1 mg of Estradiol-17β s.c. on day 0 and an i.m. injection of 100 mg of progesterone (P_4; Sigma Chemical) followed by the insertion *per vagina* of a controlled internal drug releasing device containing 1.9 g of progesterone (CIDR; Vetrepharm, Canada Inc., London, Canada). At day 8, cows received an injection of 500 mg of cloprostenol (Estrumate; Union, NJ, USA) i.m. and CIDRs were removed. Estrus was detected at day 10 using a radiotelemetric-pressure sensing system (HeatWatch, Denver, CO, USA). From treatment day 20, super-ovulated cows received eight i.m.

injections of FSH in decreasing doses every 12 h. On day 22 a dose of 375 mg of cloprostenol was given in the morning and repeated in the afternoon. Cows were inseminated with one straw containing approximately 20 x 10^6 spermatozoa at 12 h and 24 h after standing estrus was detected. At day 14 and 18 of post-estrus, both uterine horns were flushed non-surgically by using a 18-gauge two-way embryo collection catheter (Bioniche, Belleville, Ontario, Canada) and approximately 250 ml of Ringer Lactate serum per horn. Embryos were separated using a plastic filter connected by tubing to the catheter and washed in phosphate-buffered saline (PBS) under a stereoscope.

Post-attachment fetuses

Days 27- 39 of gestation. Six fetuses were collected at the Faculty of Veterinary Medicine, Austral University, Valdivia, Chile, from ten dual-purpose Overo Negro cows. To synchronize estrus, a dose of 100 μg of GnRH (Cystorelin, Merial Ltd., Duluth, GA, USA) was giving on day 0, followed the same day by the insertion *per vaginam* of a CIDR (Pfizer) device. At day 7, an injection of 500 μg of cloprostenol (Estrumate, Schering Plough, Union, HJ) was administered i.m., followed by the removal of the CIDR. A second injection of cloprostenol was administered i.m. on Day 9. Cows were observed daily for standing estrus behavior and were immediately inseminated upon detection with approximately 20 x 10^6 spermatozoa. At day 26 of gestation, cows were evaluated for pregnancy by palpation *per rectum* and confirmed using transvaginal ultrasound (Aloka, Tokyo, Japan). Feed was withheld from cows from 24 to 36 h in preparation to mid-ventral hysterotomy on days 27 (n=2), 32 (n=2) and 39 (n=2) days of gestation. Briefly, cows were sedated with 0.2 mg/kg i.m. xylazine hydrochloride (Rompun, Bayer AG, Germany). Sedated animals that adopted sternal recumbency were restrained with ropes and repositioned in dorsal recumbency. A dose of 0.06 mg/100 kg of clenbuterol hydrochloride i.m. (Planipart, Boehringer Ingelheim, Germany) was administered i.v. to induce uterine relaxation. After the operation site was disinfected, 80 ml of 2% lidocaine hydrochloride (Vedco, Inc., USA) was administered for local infiltration on the ventral mid-line between the sternum and mammary gland. A 20-cm incision was made through the skin and linea alba and the gravid uterine horn was exteriorized and incised for fetus extraction. After removal, fetuses were immediately immersed in 10% formalin or RNA later buffer (Qiagen) for further analyses. Uterine wall, peritoneum, abdominal muscles and skin were sutured. Cows were observed during recovery from anesthesia. Additional fetuses at days 27 (n=4), 32 (n=4) and 39 (n=6) were obtained from pregnant cows at a commercial abattoir for western blot and immunohistochemistry. Gestational age was estimated from crown-rump length by measuring according

to Winters et al., 1942. Fetuses were frozen in dry ice for western blot and fixed in 10% formalin for immunohistochemistry.

RNA Extraction and cDNA synthesis

Immature oocytes (n = 415), day 4 (n = 293), day 8 (n = 283), day 14 (n = 12), day 18 (n = 4) embryos and day 27 (n = 2), day 32 (n = 2), day 39 (n = 2) fetuses, spermatozoa (~75 x 10^5), and cumulus cells (~9 x 10^4) were collected and immediately fixed in RLT buffer. Total RNA was extracted using RNeasy extraction mini kit (Qiagen, Inc., Valencia, CA, USA). Oocytes and day 4 and 8 embryos were homogenized by pipetting in RLT buffer. Day 14 and 18 embryos, sperm and cumulus cells were homogenized by centrifugation in Qiashredder column (Qiagen). Day 27, 32 and 39 fetuses were homogenized in RLT buffer using a tissue homogenizer rotor (Tissuemiser, Fisher Scientific). All subsequent RNA purification steps were carried out according to the manufacturer's instructions. The concentration and purity of the RNA in each sample were determined using ribogreen RNA quantification kit (Molecular Probes, Eugene, OR, USA). Total RNA was eluted in 30-50 µl of RNase free water. cDNA was synthesized using an iScript cDNA synthesis kit (Bio-Rad Labs., Hercules, CA, USA). Reactants were incubated for 5 min at 25°C, 30 min at 42°C, 5 min at 85°C and hold at 4°C using a DNA engine PCR thermocycler (Bio-Rad).

Quantitative-PC*R*

Real-time PCR primers and TaqMan probes were designed using PrimerExpress software (Applied Biosystems) to amplify a segment of cDNA that spans the exon 2-exon 3 junction in the bovine *Prnp* sequence. Equivalence of amplification efficiencies among all primer-probe sets was confirmed using serial 5-fold dilutions of mouse or bovine brain cDNA (Huckle and Eyestone, unpublished). TaqMan probe sequence (CACAGCAGATATAAGTCATCATGGTGAAAAGCC) specific for the target was designed to contain a fluorescent 5' reporter dye (FAM) and 3' quencher dye (TAMRA). Sequence of forward and reverse bovine *Prnp* primers were at follow: CCAGAGACACAAATCCAACTTGAG and AACCAGGATCCAACTGCCTATG. Each RT-PCR reaction (25 µl) contained the following: 2X Master Mix without uracil-N-glycosidase (12.5 µl), 40X Multiscribe and RNase Inhibitor Mix (0.63 µl), target

forward primer (60 nM), target reverse primer (60 nM), fluorescent-labeled target probe (4 nM) designed for the RNA sequence isolated from bovine *Prnp* gene and a total RNA (40 ng). The PCR amplification was carried out in the 7300 Real Time PCR System (Applied Biosystems, Foster City, CA, USA). Thermal cycling conditions were 48°C for 30 min and 95°C for 10 min, followed by 40 repetitive cycles at 95°C for 15 sec and 60°C for 1 min. As a normalization control for RNA loading, parallel reactions in the same multiwell plate were performed using TaqMan Ribosomal RNA as a target (18s control kit, Applied Biosystems). Quantification of gene amplification was made following RT-PCR by determining the threshold cycle (C_T) number for FAM fluorescence within the geometric region of the semilog plot generated during PCR. Within this region of the amplification curve, each difference of one cycle is equivalent to a doubling of the amplified product of the PCR. The relative quantification of the target gene expression across treatment was evaluated using the comparative $\Delta\Delta C_T$ method. The C_T value was determined by subtracting the ribosomal C_T value from the target C_T value of the sample. Calculation of $\Delta\Delta$ C_T involved using oocyte PrP^C gene expression (sample with the highest CT value or lowest target expression) as an arbitrary constant to subtract from all other C_T sample. Relative *Prnp* expression was calculated as fold changes in relation to oocyte expression and expressed as $2^{-\Delta\Delta CT}$ value.

Western blot

Frozen day 27 (n=2), day 32 (n=2), and day 39 (n=3) fetuses were thawed and homogenized in lysis buffer (10 mM Tris, pH 7.4, 150 mM NaCl, 1% Triton-X-100, 1% deoxycholate, 0.1% SDS) using a pestle homogenizer (Fisher Scientific). Homogenates were centrifuged at 16,100 rcf for 5 min and the supernatants transferred into a new tube. Total protein concentrations were determined using a Bicinchoninic acid (BCA) kit (Pierce; Rockford, IL) according to the manufacturing's instructions. For protein denaturation, 50 µl of each homogenized sample was mixed with 50 µl of Laemmli buffer (BioRad Laboratories, Hercules, CA, USA) and heated at 98° C for 5 min. Aliquots containing 20 µg of total protein were added to each lane and separated by SDS-PAGE in 12% gels (BioRad). Electrophoresis was performed at 200V for ~60 min. Proteins were then transferred onto PDVF membranes by electroblotting at 100 V for 60 min. Membranes were immersed in blocking buffer (LI-COR Corp., Lincoln, NE, USA) for 1 h with shaking. PrP^C was detected by incubation for 1 h in SAF-32 mouse monoclonal anti-PrP (1:400; Cayman Chemical Company, Ann Arbor, MI, USA) directed against aminoacid sequence 59-89 located in the N-terminal octapeptide repeat region of the protein. For reference, membranes were co-incubated in rabbit anti-β-actin (1:1000; Santa Cruz Biotechnology, Santa

Cruz, CA, USA). Both primary antibodies were diluted in 0.1% Tween-20 in blocking buffer. After four washes in 0.1% Tween-20 in phosphate-buffered saline (PBS) for 5 min each, membranes were incubated in secondary IgG fluorescent anti-mouse and anti-rabbit antibodies (1:5000; LI-COR) diluted in 0.1% Tween-20 in blocking buffer for 30 min with shaking. Immunoreactive band intensities of PrP^C and Actin were detected and quantified as integrated intensity values using an Odyssey infrared imaging system (LI-COR). Relative expression of PrP^C was corrected by β-actin expression and standardized to the lowest expression value (Day-27 fetus).

Immunofluorescence

Bovine oocytes and pre-implantation embryos were processed for application of whole-mount immunofluorescence as described previously (Favetta et al., 2007). Briefly, embryos were fixed in 4% paraformaldehyde in PBS for 10 min, washed in PBS and then stored at 4° C for up to 1 week until processed for whole-mount immunofluorescence. Fixed embryos were permeabilized in 0.01% Triton X-100 in PBS for 1 h followed by incubation in 5% normal horse serum for 1 h at 37° C. Embryos were then incubated with SAF-32 mouse monoclonal anti-PrP (1:100; Cayman Co.) in 1% normal horse serum diluted in PBS overnight at 4°C. Next day embryos were washed three times in PBS for 30 min each and then incubated in Alexa Fluor 594 goat anti-mouse secondary antibody (1:200; Invitrogen Corp.) overnight at 4°C. Processed embryos were mounted onto glass slides in a drop of mounting solution with DAPI (Vector Lab), coverslipped with wax droplets for separation and observed under fluorescent microscope (Olympus, Japan).

Immunohistochemistry

Formalin-fixed fetuses were embedded in paraffin and sectioned at 5-7 µm using a microtome (Historange, LKB Bromma, Sweden). Tissue sections were mounted on adhesive coated slides (Newcomer supply; Middleton, Wisconsin) and incubated overnight at 37 °C. Mounted tissues were deparaffinized in xylene and dehydrated in serial alcohol solutions. Slides were subjected to an unmasking protocol that employed a commercial unmasking solution (Vector Laboratories., Burlingame, CA, USA) and autoclaving at 120°C for 5 min. Endogenous peroxidase was blocked by incubation in 3%

hydrogen peroxidase diluted in 0.1 M PBS for 30 min. Tissues were then rinsed two times in PBS and blocked in 2.5% horse serum for 15 min. PrP^C was detected by overnight incubation at room temperature with primary antibody SAF-32 (1:400; Cayman Co.) diluted in 1.5 % equine serum solution (Vector Laboratories). After two washes in PBS, bound primary antibody was detected using a horseradish-peroxidase-conjugated horse anti-mouse secondary antibody for 10 min at room temperature (Vector Laboratories). Immune complexes were visualized using 3,3'-diaminobenzidine (DAB) substrate for 5 min or until the signal became visible. Probed sections were then counterstained with hematoxilyn and rehydrated in serial alcohol solutions. Sections were mounted with permount (Fisher Scientific) under coverslips. Neighboring sections processed identically using horse serum instead of primary antibody, served as controls. Digital photos of tissue sections were obtained using light microscopy (Olympus Vanox-T, Tokyo, Japan).

Immunofluorescence on histological sections of day-14 and day-18 embryos was performed following the same protocol described for immunohistochemistry. Embryos were oriented and embedded in 4% agar (Bacto-agar, Difco Lab, Detroit, MI, USA) under a stereomicroscope. Specimens were trimmed, paraffin-embedded and transversally sectioned at 5-7 µm using a microtome. The peroxidase inhibition step was omitted and after detection with SAF-32 (1:400), slides were incubated in Alexa Fluor 594 goat anti-mouse antibody (Invitrogen Corp.). Slides were coverslipped using mounting solution with DAPI (Vector Lab) for nuclei visualization and examined under the fluorescent microscope.

Data Analysis

Statistical analyses of PrP^C mRNA expression detected by Q-PCR and PrP^C expression detected by quantitative western blot were performed using SAS software (version 9.3.1, SAS Institute Inc., Cary, North Carolina, USA). Analyses of significance ($P < 0.05$) were performed using One-way ANOVA. Expression values for each stage of development were compared to the stage at which the expression was lowest. PrP^C expression in oocytes and embryos from days 2-18 was analyzed by Q-PCR. For these stages, PrPC expression was lowest in oocytes; hence expression in all other stages was compared to that in oocytes. PrP^C expression in fetuses from day 27-39 was analyzed by Q-PCR and western blot and compared to expression level at day 27. Significant differences of expression between stages were analyzed using Duncan's multiple comparison test.

RESULTS

Expression of Prnp mRNA

The relative expression of *Prnp* mRNA was analyzed using Q-PCR in bovine granulose cells, spermatozoa, oocytes on day 0 and embryos from day 4 through day 39 of gestation (Fig. 1). *Prnp* mRNA expression was compared to 18s rRNA obtained from the same cDNA source and normalized to the level of expression in oocytes. All stages analyzed expressed detectable levels of *Prnp* mRNA expression. *Prnp* mRNA levels were 18.4-fold higher ($P < 0.05$) in granulosa cells and 1.4-fold higher in spermatozoa compared to oocytes. During pre-implantation stages, the highest level of *Prnp* mRNA were detected at day 4 (21.2-fold higher compared to oocytes; $P < 0.05$) and at day 18 (16-fold higher compared to oocytes; $P < 0.05$). In contrast, the lowest expression levels were detected at day 14 (0.98-fold higher compared to oocytes) and day 8 (2.88-fold higher compared to oocytes). Levels of *Prnp* mRNA during post-implantation stages were 1.89-fold (day 27), 2-fold (day 32) and 2.3-fold (day 39) higher than oocytes.

Expression of the PrP^C protein

Relative expression of PrP^C was analyzed by western blot using SAF-32 antibody on fetuses at days 27, 32 and 39. PrP^C immunoreactive bands were quantified by image analysis, compared to β-actin expression and normalized to day 27 expression. PrP^C immunoreactive bands were observed at all stages analyzed (Fig. 2a). The predominant immunoreactive band was observed at 31 kDa with a less intense band at 29 kDa. Comparison with adult bovine brainstem (obex) indicated that the 31 kDa band corresponded to the mono-glycosylated PrP^C with the less intense 27 kDa. The immunoreactive band at 35 kDa (di-glycosylated) normally present in several adult bovine tissues was not detected in fetal lysates. Computerized quantification of western blot bands suggested a progressive increase in the level of expression in relation to day of development; however, no significant differences were detected between days (Fig. 2b).

In order to establish the precise cellular localization of PrP^C, we performed immunofluorescence detection in whole-mounts immature oocytes and embryos at days 4 and 8 post-insemination. Results shown are typical for multiple experiments. Intensity of immunofluorescence for PrP^C protein oocytes and embryos were in general congruent with *Prnp* mRNA levels detected by Q-PCR. PrP^C was expressed with a homogeneous and punctuate pattern associated to the cytoplasm of oocytes (Fig. 3). The intensity of PrP^C immunofluorescence increased on day 4 resulting in a homogeneous labeling of the blastomere plasma membranes (Fig. 4 and 5).In blastocysts at day 8, immunofluorescence showed a punctuate and evenly distributed pattern of PrP^C in both the trophlobast and the inner cell mass (Fig. 6). Histological cross sections obtained from the embryonic disc of embryos at days 14 and 18 were also analyzed by immunofluorescence using SAF-32 antibody. Labeling associated with PrP^C was not observed either in the embryonic disc or in the trophoblast at day 14 (Fig. 7). This result was congruent with the low levels of *Prnp* mRNA detected at this stage by Q-PCR (Fig. 1). Scattered spots of specific PrP^C signal were detected in the trophoblast at day 18 (Fig. 8).

The tissue-specific pattern of PrP^C expression was studied using immunoperoxidase staining in sagittal sections of whole fetuses at days 27, 32 and 39 of gestation. Observation with low magnification at day 27 demonstrated the presence of PrP^C staining in the presumptive myelencephalic area of the brain, dorsal root ganglion and the spinal cord (Fig. 9). At higher magnification, the staining was evident in the pial regions of the brain and spinal cord (Fig. 10). In visceral organs, PrP^C was detected in scattered multinuclear cells distributed in the liver parenchyma (Fig. 11a), epithelial cells of the mesonephric duct and glomeruli (Fig. 11b). A similar pattern of staining was observed at day 32. At this stage, PrP^C labeling was present in the developing brain, dorsal root ganglion, spinal cord and mesonephros (Fig. 12). Staining in the brain and spinal cord was restricted to the pial region and no immunoreactivity was observed in the periventricular zone (Fig. 13a,c). Strong PrP^C signal was detected in the dorsal root ganglia and associated nerves of the thoracic segment (Fig. 13e). Immunodetection in the liver showed PrP^C-positive cells in higher number compared the previous stage (Fig. 14a,c,d). The relative size of the mesonephros decreased drastically compared with day 27 but continued to display a similar pattern of PrP^C labeling (Fig. 14e). Further development of the nervous system was observed at day 39, characterized by the enlargement of the brain and spinal cord (Fig. 15). As in the previous stages, PrP^C was intensely associated with the telencephalon, mesencephalon and metencephalon but also present in dorsal root ganglions, cervical ganglia, sympathetic trunks and peripheral nerves. In the CNS, PrP^C immunoreactivity was restricted to the pial region of the brain and spinal cord and was not present in the paraventricular regions (Fig. 16a,c). PrP^C staining was also strong in dorsal root ganglions and peripheral nerves originated from the cervical

and lumbar segments of the spinal cord (Fig. 17a,c). Neural trunks forming the primitive PNS were also positive for PrP^C (Fig. 17e,f). Neural tissue immunoreactive for PrP^C was also observed in the lungs and the intestinal wall (Fig 17g,i). At this stage, PrP^C-positive cells in the liver were detected in lower number compared with day 32 (Fig. 18a,c). The mesonephros continue involution but displayed PrP^C staining associated to epithelial and glomerular cells as in the previous stages (Fig 18e).

DISCUSSION

Previous studies have been conducted on *Prnp* expression during embryogenesis in an effort to better understand the cellular function of PrP^C. Activation of the *Prnp* gene in mice has been reported at approximately day 6.5 in extra-embryonic membranes (Manson et al., 1992; Tremblay et al., 2007). In the fetus, activation of *Prnp* begins at day 8.5 in the region of the mesencephalon followed by expression in radial zones of the neural tube at day 11.5 (Tremblay et al., 2007). After day 13.5, *Prnp* expression follows the development of the nervous system and is detected in telencephalon, hypothalamus, dorsal root ganglia, peripheral nerves and sympathetic ganglia. In the human, PrP^C has been detected in the forebrain in the late trimester of gestation (11^{th} week) in microglia, axonal tracts, synapses and fascicles (Adle-Biassette et al., 2006). Although, these studies provided important information about the developmental expression of PrP^C, little data is available in the bovine. The mapping of tissues involved in PrP^C expression in the bovine will provide crucial information about the potential susceptibility to BSE infection. Moreover, comparison of the PrP^C expression during bovine development with other species may facilitate the understanding of the physiological function of this protein.

Using Q-PCR, western blot and immunohistochemistry, we investigated PrP^C expression during early stages of the bovine embryonic and fetal development. Our analysis detected expression of *Prnp* mRNA in all embryonic stages beginning with the unfertilized oocyte. Granulosa cells were separated by vortex agitation from oocytes to eliminate potential contamination of oocytes. We analyzed *Prnp* expression separately in granulosa cells and found approximately 18-fold higher expression compared to the oocyte level. Analyses of expression of *Prnp* were also performed in mature sperm to estimate the potential contribution to the oocyte level during fertilization. We and others have previously shown that the PrP^C protein is present in the mature sperm (Chapter II; Shaked et al., 1999). However, we found no significant differences in the amount of mRNA expression between the sperm and the oocyte, suggesting that the

potential increase of *Prnp* expression after fertilization is a consequence of embryonic regulation. The onset of embryonic gene transcription and translation in the bovine begins as early as the zygote stage and increases gradually until 2- and 4-cell stages (Viuff et al., 1996; Hytell et al., 1996; Memili and First, 1998; Memili and First, 2000). A previous study reported that the peak in PrP^C expression during pre-implantation occurred at the zygote stage in contrast to insignificant levels at the 8- and 16-cell stages (Thumdee et al., 2007). However, our data both at the mRNA and protein level showed that the peak in PrP^C expression occurs at 8-to-16-cell stage. Differences between both studies may be attributed to the use of *in vivo* versus *in vitro* produced embryos that may influence the timing of gene activation. Our data indicates that the up-regulation of *Prnp* expression occurs during the maternal-zygote transition (MZT). This process is the major onset in embryonic transcription, characterized by the gradual degradation of maternal RNAs and protein, and the activation of embryonic gene transcription (Barnes and First, 1991; Memili and First, 1999). Several proteins detected before or during MZT have been shown to be essential for the development of the embryo beyond the 9- to 16-cell stages (Memili and First, 1998). Up-regulation of *Prnp* at the MZT suggests a potential role for PrP^C during subsequent stages of embryonic development. Our analyses showed a second peak in *Prnp* expression at day 18. At this time, PrP^C protein was localized to trophoblast cells. Beginning at day 18 after estrus, the bovine embryo undergoes a critical process of maternal recognition and very early stages of a gradual attachment to the uterus. The cotyledonary chorioallantois formed from the trophoblast is the tissue that attaches to the uterine caruncular endometrium. A previous study reported that PrP^C levels are up-regulated in uterine caruncles during pregnancy in the sheep (Tuo et al., 2001). PrP^C has been found to support cell-to-cell adhesion by interacting with several binding partners including the major basement membrane component laminin (Graner et al., 2000). Taken together, this data suggests that the up-regulation of PrP^C at day 18 may be associated with participation of PrP^C as a cell adhesion factor.

Our study showed an intense expression of PrP^C in the developing nervous system during early fetal development. PrP^C staining was observed as early as day 27 in the CNS and was detected at day 39 in the brain, spinal cord, dorsal root ganglia, cervical ganglia, sympathetic trunks and peripheral nerves. The development of the primitive peripheral nervous system was evident on day 39, characterized by PrP^C-positive neural trunks emerging from the cervical and lumbar segments of the spinal cord. Throughout all stages of development, the staining of PrP^C was detected in more differentiated neural cells located in the pial region of the CNS and not in mitotically active cells of the periventricular zone. This pattern of expression in the nervous system appears to persist during the adult life in mammals (Kretzschmar et al., 1986). These observations are consistent with the role of PrP^C in neuronal migration, adhesion and

differentiation as previously reported. PrP^C have been shown to enhanced neurite outgrowth when added to neurons cultured *in vitro* (Kanaai et al., 2005). PrP^C may activate signaling pathways associated with neuritogenesis and neural migration by interaction with laminin (Graner et al., 2000; Martins et al., 2001). Moreover, PrP^C facilitates axonal growth via *cis* and *trans* interactions with N-CAM, a process that involves recruitment of N-CAM to lipid rafts and activation of fyn kinase (Santuccione et al., 2005).

Throughout our analysis in bovine fetuses, we detected PrP^C expression in several peripheral organs. Intense PrP^C staining was observed in nervous tissue associated with the intestine and lungs. PrP^C labeling in one of the layers of the intestinal wall appeared to be associated with the parasympathetic myenteric plexus as showed by analyses in adult stages (Chapter II; Lemaire-Vieille et al., 2000; Ford et al., 2002). PrP^C staining was also detected in scattered multinuclear cells in the liver. These cells showed a pattern of staining similar to that of macrophages previously reported in fetal liver at day 34 (Kritzenberger and Wrobel, 2004). Primitive macrophages at this stage participate in erythropoiesis and later differentiate into Kupffer cells (Sasaki and Sonoda, 2000). Alternatively, megakaryocytes have displayed a similar cell-specific staining in day-34 fetuses and have been shown to express PrP^C in adult stages (Kritzenberger and Wrobel, 2004; Starke et al., 2005). Further analyses using double-immunodetection techniques with markers for the erythropoyetic cell lineage would allow identification of these cells. Glomerular and tubule epithelial cells of the mesonephric duct displayed intense labeling for PrP^C during all stages of fetal development. The mesonephric duct differentiates into structures of the reproductive system including the epididymis and the ductus deferens. Analyses of the male reproductive system indicate that these structures continued showing expression of PrP^C during adulthood (see Chapter III).

In the present study we documented the relative levels of *Prnp* and the tissue-specific expression of PrP^C during bovine embryonic and early fetal development. We showed that *Prnp* is up-regulated at the MZT suggesting that PrP^C may exert a potential function during subsequent stages of development. Thereafter, PrP^C was up-regulated at day 18 suggesting the participation in the cell adhesion process associated to the attachment of the embryo. Throughout the fetal stages, PrP^C expression showed a close relation to the development of the nervous system. During this process PrP^C was widely distributed in the CNS and peripheral neurons and displayed a selective expression in post-mitotic and differentiated neural cells. In conclusion, our study suggests the participation of PrP^C in several cellular processes occurring during development including cell adhesion, differentiation, and migration.

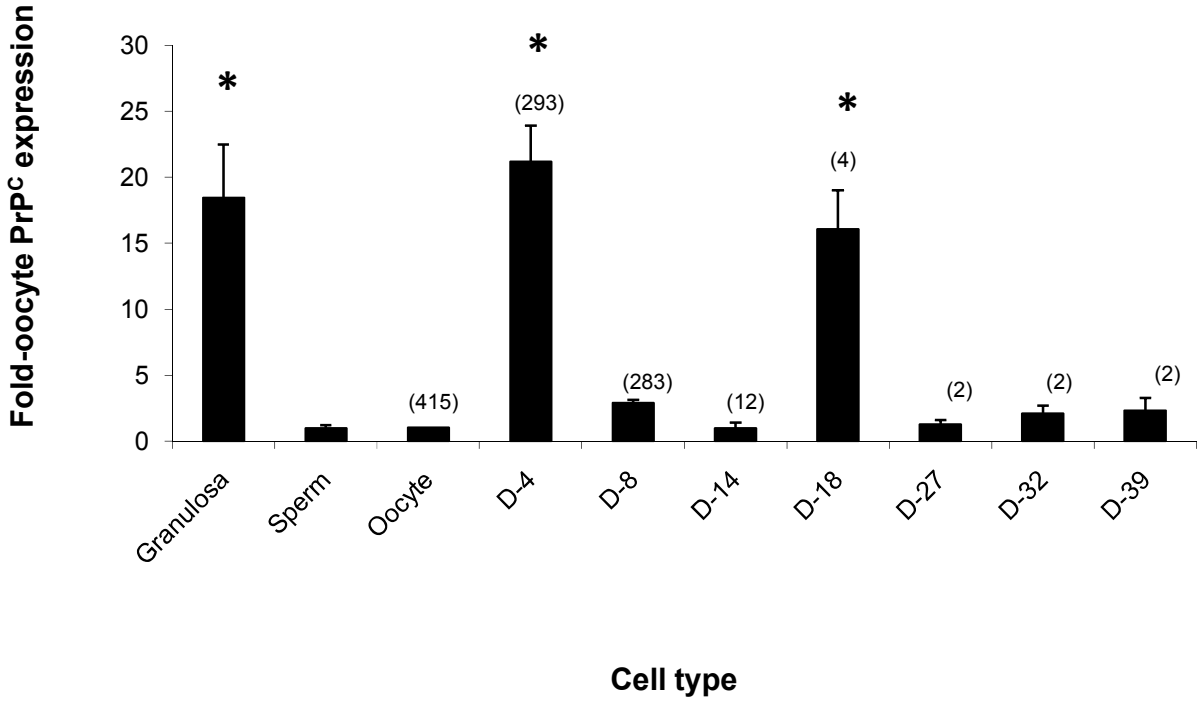

Figure 1. Relative expression of *Prnp* mRNA in granulosa cells, sperm, oocytes and during bovine embryonic and early fetal development. *Prnp* mRNA levels were detected using Q-PCR, compared to 18s rRNA and standarized to oocyte expression value. Granulosa cells showed significantly higher expression compared to oocytes. The highest ($P<0.05$) levels of relative *Prnp* expression were detected at day 4 and at day18of bovine development. (*) Indicates significant difference ($P<0.05$).

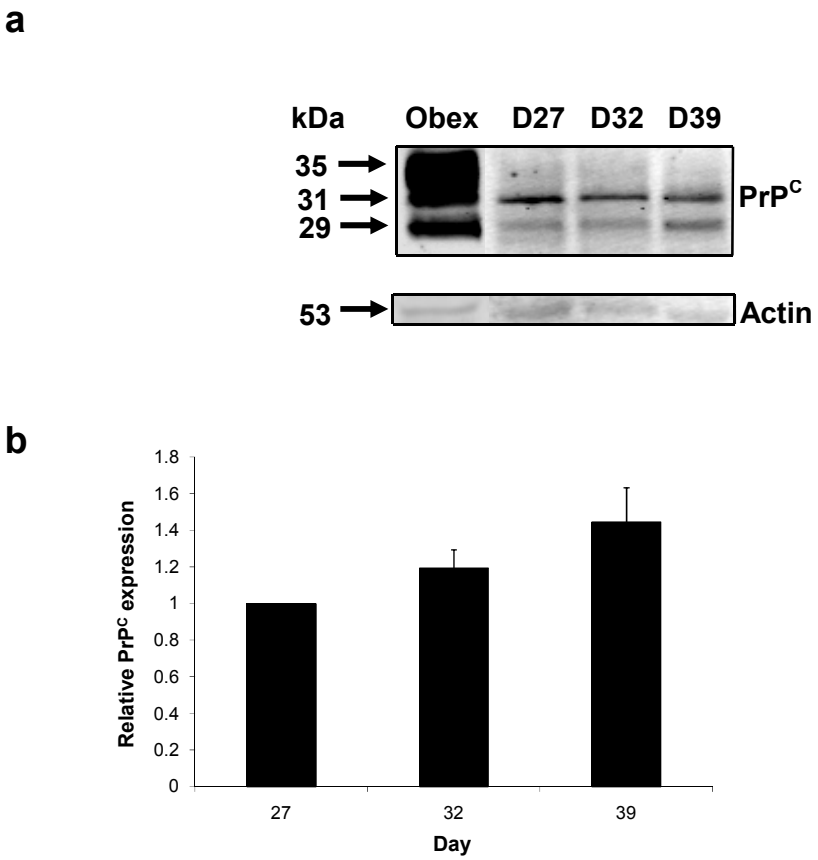

Figure 2. Expression of PrP^C protein during early bovine fetal development. PrP^C was detected by western blot using SAF-32 anti-PrP antibody. Migratory bands were computarized quantified using an Odyssey infrared imaging system. (a) PrP^C displayed two migratory bands representative of different isoforms of the protein. (b) Relative levels of PrP^C protein expression were standarized to Day-27 fetus level of expression.

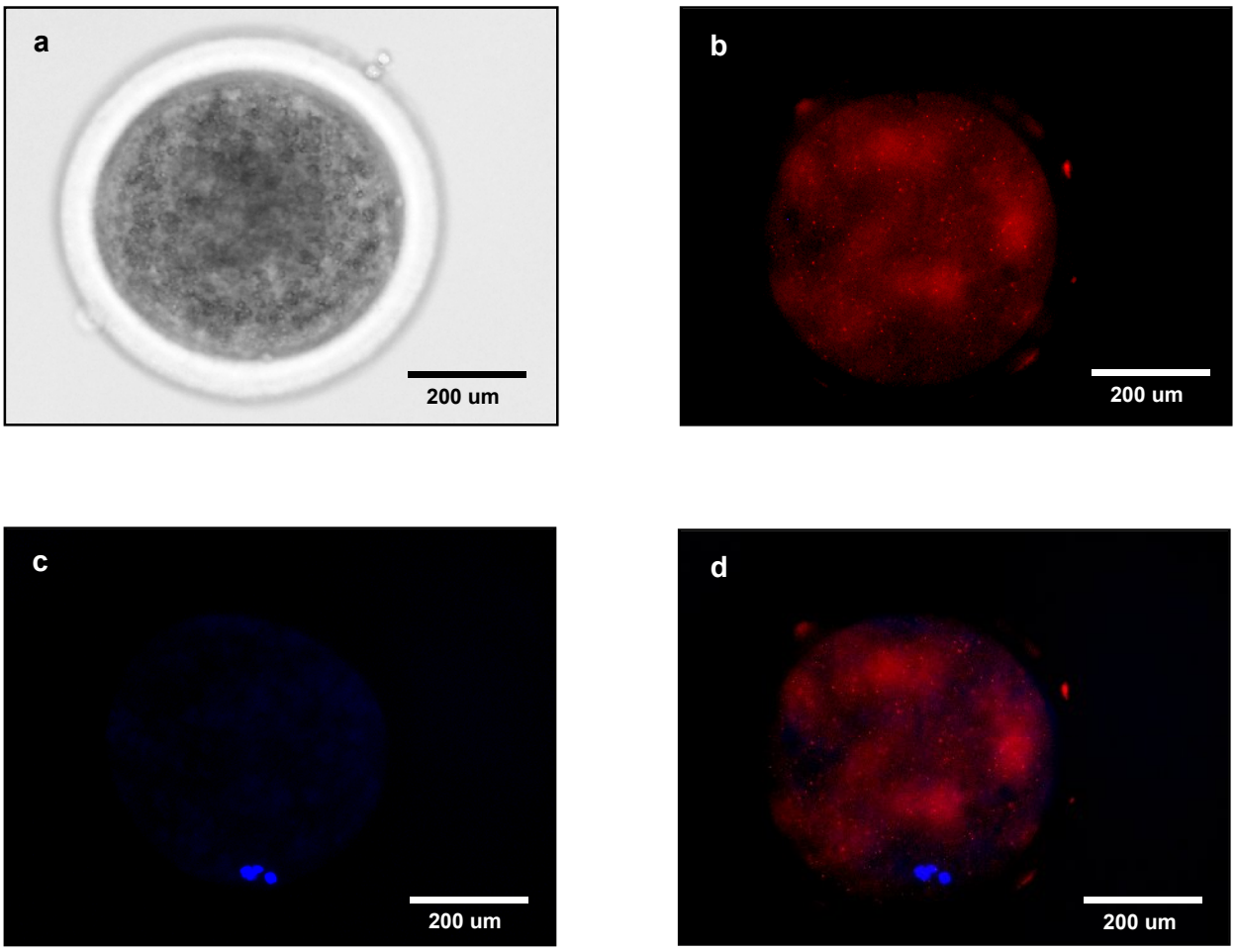

Figure 3. Expression of PrP^C protein in bovine oocytes. PrP^C was immunodetected using SAF-32 antibody followed by Alexa Fluor 594 secondary antibody and counterstained with DAPI. A puntuate pattern of specific immunofluorescence was homogeneously distributed on the oocyte cytoplasm. (a) Phase contrast; (b) PrP^C; (c) DAPI; (d) Merged PrP^C-DAPI.

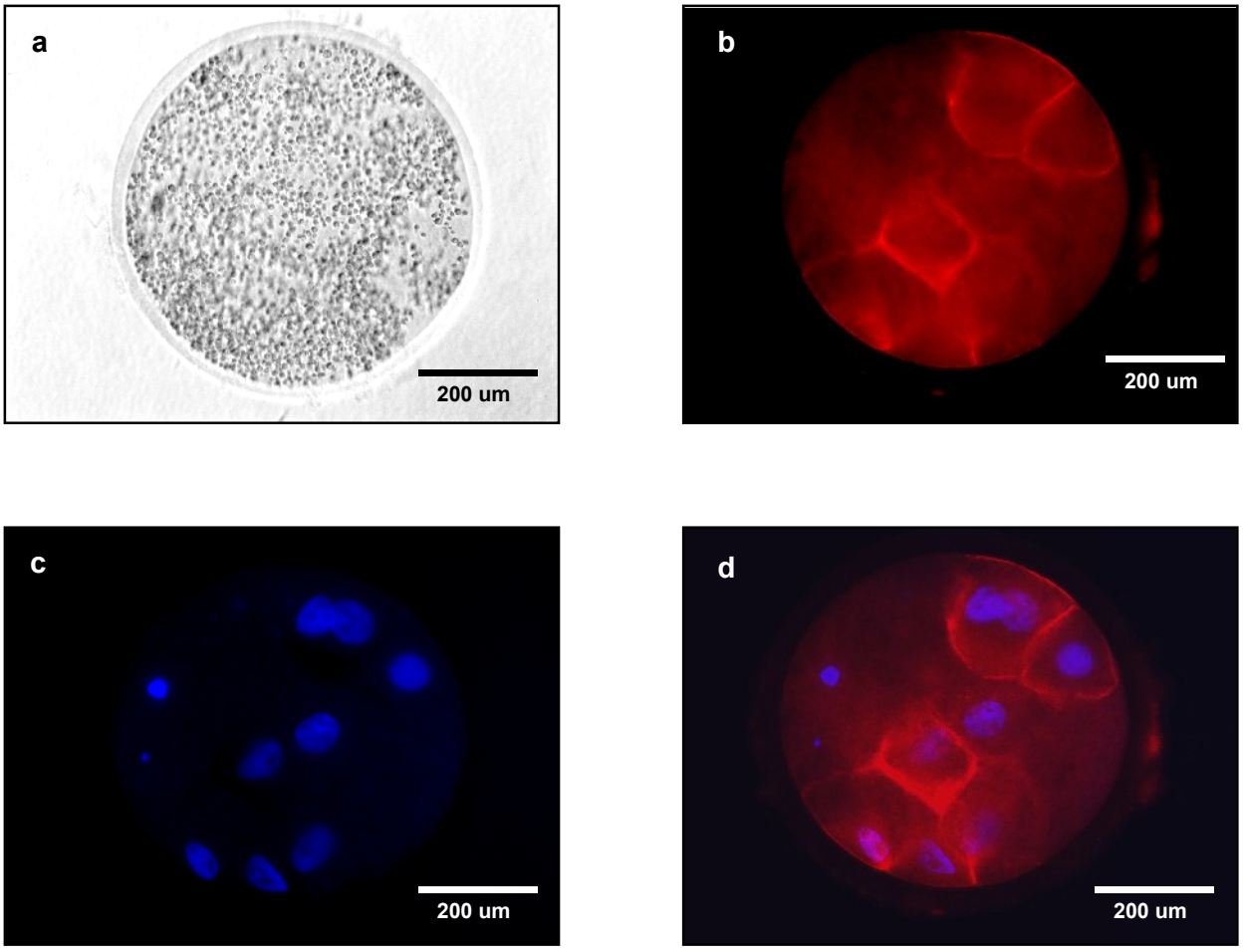

Figure 4. Expression of PrP^C protein in the 8-cell bovine embryo (day 4). PrP^C was immunodetected using SAF-32 antibody followed by Alexa Fluor 594 secondary antibody and counterstained with DAPI. Intense PrP^C specific immunofluorescence was observed in the plasma membrane of blastomeres. (a) Phase contrast; (b) PrP^C; (c) DAPI; (d) Merged PrP^C-DAPI.

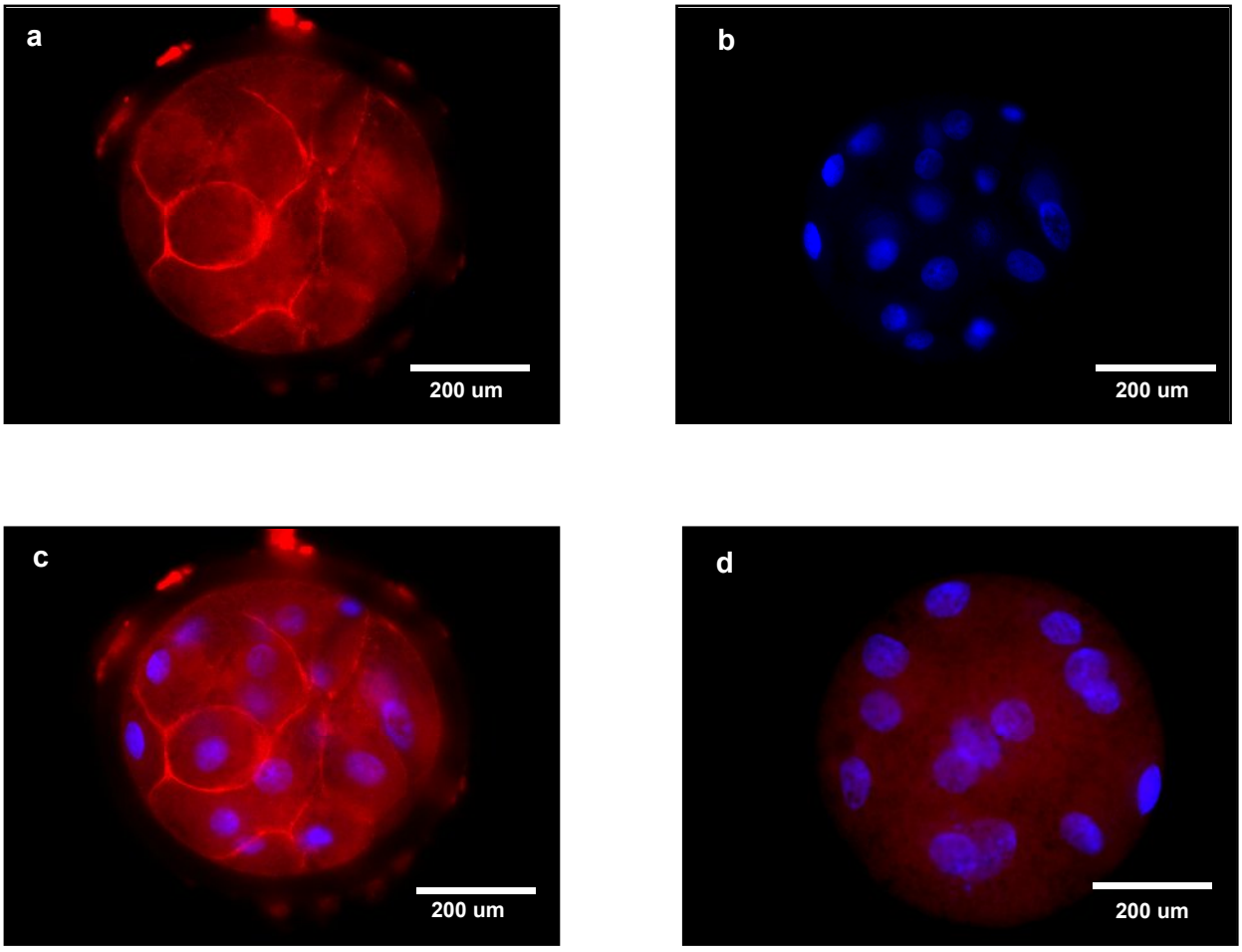

Figure 5. Expression of PrP^C protein in the 16-cell bovine embryo (day 4). PrP^C was immunodetected using SAF-32 antibody followed by Alexa Fluor 594 immunofluorescent secondary antibody and counterstained with DAPI. PrP^C specific immunofluorescence was observed in the plasma membrane of blastomeres. (a) PrP^C; (b) DAPI; (c) Merged PrPC-DAPI; (d) Negative control incubated with non-immune hose serum instead of SAF-32.

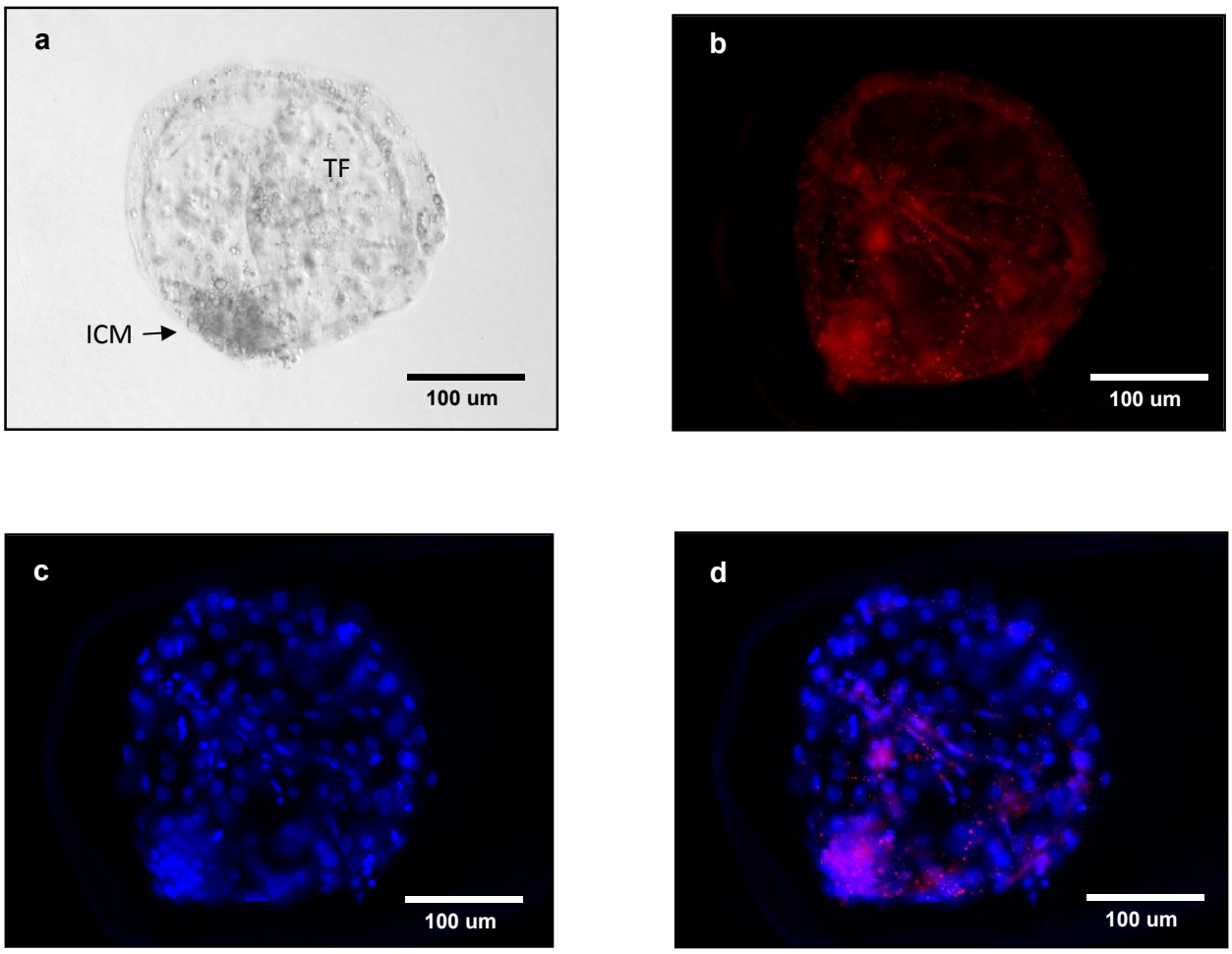

Figure 6. Expression of PrP^C protein in the bovine blastocyst (day 9). PrP^C was immunodetected using SAF-32 antibody followed by Alexa Fluor 594 immunofluorescent secondary antibody and counterstained with DAPI. Spots of specific PrP^C immunofluorescence were observed homogeneously distrubuted on cells in the trophoblast (TF) and intensely present in the inner cell mass (ICM). (a) Phase contrast; (b) PrP^C; (c) DAPI; (d) Merged PrP^C-DAPI.

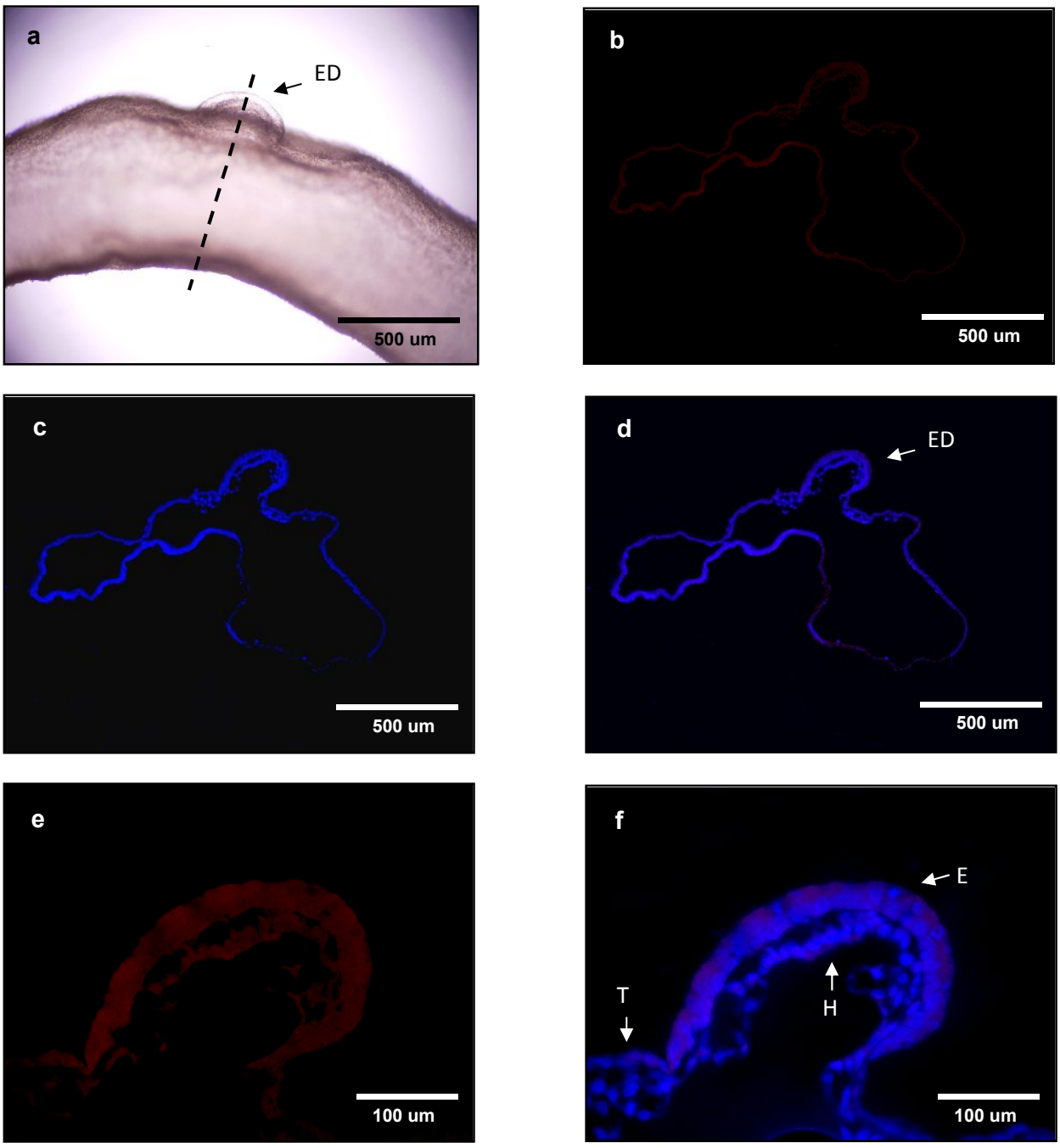

Figure 7. Expression of PrP^C protein in bovine embryo (day 14). PrP^C was immunodetected using SAF-32 antibody followed by Alexa Fluor 594 secondary antibody and counterstained with DAPI. (a) Phase contrast view of the embryonic disc (ED). Line indicates orientation of the histological sections. Non-specific immunofluorescence was detected in the embryonic disc and the trophoblast (T). (b) PrP^C; (c) DAPI; (d) Merged PrP^C-DAPI; (E) Embryonic disc PrP^C; (f) PrP^C-DAPI. Abbreviations: E, Epiblast; ED, Embryonic Disc, H, Hypoblast; T, Trophoblast.

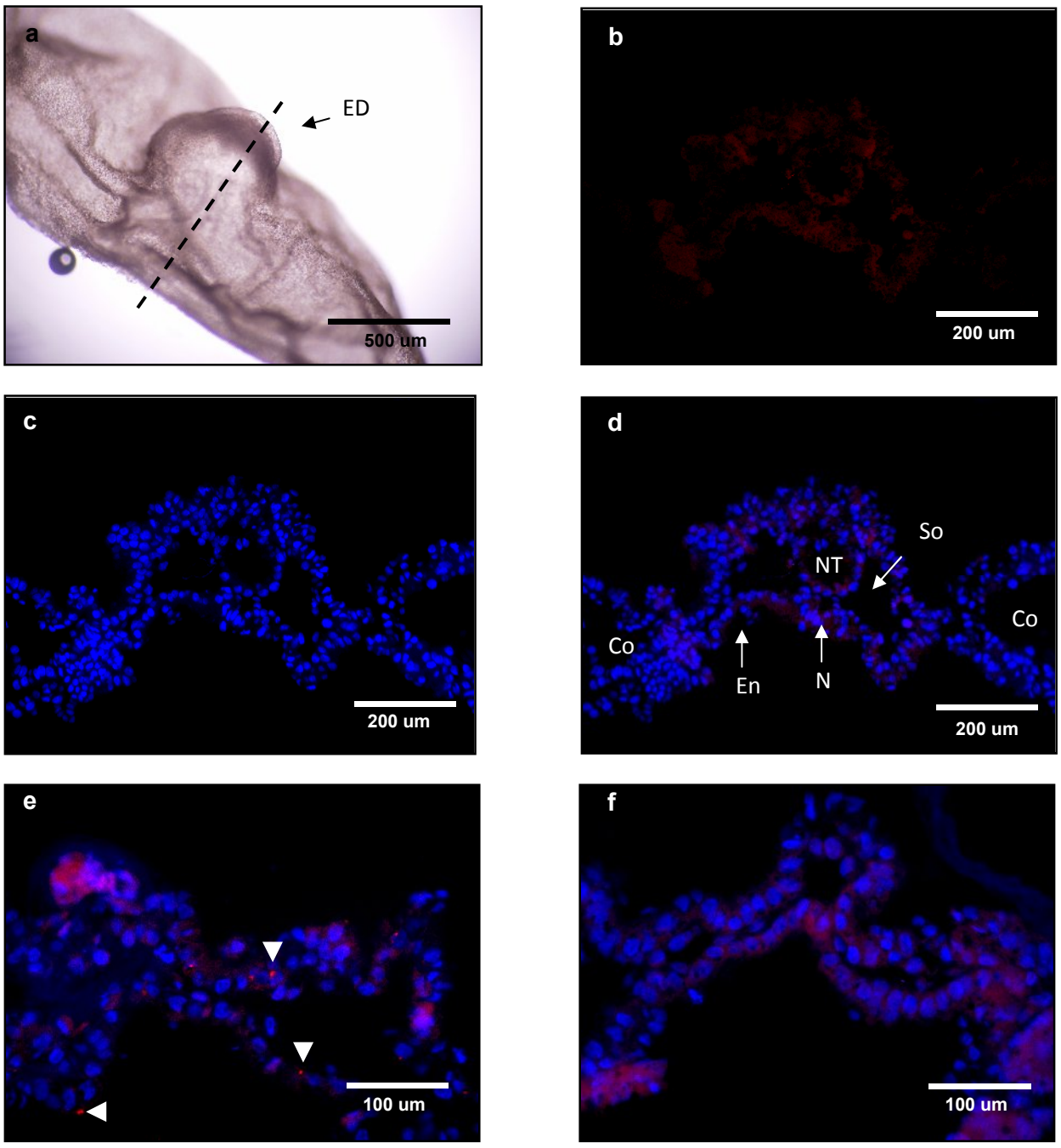

Figure 8. Expression of PrP^C protein in bovine embryo (day 18). PrP^C was immunodetected using SAF-32 antibody followed by Alexa Fluor 594 secondary antibody and counterstained with DAPI. (a) Phase contrast view of the embryonic disc (ED). The embryonic disc showed non-specific labeling; however, spots of PrP^C-specific immunofluorescence were observed in areas of the trophoblast (e,white arrows). (f) Negative control of (e); (b) PrP^C, (c) DAPI; (d) Merged PrP^C-DAPI. Abbreviations: Co, Coelom; En, Endoderm; N, Notocord; NT, Neural Tube; So, Somite.

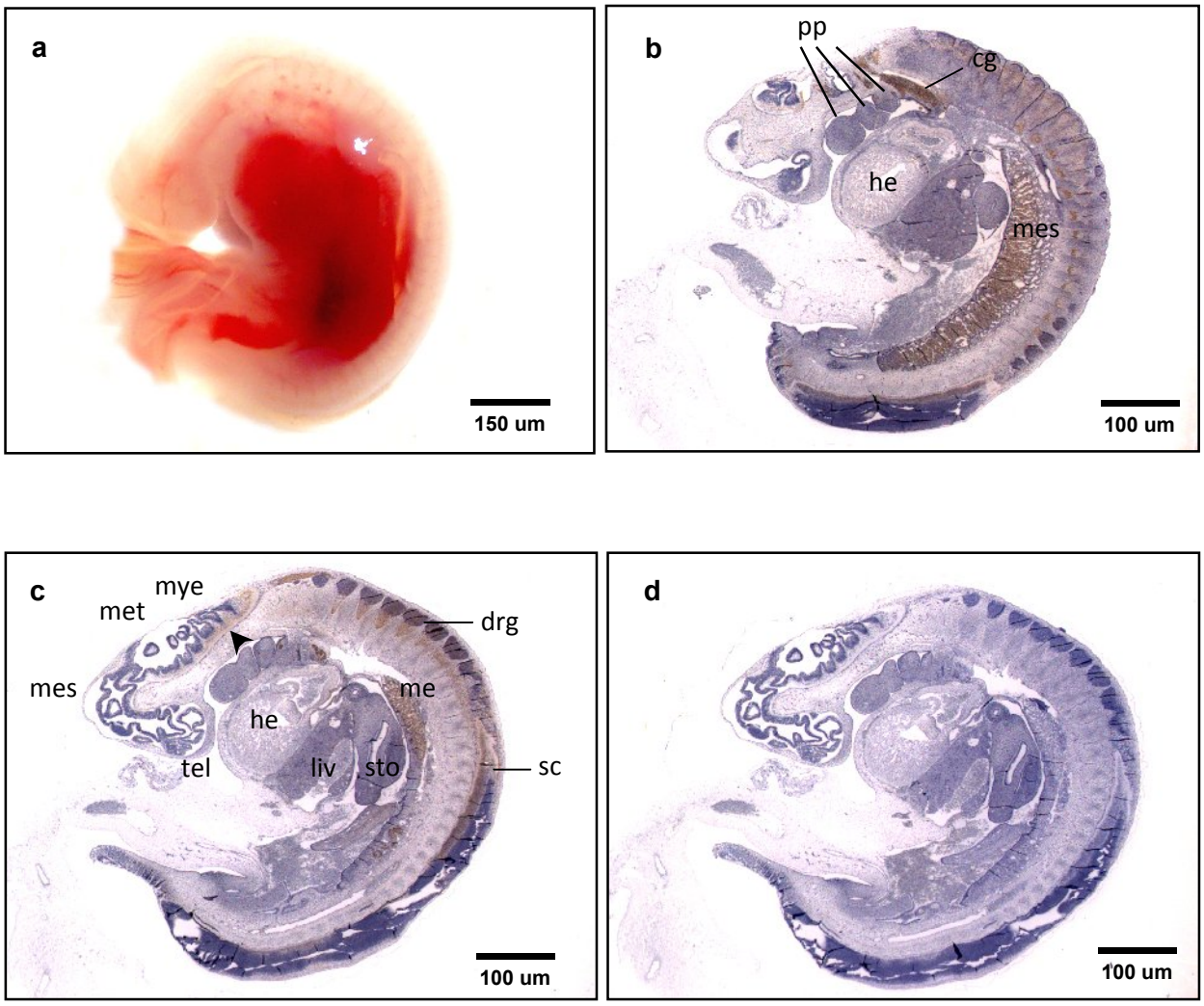

Figure 9. Expression of PrP^C protein in bovine fetus (day 27). PrP^C was immunodetected using SAF-32 antibody followed by peroxidase-conjugated goat anti-mouse IgG and counterstained with hematoxylin. PrP^C specific immunostaining was detected un the brain at the level of the myelencephalon (*arrow-head*), dorsal root ganglion, spinal cord and mesonephros. (a) Phase contrast; (b) Lateral and (c) medial sections; (d) Negative control incubated with with non-immune horse serum instead of SAF-32 and counterstained with hematoxilyn. Abbreviations: cg, cervical ganglia; drg, dorsal root ganglion; he, heart; li, liver; me, mesonephros, mes, mesencephalon; met, metencephalon; mye, myelencephalon; pp, pharyngeal pouches; sc, spinal cord; sto, stomach; tel, telencephalon.

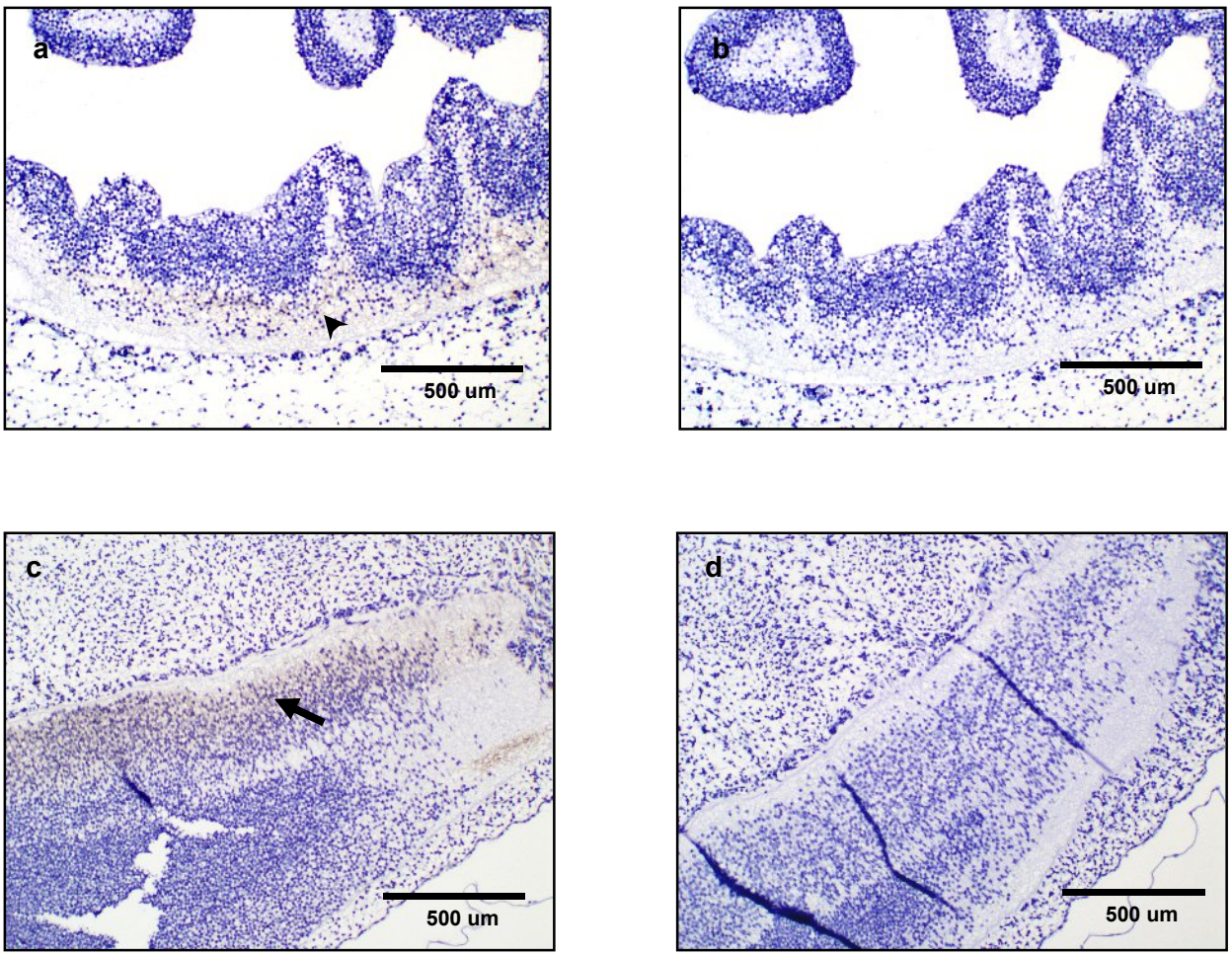

Figure 10. Expression of PrP^C protein in the CNS of the bovine fetus (day 27). PrP^C was immunodetected in the pial region of the neuroepithelium in the (a) brain (*arrow-head*) and (c) spinal cord (*black arrow*). No staining was detected in the ventricular region of the spinal cord (b,d) Negative controls incubated with with non-immune horse serum instead of SAF-32 and counterstained with hematoxilyn.

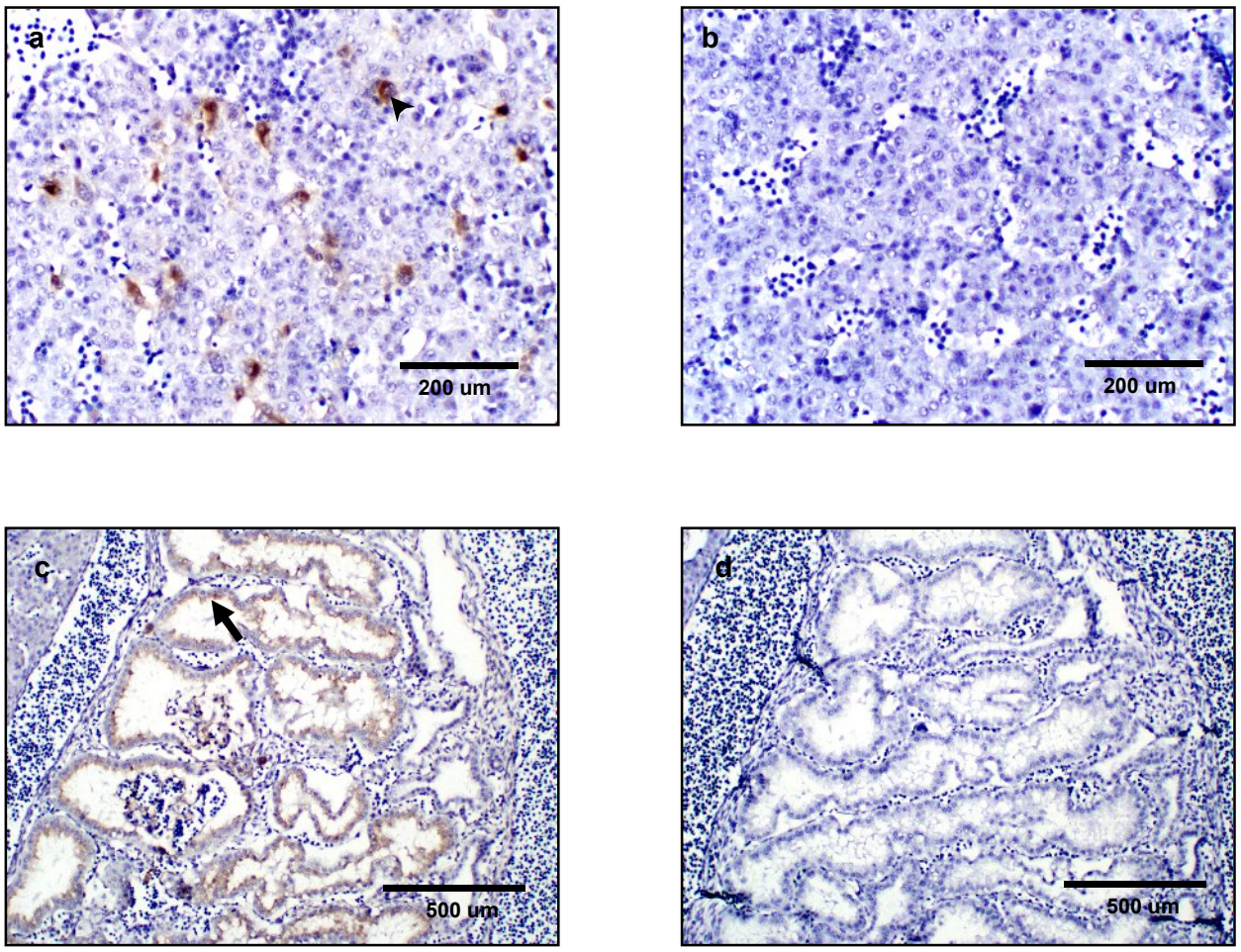

Figure 11. Expression of PrP^C protein in non-neural tissues of the bovine fetus (day 27). PrP^C cellular-specific immunostaining was observed in (a) scattered multinuclear cells in the liver (*arrowhead*) and (c) epithelial cells and glomeruli of the mesonephros (*black arrow*). (b,d) Negative controls incubated with with non-immune horse serum instead of SAF-32 and counterstained with hematoxilyn.

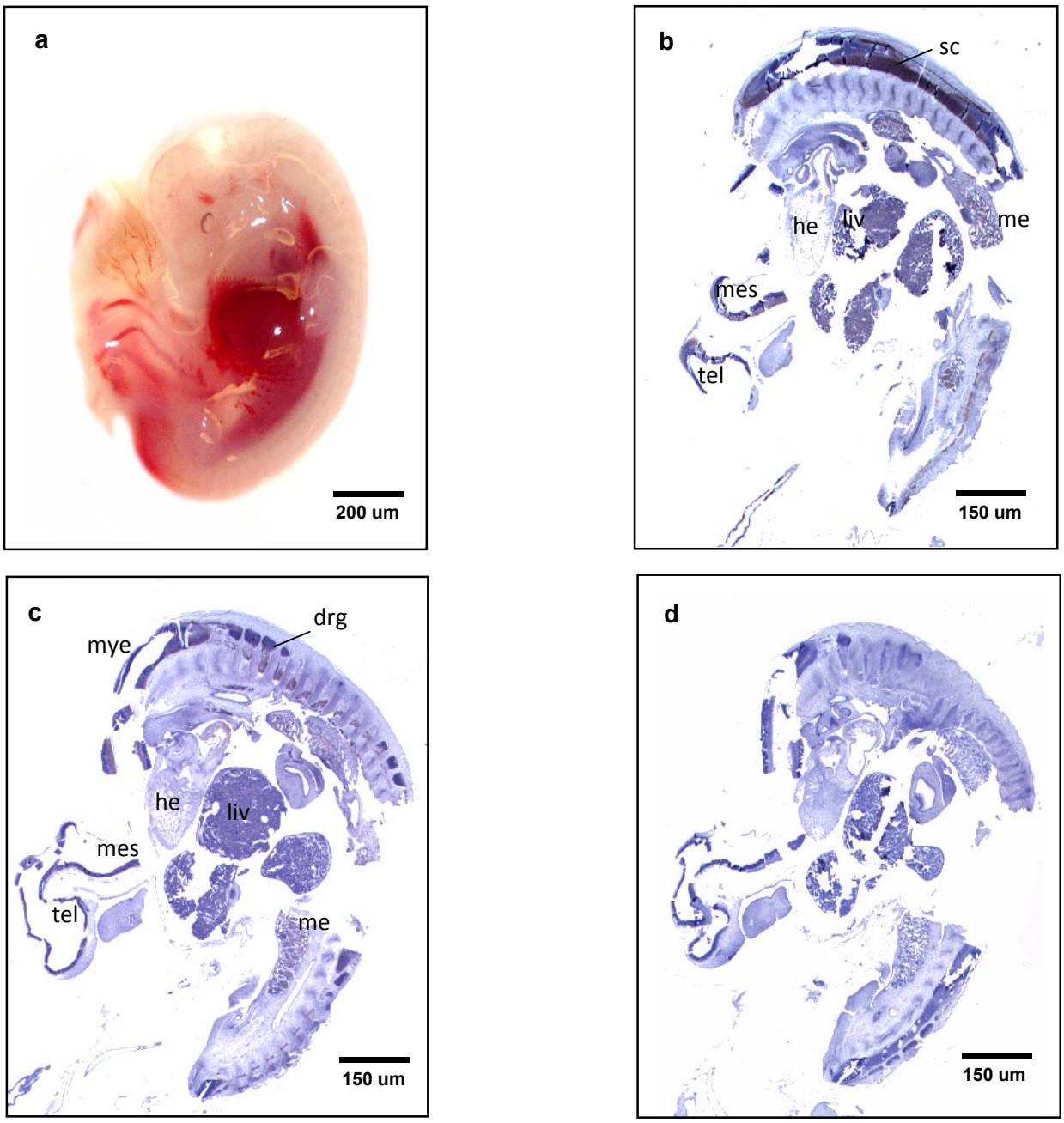

Figure 12. Expression of PrP^C protein in bovine fetus (day 32). PrP^C was immunodetected using SAF-32 antibody followed by peroxidase-conjugated goat anti-mouse IgG and counterstained with hematoxylin. (a) Phase contrast; (b,c) PrP^C specific immunostaining was detected in the developing brain, dorsal root ganglion, and spinal cord. (d) Negative control incubated with with non-immune horse serum instead of SAF-32 and counterstained with hematoxilyn. Abbreviations: drg, dorsal root ganglion; he, heart; li, liver; me, mesonephros, mes, mesencephalon; met, metencephalon; mye, myelencephalon; sc, spinal cord.

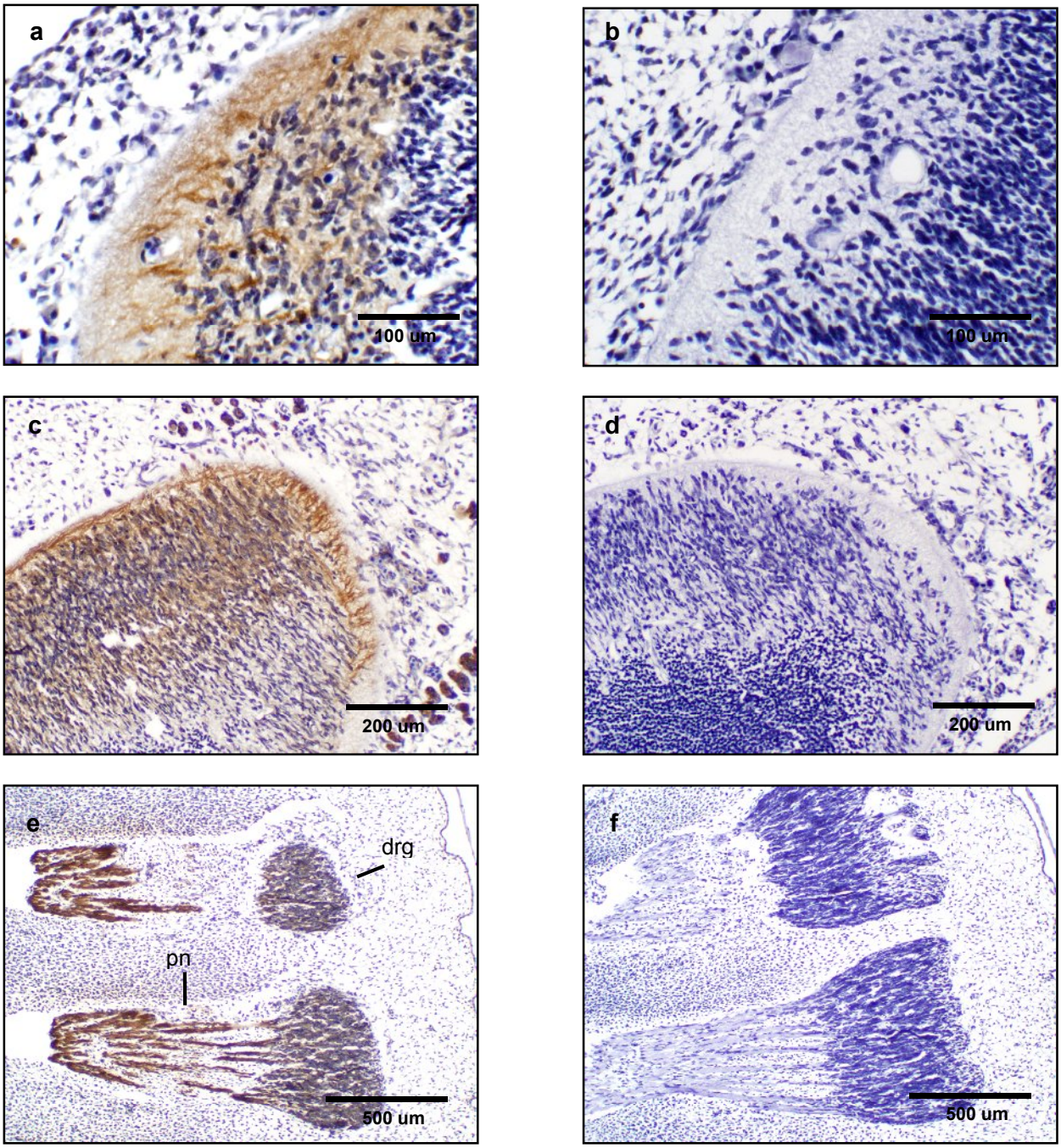

Figure 13. Expression of PrP^C protein in the nervous system of the bovine fetus (day 32). (a) PrP^C specific immunostaining was detected un the (a) pial region of the developing brain and (c) spinal cord. (e) Dorsal root ganglions (drg) and peripheral nerves (pn) were also immunopositive for PrP^C. (b,d,f) Negative controls incubated with with non-immune horse serum instead of SAF-32 and counterstained with hematoxilyn.

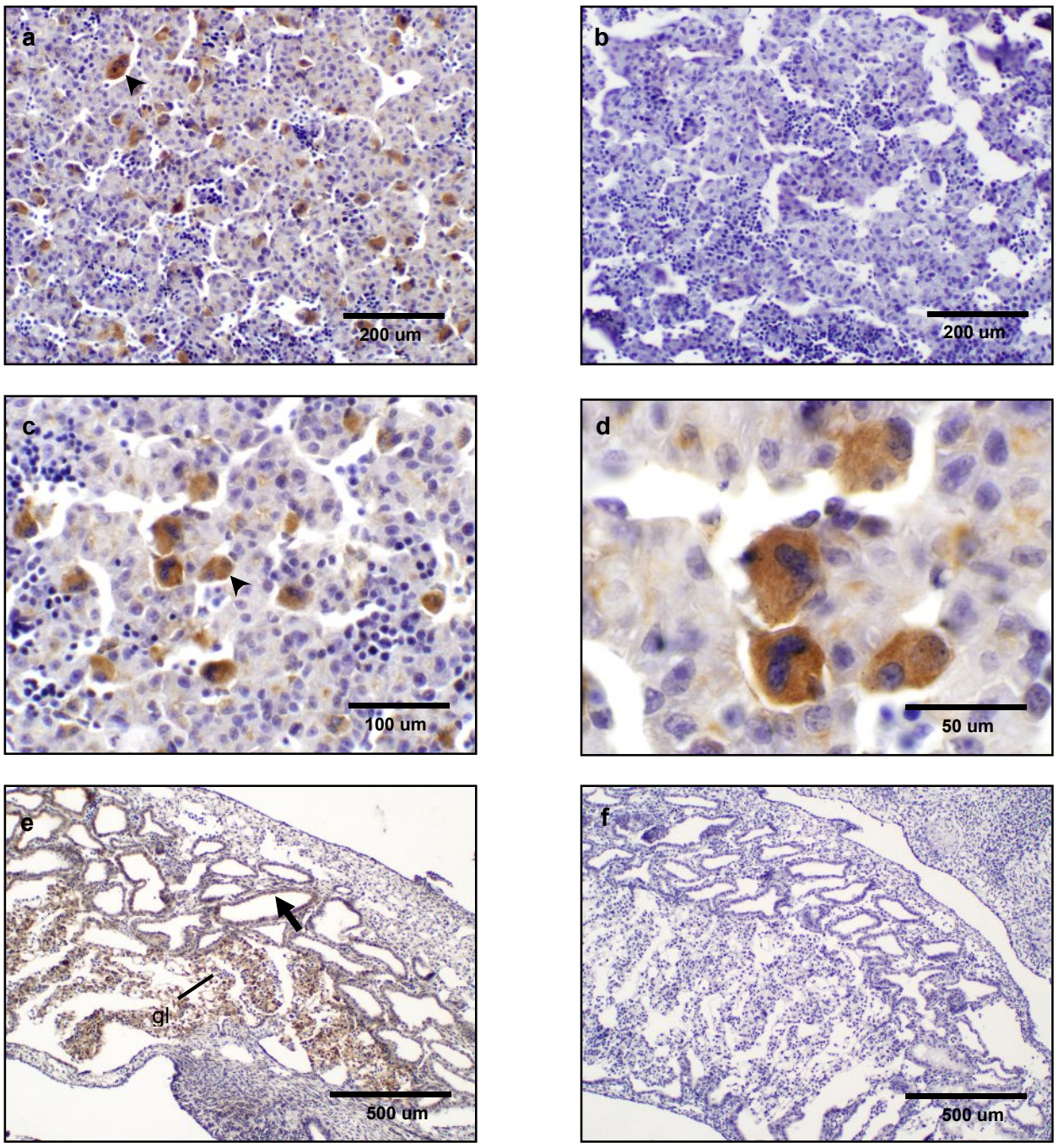

Figure 14. Expression of PrP^C protein in non-neural tissues of the bovine fetus (day 32). PrP^C cellular-specific immunostaining was observed in (a,c,d) scattered multinuclear large cells in the liver (*arrow-heads*) and epithelial cells of the (e) mesonephric duct (*black arrow*) and glomeruli (gl); (b,f) Negative control incubated with with non-immune horse serum instead of SAF-32 and counterstained with hematoxilyn.


a
300 um

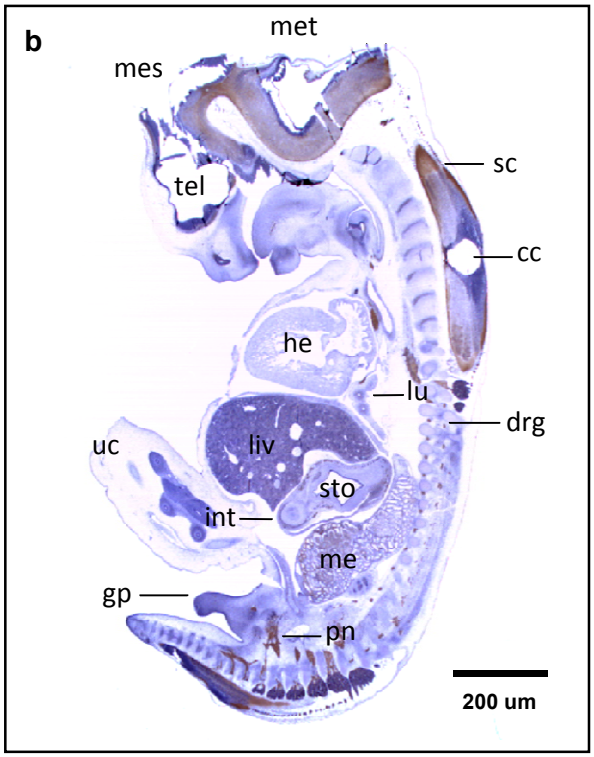
b
met
mes
tel
sc
cc
he
lu
drg
uc
liv
sto
int
me
gp
pn
200 um

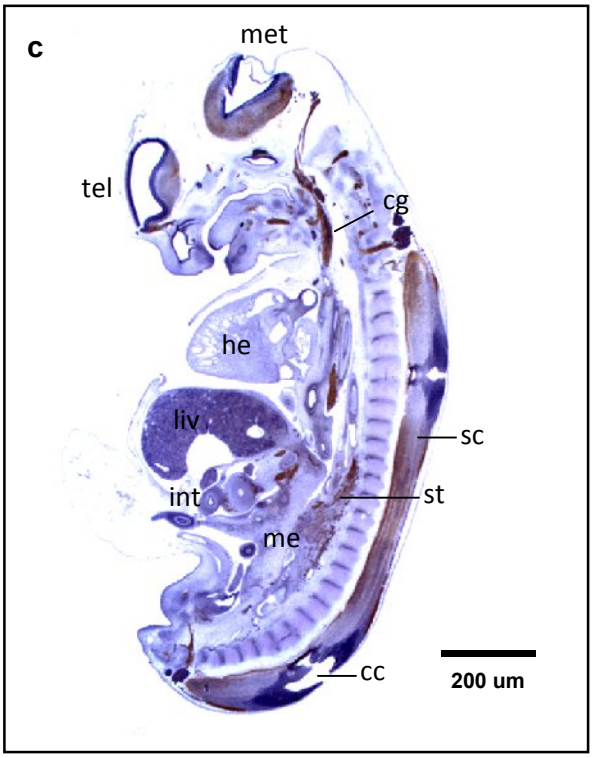
c
met
tel
cg
he
liv
sc
int
st
me
cc
200 um

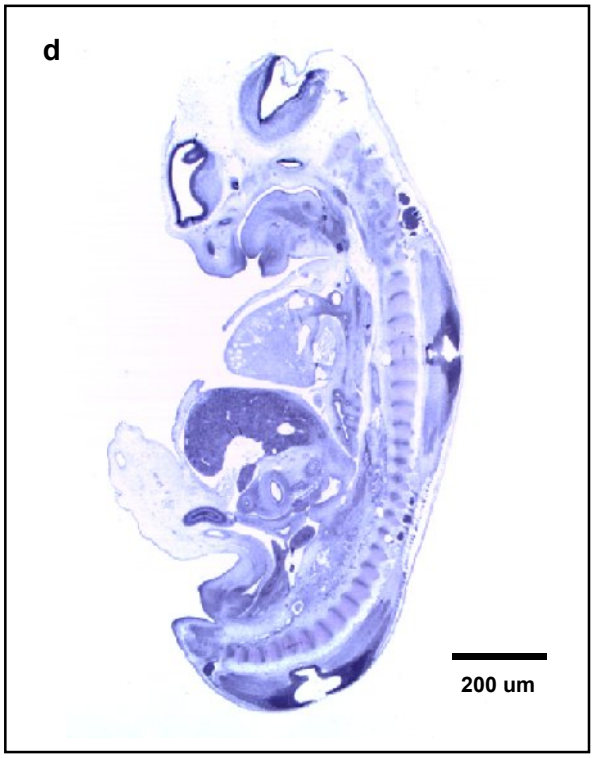
d
200 um

Figure 15. Expression of PrP^C protein in bovine fetus (day 39). (a) Phase contrast; (b,c) PrP^C specific immunostaining was detected in the (a) telencephalon, mesencephalon and myelencephalon. PrP^C labelling was also observed in the dorsal root ganglions, cervical ganglia, sympathetic trunks, peripheral nerves, spinal cord and mesonephros. (d) Negative control incubated with with non-immune horse serum instead of SAF-32 and counterstained with hematoxilyn. Abbreviations: cc, cord canal; cg, cervical ganglia; drg, dorsal root ganglion; gp, genital papila; he, heart; li, liver; lu, lung; me, mesonephros; mes, mesencephalon; met, metencephalon; pn, peripheral nerve; tel, telencephalon; sc, spinal cord; st, sympathetic trunks.

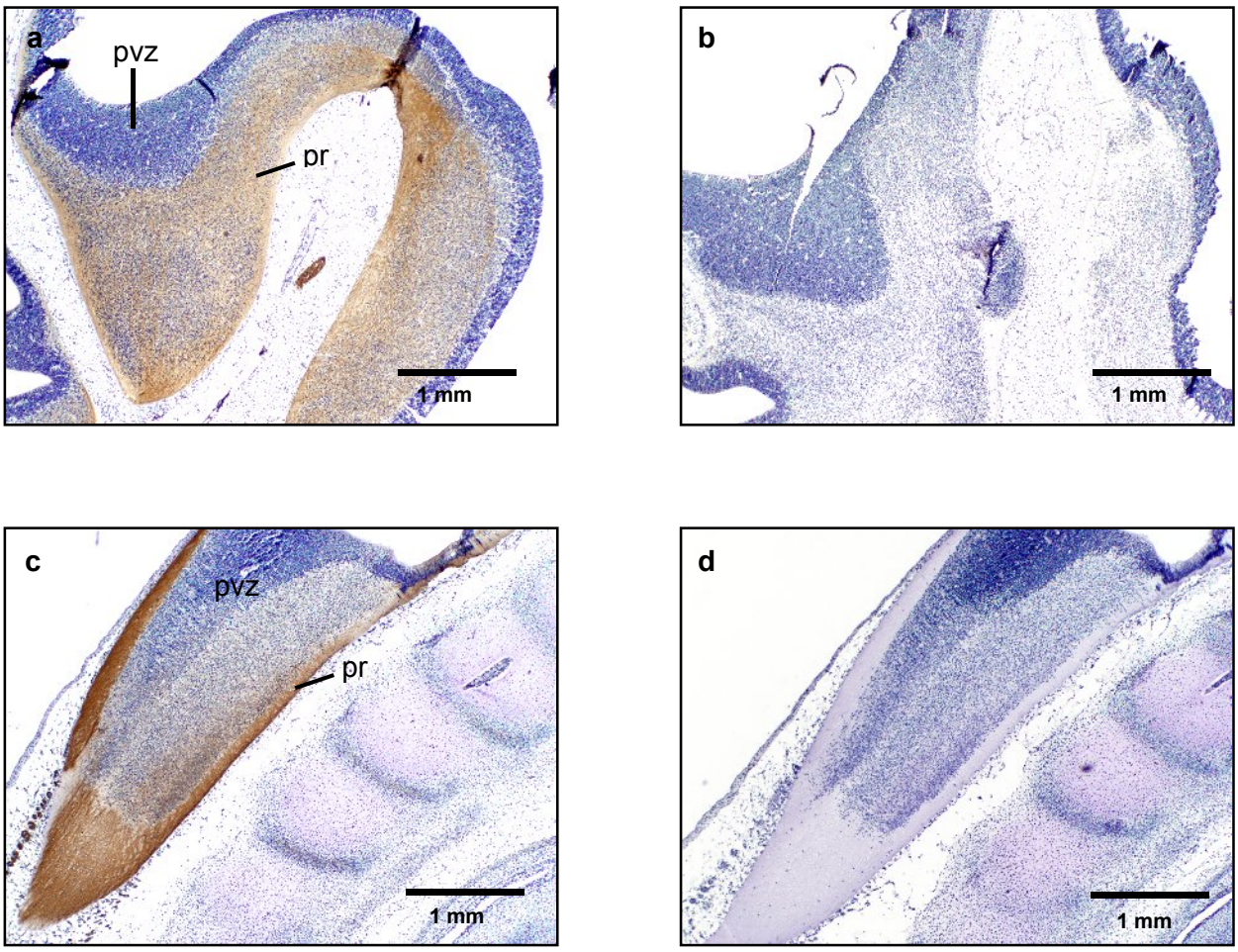

Figure 16. Expression of PrP^C protein in the central nervous system of the bovine fetus (day 39). (a) PrP^C specific immunostaining was detected in the pial region (pr) of the brain (a) and spinal cord. No immunoreactivity for PrP^C was observed in the paraventricular zone (pvz). (b,d) Negative control incubated with horse serum instead of SAF-32 and counterstained with hematoxilyn.

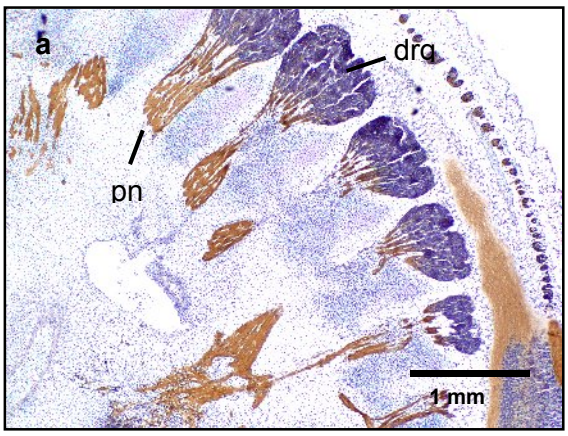
a
drg
pn
1 mm

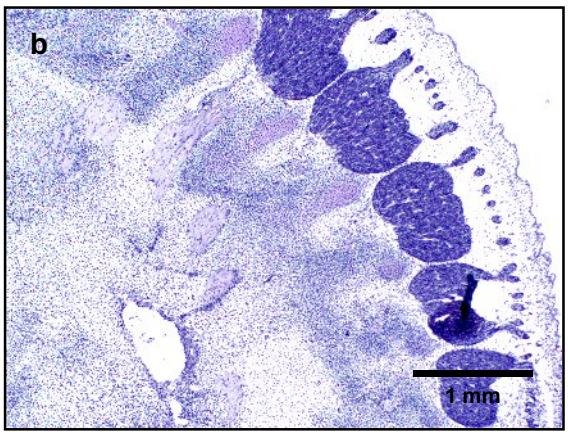
b
1 mm

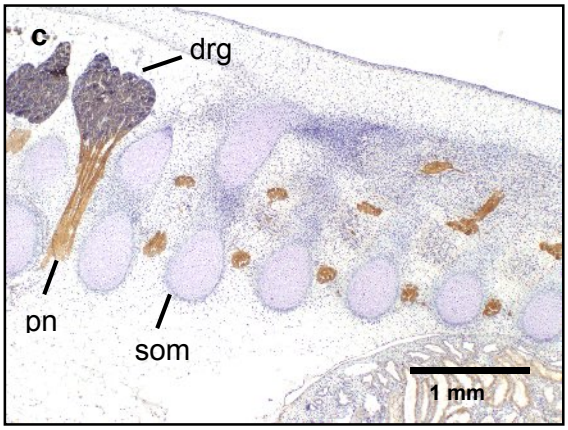
c
drg
pn
som
1 mm

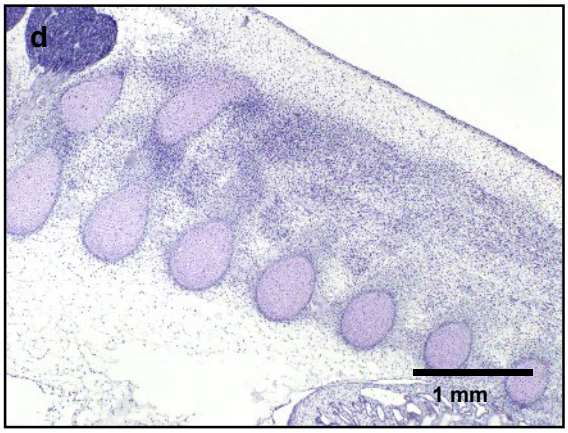
d
1 mm

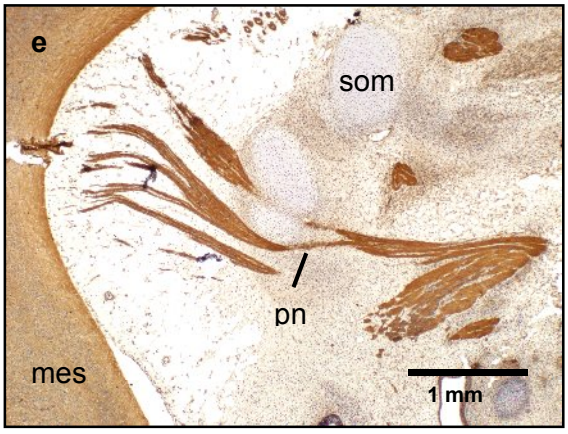
e
som
pn
mes
1 mm

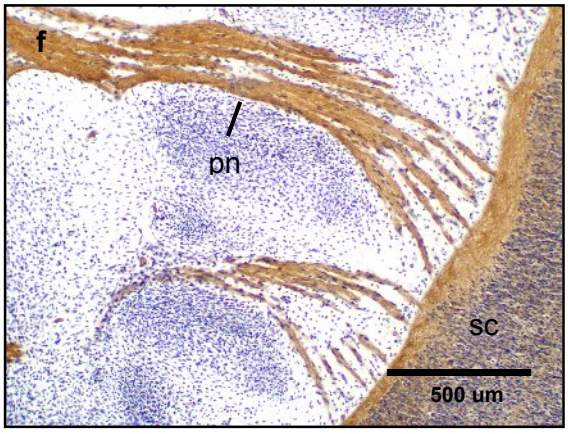
f
pn
sc
500 um

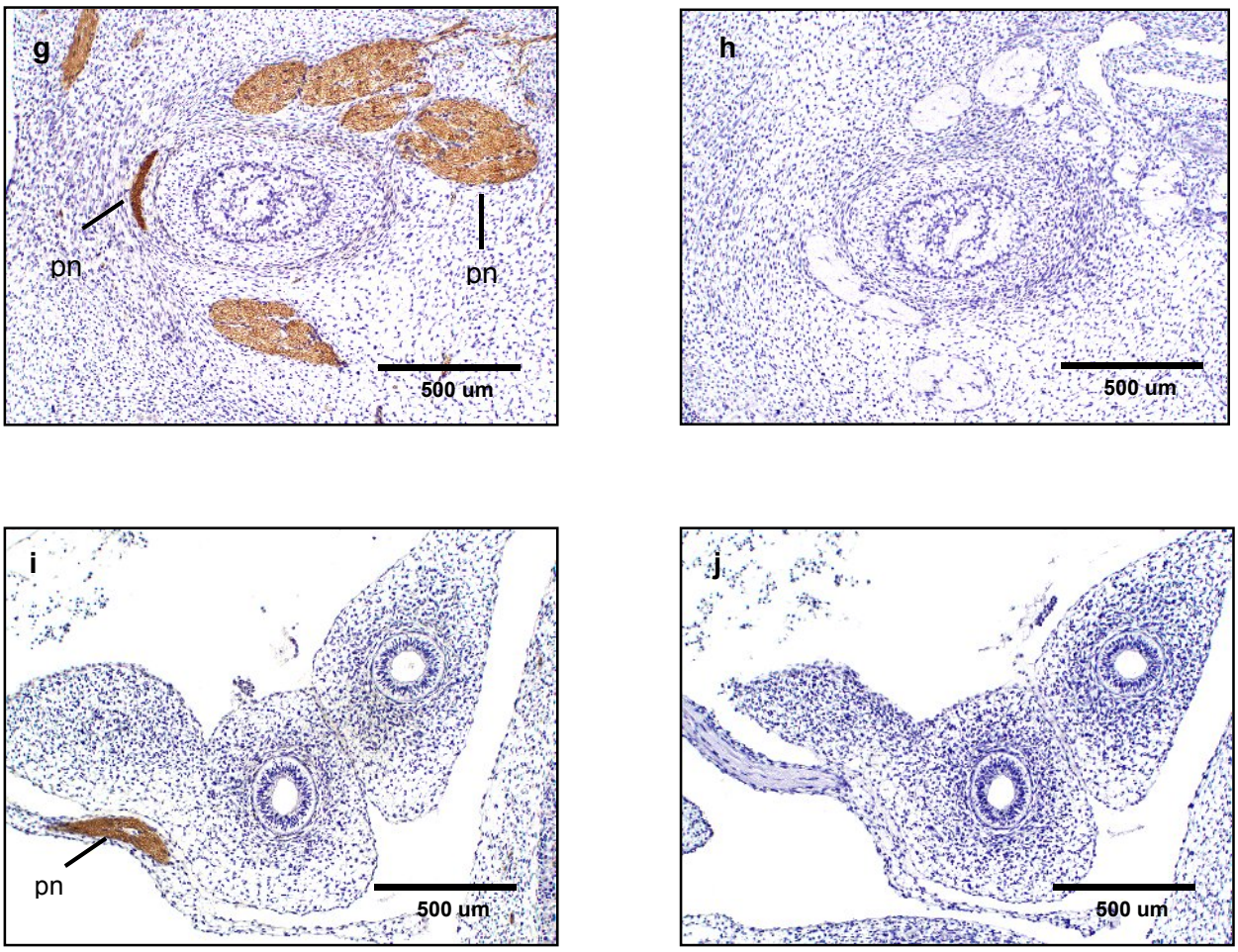

Figure 17. Expression of PrP^C protein in the peripheral nervous system of the bovine fetus (day 39). (a) PrP^C specific immunostaining was detected in (a,c) peripheral nerves (pn) emerging from the dorsal root ganlgions and (c) from the mesencephalon and (d) spinal cord. PrP^C labelling was evident in peripheral nerves (pn) associated with the (g) intestine and the intestinal wall (black arrows) and (i) lungs; (b,d,h,j) Negative control, incubated with with non-immune horse serum instead of SAF-32 and counterstained with hematoxilyn.

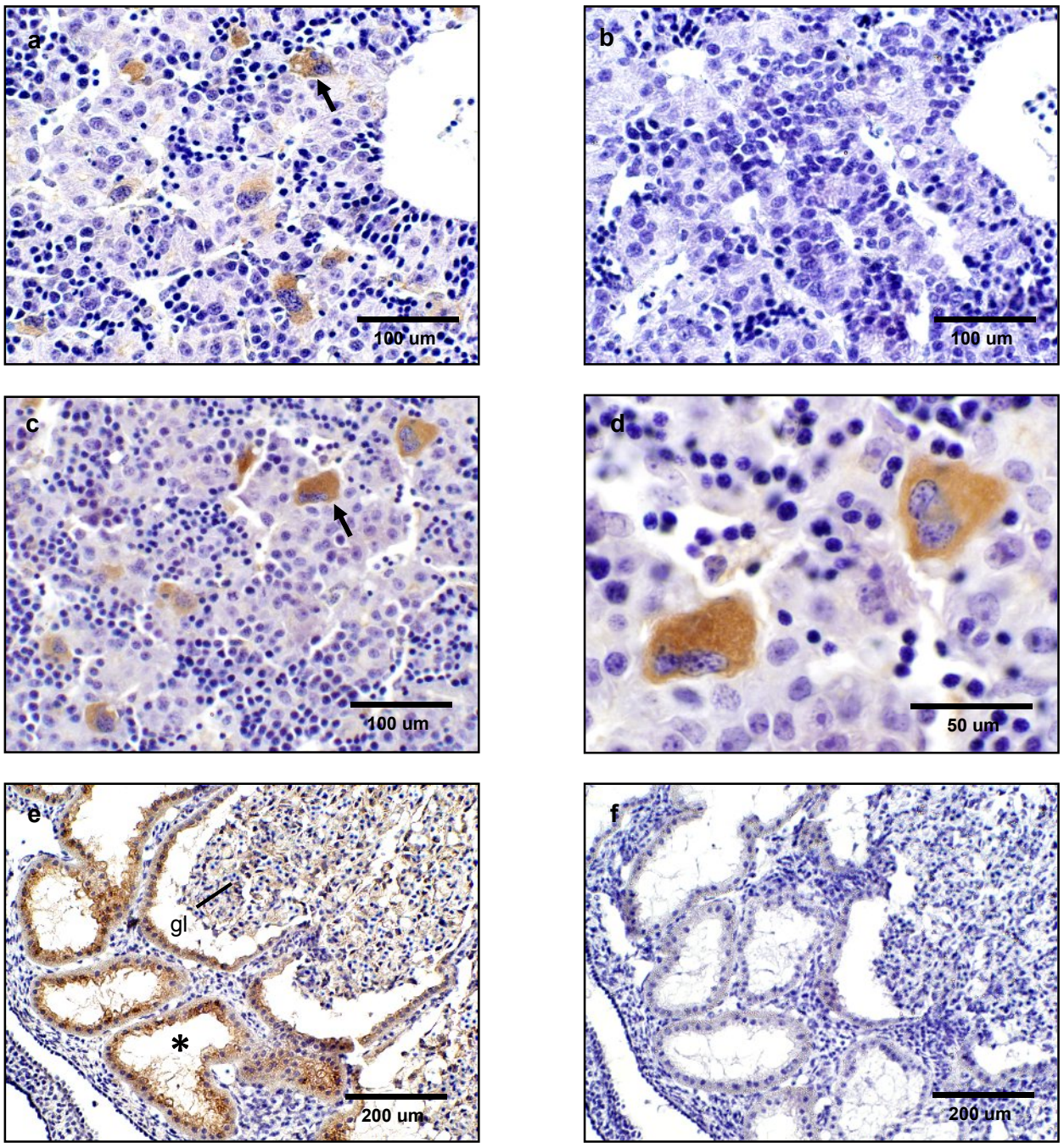

Figure 18. Expression of PrP^C protein in non-neural tissues of the bovine fetus (day 39). PrP^C cellular-specific immunostaining was observed in (a,c,d) scattered multinuclear cells in the liver (*black arrow*), (e) epithelial cells of the mesonephric duct (*) and glomeruli (gl); (b,f) Negative control incubated with non-immune horse serum instead of SAF-32 and counterstained with hematoxilyn.

LITERATURE CITED

Abid K, Soto C. 2006. The intriguing prion disorders. Cell Mol Life Sci 63, 19-20, 2342-2351.

Addle-Biassette H, Verney C, Peoc'h K, Dauge MC, Razavi F, Choudat L, Gressens P, Budka H, Henin D. 2006. Immunohistochemical expression of prion protein (PrPC) in the human forebrain during development. J Neuropathol Exp Neurol 65, 7, 698-706.

Bailly Y, Haeberle A-M, Blanquet-Grossard F, Chasserot-Golaz S, Grant N, Schulze T, Bombarde G, Grassi J, Cesbron J-Y, Lemaire-Vieille C. 2004. Prion protein (PrPC) immunocytochemistry and expression of the green fluorescent protein reporter gene under control of the bovine PrP gene promoter in the mouse brain. J Comp Neurol 473, 244-269.

Barnes FL, First NL. 1991. Embryonic transcription in in vitro cultured bovine embryos. Mol Reprod Dev 29, 117-123.

Bueler H, Fischer M, Lang Y, Bluethmann H, Lipp H-P, DeArmond SJ, Prusiner SB, Aguet M, Weissmann C. 1992. Normal development and behavior of mice lacking the normal cell-surface PrP protein. Nature 356, 577-582.

Bueler H, Aguzzi A, Sailer A, Greiner RA, Autenried P, Aguet M and Weissman C. 1993. Mice devoid of PrP are resistant to scrapie. Cell 73, 1339-1347.

Chesebro B, Race R, Wehrly K, Nishio J, Bloom M, Lechner D, Bergstrom S, Robbins K, Mayer L, Keith JM, Garon C, Haase A. 1985. Identification of scrapie prion protein-specific mRNA in scrapie-infected and uninfected brain. 315, 6017, 331-333.

Collee JG, Bradley R, Liberski PP. 2006. Variant CJD (vCJD) and bovine spongiform encephalopathy (BSE): 10 and 20 years on: part 2. Folia Neuropathol 44, 2, 102-110.

Collinge J. 2001. Prion diseases of humans and animals: their causes and molecular basis. Annu Rev Neurosci 24, 519-550.

Collinge J, Whittington MA, Sidle KCL, Smith CJ, Palmer MS, Clarke AR, Jefferys JGR. 1994. Prion protein is necessary for normal synaptic function. Nature 370, 295-297.

DeMarco ML, Daggett V. 2005. Local environmental effects on the structure of the prion protein. C R Biol 328, 847-862.

Ford MJ, Burton LJ, Morris RJ, Hall SM. 2002. Selective expression of prion protein in peripheral tissues of the adult mouse. Neuroscience 113, 1, 177-192.

Fournier JG, Escaig-Haye F, Billette de Villemeur T, Robain O, Lasmezas CI, Deslys JP, Dormont D, Brown P. 1998. Distribution and submicroscopic immunogold localization of cellular prion protein (PrPc) in extracerebral tissues. Cell Tissue Res 292, 1, 77-84.

Graner E, Mercandante AF, Zanata SM, Forlenza OV, Cabral AL. Veiga SS, Juliano MA, Roesler R, Walz A, Minetti A, Izquierdo I, Martins VR, Brentani RR. 2000. Cellular prion protein binds laminin and mediates neuritogenesis. Mol Brain Res 76, 85-92.

Eyestone WH. 1999. Production and breeding of transgenic cattle using in vitro embryo production technology. Therio 51: 509-517.

Harris DA, Lele P, Snider WD. 1993. Localization of the mRNA for a chicken prion protein by in situ hybridization. Proc Natl Acad Sci USA 1, 90, 9, 4309-4313.

Hyttel P, Viuff D, Avery B, Laurincik J, Greve T. 1996. Transcription and cell cycle-dependent development of intranuclear bodies and granules in two-cell bovine embryos. J Reprod Fertil 108, 263-270.

Inoue S, Tanaka M, Horiuchi M, Ishiguro N, Shinagawa M. 1997. Characterization of the bovine protein gene: The expression requires interaction between the promoter and intron. J Vet Med Sci, 59, 3, 175-183.

Kanaani J, Prusiner SB, Diacovo J, Baekkeskov S, Legname G. 2005. Recombinant prion protein induces rapid polarization and development of synapses in embryonic rat hippocampal neurons in vitro. J Neurochem 95, 1373-1386.

Kretzschmar HA, Prusiner SB, Stowring LE, DeArmond SJ. 1986. Scrapie prion proteins are synthesized in neurons. Am J Pathol 122, 1-5.

Kritzenberger M, Wrobel K-H. 2004. Histochemical in situ identification of bovine embryonic blood cells reveals differences to the adult haematopoietic system and suggests a close relationship between haematopoietic stem cells and primordial germ cells. Histochem Cell Biol 121, 273-289.

Lemaire-Vieille C, Schulze Tobias, Podevin-Dimster V, Follet J, Bailly Y. Blanquet-Grossard F, Decavel J-P, Heinen E, Cesbron J-Y. 2000. Epithelial and endothelial expression of the green fluorescent protein

reporter gene under the control of bovine prion protein (PrP) gene regulatory sequences in transgenic mice. PNAS 97, 10, 5422-5427.

Mange A, Milhavet O, Umlauf D, Harris S, Lehmann. 2002. PrP-dependent cell adhesion in N2a neuroblastoma cells. FEBS Lett 514, 159-162.

Manson J, West JD, Thomson V, McBride P, Kaufman MH, Hope J. 1992. The prion protein gene: a role in mouse embryogenesis? Development 115, 1, 117-122.

Martins VR, Mercadante AF, Cabral AL, Freitas AR, Castro RM. 2001. Insights into the physiological function of cellular prion protein. Braz J Med Biol Res 34, 5, 585-595.

Martins VR, Linden R, Prado M, Walz R, Sakamoto AC, Izquierdo I, Brentani RR. 2002. Cellular prion protein: on the road for functions. FEBS Letters 512, 25-28.

Memili E, First NL. 1998. Developmental changes in RNA polymerase II in bovine oocytes, early embryos and effect of alpha-amanitin on embryo development. Mol Reprod Dev 51, 381-389.

Memili E, First NL. 1999. Control of gene expression at the onset of bovine embryonic development. Biol Reprod 61, 1198-1207.

Memili E, First NL. 2000. Zygotic and embryonic gene expression in cow: a review of timing and mechanisms of early gene expression as compared with other species. Zygote 8, 87-96.

Miele G, Jeffrey M, Turnbull D, Manson J, Clinton M. 2002. Ablation of cellular prion protein affects mitochondrial numbers and morphology. Biochem Biophys Res Comm 291, 372-377.

Miele G, Alejo Blanco AR, Baybutt H, Horvat S, Manson J, Clinton M. 2003. Embryonic activation and developmental expression of the murine prion pprotein gene. Gene Exp 11, 1, 1-12.

Moser, M, Colello RJ, Pott U, Oesch B. 1995. Developmental expression of the prion protein gene in glial cells. Neuron 14, 509-517.

NCJDSU. The National Creutzfeldt-Jakob Disease Surveillance Unit. Variant Creutzfeldt-Jakob disease, current data. The University of Edinburgh. 2008.

Oesch B, Westaway D, Walchili M, Mckinley MP, Kent SB, Aebersol R, Barry RA, Tempst P, Teplow DB, Hood LE, Prusiner SS and Weissman C. 1985. A cellular gene encodes scrapie PrP 27-30 protein. Cell 40, 735-746.

Priola S, Vorberg I. 2006. Molecular aspects of disease pathogenesis in the transmissible spongiform encephalopathies. Mol Biotech 33, 71-88.

Prusiner SB. 1998. Prions. Proc Natl Acad Sci USA 95, 13363-13383.

Prusiner SB and Scott MR. 1997. Genetics of prions Annu Rev Genet 31, 139-175.

Richt JA, Kasinathan P, Hamir AN, Castilla J, Sathiyaseelan T, Vargas F, Sathiyaseelan J, Wu H, Matsushita H, Koster J, Kato S, Ishida I, Soto C, Robl JM, Kuroiwa Y. 2006. Production of cattle lacking prion protein. Nature Biotech 25, 132-138.

Russelakis-Carneiro M, Saborio GP, Anderes L, Soto C. 2002. Changes in the glycosylation pattern of prion protein in murine scrapie. Implications for the mechanism of neurodegeneration in prion diseases. J Biol Chem 277, 36872-36877.

Ryan AM, Womack JE. 1993. Somatic cell mapping of the bovine prion protein gene and restriction fragment length polymorphism studies in cattle and sheep. Anim Genet 24, 1, 23-26.

Santuccione A, Sytnyk V, Leshchyns'ka I, Schachner M. 2005. Prion protein recruits its neuronal receptor NCAM to lipid rafts to activate p59fyn and to enhance neurite outgrowth. J Cell Biol 169, 341-354.

Sasaki K, Sonoda Y. 2000. Histochemical and three-dimensional analyses of liver hematopoiesis in the mouse embryo. Arch Histol Cytol 63, 2, 137-146.

Scmitt-Ulms G, Legname G, Baldwin MA, Ball HL, Brandon N, Bosque PJ, Crossin KL, Edelman GM, DeArmond SJ, Cohen FE, Prusiner SB. 2001. Binding of neural cell adhesion molecules (N-CAMs) to the cellular prion protein. J Mol Biol 314, 1209-1225.

Shaked Y, Rosenmann H, Talmor G, Gabizon R. 1999. A C-terminal truncated PrP isoform is present in mature sperm. J Biol Chem 274, 32153-32158.

Sparkes RS, Simon M, Cohn VH, Fournier RE, Lem J, Klisak I, Heinzmann C, Blatt C, Lucero M, Mohandas T, DeArmond SJ, Westaway D, Prusiner SB, Weiner LP. 1986. Assignment of the human and mouse prion protein genes to homologous chromosomes. Proc Natl Acad Sci USA 83, 7358-7362.

Starke R, Harrison P, Mackie I, Wang G, Erusalimsky JD, Gale R, Masse JM, Cramer E, Pizzey A, Biggerstaff J, Machin S. 2005. The expression of prion protein (PrP(c)) in the megakaryocyte lineage. J Thromb Haemost 3, 6, 1266-73.

Steele AD, Emsley JG, Ozdinler PH, Lindquist S, Macklis JD. 2006. Prion protein (PrPc) positively regulates neural precursor proliferation during developmental and adult mammalian neurogenesis. Proc Natl Acad Sci USA 14, 103, 7, 2184-2189.

Thumdee P, Ponsuksili S, Murani E, Nganvongpanit K, Gehrig B, Tesfaye D, Gilles M, Hoelker M, Jennen D, Griese J, Schellander K, Wimmers K. 2007. Expression of the prion protein gene (PRNP) and cellular prion protein (PrPc) in cattle and sheep fetuses and maternal tissues during pregnancy. Gene Exp 13, 283-297.

Tremblay P, Bouzamondo-Bernstein E, Heinrich C, Prusiner SB, DeArmond SJ. 2007. Developmental expression of PrP in the post-implantation embryo. Brain Res 30, 1139, 60-67.

Tuo W, Zhuang D, Knowles DP, Cheevers WP, Syl M-S, O'Rourke K I. 2001. PrP-C and PrP-Sc at the Fetal-Maternal Interface. J Biol Chem 276, 21, 18229-18234.

Viuff D, Avery B, Greve T, King WA and Hyttel P. 1996. Transcriptional activity in vitro produced bovine two- and four-cell embryos. Mol Reprod Dev 43, 171-179.

Winters LM, Green WW, Comstock RE. 1942. Prenatal development of the bovine. University of Minnesota, Agricultural Experiment Station, Division of Animal Husbandry.

CHAPTER V

EXPRESSION AND KNOCKDOWN OF PRION EXPRESSION IN DIFFERENTIATING MOUSE EMBRYONIC STEM CELLS

INTRODUCTION

The host encoded cellular prion protein (PrP^C) is an N-linked glycoprotein tethered to the cell membrane by a glycophosphatidylinositol anchor. Under certain conditions, PrP^C can undergo conversion into a conformationally-altered isoform (PrP^{Sc}) widely believed to be the pathogenic agent of transmissible spongiform encephalopathies (TSEs). Although much is known about the role of PrP^{Sc} in prion diseases, the normal function of PrP^C is poorly understood. Suggested roles include cell signaling, protection against oxidative stress and differentiation (Hetz et al., 2003, Westergard et al., 2007; Steele et al., 2007). Despite these putative functions, lines of mice and cattle in which PrP^C has been ablated have showed no phenotypical alterations and therefore offered no clues on the potential role of PrP^C (Bueler et al., 1992; Richt et al., 2006). However, a recent report indicated that PrP^C-null mice exhibited an impaired self-renewal capacity of hematopoietic stem cell populations after serial transplantation in the bone marrow (Zhang et al., 2005). Furthermore, multipotent neural precursors obtained from PrP^C knockout, wild-type and overexpresser mice, showed a dose-dependent correlation between PrP^C levels and the capacity to differentiate into mature neurons (Steele et al., 2007). These studies have contributed important evidence for the participation of PrP^C in neural stem/progenitor cell proliferation and differentiation.

Several studies have reported strong expression of PrP^C in the neuroepithelium of the central nervous system (CNS) during embryogenesis (see chapter IV; Manson et al., 1992; Ford et al., 2002; Miele et al., 2003; Tremblay et al., 2007). As the CNS develops, post-mitotic neurons which go through their last mitosis at the ventricular surface of the epithelium migrate towards the opposite pial surface where they extend axons (Frederiksen and McKay, 1988). In the adult brain, PrP^C has been mostly localized in elongated axons and pre-synaptic terminals (Sales et al., 2002; Adle-Biassette et al., 2006; Tremblay et al., 2007). We and others have observed that PrP^C is specifically expressed by neural cells in the neuroepithelium (see chapter IV; Miele et al., 2003; Tremblay et al., 2007); however, the state of differentiation of these cells has not been fully determined. In the present study we used immunohistochemical analyses to characterize the state of differentiation of PrP^C-positive cells in the bovine neuroepithelium during embryogenesis. We were able to identify PrP^C in the pial surface of the neural tube sharing a common location with nestin. These data suggest that PrP^C is differentially expressed in the neuroepithelium and that PrP^C is associated with more differentiated states of neurogenesis.

Expression of PrP^C has been positively correlated with differentiation in several lines of neural (Steele et al., 2006; Witusik et al., 2007) and non-neural cells (Dodelet and Cashman, 1998; Starke et al., 2005). However, PrP^C expression has not been characterized during earlier stages of development. We have characterized the expression of PrP^C during cellular differentiation using mouse embryonic stem cells (mESCs) as a model for PrP^C expression during early embryogenesis. mESCs are derived from the inner cell mass of pre-implantation embryos showing the capacity of self-renewal and broad differentiation plasticity. The potential of pluripotent mESC to differentiate into a wide variety of cell types in vitro, including neural cells, provides an excellent model for experimental analysis of PrP^C expression during cell commitment and differentiation in early embryogenesis. Our aims for the present study were to characterize the expression of PrP^C during mESC differentiation and to test the hypothesis that the PrP^C regulates differentiation of mESCs into neural derivatives.

MATERIAL AND METHODS

Culture Conditions

Undifferentiated mouse D3 ES cells (ATCC, Manassas, VA, USA) were co-cultured on mitotically inactivated STO feeder cells (10µl/ml of mitomycin-C for 1h) in tissue culture dishes coated with 0.1% gelatin as described by Robertson (1987). Standard medium consisted of DMEM supplemented with 1% non-essential aminoacids, 10^{-4} M β-Mercaptoethanol and 15% bovine serum (FBS, Hyclone) screened to support growth of undifferentiated ESC. Leukemia inhibitory factor (LIF; Esgro, Chemicon) at a final concentration of 1000 units/ml were added to the medium to inhibit differentiation. Under these conditions, mESCs formed typical compacted colonies attached to monolayer of STO cells. When mESC were 80% confluent, cells were harvested with 0.25% trypsin and 1 mM EDTA in 0.1% PBS (trypsin/EDTA). mESC were separated from STO cells by differential sedimentation and plating twice for 10 min each. mESCs were then induced to form embryoid bodies (EBs) by placing them in differentiation medium (standard medium without LIF) on day 0. After four days, EBs were disaggregated in

trypsin/EDTA, after which cells were seeded into tissue culture dishes and cultured in differentiation medium for 17 additional days. During the 20-day experimental period, cells were sampled on day 0 and at three- or four-days intervals thereafter for analysis of PrP^C expression by Q-PCR and quantitative western blot. To study the effect of retinoic acid (RA) on mESCs differentiation and PrP^C expression, cells were cultured following the 4-/4+ protocol described by Bain et al., 1995. Briefly, mESCs were allowed to form EBs for 4 days without RA followed by 4 days of culture in the presence of RA. Undifferentiated mESCs were trypsinized to remove cells from stratum. Cells were pipetted up and down several times for mild disaggregation and mESCs were separated from STO cells by differential sedimentation and plating. To standardize cell input, mESCs from two 100-mm tissue culture dishes were seeded in two non-adhesive petri dishes in differentiation medium consisting in DMEM supplemented with 10% non-selected fetal calf serum, without LIF and β-mercaptoethanol. Under these conditions mESCs did not attach to the surface of the dish and formed EBs. Medium was changed after two days and EBs were cultured for 2 more days under similar conditions. At this time, medium was changed and supplemented with 5×10^{-7} M of RA. After 2 days, medium was replaced with fresh RA-supplemented medium and allowed 2 more days for culture in suspension. At this point, about 100 EBs were transferred to each of six 35-mm tissue culture dishes with differentiation medium without RA. Culture of EBs was continued for 12 days with changes of medium every 2 days.

siRNA expression vector

Double-stranded siRNA sequences predicted to target the mouse *Prnp* mRNA as well as a scrambled sequence were designed using the OligoEngine online utility and were synthesized as individual DNA oligonucleotides by the same vendor for expression vector construction. Target siRNA and scramble sequences were at follows: AACCAGAACAACUUCGUGC and GGGUAUGGAGAGACACGCA. RNA pairs were annealed and ligated to the pSuperNeo vector that had been previously digested with BamHI and HindIII and gel-purified. Positive clones were identified by PCR across the insertion site and confirmed by DNA sequencing. Bacterial clones harboring plasmids with the desired sequences were expanded in 100 ml liquid culture, and plasmids were purified using Qiagen Maxi-prep reagents in preparation for transfection of mESC (Huckle and Eyestone, unpublished). The candidate siRNA target sequence in the bovine PrP^C gene (*Prnp*) coding region was identified using siRNA design software (OligoEngine). A DNA insert designed to encode a shRNA was ligated into the pSUPER.neo vector

(Brummelkamp et al., 2002). A control vector was also made using a scrambled version of the shRNA sequence.

mESC transfection and selection of neoR clones

Linearized pSUPER.neo was transfected into mESCs using Lipofectamine Plus (Invitrogen). After 24 hours, 800 µl/ml G418 was added to select for neomycin-resistant (neoR) cells over the next 7 days. Clonal lines were established by culturing neoR cells at limiting dilution on mitotically-inactivated STO in 96-well plates. Colonies were expanded to obtain sufficient quantities for PrP^C mRNA and protein analysis (confluent, 60 mm dishes) and cryopreservation (100 mm dishes).

Immunohistochemistry

Bovine fetuses at days 27 (n=2) and 39 (n=3) were obtained from five clinically healthy cows slaughtered at a local abattoir. After extraction from the uterus, fetal age was estimated after measuring crown-rump length (Winters et al., 1942) and fixed in 10% formalin. Formalin-fixed fetuses were embedded in paraffin and sectioned at 5-7 µm using a microtome (Historange, LKB Bromma, Sweden). Tissue sections were mounted on adhesive coated slides (Newcomer supply; Middleton, Wisconsin) and incubated overnight at 37 °C. Mounted tissues were deparaffinized in xylene and dehydrated in serial alcohol solutions. Slides were subjected to an unmasking protocol that employed unmasking solution (Vector Laboratories., Burlingame, CA, USA) and autoclaving at 120°C for 5 min. Endogenous peroxidase was blocked by incubation in 3% hydrogen peroxidase diluted in 0.1 M PBS for 30 min. Tissues were then rinsed two times in PBS and blocked in 2.5% horse serum for 15 min. PrP^C was specifically detected by overnight incubation at room temperature with primary antibody SAF-32 (1:400; Cayman Co.) diluted in 1.5 % equine serum solution (Vector Laboratories). Serial slides were incubated with polyclonal antibodies anti-nestin (1:200) and anti-MAP-2 (1:200) (Santa Cruz Biotechnology). After two washes in PBS, bound primary antibody was detected using a horse anti-mouse secondary antibody conjugated to horseradish-peroxidase for 10 min at room temperature (Vector Laboratories). Immune complexes were visualized using 3, 3'-diaminobenzidine (DAB) substrate for 5 min or until the signal became visible.

Probed sections were then counterstained with hematoxilyn and rehydrated in serial alcohol solutions. Sections were mounted with permount (Fisher Scientific) under coverslips. Neighboring sections processed identically using horse serum instead of primary antibody, served as controls. Digital photos of tissue sections were obtained using light microscopy (Olympus Vanox-T, Tokyo, Japan).

Western blot

Cultured mESCs were washed with PBS and homogenized by pipetting in lysis buffer (10 nM Tris, pH 7.4, 150 mM NaCl, 1% Triton-X-100, 1% deoxycholate, 0.1% SDS). Homogenates were centrifuged at 13,500 rpm for 5 min and the supernatants transferred into a new tube. Total protein concentrations were determined using a Bicinchoninic acid (BCA) kit (Pierce; Rockford, IL) according to the manufacturing's instructions. For protein denaturation, 50 µl of each homogenized sample was mixed with 50 µl of Laemmli buffer (BioRad Laboratories, Hercules, CA, USA) and heated at 98° C for 5 min. Aliquots containing 20 µg of total protein were added to each lane and separated by SDS-PAGE in 12% gels (BioRad). Electrophoresis was performed at 200V for 60 min. Proteins were then transferred onto PDVF membranes by electroblotting at 100 V for 1h. Membranes were immersed in blocking buffer (LI-COR Corp., Lincoln, NE, USA) for 1 h with shaking. PrP^C was detected by incubation for 1 h in SAF-32 mouse monoclonal anti-PrP (1:400; Cayman Chemical Company, Ann Arbor, MI, USA) directed against amino acid sequence 59-89 located in the N-terminal octapeptide repeat region of the protein. For reference, membranes were co-incubated in rabbit anti-β-actin (1:1000; Santa Cruz Biotechnology, Santa Cruz, CA, USA). Both primary antibodies were diluted in 0.1% Tween-20 in blocking buffer. After four washes in 0.1% Tween-20 in PBS for 5 min each, membranes were incubated in secondary IgG fluorescent anti-mouse and anti-rabbit antibodies (1:5000; LI-COR) diluted in 0.1% Tween-20 in blocking buffer for 30 min with shaking. Immunoreactive band intensities of PrP^C and β-actin were detected and quantified as integrated intensity values using an Odyssey infrared imaging system (LI-COR). Relative expression of PrP^C was corrected by β-actin expression and standardized to the lowest expression value (Day-27 fetus).

RNA Extraction and cDNA synthesis

Approximately 3 x 10^5 mESCs were collected and immediately fixed in RLT buffer. Total RNA was extracted using RNeasy extraction mini kit (Qiagen, Inc., Valencia, CA, USA) according to the manufacturing's instructions. The concentration and purity of the RNA in each sample were determined using Ribogreen RNA quantification kit (Molecular Probes, Eugene, OR, USA). Total RNA was eluted in 30-50 µl of RNase free water. Samples were subjected to RT-PCR using an iScript cDNA synthesis kit (Bio-Rad Labs., Hercules, CA, USA). The reaction protocol consisted of incubation for 5 min at 25°C, 30 min at 42°C, 5 min at 85°C and hold at 4°C using a DNA engine PCR thermocycler (Bio-Rad).

Quantitative-PCR

Real-time PCR primers and TaqMan probes were designed using PrimerExpress software (Applied Biosystems) to amplify a segment of cDNA that spans the exon 2-exon 3 junction in the mouse *Prnp* sequence. Equivalence of amplification efficiencies among all primer-probe sets was confirmed using serial 5-fold dilutions of mouse or bovine brain cDNA (Huckle and Eyestone, unpublished). TaqMan probe sequence (AGCAGACTATCAGTCATCATGGCGAACCTTG) specific for the target was designed to contain a fluorescent 5' reporter dye (FAM) and 3' quencher dye (TAMRA). Sequence of forward and reverse mouse *Prnp* primers were at follow: AGCATTCTGCCTTCCTAGTGCTA and GAGGGCCAGCAGCCAGTAG. Taqman probe specific for the target was designed to contain a fluorescent 5' reporter dye (FAM) and 3' quencher dye (TAMRA). Each RT-PCR reaction (25 µl) contained the following: 2X Master Mix without uracil-N-glycosidase (12.5 µl), 40X Multiscribe and RNase Inhibitor Mix (0.63 µl), target forward primer (60 nM), target reverse primer (60 nM), fluorescent-labeled target probe (4 nM) designed for the RNA sequence isolated form bovine and a total RNA (40 ng). The PCR amplification was carried out in the 7300 Real Time PCR System (Applied Biosystems, Foster City, CA, USA). Thermal cycling conditions were 48°C for 30 min and 95°C for 10 min, followed by 40 repetitive cycles at 95°C for 15 sec and 60°C for 1 min. As a normalization control for RNA loading, parallel reactions in the same multiwell plate were performed using TaqMan Ribosomal RNA as a target (18s control kit, Applied Biosystems). Quantification of gene amplification was made following RT-PCR by determining the threshold cycle (C_T) number for FAM fluorescence within the geometric region of the semilog plot generated during PCR. Within this region of the amplification curve, each difference of one cycle is equivalent to a doubling of the amplified product of the PCR. The relative

quantification of the target gene expression across treatment was evaluated using the comparative $\Delta\Delta C_T$ method. The C_T value was determined by subtracting the ribosomal C_T value from the target C_T value of the sample. Calculation of $\Delta\Delta$ C_T involved using PrP^C gene expression on day 0 (sample with the highest CT value or lowest target expression) as an arbitrary constant to subtract from all other C_T sample values. Relative PrP^C expression was calculated as fold changes in relation to day 0 sample and expressed as $2^{-\Delta\Delta CT}$ value.

Immunofluorescence

mESC were expanded in DMEM containing LIF (day 0) and differentiating medium (day 20) in 35-mm dishes, fixed in a mixture of methanol and acetone (1:1) at -20 °C for 5 min and stored at 4 °C under PBS. Dishes were washed in PBS twice and blocked in blocking buffer (1:1; Odyssey blocking solution and PBS, 0.1% Tween-20) for 30 min at room temperature (RT). Cells were incubated in primary antibodies diluted in blocking buffer including mouse anti-PrP SAF-32 (1:400; Cayman Chemical) and rabbit anti-nestin (1:200; Santa Cruz Biotechnology). After three washes with PBST (PBS, 0.1% Tween), cells were incubated with secondary antibodies goat anti-rabbit IgG labeled with Alexa Fluor 488 goat anti-mouse IgG labeled with Alexa Fluor 594 (both diluted 1:400 in blocking buffer). Then cells were washed three times in PBST and coverslipped using mounting solution with 4', 6-diamidino-2-phenylindole (DAPI) (Vector Laboratories) for nuclei visualization and examined under the fluorescent microscope (Olympus, Japan).

Data Analysis

All statistical analyses were performed using SAS software (version 9.3.1, SAS Institute Inc., Cary, North Carolina, USA). Analyses of significance ($P < 0.05$) for PrP^C expression values were performed using one-way ANOVA. Expression values for individual tissues were compared to the lowest expression (day 0) using Dunnet's t-test; whereas, significant differences between tissues were analyzed using Duncan's multiple comparison test. Differences between treatments for each individual day were compared using student T-test. PrP^C and Oct-4 values for the 20-day period were compared using correlation coefficients.

RESULTS

Immunolocalization of PrP^C, MAP-2 and nestin during development in vivo

In order to establish the localization of PrP^C and its association with cellular differentiation in vivo, we performed immunohistochemical analyses in bovine fetuses and determined the spatial relation between PrP^C, MAP-2 and nestin. We have previously characterize the expression of PrP^C during bovine embryogenesis and shown a close relationship between this protein and the development of the nervous system (see Chapter IV). In the present study, PrP^C expression was detected as expected in CNS areas including the encephalon and the spinal cord (Fig. 1a and 5a). PrP^C seems to be localized with higher intensity in the peripheral or pial region of the neuroepithelium associated to post-mitotic and more differentiated states of neurogenesis (Fig. 2a, 3a, 6a and 7a). The strongest staining for PrP^C was observed in the molecular layer of the pial surface formed by neurites of the differentiated neurons. By contrast, periventricular region the levels of PrP^C were undetectable, indicating low expression in mitotically active and less differentiated neural cells.

MAP-2 staining was mostly detected in the CNS (Fig 1b and 5b) and confined to intermediate regions of the neuroepithelium (Fig. 2b and 3b). MAP-2 and PrP^C common pattern of staining in the intermediate zone was more distinguishable at day 39 compared to day 27 (Fig. 6a,b and 7a,b). However, observations both in the brain and spinal cord at day 39 indicated that MAP-2 did not stain the molecular region of the pial surface where most of the PrP^C immunoreactivity is located (Fig 6a,b; 7 a,b). These data indicate that both PrP^C and MAP-2 share localization in the intermediate region of the neuroepithelium but only PrP^C is present in the molecular region.

In serial sections, nestin immunoreactivity was also observed in the CNS (Fig. 1c and 5c). In contrast to both PrP^C and MAP-2, nestin staining extended across the surface of the neuroepithelium showing immunoreactivity in both pial and periventricular areas (Fig. 2c, 3c, 6c, 7c). Detection of nestin in the periventricular area suggested the expression in mitotically active cells (Fig. 7c); whereas, nestin

immunoreactivity in the pial surface was probably associated to post-mitotic cells (Fig. 6c and 7c). Nestin and PrP^C share a similar intensity of staining in the molecular layer of the pial surface. Thus, the lack of PrP^C staining in the ventricular region where nestin-positive cells were observed indicated that PrP^C may not expressed by mitotically active cells. However, nestin and PrP^C co-localization in the molecular layer of the pial surface suggest that both proteins are expressed by differentiated neural cells. Moreover, both PrP^C and nestin stained peripheral nerves indicating co-localization in the developing nervous system.

Outside the nervous system, scattered multinuclear cells in the parenchyma of the liver showed a similar pattern of staining for PrP^C and MAP-2 (Fig.8a,b). Moreover, intense immunoreactivity for nestin was also observed throughout the parenchyma of the liver (Fig. 8c).

Analysis and knockdown of PrP^C expression during ESC differentiation

ESCs were expanded in co-culture with STO-feeder under media supplemented with LIF and B-mercaptoethanol to obtain a sufficient number of cells in the undifferentiated state for analyses (Fig. 9a). mESCs were induced to form aggregates or embryoid bodies (EBs) in suspension for 4 days (Fig. 9b) and were transferred to adhesive tissue culture dishes (Fig. 9c) for further differentiation during a total period of 21 days. During this period, a number of different cell types were visualized including cardiac- (Fig. 9d) and neuron-like cells (Fig. 9e,f).

In a first experiment, PrP^C expression was analyzed by western blot every 3 days during a 20-day period (Fig. 10). Several immunoreactive bands were observed at 35, 32 and 27 kDa confirming the presence of different isoforms of PrP^C. Immunoreactive bands were computerized quantified and relative expression for each day was calculated by normalizing PrP^C value to Actin expression and comparing them to day 0. In differentiating mESCs, PrP^C appeared first on day 9 (3.7-fold relative to day 0; $P < 0.05$) and rose progressively until day 18 (19-fold relative to day 0; $P < 0.05$). Numerous neurons where observed in culture at this time (Fig 9ef). Correspondingly, levels of Oct-4 decreased progressively after day 3 (0.63-fold; $P < 0.05$) until day 21 (0.079-fold; $P < 0.05$). PrP^C expression was negatively correlated with Oct-4 expression for the 21-day period ($r = -0.85$; $P < 0.05$). Levels of *Prnp* mRNA expression, analyzed by Q-

PCR in the same cell cultures, were normalized to 18s rRNA and compared to the value at day 0 (Fig. 11). *Prnp* mRNA expression was similar to protein expression. *Prnp* values increased progressively after day 9 (1.8-fold) to approximately 4 times at day 18 (3.9-fold; $P < 0.05$).

To promote differentiation along the neuronal pathway, after 4 days of aggregation EBs were induced in media containing RA (5×10^{-7} M) for additional 4 days. We hypothesized that RA induction would increase expression of PrP^C in mESCs during differentiation. During a total period of 20 days, ESCs were analyzed for levels of PrP^C expression to see if RA-induced neurons expressed higher levels of PrP^C expression. We observed a significant rise in PrP^C expression after day 16 (14-fold; $P < 0.05$) that stabilized at day 20 showing 25 times higher expression compared to day 0 (Fig. 12). Immunofluorescence analyses also evidenced an important increase in PrP^C signal from day 0 (Fig. 16a) to day 20 (Fig. 17 a) of differentiation. Induction with RA resulted in an earlier up-regulation of PrP^C during differentiation (day 12 vs. day 16; $P < 0.05$) (Fig. 12a,b). In addition, RA-treated mESCs showed higher PrP^C expression compared to untreated control at days 12 (4.0- vs. 10.3-fold; $P < 0.05$) and 16 (14- vs. 24.8-fold; $P < 0.05$). Induction with RA resulted in a greater decrease in Oct-4 levels at day 8 compared to the untreated control (0.13- vs. 0.58-fold; $P < 0.05$) (Fig 12a,b). Nestin levels were analyzed in the same cell lysates by western blot for the effect of RA-induction. Untreated mESCs showed a progressive increase in nestin levels since day 16 of differentiation (11.8-fold; $P < 0.05$) (Fig 12c). Nestin increased after day 12 (26.5-fold; $P < 0.05$) in the RA-treated cells (Fig. 12b). In addition, 25.1- and 16.6-fold higher levels of nestin were detected in the RA mESCs at day 12 and 16 compared to the untreated control ($P < 0.05$). These results were supported by a higher nestin-specific fluorescence observed in mESC at day 20 compared to day 0 (Fig. 16c and 17c).

We next investigated the effects of PrP^C knockdown on nestin expression in RA-treated mESCs during differentiation. We hypothesized that the knockdown in PrP^C would reduce neural differentiation as reflected by a reduction in expression of the neural marker nestin. mESCs were transfected with pSUPER.neo vector containing a siRNA target sequence directed against the *Prnp* coding region (Fig. 13a,b). PrP^C siRNA induced a significant reduction in PrP^C expression in differentiating mESCs after day 12 (55.7 %) compared to the control (Fig. 14a,b). Further in differentiation, PrP^C values were reduced in 70.9 % (day 16) and 60% (day 20), respectively ($P < 0.05$). siRNA cells displayed a reduction in PrP^C immunofluorescence compared to the control (Fig. 17 a,b). Analysis by Q-PCR in the same cell cultures

showed that *Prnp* mRNA expression was reduced in 48.8 % (day 16) and 53.1 % (day 20; Fig. 15) in PrP^C siRNA mESCs. Oct-4 expression showed a drastic decrease associated with the RA induction of PrP^C at day 8 in both groups (Control=0.036-fold and PrP^C siRNA=0.14-fold) (Fig. 14a,b). However, no significant differences were found between treatments. We found that nestin levels were reduced in the PrP^C siRNA group by 61.3 % (day 16) and 70.7 (day 20) ($P < 0.05$) compared to the control (Fig. 14c). Immunofluorescence analyses showed also lower nestin signal in the PrP^C siRNA cells compared to the control (Fig. 17 c,d). These results support our hypothesis and give evidence for a significant role of PrP^C in mESC differentiation.

DISCUSSION

We have previously showed the specific localization of PrP^C in the neuroepithelium during bovine embryogenesis (see chapter IV). In the present study, using immunohistochemical analyses in bovine fetuses, we found that PrP^C shared a common niche of cells with nestin in the peripheral area of the neuroepithelium. PrP^C and nestin common location indicate that both proteins are expressed by the same population of neural cells that have undergone differentiation. Our analyses showed that PrP^C is intensely expressed in the molecular layer of the pial surface composed by a high proportion of dendrites and axons. As the nervous system develops, this area will give rise to the gray matter where most of the PrP^C is localized in the adult CNS (Sales et al., 2002; Adle-Biassette et al., 2006). Despite the high concentration of neurites in the molecular layer, we observed no immunoreactivity for MAP-2 in this region. This phenomenon may be explained by the complex regulation of MAP-2 during neural development. MAP-2 plays an active role in cytoskeleton dynamics necessary for earlier axonal growth; however, its expression is reduced after establishment of synaptic contact to give rise to a more stable cytoskeleton (Sanchez et al., 2000).

We found that nestin immunoreactivity was extended across the neuroepithelium from the periventricular area to the pial surface. This may be explained by its expression in a wide variety of neural cells including stem/progenitor of the ventricular area and glial precursor cells located in the pial surface (Frederiksen and McKay, 1988). Nestin has been associated as a marker of neural stem/progenitor cells based on

several evidences. These include its expression in neural and glial precursors (Fukuda et al., 2003), its reduction in expression as differentiation of the nervous system proceeds (Luskin, 1998) and its reclusion to mitotically active zones of the brain in the adult stages (Ernst and Christie, 2005). However, its expression in other tissues including muscle, cardiac and skin indicates that it is not exclusively of neuroepithelial origin (Gilyarov, 2008). Although the expression of nestin is not exclusively in neural/stem progenitor cells, we observed a high proportion of nestin-positive cells in the periventricular area indicating its association with mitotically active neural cells. In this area, we found no immunoreactivity for PrP^C, supporting the association of PrP^C with more differentiated cells. Based on this data, we can conclude that PrP^C as well as nestin are expressed by differentiated neural cell population and that the cellular localization of PrP^C seems to be associated with the neurite compartment.

We have previously showed in the bovine that PrP^C is highly regulated during early stages of embryonic development (see Chapter 4). *Prnp* is expressed on day 4, at the 8-to-16 cell stage, showing intense expression in the blastomeric membrane. Later in development, PrP^C was localized in the inner cell mass and trophoblast of blastocysts and was also detected in trophoblast cells on day 18. In mice, *Prnp* expression has been detected as early as day 6.5 in extraembryonic membranes including decidua and amnion (Manson et al., 1992). At day 8, *Prnp* expression is evident in the cephalic folds and becomes intensified toward the mesencephalon, neural tube and peripheral nerves on day 11.5. In the present study, mESCs were induced to differentiate under in vitro conditions to create a model for the study of PrP^C expression during early embryogenesis. Under these conditions, our analyses showed that *Prnp* expression is significantly increased beginning on day 9 of differentiation. The rise in PrP^C levels seems to occur before the visualization of neuron-like cells at day 12. However, for day 20 a high proportion of mESCs displayed intense neurite formation associated with high levels of PrP^C detected by western blot. In coincidence with the increase in PrP^C expression, we also observed a progressive reduction in Oct-4 levels indicating the loss of pluripotency in the mESC population. These data suggests that our *in vitro* cellular model simulates important events occurring during mice embryogenesis and is suitable for the study of PrP^C expression during development. At the end of the 20-day *in vitro* differentiation period, we found a negative coefficient correlation between PrP^C and Oct-4 (r = -0.85) indicating that PrP^C levels are positively associated with the loss of pluripotency in the mESC population.

The capacity of RA to promote neurogenesis and formation of neuron-like cells in ESC cultures has been documented (Bain et al., 1995). The mechanism by which RA exerts this effect is not clearly understood; however, two classes of receptors which bind RA, the retinoic acid receptors (RARs) and the retinoid X receptor (RXRs) have been identified (Bain et al., 1995). In our study, culture of EBs for four days with RA resulted in the promotion of a higher proportion of mESCs showing signs of neuritogenesis. We evaluated the effect of RA induction on PrP^C levels during the differentiation process and found that RA induced an earlier rise in PrP^C expression compared to the untreated cells. PrP^C expression was up-regulated by RA during an 8-day period after which PrP^C levels returned to normal values. Moreover, the significant decrease of Oct-4 levels at day 8 indicated that RA induced an earlier differentiation of mESC during development. In order to analyze the fate of the mESC population, we measured levels of nestin expression to estimate the proportion of cells following the stem/progenitor lineage. Our attempts to detect MAP-2, a marker of more advanced states of neural cell differentiation failed suggesting that the period covered in our experiments did not cover the emergence of more mature neurons capable of expressing MAP-2. We found that RA advanced the onset of nestin expression during differentiation but that showed no effect on the nestin levels at the end of the differentiation period. This pattern of expression, along with the increasing expression of PrP^C and decreasing levels of Oct-4, suggests that RA induced stronger differentiation of mESCs.

Ablation or knockdown of *Prnp* gene expression offers an effective strategy for better understanding the potential role of PrP^C during differentiation. Our lab developed a line of mESCs that stably integrated a transgene containing a PrP^C siRNA construct. First, we wanted to test if the siRNA construct was able to efficiently reduce PrP^C expression in differentiating mESCs. We found that PrP^C siRNA cells showed a significant reduction both in PrP^C protein and mRNA levels. We also observed that the knockdown in PrP^C along the differentiation process did not affect the level of Oct-4 expression. This data suggests either that PrP^C had no direct effect on the pluripotency of mESCs or that the knockdown in PrP^C expression was not sufficient to induce a detectable effect in Oct-4. We then estimated the effect of the PrP^C knockdown in the levels of nestin expression. PrP^C knockdown resulted in significant reduction in nestin levels that ranged from 61.3% (day 16) to 70.7% (day 20). This result indicates that PrP^C might have a direct effect on the expression of the nestin gene in the mESC population or that the proportion of cells expressing nestin was reduced after the knockdown of PrP^C. Both alternatives indicate that the reduction in PrP^C levels resulted in a lower proportion of cells differentiating into the stem/precursor lineage. Thus, this data represent evidence on the participation of PrP^C in the process of mESC

differentiation. This conclusion is consistent with results from several recent studies arguing that PrP^C participate in cellular differentiation. The mechanism involved in this function of PrP^C is not clear. However, the use of differentiating mESc as a model for the study of PrP^C interactions with other cellular markers can provide more clues about the signaling pathways that mediate this function.

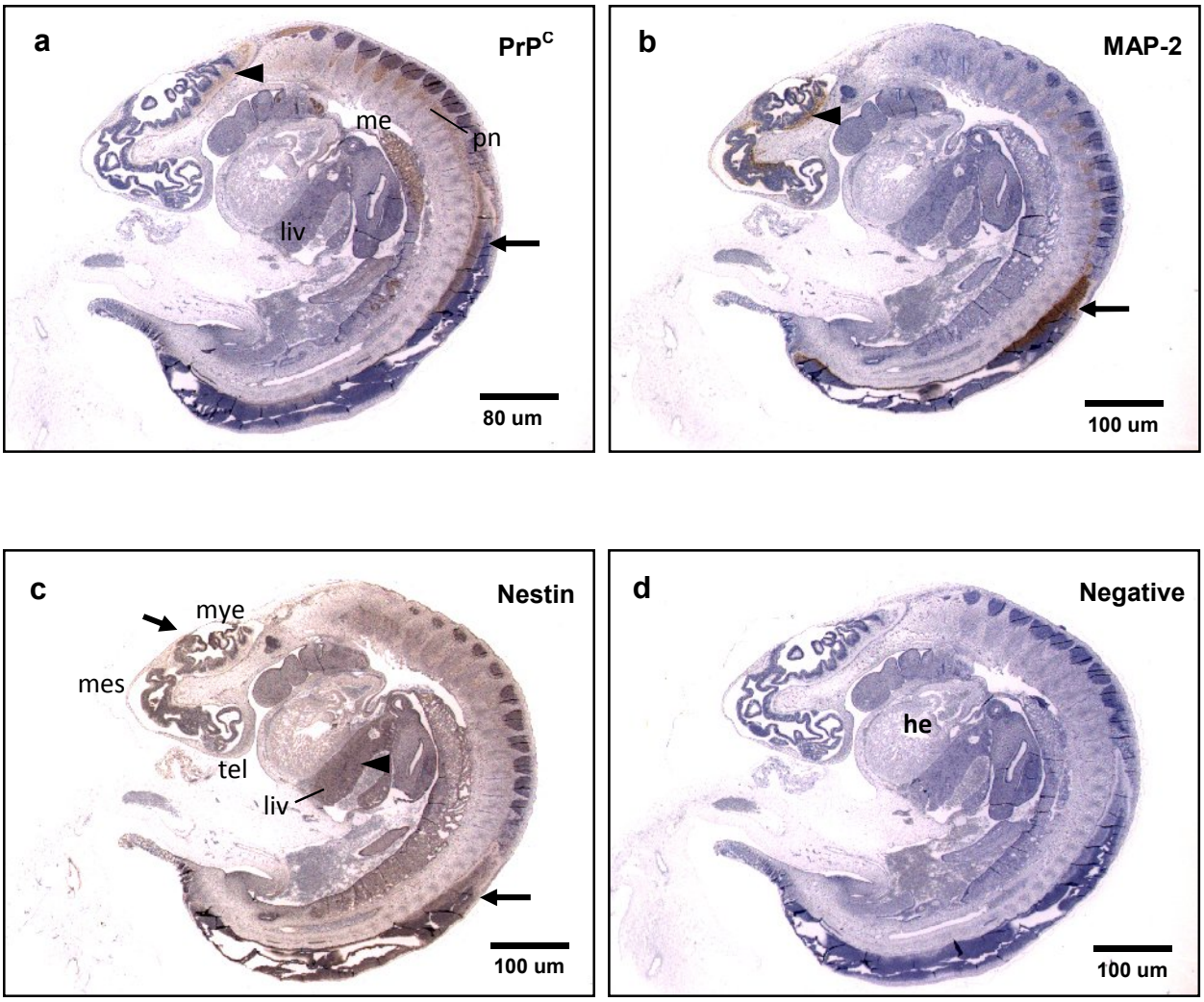

Figure 1. Immunohistochemical analysis of PrP^C, MAP-2 and nestin expression in bovine fetuses (day 27). (a) PrP^C and (b) MAP-2 staining were detected in the developing brain (*arrow-head*) and spinal cord (*arrow*). (c) Nestin showed a wide pattern of staining mainly localized in the CNS (*arrow*) and liver (*arrow head*). (d) Negative control incubated with non-immune horse serum instead of primary antibody. Abbreviations: sc, spinal cord; he, heart; liv, liver; mes, mesencephalon; me, mesonephros; mye, myelencephalon; tel, telencephalon; pn, peripheral nerve.

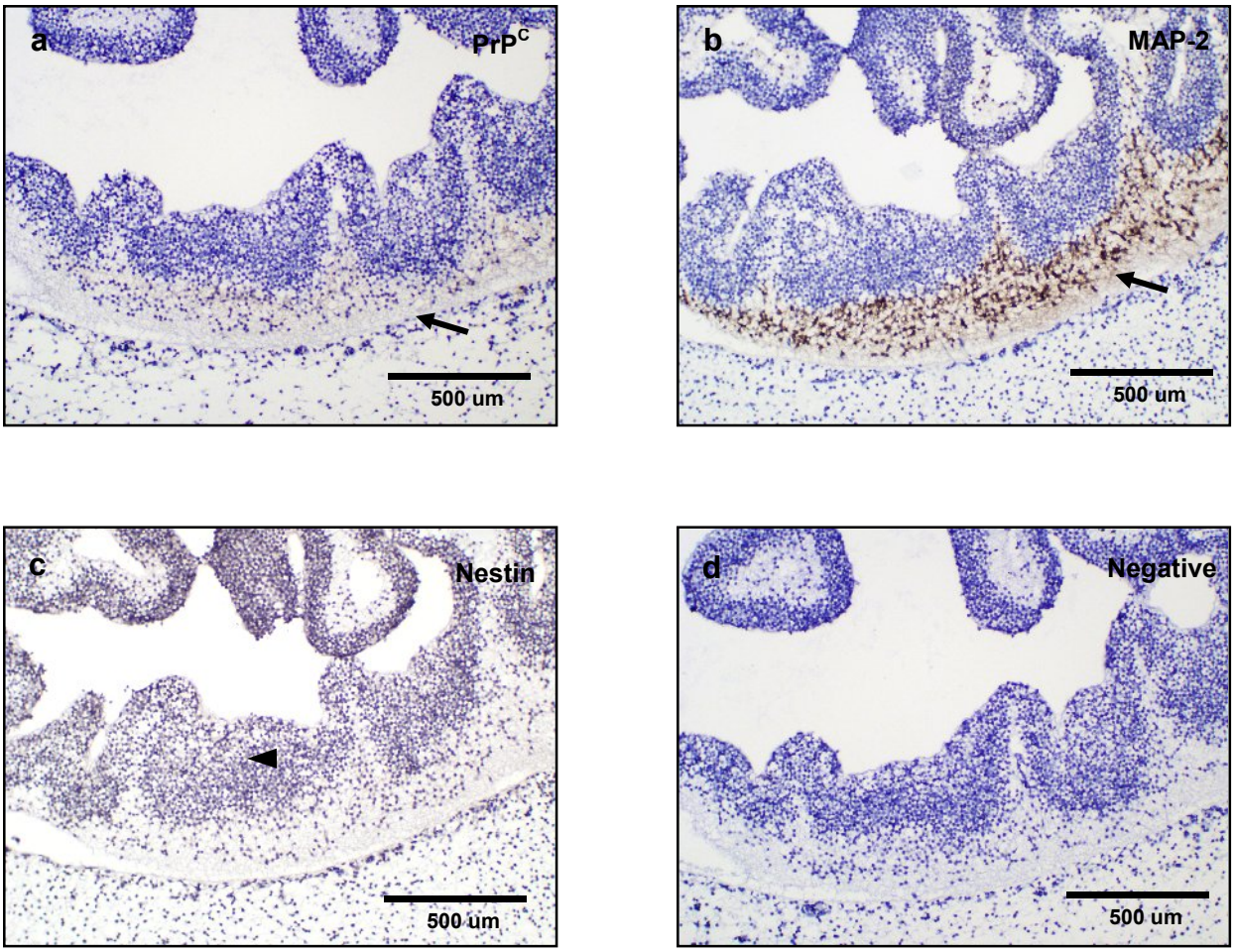

Figure 2. Expression of PrP^C, MAP-2 and nestin in the developing brain (day 27). (a) Weak PrP^C staining was observed in the marginal layer of the myelencephalon. (b) MAP-2 showed intense staining in the intermediate layer in the same brain region (*arrow*). (c) Nestin immunoreactions was diffuse in all regions of the neuroepithelium (*arrow-head*). (d) Negative control.

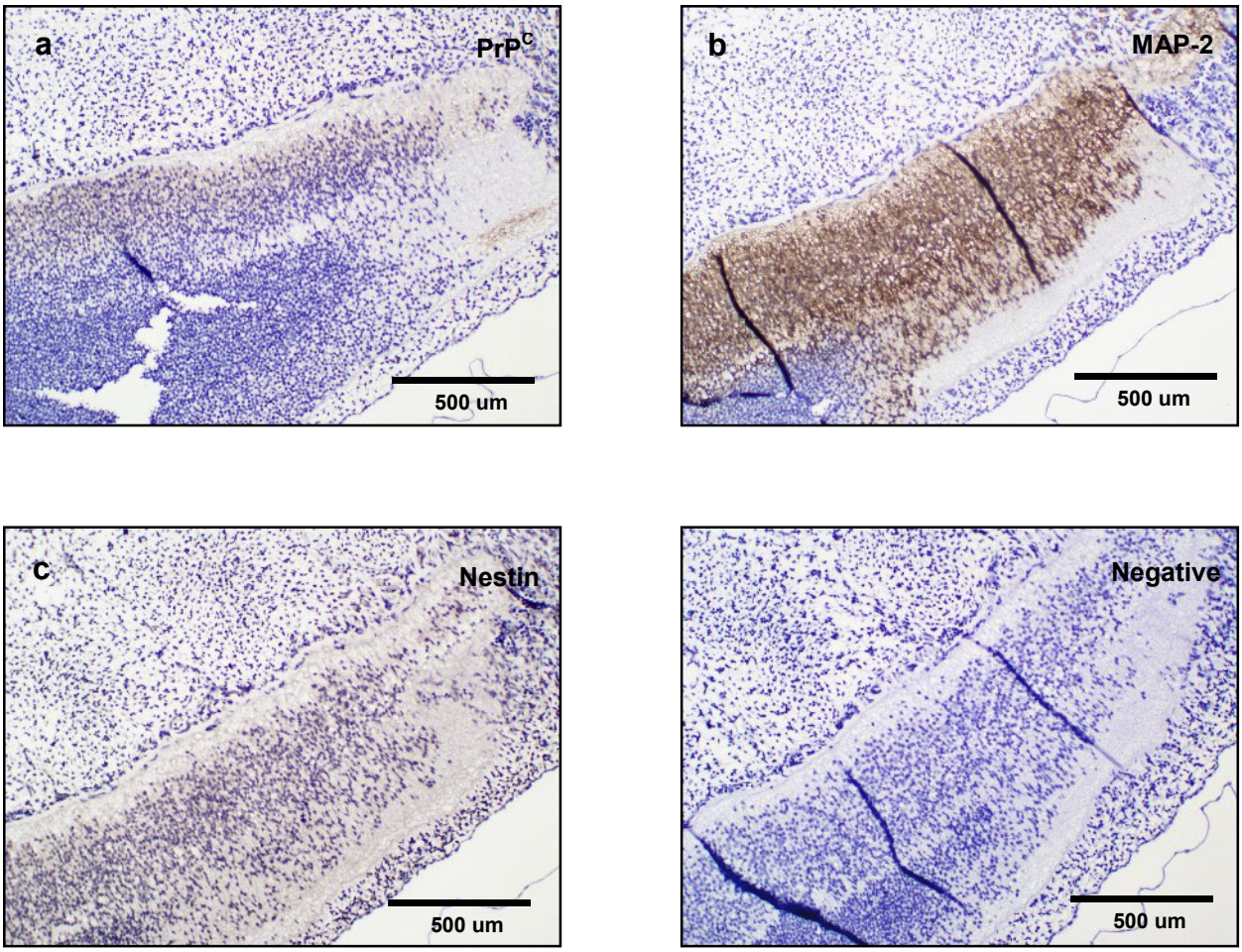

Figure 3. Expression of PrP^C, MAP-2 and nestin in the spinal cord (day 27). PrP^C immunoreactivity was observed in the pial region (a); whereas, MAP-2 staining was intense in the intermediate zone (b). Nestin staining was weak and diffuses in the periventricular and ventricular regions. (c) Negative control.

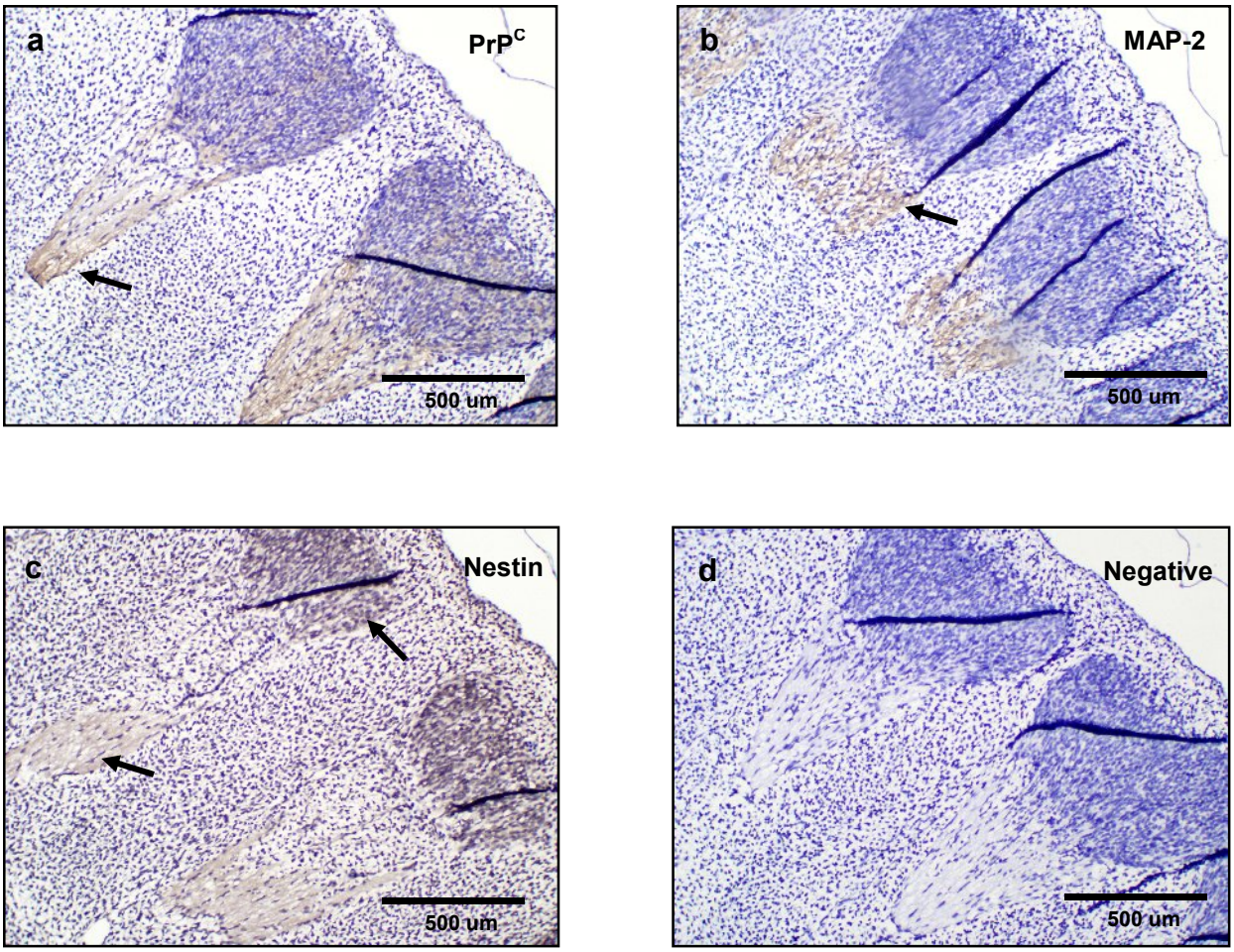

Figure 4. Expression of PrP^C, MAP-2 and nestin in the peripheral nerves (day 27). PrP^C (a) and MAP-2 (b) showed staining in peripheral nerves emerging from somites (*arrows*). (c) A weak labeling was observed after nestin immunoreaction analysis. (d) Negative control.

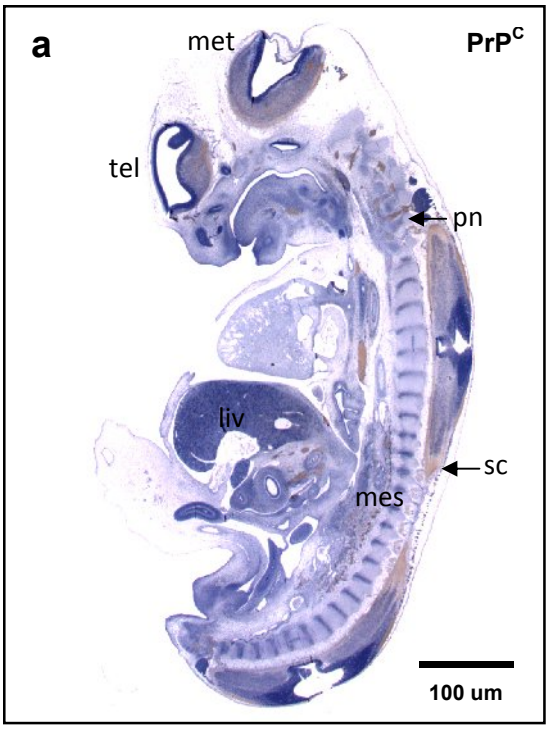
a
met
PrP^c
tel
pn
liv
sc
mes
100 um


b
MAP-2
100 um


c
Nestin
200 um

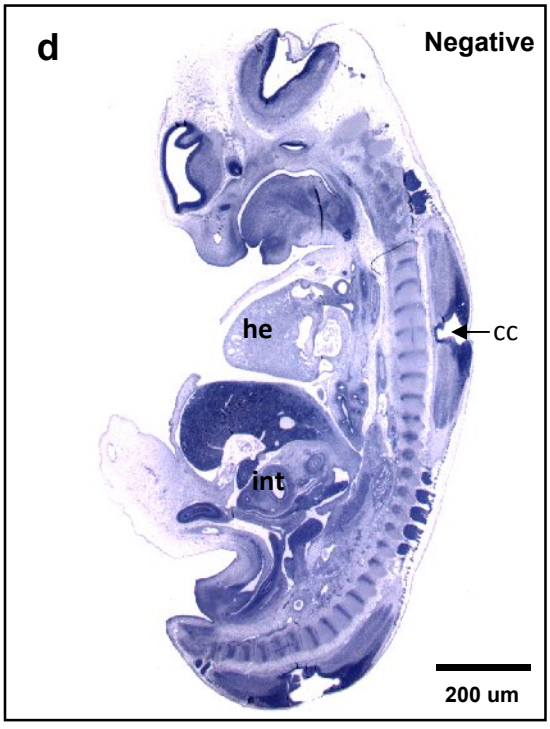
d
Negative
he
cc
int
200 um

Figure 5. Immunohistochemical analysis of PrP^C, MAP-2 and nestin expression in bovine fetuses (day 39). PrP^C immunoreactivity was observed in the brain, spinal cord, mesonephros and cells of the liver (a). MAP-2 staining was confined to the brain and spinal cord (b). Nestin showed diffuse staining with higher immunoreactivity in the brain, spinal cord and liver (c). Negative control (d). Abbreviations: cc, cord canal; he, heart; int, intestine; li, liver; me, mesonephros; mes, mesencephalon; tel, telencephalon; sc, spinal cord.

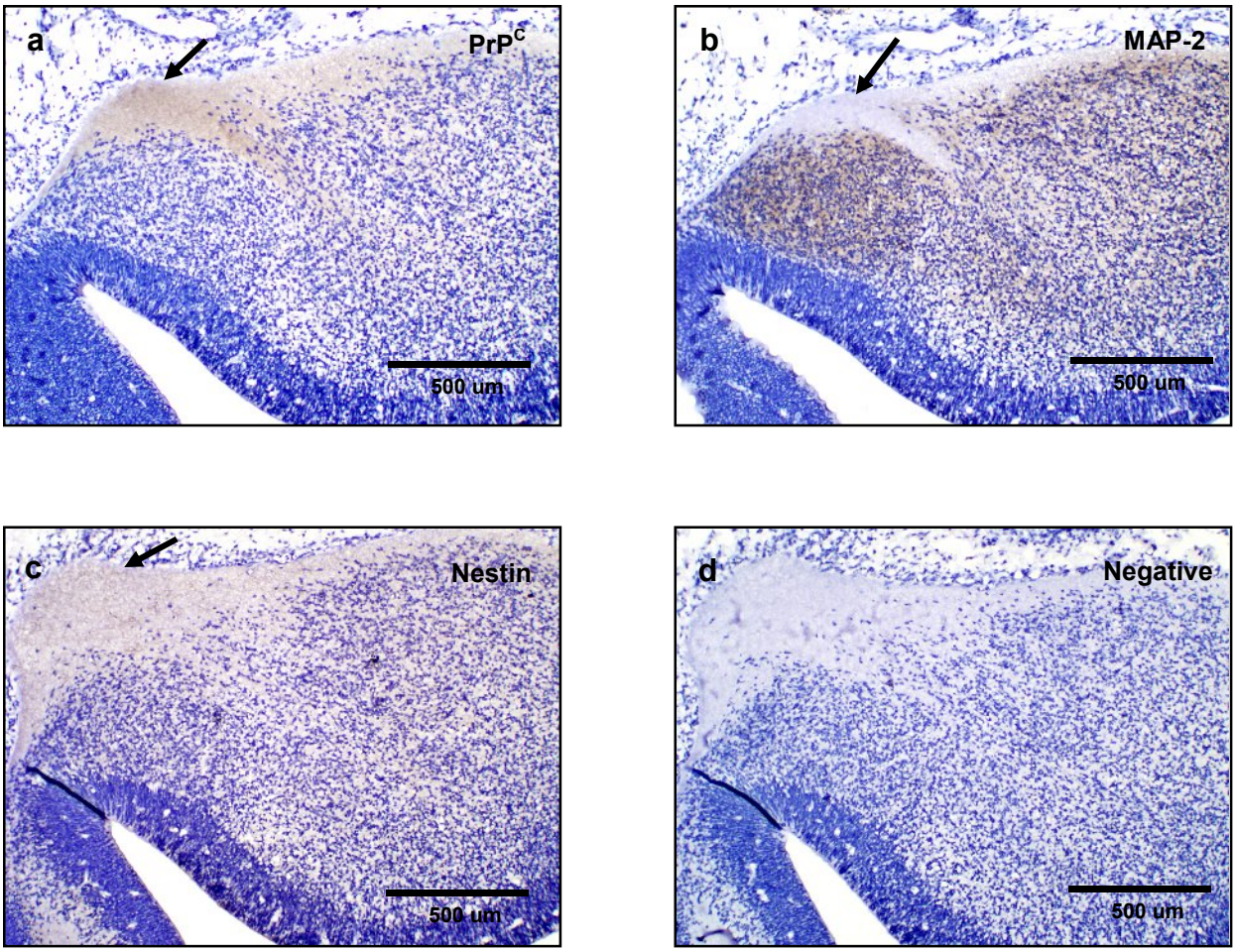

Figure 6. Expression of PrP^C, MAP-2 and nestin in the developing brain (day 39). (a) PrP^C showed intense staining in the molecular layer of the pial region of the brain (*arrows*) in contrast to the lack of immunoreactions by MAP-2 (b). (c) Nestin labeling covered all regions of the neuroepithelium. (d) Negative control.

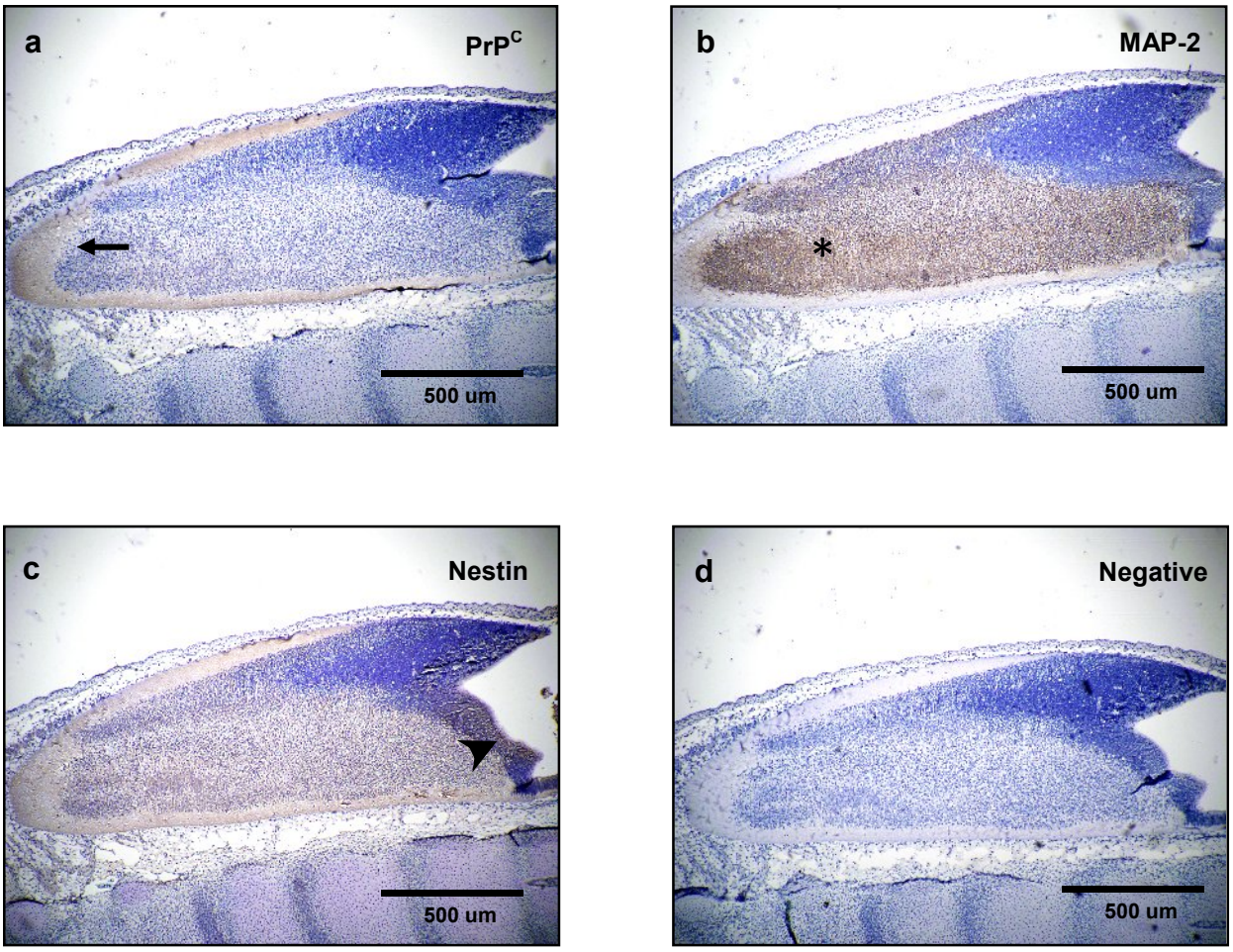

Figure 7. Expression of PrP^C, MAP-2 and nestin in the spinal cord (day 39). (a) PrP^C staining was observed in the pial region of the spinal cord (*black arrow*). (b) MAP-2 showed positive reaction in the intermediate region but no labeling in the pial region (*). (c) Nestin immunoreacted with all regions of the neuroepithelium including the ventricular zone (*arrow-head*). (d) Negative control.

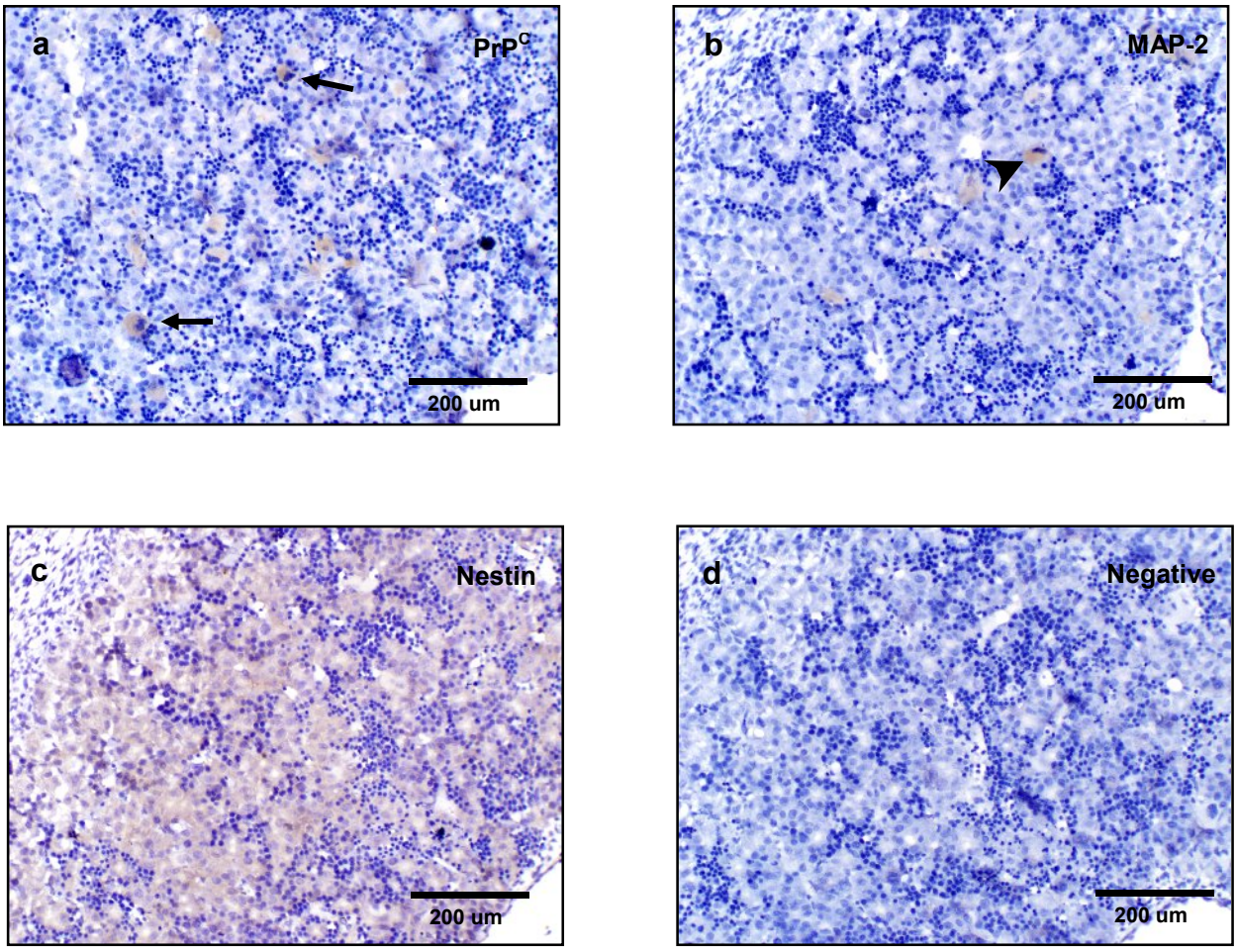

Figure 8. Expression of PrP^C, MAP-2 and nestin in the liver (day 39). (a) PrP^C staining was observed in the multinucleated cells in the liver parenchyma (*black arrow*). (b) MAP-2 showed similar cellular-specific immunoreactivity with PrP^C (*arrow-head*). (c) Nestin displayed a wide immunoreactivity with cells in the liver parenchyma. (d) Negative control.

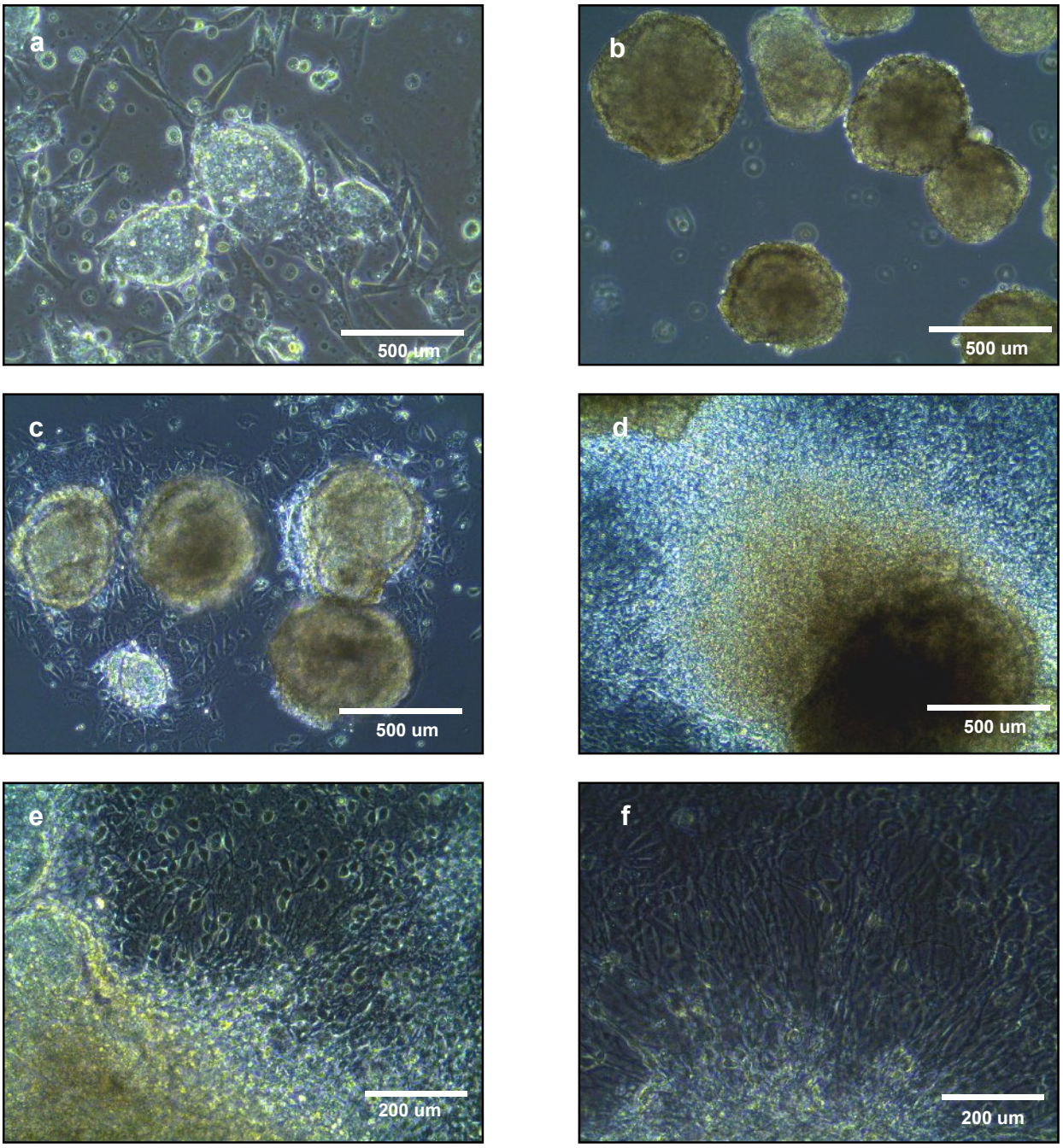

Figure 9. mESC morphology during differentiation. (a) day 0; mESC colonies were expanded in co-culture with STO cells. (b) day 5; mESCs formed EBs after separation of STO cells and culture in suspension under differentiating conditions. (c) day 10; EBs were cultured in differentiating media, attaching to tissue culture dishes and showing expansion of mESC-derived cells. (d) day 15; mESCs expanded from EBs and showing precursors of beating cardiomyocytes. (e) Day 20; ESC showed signs of differentiation into neural-like cells by formation of neurites.

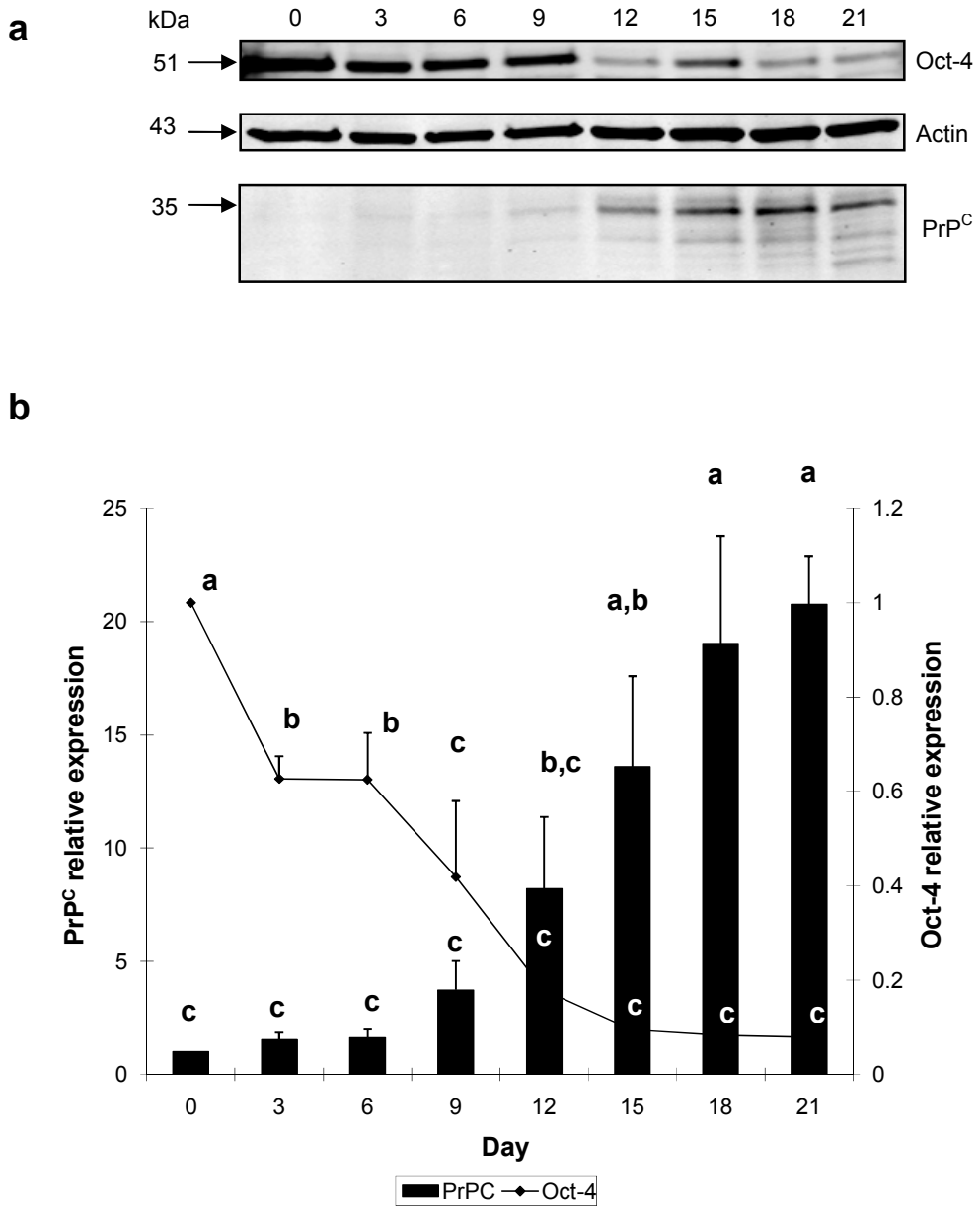

Figure 10. Expression of PrP^C in differentiating mESC cells. (a) PrP^C displayed characteristic glycosilated isoforms at 35 kDa with increasing intensity after western blot analysis during ESC differentiation. In contrast, Oct-4 expression showed decreasing levels at 51 kDa. (b) Computerized quantification of migration bands (n=3) indicated that PrP^C expression was significantly ($P < 0.05$) higher since day 12 of differentiation compared to day 0. Oct-4 expression showed lower ($P < 0.05$) values since day 3 of differentiation. Furthermore, values were significantly reduced at day 12.

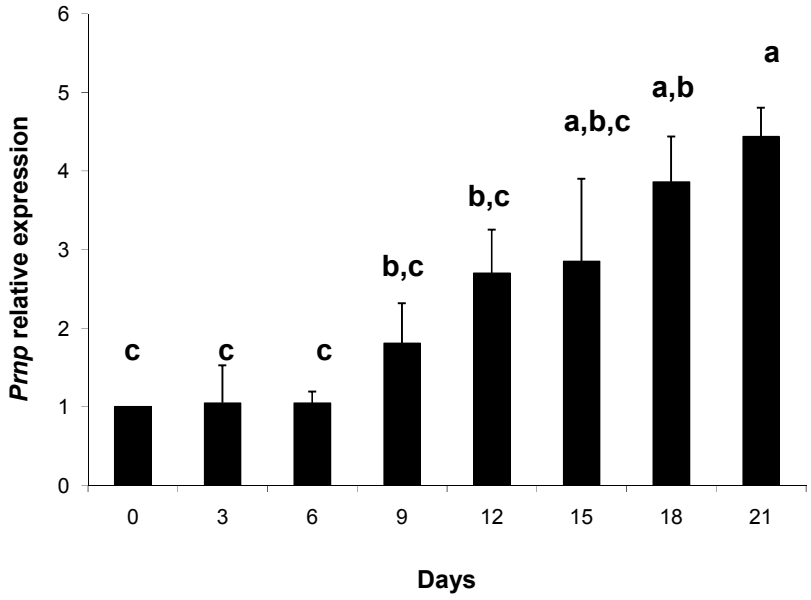

Figure 11. Expression of *Prnp* in differentiating mESCs. *Prnp* mRNA expression was analyzed using Q-PCR. *Prnp* mRNA values were significantly ($P < 0.05$) increased after day 9 of differentiation. (a,b) different superscripts indicate significant ($P < 0.05$) difference.

a

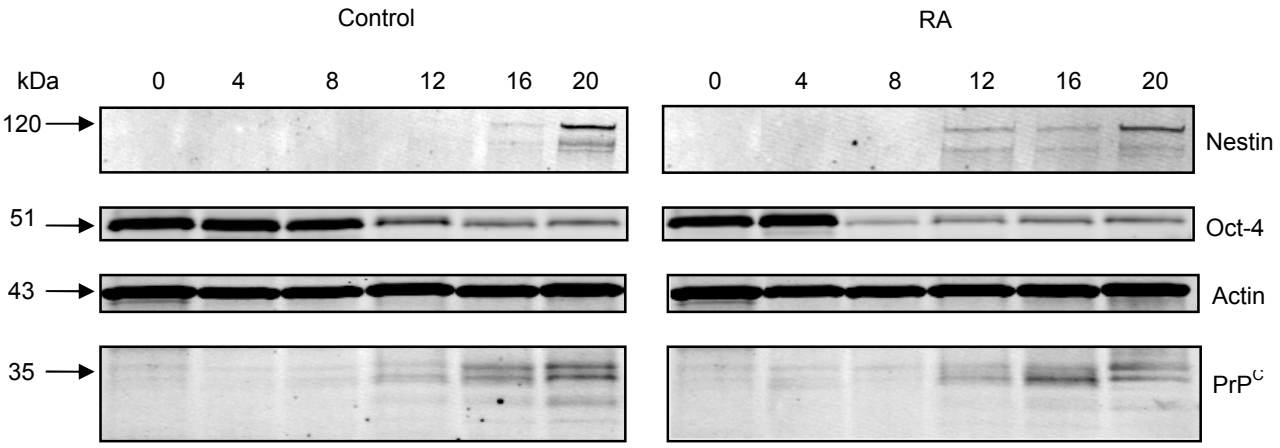
Control
RA
kDa
0
4
8
12
16
20
120
51
43
35
Nestin
Oct-4
Actin
PrP^C

b

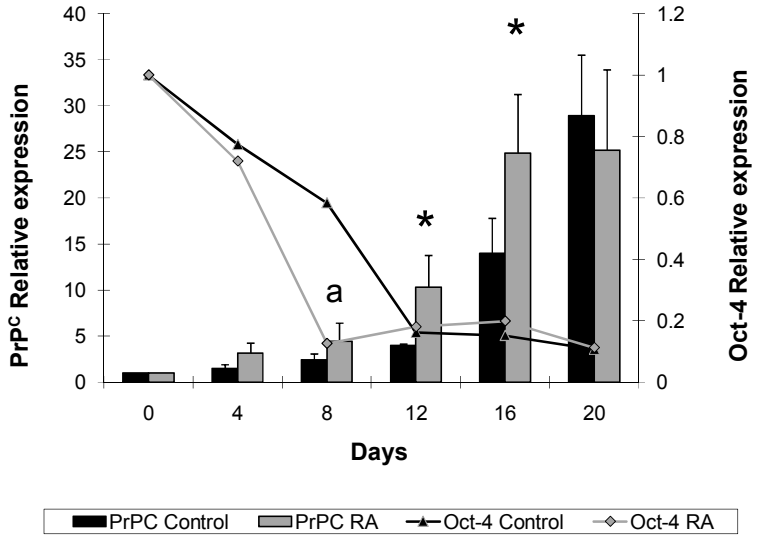
PrP^C Relative expression
Oct-4 Relative expression
Days
a
*
*
PrPC Control
PrPC RA
Oct-4 Control
Oct-4 RA

c

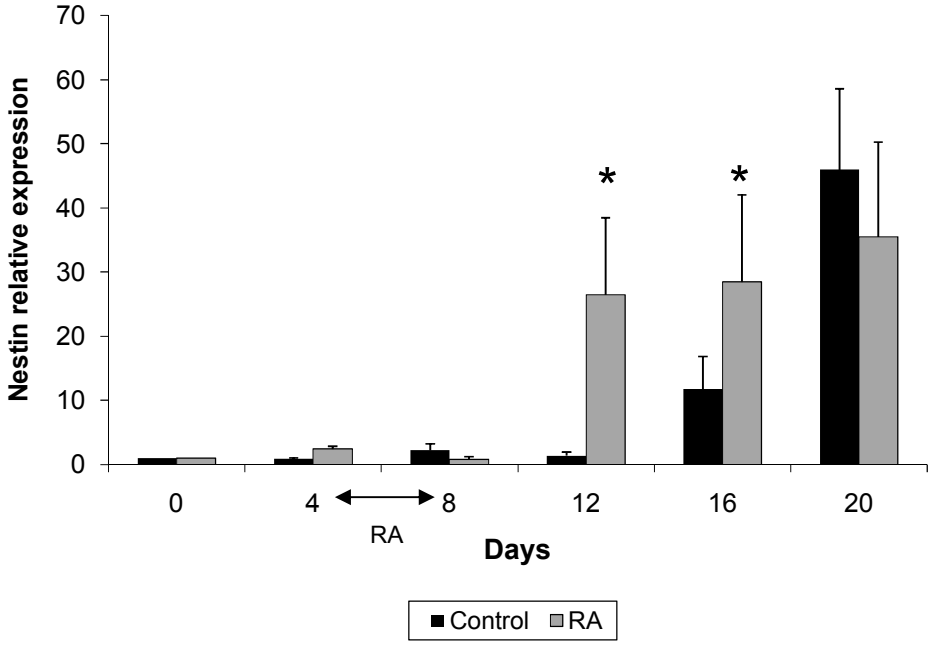

Figure 12. Expression of PrP^C, Oct-4 and nestin in differentiating mESCs after induction with RA. (a) PrP^C displayed characteristic glycosilated isoforms at 35 kDa, Oct-4 at 51 kDa and nestin at 120kDa. (b) Computerized quantification of migration bands showed a higher ($P < 0.05$) expression of PrP^C in RA-treated mESCs compared to the controls at days 12 and 16 of differentiation. Oct-4 expression in RA-treated mESC showed an earlier reduction (a; $P < 0.05$) at day 8 compared to the control. (c) RA-treated mESCs displayed an earlier increase in nestin levels compared to controls (*; $P < 0.05$).

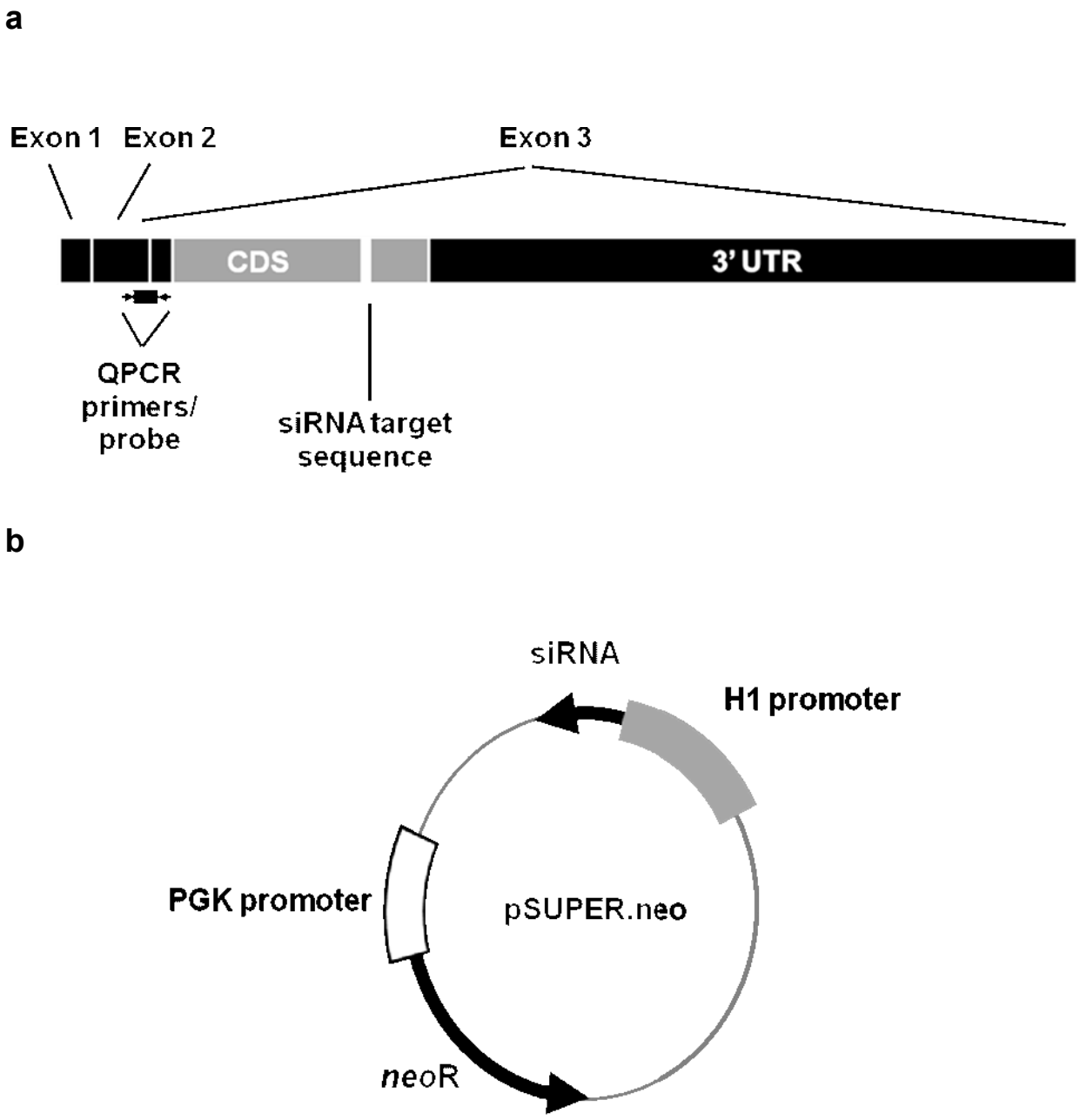

Figure 13. Structure of the *Prnp* gene and pSUPER.neo vector used to knockdown *Prnp* expression through siRNA. (a) Bovine *Prnp* gene, showing location of siRNA target sequence, probe and primer location for QPCR. pSUPER.neo vector. (b) Expression of siRNA, driven by the H1 RNA promoter, yields mRNA that contains two 19-base pallindromic targeting sequences separated by nine bases that form a hairpin loop after folding of the pallindromes to form a double-stranded RNA. Control vector was identical, save for substitution of a scrambled version of the targeting sequence.

a

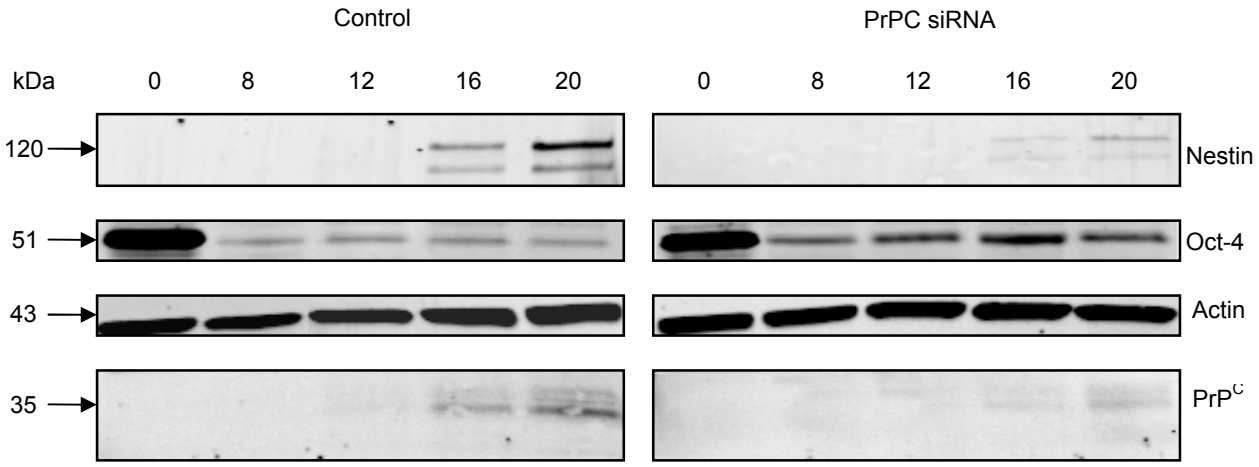
Control
PrPC siRNA
kDa
0
8
12
16
20
120
51
43
35
Nestin
Oct-4
Actin
PrP^C

b

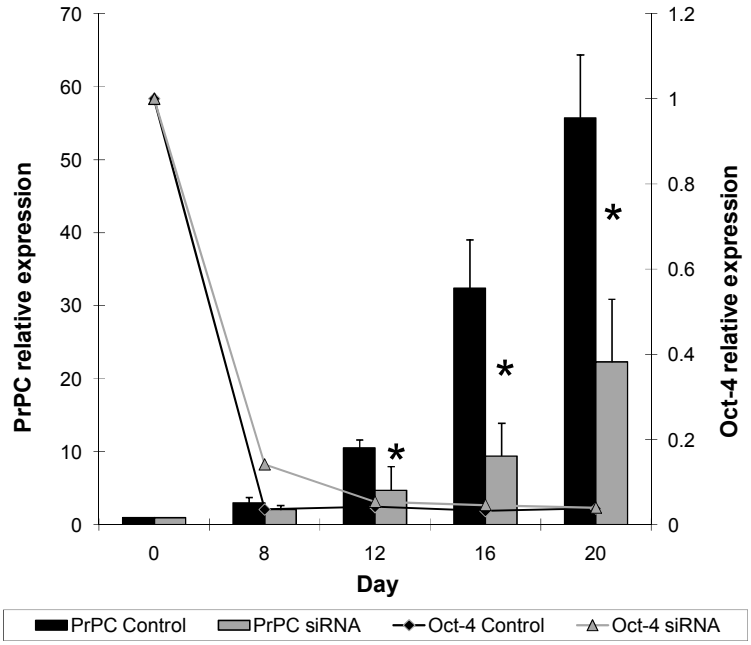
PrPC relative expression
Oct-4 relative expression
Day
0
8
12
16
20
70
60
50
40
30
20
10
0
1.2
1
0.8
0.6
0.4
0.2
0
*
PrPC Control
PrPC siRNA
Oct-4 Control
Oct-4 siRNA

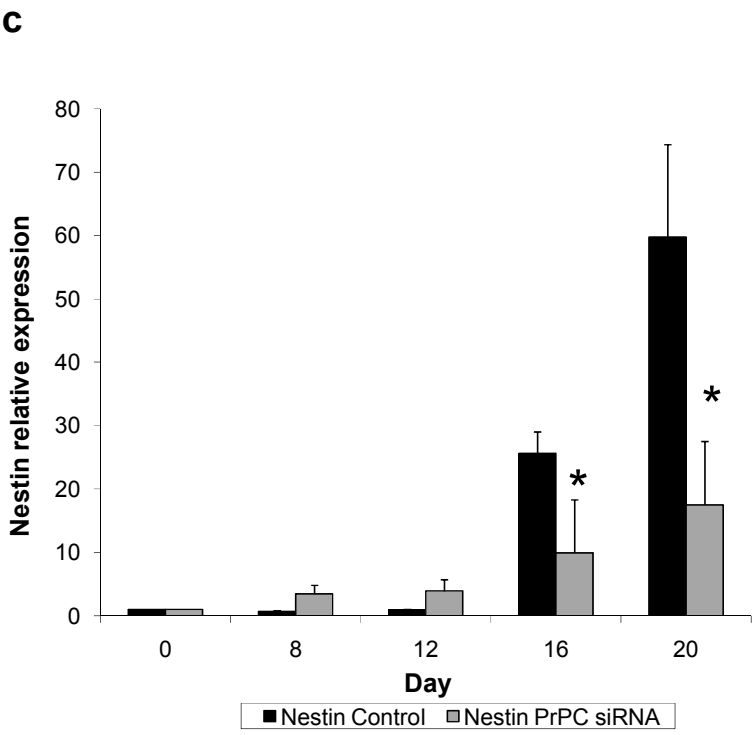

Figure 14. Expression of PrP^C, Oct-4 and nestin in differentiating mESCs after knockdown of PrP^C. (a) PrP^C displayed less intense immunoreactive bands compared to control. (b) Computerized quantification of migration bands indicated that PrP^C expression was significantly ($P < 0.05$) reduced on days 12 and 16 compared to control. Oct-4 levels were reduced at day 8 and showed no differences between groups. (c) Nestin levels were significantly reduced on days 16 and 20 compared to control.

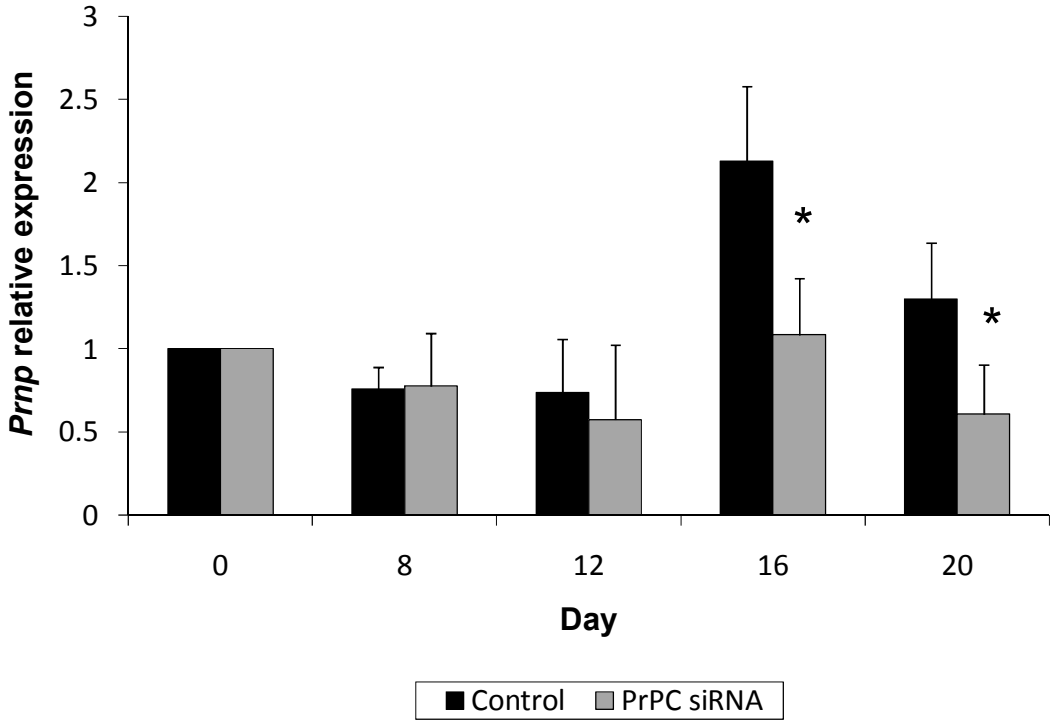

Figure 15. Expression of *Prnp* mRNA in differentiating mESCs after knockdown of PrP^{C}. Q-PCR analyses evidenced the significant reduction in *Prnp* mRNA levels in the siRNA mESCs at days 16 and 20 of differentiation compared to control.

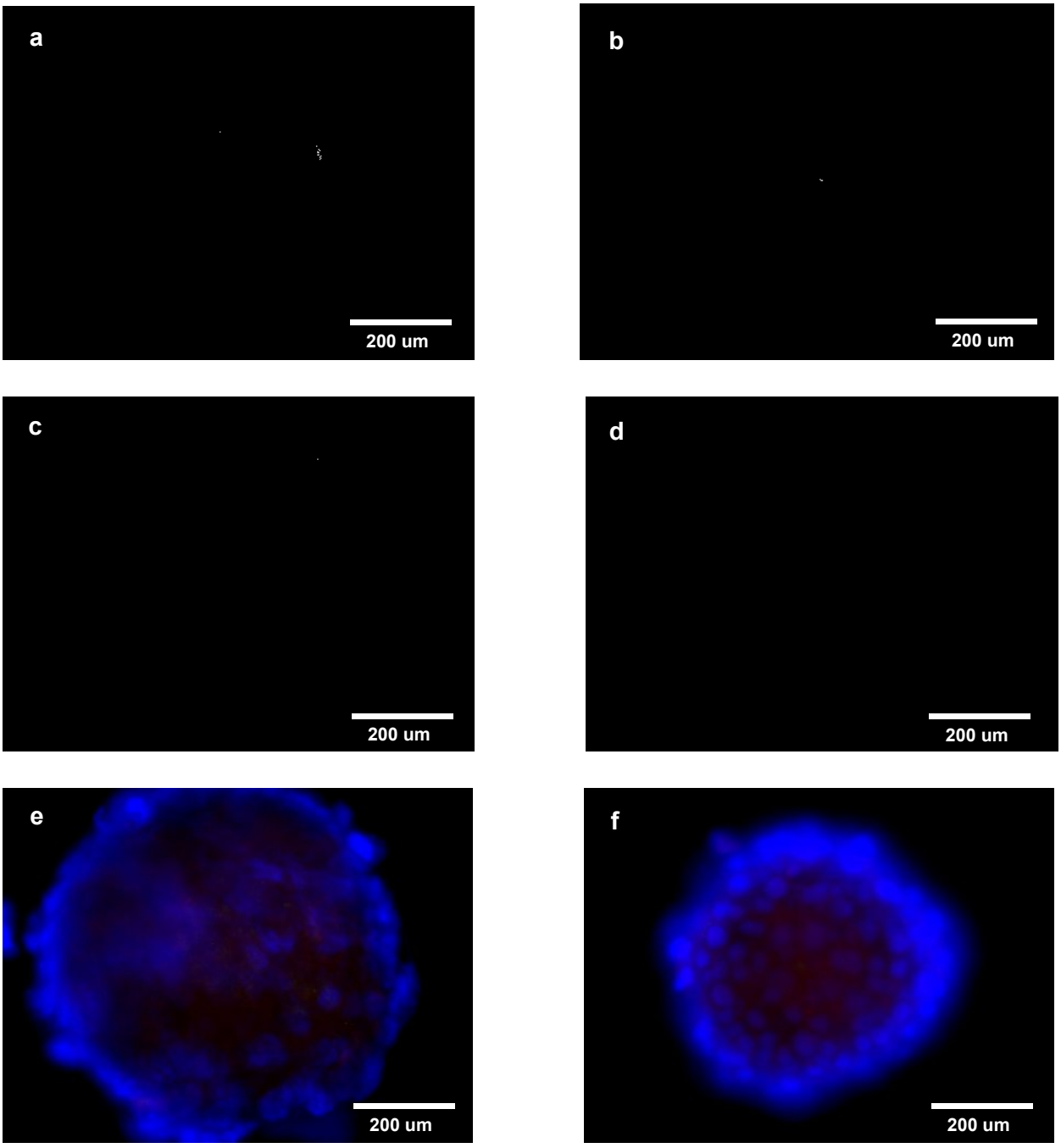

Figure 16. Expression of PrP^C in siRNA PrP^C mESC and control mESCs at day 0 of differentiation. Undetectable levels of PrP^C were detected in (a) control and (b) siRNA mESCs at day 0 of differentiation. Similarly, nestin showed no immunoreactivity in (c) control and (d) siRNA mESCs. Merged PrP^C, nestin and DAPI for (e) control and (f) siRNA mESCs.

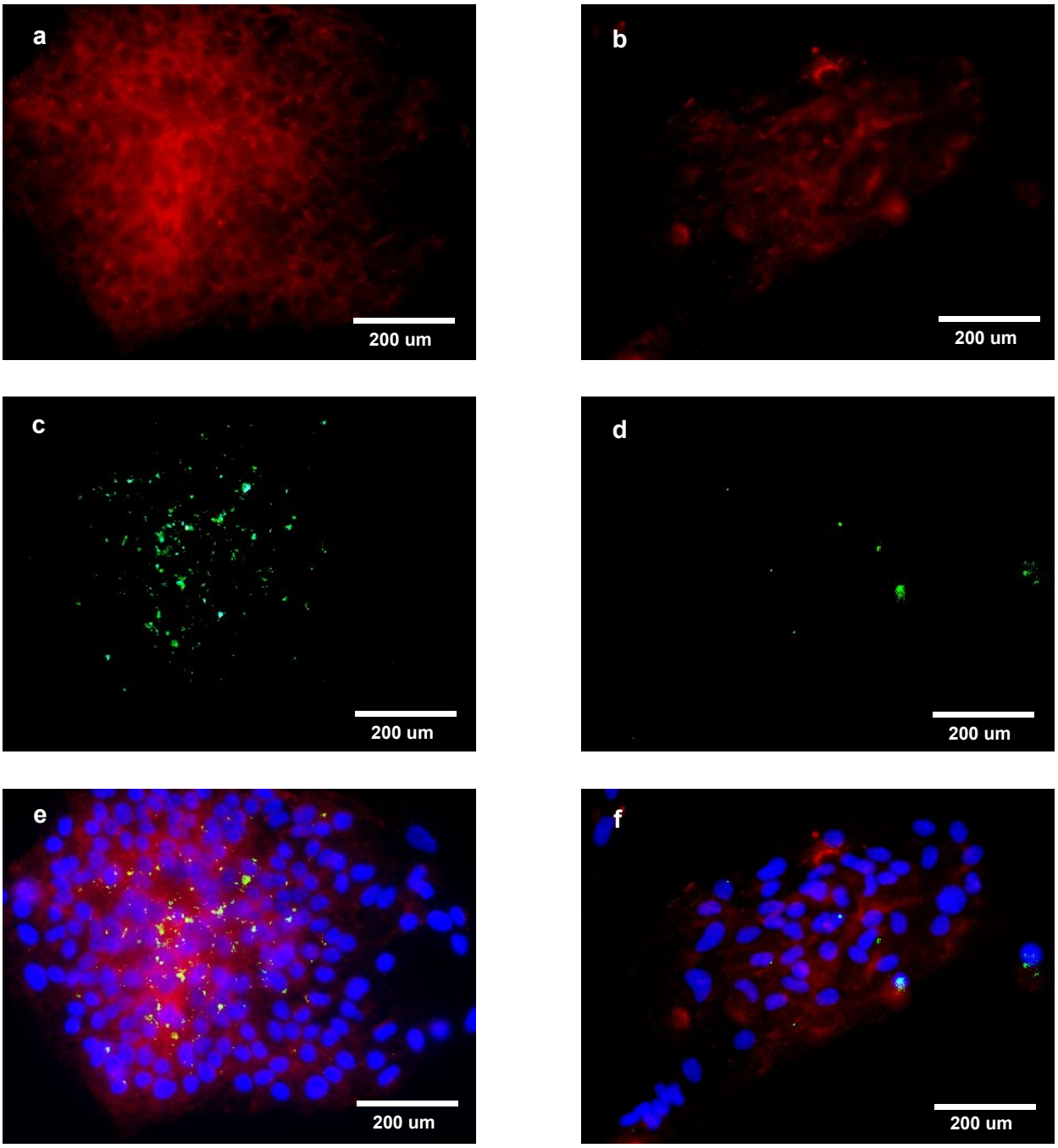

Figure 17. Expression of PrP^C in control PrP^C mESCs and siRNA mESCs at day 20 of differentiation. PrP^C labeling was strongly detected in (a) mESC control colonies but showed decreased levels of intensity in (b) siRNA mESCs at day 20 of differentiation. Similarly, nestin signal was detected in (c) control mESC but showed les immunoreactivity in (s) siRNA mESCs. Merged PrP^C, nestin and DAPI for (e) control and (f) siRNA mESCs.

LITARATURE CITED

Adle-Biassette H, Verney C, Peoc'h K, Dauge M-C, Razavi F, Choudat L, Gressens P, Budka H, Henin D. 2006. Immunohistochemical expression of prion protein (PrPC) in the human forebrain during development. J Neuropathol Exp Neurol, 65, 7, 698-706.

Bain G, Kitchens D, Yao M, Huettner JE, Gottlieb DI. 1995. Embryonic stem cells express neuronal properties *in Vitro*. Dev Biol, 168, 342-357.

Brummelkamp TR, Bernards R, Agami R. 2002. A system for stable expression of short interfering RNAs in mammalian cells. Science 296, 550-553.

Bueler H, Fischer M, Lang Y, Fluethmann H, Lipp H-P, DeArmond SJ, Prusiner SB, Aguet M, Wissmann C. 1992. Normal development and behavior of mice lacking the neuronal cell-surface PrP protein. Nature 356, 577-582.

Dodelet VC, Cashman NR. 1998. Prion protein expression in human leukocyte differentiation. Blood 91, 1556-1561.

Ernst C and Christie BR. 2005. Nestin-expressing cells and their relationship to mitotically active cells in the subventricular zones of the adult rat. Eur J Neurosci 22, 12, 3059-3066.

Ford MJ, Burton LJ, Morris RJ, Hall SM. 2002a. Selective expression of prion protein in peripheral tissues of the adult mouse. Neuroscience 113, 1, 177-192.

Frederiksen K and McKay RDG. 1988. Proliferation and differentiation of rat neuroepithelial precursor cells *in vivo*. J Neurosci 8, 4, 1144-1151.

Fukuda S, Kato F, Tozuka Y, Yamaguchi M, Miyamoto Y, Hisatsune T. 2003. Two distinct subpopulations of nestin-positive cells in adult mouse dentate gyrus. J Neurosci 23, 28, 9357-9366.

Gilyarov AV. 2008. Nestin in central nervous system cells. Neurosci and Behavior Phys 38, 2, 165-169.

Graner E, Mercadante AF, Zanata SM, Martins VR, Jay DG, Brentani RR. 2000. Laminin-induced PC-12 cell differentiation is inhibited following laser inactivation of cellular prion protein. FEBS Lett 482, 257-260.

Hetz C, Maundrell K, Soto C. 2003. Is loss of function of the prion protein the cause of prion disorders? Trends Mol Med 9, 237-243.

Luskin MB. 1998. Neuroblasts of the postnatal mammalian forebrain: their phenotype and fate. J Neurobiol 36, 221-233.

Manson J, West JD, Thomson V, McBride P, Kaufman MH, Hope J. 1992. The prion protein gene: a role in mouse embryogenesis? Development 115, 117-122.

Miele G, Alejo Blanco AR, Baybutt H, Horvat S, Manson J, Clinton M. 2002. Embryonic activation and developmental expression of the murine prion protein gene. Gene Expression 11, 1-12.

Robertson EJ. 1987. Teratocarcinomas and embryonic stem cells: a practical approach. Oxford: IRL Press.

Richt JA, Kasinathan P, Hamir AN, Castilla J, Sathiyaseelan T, Vargas F, Sathiyaseelan J, Wu H, Matsushita H, Koster J, Kato S, Ishida I, Soto C, Robl JM, Kuroiwa Y. 2007. Production of cattle lacking prion protein. Nat Biotechnol 1, 132-138.

Sales N, Hassig R, Katia R, Giamberardino LD, Traiffort E, Ruat M, Fretier P, Moya L. 2002. Developmental expression of the cellular prion protein in elongating axons. Eur J Neurosci 15, 1163-1177.

Sanchez C, Diaz-Nido J, Avila J. 2000. Phosphorylation of microtubule-associated protein 2 (MAP2) and its relevance for the regulation of the neuronal cytoskeleton function. Prog Neurobiol 61, 133-168.

Santuccione A, Sytnyk V, Leeshchyns'ka I, Schachner M. 2005. Prion protein recruits its neuronal receptor NCAM to lipid rafts to activate p59fyn and to enhance neurite outgrowth. J Cell Biol 169, 341-354.

Starke R, Harrison P, Mackie I, Wang G, Erusalimsky JD, Gale R, Masse JM, Cramer E, Pizzey A, Biggerstaff J, Machin S. 2005. The expression of prion protein (PrP(C)) in the megakaryocyte lineage. J Thromb Haemost 3, 1266-1273.

Steele AD, Emsley JG, Ozdinler PH, Lindquist S, and Macklis J. 2006. Prion protein (PrPC) positively regulates neural precursor proliferation during developmental and adult mammalian neurogenesis. PNAS, 103 (9): 3416-3421.

Tremblay P, Bouzamondo-Bernstein E, Heinrich C, Prusiner SB, DeArmond SJ. 2007. Developmental expression of PrP in the post-implantation embryo. Brain Res 30, 1139, 60-67.

Westergard L, Christensen HM, Harris DA. 2007. The cellular prion protein (PrPC): Its physiological function and role in disease. Biochim. Biophys. Acta. 1772, 6, 629-644.

Winters LM, Green WW, Comstock RE. 1942. Prenatal development of the bovine. University of Minnesota, Agricultural Experiment Station.

Witusik M, Gresner SM, Hulas-Bigoszewska K, Krynska B, Azizi SA, Liberski PP, Brown P, Rieske P. 2007. Neuronal and astrocytic cells, obtained after differentiation of human neural GFAP-positive progenitors, present heterogeneous expression of PrPC. Brain Res 1186, 65-73.

CONCLUSIONS

The controversial report of the study by Prusiner in 1981 opened a new perspective in the prion biology that involved the autocatalytic capacity of these proteins to replicate in absence of DNA. Currently, there are no ways to cure, treat or immunizes against TSEs, and the consequences for public health and economic costs have proven to be tremendous. However, important advances during the last years in the understanding of prion biology have allowed the development of better strategies for the control of this disease and have opened new opportunities for treatment. One of the most intriguing aspects in prion biology is the still enigmatic physiological function of the PrP^C. Recently, important evidence has been reported supporting the idea that PrP^C is involved in signaling pathways associated with cellular proliferation and differentiation. In the present work, we showed that PrP^C is intensely expressed in the bovine CNS but also widely distributed in peripheral tissues including the reproductive system. These analyses suggest the participation of PrP^C in various physiological processes involving cellular protection, proliferation and differentiation. Moreover, the developmental regulation of PrP^C during embryogenesis suggests that this physiological role is active since early stages of development. One of the most interesting conclusions of the analyses of PrP^C in fetuses is the close association that this protein has with the early development of the nervous system. The use of mESC cell to study the potential role or PrP^C in neurogenesis allowed us to conclude that PrP^C is positively associated with differentiation of ESC into neural stem/progenitor cells. Moreover, in the present work we showed evidence for the association between PrP^C and nestin indicating the contribution of PrP^C in neurogenesis.

SUMMARY

In the present work, we describes on our efforts to better understand the biological function of PrP^C. Our first approach involved the elaboration of a map of PrP^C expression by analyzing fifteen different somatic tissues in cattle. PrP^C expression was detected by quantitative western blot and immunohistochemistry. Tissues analyzed included cerebellum, obex, spinal cord, sciatic nerve, mesenteric lymph node, thymus, spleen, liver, pancreas, ileum, kidney, heart, lung, skin and skeletal muscle. Western blot analysis showed immunoreactive bands for PrP^C at 35, 28 and 25 kDa suggesting the presence of di-, mono- and un-glycosylated isoforms. The di-glycosylated isoform predominated across all tissues and displayed strong bands in the CNS and thymus. In contrast, immunoreactivity of di-glycosylated PrP^C was low in pancreas and liver. Relative expression of PrP^C was calculated by comparing PrP^C levels to GAPDH levels and normalizing the expression of each tissue to PrP^C expression in the cerebellum. Cerebellum and obex showed the highest ($P < 0.05$) expression of PrP^C. Among non-neural tissues, the highest ($P < 0.05$) level of PrP^C was detected in the thymus. The tissue-specific location of PrP^C was analyzed in the same tissues using immunohistochemistry. Intense immunostaining was observed in the nervous system and thymus. In contrast, PrP^C was undetectable in the liver and muscle. Cell-specific staining was observed in perilymphoid areas in the lymph node and spleen, mucosa and submucosa of the intestine, Islets of langerhans in the pancreas and dermis of the skin. PrP^C labeling was also observed in the kidney, cardiac muscle and lung. Although PrP^C was widely distributed in bovine somatic tissues, the most intense expression of PrP^C was detected in the nervous system. PrP^C was most commonly localized in neurons and lymphoreticular cells.

In a second study we used western blot and immunohistochemistry to characterize the expression of PrP^C in the bovine and ovine reproductive system. Tissue samples were collected from ovary, uterus, vagina, oviduct, mammary gland, testis, epididymis, penis, glans, prepuce, vas deferens, vesicular gland and prostate. Immunoreactive PrP^C bands were observed at 35, 28 and 25 kDa suggesting the presence of di-, mono- and un-glycosylated isoforms. The di-glycosylated isoform showed variable intensities between tissues with some displaying strong immunoreactivity and others lower levels. Relative expression of PrP^C was calculated by comparing PrP^C levels to GAPDH and normalizing expression of each tissue to obex expression. Among male tissues, the highest ($P < 0.05$) levels of PrP^C were detected in testis and epididymis. Ovine testes showed similar levels of PrP^C compared to the ovine obex ($P < 0.05$). All female tissues showed lower ($P < 0.05$) levels of PrP^C expression compared to the obex. Immunohistochemical analyses showed intense PrP^C staining in seminiferous tubules associated to spermatids, spermatogonia

and sertoli cells. Immunofluorescence analyses revealed the presence of PrP^C in the bovine and ovine spermatozoa associated to the equatorial and acrosomal areas, respectively. PrP^C immunoreactivity was observed in the pseudostratified epithelium lining the epididymal duct and vas deferens. Secretory epithelium in seminal vesicles and prostate also showed immunoreactivity for PrP^C. In female tissues, PrP^C was detected in neurons of the mesovarium and secretory glands of the endometrium. PrP^C expression was higher in male compared to the female reproductive tissues. Thus PrP^C was widely distributed in the reproductive system with intense expression in male tissues associated with the development, maturation and transportation of the spermatozoa.

In a third study, we analyzed the developmental expression of PrP^C during bovine embryogenesis. Bovine embryos at days 4 and 8 were produced by *in vitro* fertilization (IVF) and culture of abattoir-derived oocytes. To obtain embryos at days 14 and 18, IVF embryos were cultured to day 8, transferred to recipient cattle and collected by non-surgical uterine flushing. Fetuses from days 27, 32 and 39 were obtained from cows bred by artificial insemination and collected by mid-line hysterotomy. Expression of PrP^C was analyzed by Q-PCR, immunofluorescence, immunohistochemistry and western blot. During pre-implantation stages, the highest level of *Prnp* mRNA were detected at day 4 (21.2-fold higher vs. unfertilized oocytes at day 0; $P < 0.05$) and again at day 18 (16-fold higher vs. unfertilized oocytes at day 0; $P < 0.05$). In contrast, the lowest expression levels were detected at day 14 (0.98-fold vs. day 0 oocytes) and day 8 (2.88-fold vs. day 0 oocytes). PrP^C labeling was present in blastomeres and trophoblast cells at days 4 and 18, respectively. Immunohistochemical analyses on day 27, 32 and 39 fetuses showed intense immunoreactivity in the developing brain, spinal cord and peripheral nerves. Cellular specific staining was detected in the liver and mesonephros. Immunoreactive bands for PrP^C were observed at 28 and 25 kDa suggesting the presence of mono- and un-glycosylated isoforms. Thus, PrP^C was developmentally regulated during bovine embryogenesis. The highest levels of PrP^C were temporally associated to maternal-zygote transition and maternal recognition stages (days 4 and 18, respectively). PrP^C was immunolocalized in mature neurons of the neuroepithelium and emerging neural trunks of the CNS. This data suggest the participation of PrP^C in the development of the nervous system.

In a final experiment, we utilized differentiating mESC to test whether PrP^C contributed to the process of neurogenesis. mESC were induced to form embryoid bodies (EBs) by placing them in suspension culture under differentiating conditions. EBs were disaggregated in trypsin-EDTA and cells were seeded into tissue culture dishes and cultured for up to 21 days. We detected increasing levels of PrP^C starting on day 12 (8.21- fold higher vs. day 0; $P < 0.05$) and continuing until day 20 (20.77-fold higher vs. day 0; $P < 0.05$). PrP^C expression was negatively correlated with pluripotency marker Oct-4 ($r = -0.85$) confirming

that mESC had indeed differentiated. Then mESC were cultured with or without retinoic acid (RA) to encourage differentiation into neural lineages. Induction of EBs in the presence of retinoic acid (RA) advanced the up-regulation of both PrP^C and the neural progenitor marker nestin (day 12 vs. day 16; $P < 0.05$). In addition, immunofluorescence studies indicated co-expression of PrP^C and nestin in the same cells. These data suggested a temporal association between PrP^C expression and expression of nestin during mESC differentiation into neural progenitor cells. We next tested whether PrP^C was involved in RA-enhanced neural differentiation from mESC using a PrP^C knockdown model. Plasmid vectors designed to express either a PrP-targeted shRNA or scrambled, control shRNA were transfected into mESC. Stable transfectants were selected under G418 and cloned. PrP-targeted and control shRNA clones, as well as wild-type mESC, were differentiated and sampled as above. PrP^C expression was knocked down in PrP-targeted shRNA cultures between days 12 and day 20 (62.2 % average reduction vs. scrambled shRNA controls). Moreover, nestin expression was reduced at days 16 and 20 (61.3% and 70.7%, respectively vs. scrambled shRNA controls). These results provide evidence for the contribution of PrP^C to mESC differentiation into neural progenitor cells.

In conclusion, a widely distributed expression of PrP^C in ruminant tissues suggests an important biological role for this protein. PrP^C was immunodetected in organs undergoing an active process of cellular differentiation (i.e. T-cell activation in the thymus and spermatogenesis in the testis). Regulation of PrP^C expression during embryogenesis and intense localization of PrP^C in the developing nervous system suggest the participation of PrP^C in neurogenesis. Furthermore, our experimental work provided evidence of a role of PrP^C in the differentiation of neural cells from pluripotent mESC.